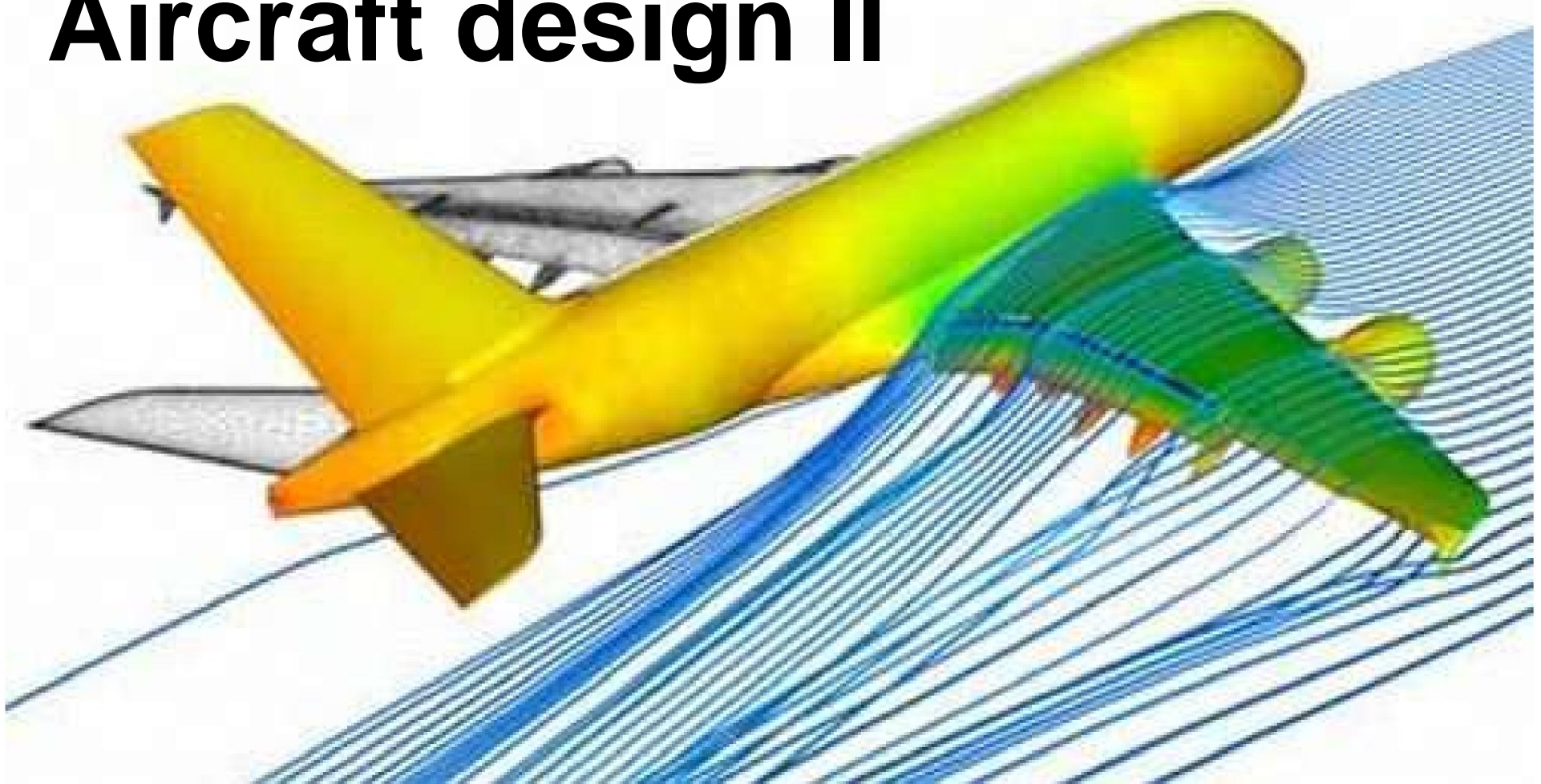


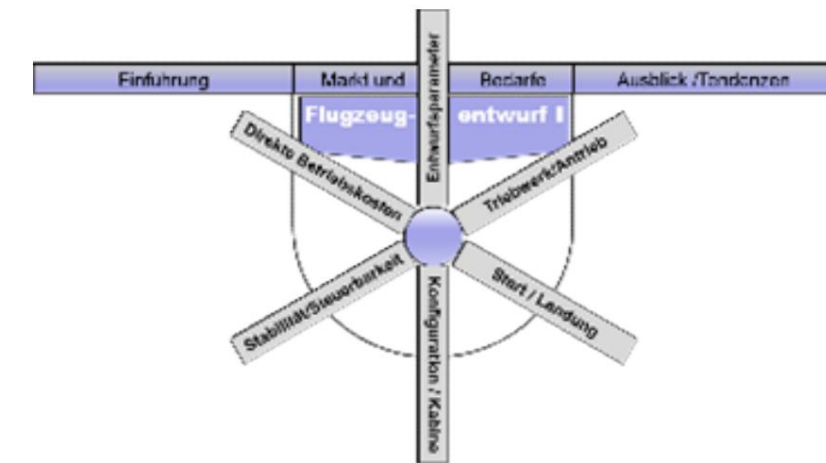
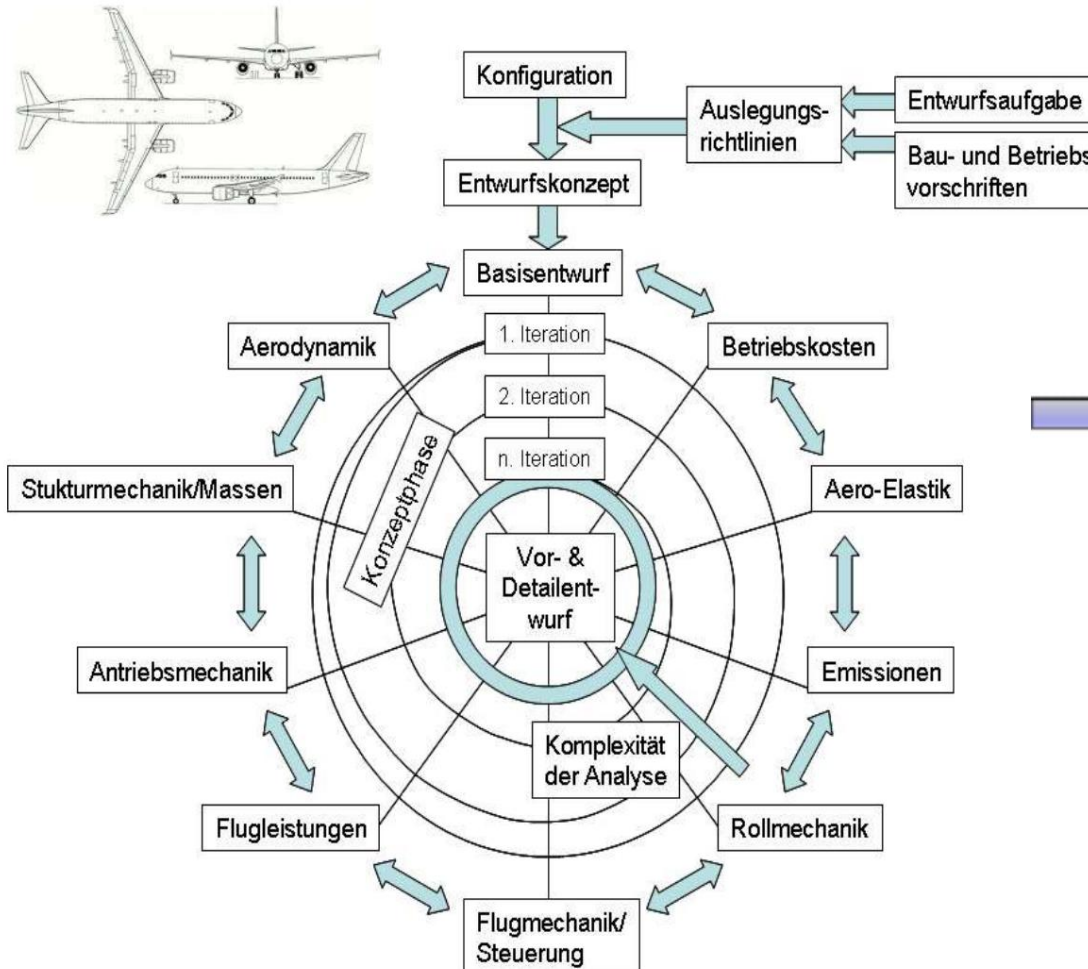
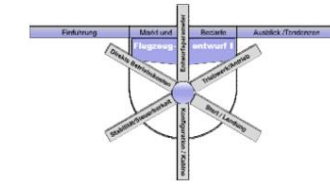
Welcome to the course

# Aircraft design II

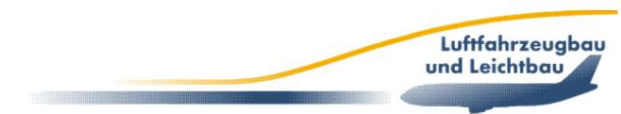


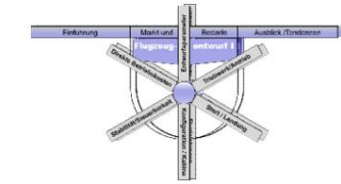
**Andreas Bardenhagen  
Andreas Gobbin**

# Introduction



**As knowledge of the design increases, more precise procedures and in-depth Analyses carried out**





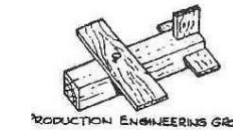
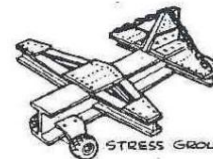
# Airplane Throwing – Basic Aspects

What if only...

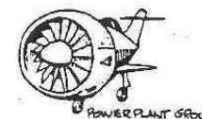
- Aerodynamics



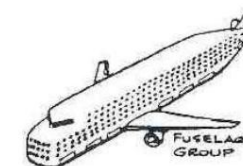
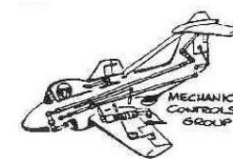
- Structure



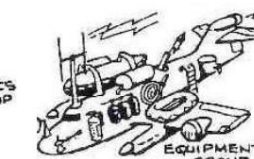
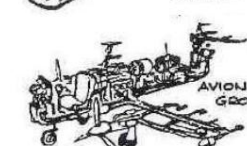
- Engine



- Flight behaviour

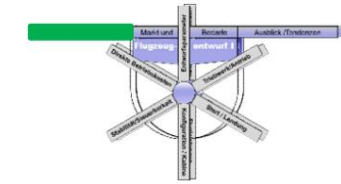


- Configuration and cabin



- Aircraft systems

The aircraft design considers the overall system “aircraft”



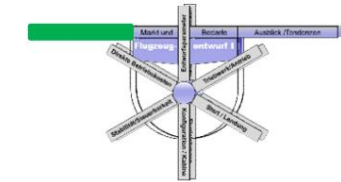
# Aircraft Design 1 - Table of Contents

- ✓ A Introduction to Preliminary Aircraft Design
- ✓ B Influence of important design parameters
- ✓ C Basics of drive technology
- ✓ D Mass and range
- ✓ E Take-off and landing
- ✓ F Aircraft configuration & cabin
- G Stability / Controllability and Tail
- H Direct operating costs
- I Basics of aerodynamic design

**FE I**

**FE II**





# Aircraft Design 2 - Table of Contents

**FE I**

I      **Basics of aerodynamic design**

J      **Weights, centre of gravity and roles on  
Floor**

**FE II**

K      **Basics of flight mechanical design**

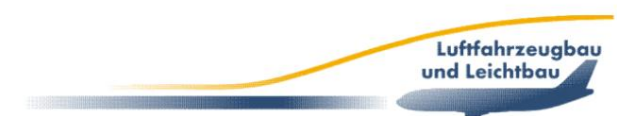
G      **Flight services**

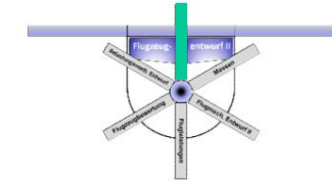
I      **Basics of load mechanics**  
Draft

**J(H) Direct operating costs // Aircraft valuation**

K      **Introduction to engineering**  
**Use of statistical methods**

**manuscript**





# D Basics of aerodynamic design

## Overview

### Basics of aerodynamic design

#### D.1 Wing design

##### D.1.1 Wing geometry

##### D.1.2 Wing area

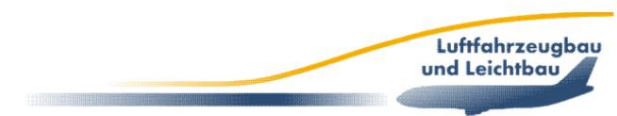
##### D.1.3 Wing profile

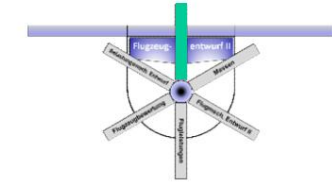
###### D.1.3.1 Influence of profile geometry parameters

###### D.1.3.2 Influence of Reynolds number/roughness

**Manuscript** D.1.3.3 Influence of the Mach number

###### D.1.3.4 Profile developments





# D Basics of aerodynamic design

## Overview

### Basics of aerodynamic design

#### D.1 Wing design

##### D.1.4 Influence of the wing plan

**FE1**

###### D.1.4.1 Wing plan parameters

D.1.4.2 Wing lift distribution

D.1.4.3 Wing moment

D.1.4.4 Wing resistance

D.1.4.5 Influence of wing extension

D.1.4.6 Influence of escalation

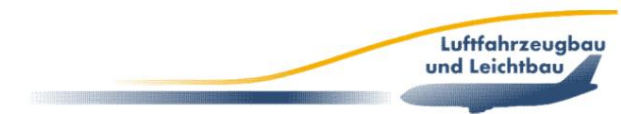
D.1.4.7 Influence of the arrowhead

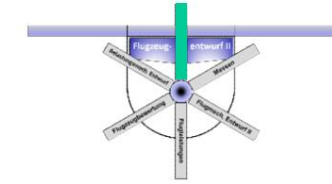
D.1.4.8 Influence of torsion

D.1.5 Optimal wing design

D.1.6 Lift characteristics during take-off and landing

D.1.7 Wings without lift aids





# D Basics of aerodynamic design

## Overview

### Basics of aerodynamic design

#### D.1 Wing design

##### D.1.8 Wings with lift aids (HA)

###### D.1.8.1 Lift change by different flap systems Leading edge lift aids

###### D.1.8.2

###### D.1.8.3 Profile values for different HA systems

###### D.1.8.4 Thrust-assisted high-lift devices

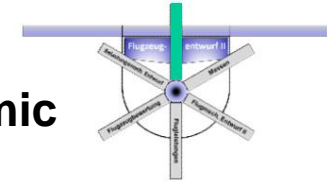
##### D.1.9 Drag increase during flap deflection

###### D.1.9.1 Profile drag at flap deflection

###### D.1.9.2 Induced resistance at KI deflection

###### D.1.9.3 Interference resistance at KI deflection

##### D.1.10 Moment change during flap deflection



## D Basics of aerodynamic design Overview Basics of aerodynamic design D.2

Fuselage design D.3 Tail design D.4 Engine

installation D.5 Landing

gear installation D.6 Wave drag

D.7 Interference drag D.8 Aircraft

drag polars

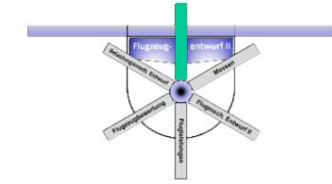
D.8.1 Quadratic drag polars D.8.2 Trim drag

D.8.3 Total drag balance

D.8.4 Ground effect D.8.5 Take-off and

landing polars



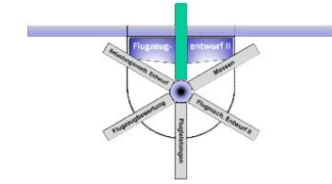


# D Basics of aerodynamic design

## 1. Wing design

- **Task of the wing: Generating the lift forces necessary to balance the mass forces of the aircraft.**
- **Wing:**
  - 50% share of the total drag of the aircraft
  - 30% share of the aircraft's operating empty weight
  - Up to 60% share of development costs
- **Transport quality is largely determined by the aerodynamic and structural quality of the wing → optimal wing design is essential!**

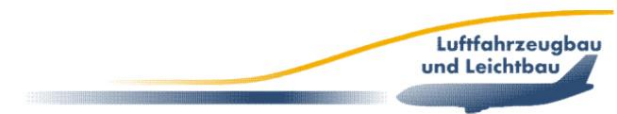


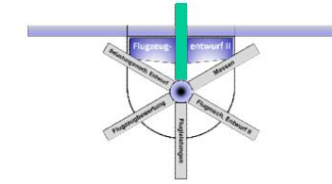


# D Basics of aerodynamic design

## 1. Wing design

- Complex optimization task: –
  - aerodynamically optimized wing with
    - minimal weight and
    - minimal production and maintenance costs
- Requirements of a flight mission vary greatly and partly contradictory:
  - Cruise flight: sufficient lift and as little drag as possible at high Mach numbers
  - Landing: maximum lift with large Resistance
  - Start: maximum lift with minimum Resistance

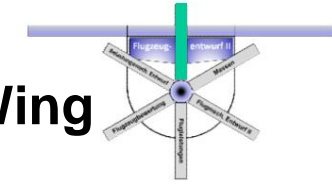




# D Basics of aerodynamic design

## 1. Wing design

- Also required:
  - good stalling behaviour Ѽ safe operation in High angle of attack range
  - Flight characteristics: Requirements for the maneuverability of the aircraft Ѽ impact on the Wing control surface concept



## D Basics of aerodynamic design 1.1 Wing geometry • Wing design:

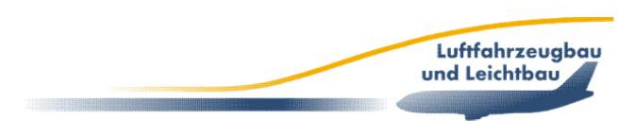
**Determination of the geometric and structural shape of the wing in all details**

- First floor plan with the parameters

- span, • depth distribution and • sweep,

**from this follow the sizes**

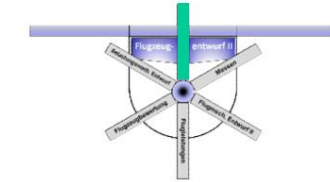
- Wing area, • aspect ratio and
- taper

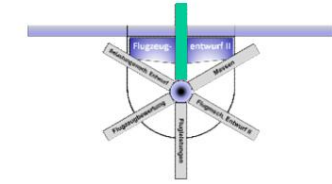


# D Basics of aerodynamic design

## 1.1 Wing geometry

- Wing design also in third dimension with
  - profile variable across the wingspan – torsion distribution – size and position of the ailerons – high-lift aids and spoilers with their corresponding activation kinematics or Travel trajectories
  - location of the spar bridges
- Define these parameters
  - Wing stiffness –
  - Tank capacity –
  - Location of main landing gear.





# D Basics of aerodynamic design

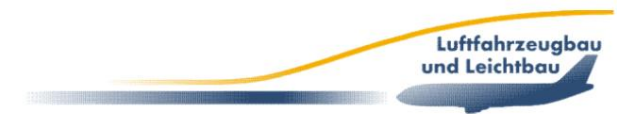
## 1.1 Wing geometry

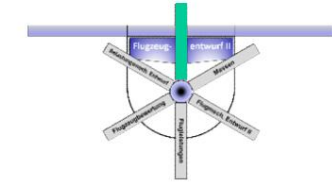
The geometric diversity of the profiles alone, which is characterized by characteristic parameters such as

- Profile thickness and
- Thickness reserve,
- Curvature and
- Arch reserve,
- Nose radius and
- Trailing edge angle

shows the complexity of describing a wing.

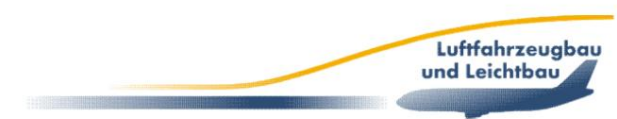
If the aircraft configuration provides for the engines and landing gear to be mounted on the wing, additional design features are added.

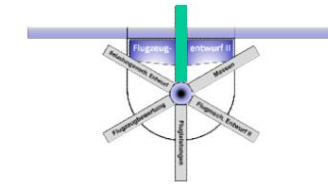




## D Basics of aerodynamic design 1.2 Wing area

- Most important parameter of the wing geometry: wing area
- This largely determines the performance of the aircraft.
- Characteristic reference dimension: wing loading
- Wing loading influences:
  - the approach speed and the landing distance with landing weight,
  - the take-off distance with take-off weight,
  - the initial cruise and service ceiling altitude and
  - the economical cruise speed,
- Surface loading is one of the main design parameters





# D Basics of aerodynamic design

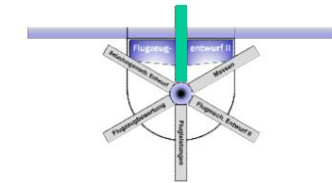
## 1.2 Wing area from approach speed

- From a given maximum approach speed,  
Given a landing weight and a given airfield altitude, a first specification for the wing loading follows:

$$G A_L c_{A_{\text{Max}}} = \frac{\rho}{2} v^2 F$$

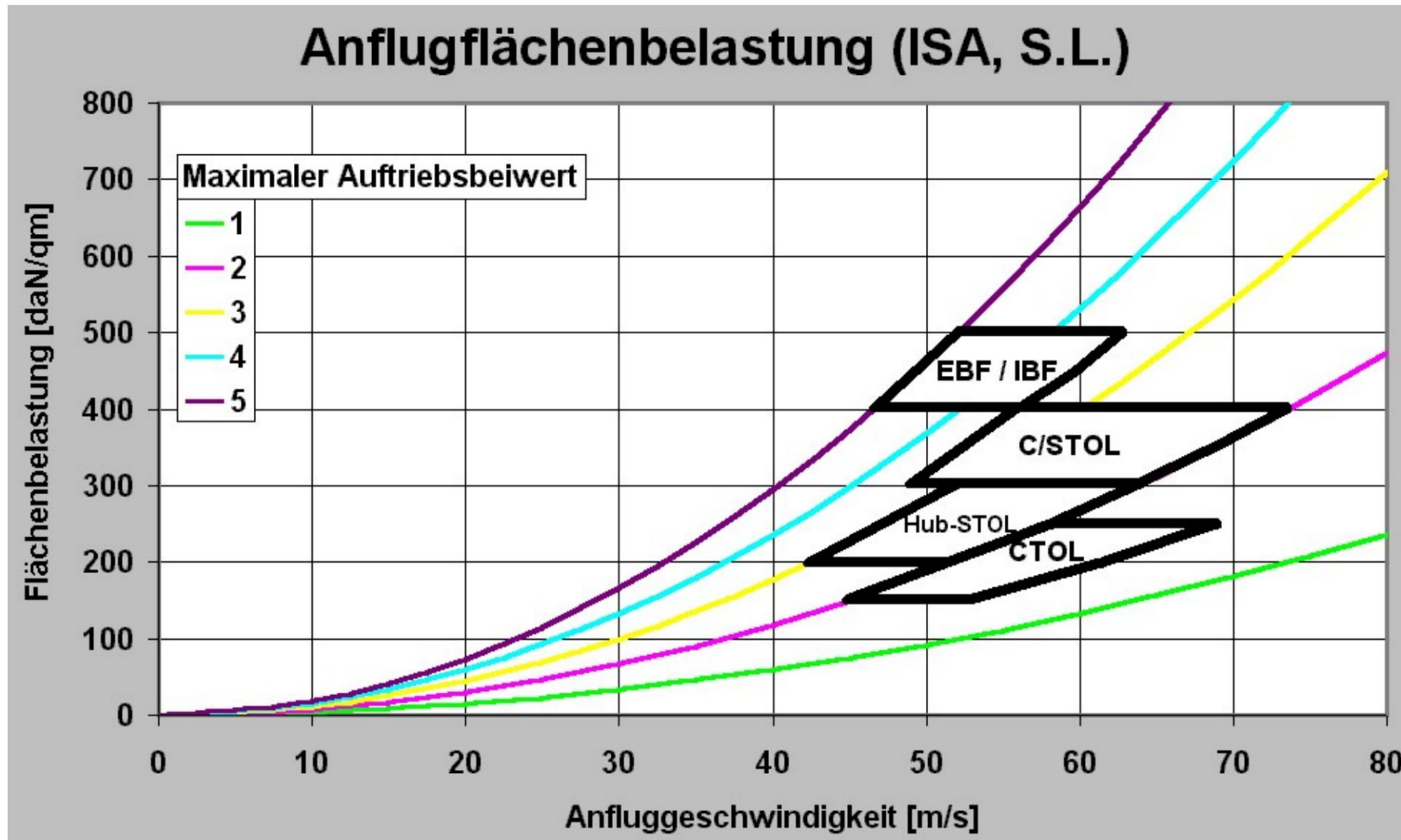
- Taking into account the company regulation that the Approach speed must be 30% higher than the Minimum speed for unaccelerated flight is thus:

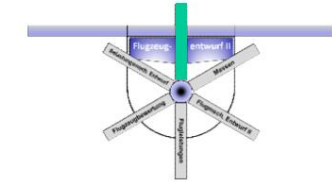
$$\frac{\rho G_L}{F} = \frac{\rho}{2} c_{A_{\text{Max}}} \cdot \frac{v_{\text{min}}^2}{1.3^2} \approx 0.6 \frac{\rho}{2} c_{A_{\text{Max}}} \cdot v_{\text{min}}^2$$



# D Basics of aerodynamic design

## 1.2 Wing area from approach speed





# D Basics of aerodynamic design

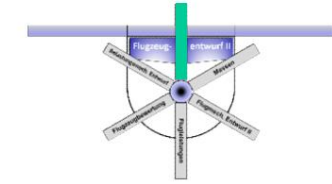
## 1.2 Wing area from approach speed

- The landing or approach surface loading can be converted into the departure surface loading using the fuel factor  $k$ , because

$$\frac{G_L}{G_A} = \frac{G_L}{G_A} \cdot k$$

- Related to the wing area and transformed:

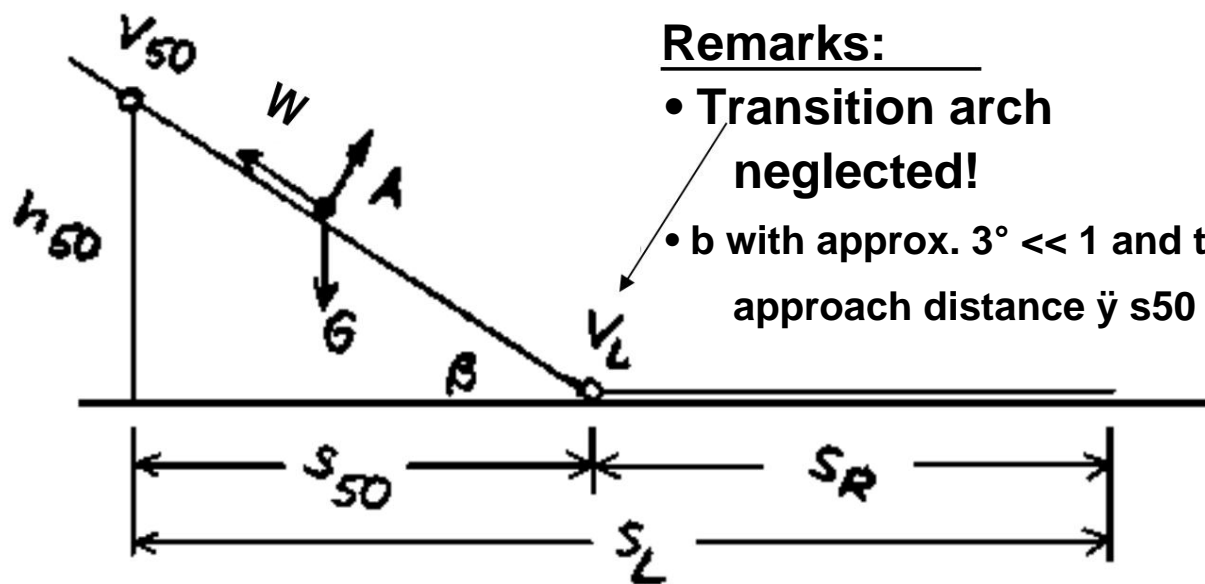
$$\frac{F_A}{F_{Max}} = \frac{F_L}{F_{Max}} \cdot \frac{1}{k}$$

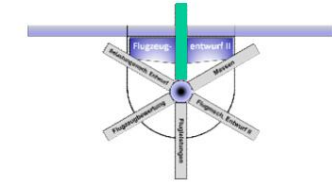


# D Basics of aerodynamic design

## 1.2 Wing area from approach speed

- The approach speed is a decisive factor for the landing distance. • This consists of 1.) the approach distance from 50 ft flight altitude to touchdown and 2.) a braking distance. • Legislator requirement: The calculated landing distance to cover the influences of weather and runway conditions may only be 60% of the design landing distance





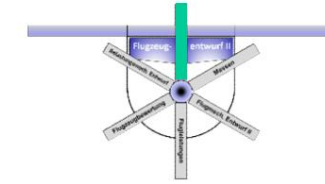
# D Basics of aerodynamic design

## 1.2 Wing area from landing distance

- If the approach distance ( $s_{50}$ ) is calculated using the energy method, the shape and length of the transition curve can be disregarded. The following applies:
  - The sum of kinetic and potential energy at the obstacle point (50 ft) is completely converted into kinetic energy by the aircraft drag, which corresponds to the **touchdown speed** at altitude “0” when touching down.
  - **Thrust S is set to “0” (see chapter Takeoff & Landing)**

$$\begin{aligned}
 & \frac{G v_{L50}^2}{2g} \quad G h_{L50} \quad \frac{G v_{LL}^2}{2g} \quad \ddot{y} \ddot{y} \ddot{W} \ddot{s} \ddot{y} \quad 50 \quad L \quad G s_{L50} \\
 & \frac{s_{50}}{2g} = \frac{v_{50}^2}{2g} + \frac{v_L^2}{2g} - \frac{h_{50}}{2g} + \frac{1}{2g} \ddot{y}_{50}^2 \quad L \quad \frac{H_{50}}{\ddot{y}_L}
 \end{aligned}$$

$\uparrow$   
 $S_{50} = S_2 + S_3$



# D Basics of aerodynamic design

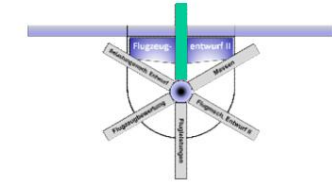
## 1.2 Wing area from landing distance

- At 50ft altitude, fly at the given approach speed (must be 30% higher than minimum speed)
- For the touchdown speed, the legislator specifies a safety margin on the minimum speed for the load factor during recovery and for weather-related disruptions of 20% for 2- and 3-engine aircraft and 15% for aircraft with more than 3 engines.

This results in the approach distance for 2-engine aircraft, for example

$$s_{50} = \frac{v_{min}^2}{2 \cdot G \cdot \ddot{y}_L} \cdot \ddot{y}_{1.3}^2 \cdot 1.2 \cdot \frac{\ddot{y}_L^2 \cdot \ddot{y}_{\infty}^2 \cdot \frac{h_{50}}{G}}{\ddot{y}_L} \cdot \frac{L}{Fg} \cdot \frac{1}{4 \cdot \ddot{y}_L \cdot \ddot{y}_{\infty} \cdot c_{A_{Max}}} \cdot \frac{H_{50}}{\ddot{y}_L}$$

with  $v_{min}^2 = \frac{2G}{F} \cdot \frac{L}{c_{A_{Max}}}$  from the equilibrium relationship.



**D Basics of aerodynamic design 1.2 Wing area from landing distance • The braking distance is also dependent on the landing area load. It is obtained by evaluating the differentials**

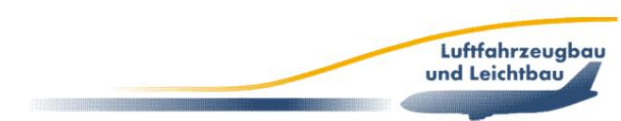
$$\frac{ds}{v \ddot{y} \ddot{y} \ddot{y} \ddot{y}} = \frac{ds}{v dt} \text{ and } b$$

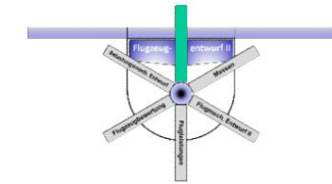
$$\frac{dv}{\ddot{y}}$$

engl

with the relationship

$$s_R = \frac{v^0}{v_L} \frac{dV}{\ddot{y} \ddot{y} \ddot{y} \ddot{y}}$$





# D Basics of aerodynamic design

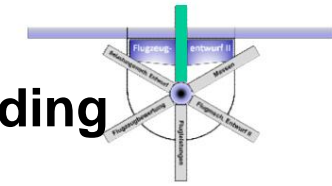
## 1.2 Wing area from landing distance

- Assumption: braking deceleration (resistance, braking, rolling friction, thrust reversal) is approximately constant along the rolling path
- This results in the following for a 2-engine aircraft:

$$s_R = \frac{v_L^2}{2B_m} \cdot \frac{G_L}{F_c} \cdot \frac{1.2^2}{A_{Max} \cdot b_m}$$

and thus for the 60% increased landing distance

$$s_L = \frac{1.6s_R}{0.6} = \frac{\frac{1}{F_c} \cdot \frac{1}{A_{Max}} \cdot \frac{1}{b_m} \cdot \frac{1.44}{H_{50}} \cdot \frac{1}{0.6}}{\frac{1}{G_L} \cdot \frac{1}{4} \cdot \frac{1}{G_L}}$$

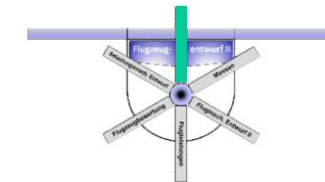


## D Basics of aerodynamic design 1.2 Wing area from landing distance • Solution for maximum landing area loading results in:

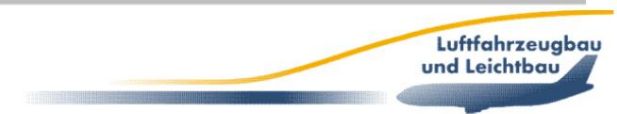
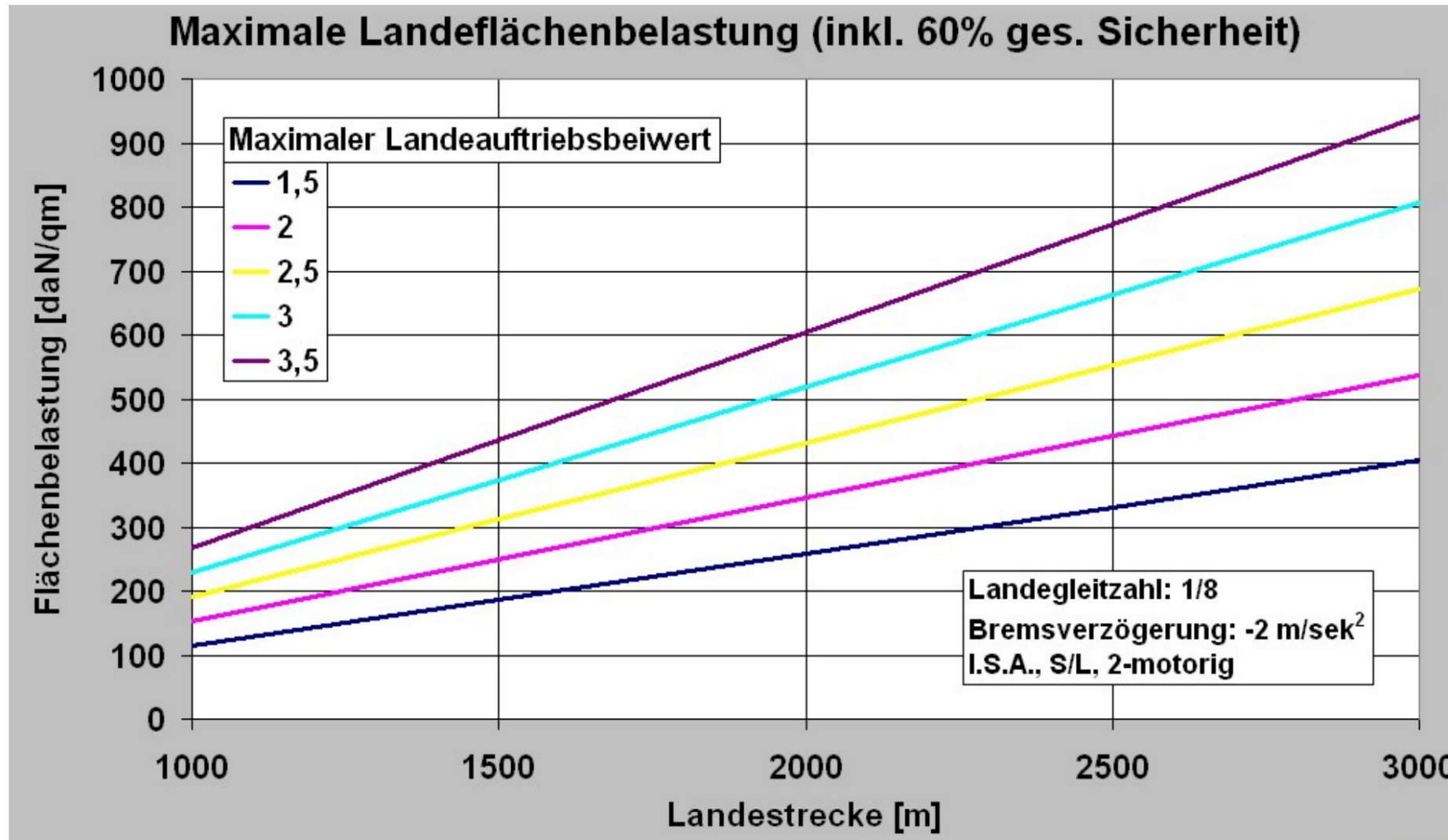
$$\frac{\frac{0.6 \cdot s_L}{H_{50}}}{\frac{1}{F_{Max}} + \frac{1}{c_{A_{Max}} \cdot G_L^4}} = \frac{1.44}{b_m}$$

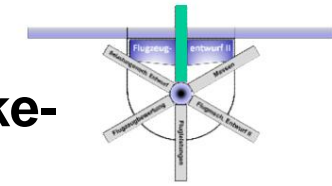
- Calculation of the take-off surface load from the Landing area loading using the fuel factor:

$$\frac{G_A}{F_{Max}} = \frac{G_L}{F_{Max}} \cdot k$$



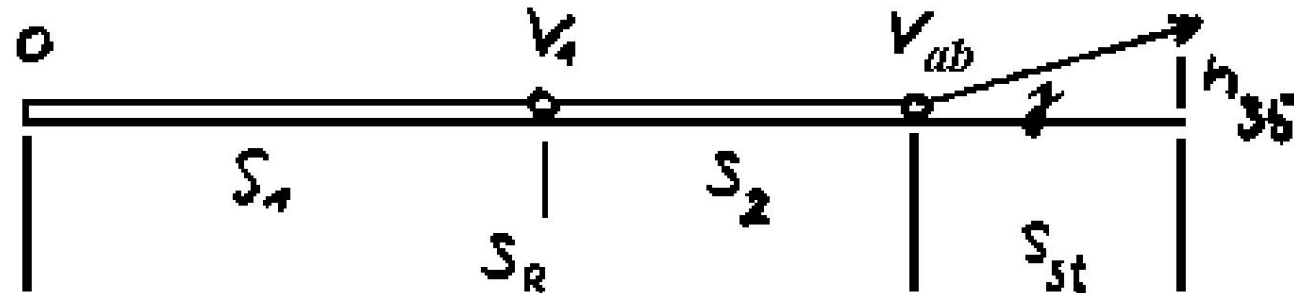
## D Basics of aerodynamic design 1.2 Wing area from landing distance





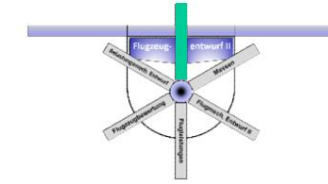
## D Basics of aerodynamic design 1.2 Wing area from take-off distance

- The required take-off distance also significantly influences the maximum wing loading.
- A simplified take-off distance calculation gives its limit value.



- Take-off roll distance s<sub>R</sub> from integration of the speed during accelerated rolling to the take-off point:

$$s_R = \frac{\ddot{y}}{b} \int_0^{v_{\text{from}}} v^2 dv = \frac{v_{\text{from}}^2}{2B}$$



# D Basics of aerodynamic design

## 1.2 Wing area from take-off distance

- Assumptions: constant average acceleration and take-off speed ~15% above minimum speed (relevant vMU & vMCG not yet known at this stage)
- The square of the take-off speed is:

$$v_{\text{from}}^2 = \frac{G}{F} \cdot \frac{2 \cdot 1.15}{c_{A_{\text{Max}}}}^2$$

- For the rolling distance, this means:

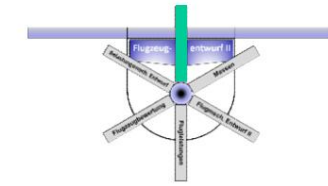
$$s_R = \frac{v_{\text{away}}^2}{2B} = \frac{1.32}{c_{A_{\text{Max}}} \cdot b} \cdot \frac{G}{F}$$

Remark:

vMU = Minimum Unstick Speed

vMCG = Minimum Control Speed Ground





# D Basics of aerodynamic design

## 1.2 Wing area from take-off distance

- Assumption when estimating the average rolling acceleration: Total installed thrust  $S$  up to a decision speed  $v_1$ ; then with residual thrust after failure of one engine  $S \cdot (1 - 1/z_{TW})$  until take-off:

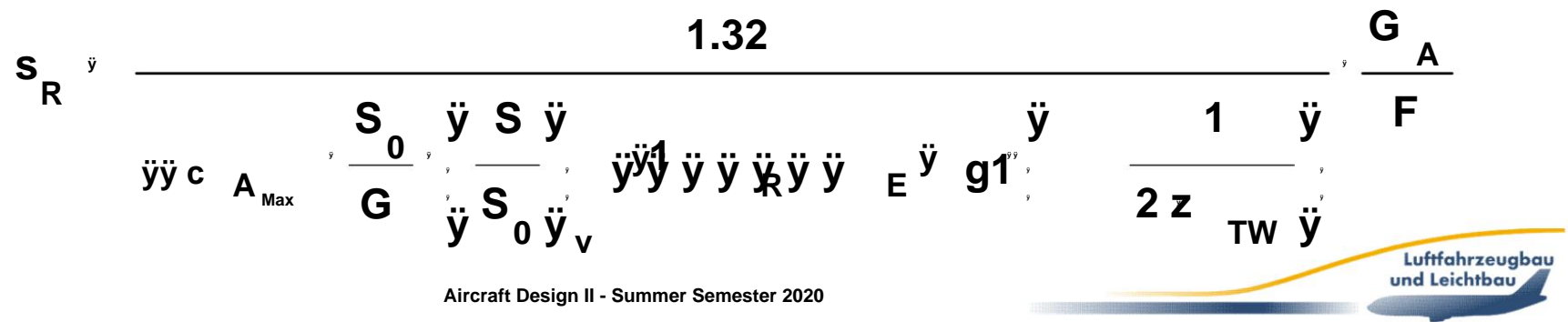
$$\frac{\ddot{y}_{SW}}{G}$$

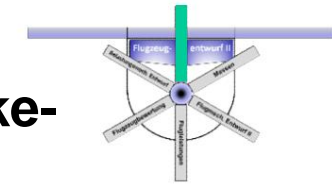
$\ddot{y}_{bg}$

- Average acceleration:

$$b_m = \frac{S_0}{G} \cdot \frac{\ddot{y}_S}{\ddot{y}_v} \cdot \frac{1}{2z_{TW}}$$

- Total rolling distance:





## D Basics of aerodynamic design 1.2 Wing area from take-off distance

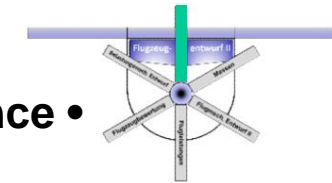
- $\ddot{y}R$  : Loss from rolling and aerodynamic drag  $\ddot{y}E$  :
- Inlet pressure loss
- $zTW$  the number of engines
- $(S/S_0)v$  : average effective thrust ratio in the rolling acceleration phase at an average speed. • This is approximately calculated at constant acceleration) of the take-off 1 2

• The thrust factor  $(1 - 1 / 2.zTW)$  is determined by averaging the thrust

at the start of take-off ( $S_0$ ) and after engine failure  $S_0$ .  $(1 - 1/zTW)$  , because  $\ddot{y} \ddot{y}$   
 $\ddot{y} \ddot{y} \ddot{y} \ddot{y} 2$

$$\frac{s_0}{e_{TW}} = \frac{1}{\sqrt{\frac{1}{2} + \frac{1}{zTW}}}$$

Luftfahrtbau  
und Leichtbau



## D Basics of aerodynamic design 1.2 Wing area from take-off distance •

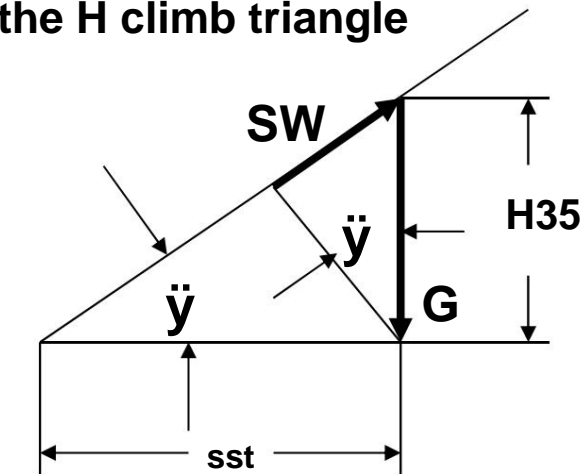
The climb distance is defined by

reaching an obstacle height of 35 ft and results from the H climb triangle

to  $\frac{H}{s_{st}} = \tan \alpha$

- With the weight-related thrust surplus after failure of a Engine

$$\frac{H}{s_{st}} = \frac{35}{s_{st}}$$



$$\sin \alpha = \frac{SW}{G} = \frac{s_{st}}{G}$$

$$\frac{S_0}{G_{A0}} = \frac{S}{G} = \frac{\sin \alpha}{\cos \alpha} = \frac{\ddot{y}_1}{\ddot{y}_{Ez}} = \frac{1}{e_{TW}}$$

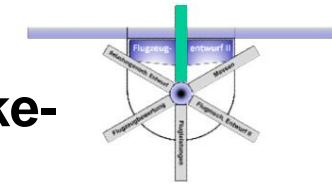
- It follows:

$$s_{st} = \frac{H_{35}}{\tan \alpha} = \frac{35}{\tan \alpha}$$

$$\arcsin \frac{H_{35}}{s_{st}} = \alpha$$

$$\frac{S_0}{G_{A0}} = \frac{s_{st}}{S} = \frac{\ddot{y}_1}{\ddot{y}_{Ez}} = \frac{1}{e_{TW}}$$



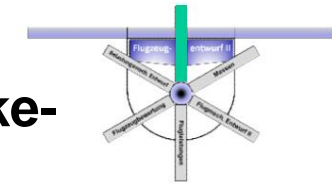


## D Basics of aerodynamic design 1.2 Wing area from take-off distance • After applying some trigonometric rules, the climb distance is:

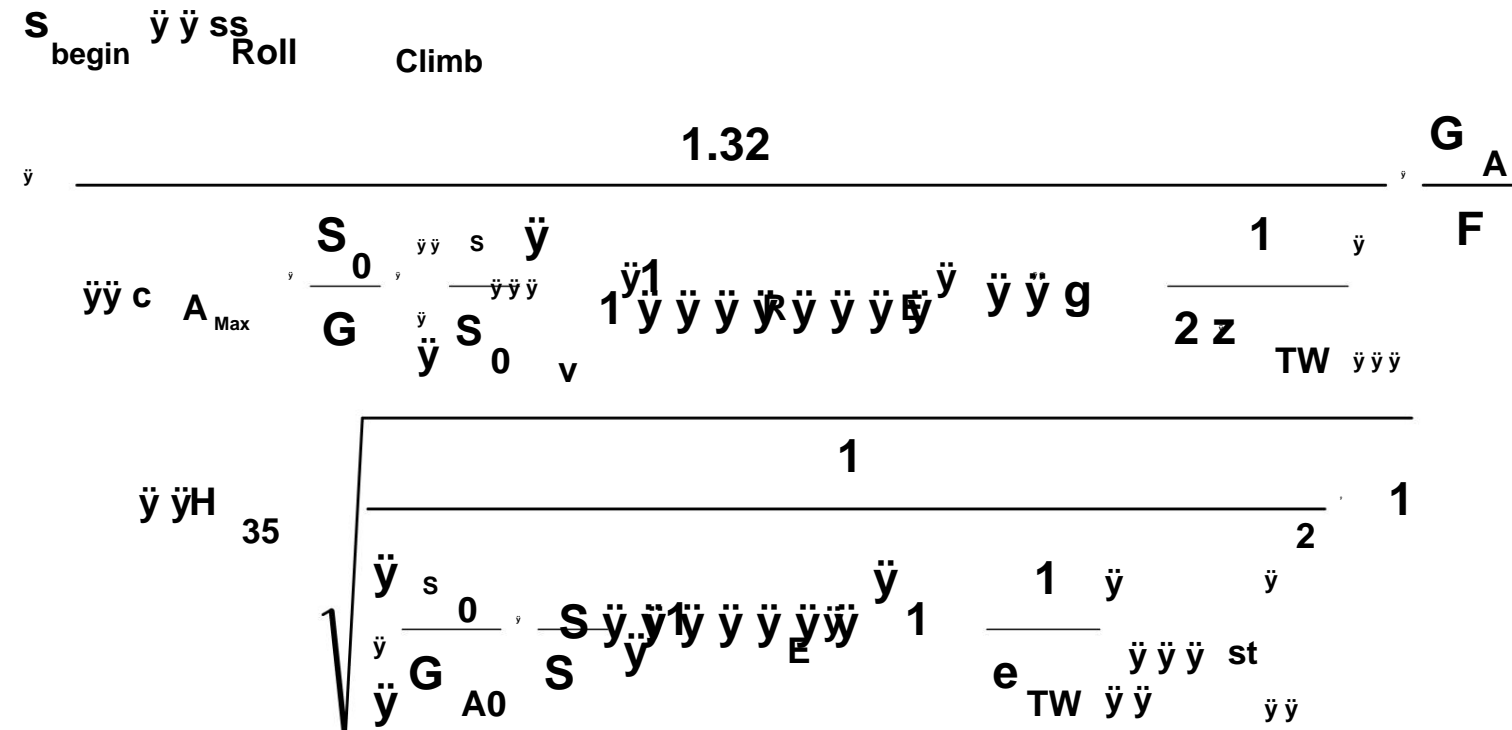
$$s_{st} = \frac{H}{G_{A0}} \cdot \sqrt{\frac{1}{e_{TW}}}$$

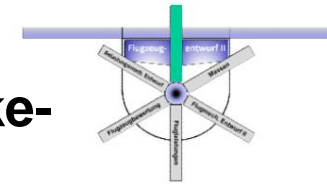
The diagram shows a right-angled triangle with the hypotenuse labeled  $H$ . The vertical leg is labeled  $G_{A0}$  and the horizontal leg is labeled  $e_{TW}$ . The angle at the bottom-left vertex is labeled  $\alpha$ .

- The climb distance is therefore not dependent on the wing loading dependent!



## D Basics of aerodynamic design 1.2 Wing area from take-off distance • The sum of roll and climb distance is thus





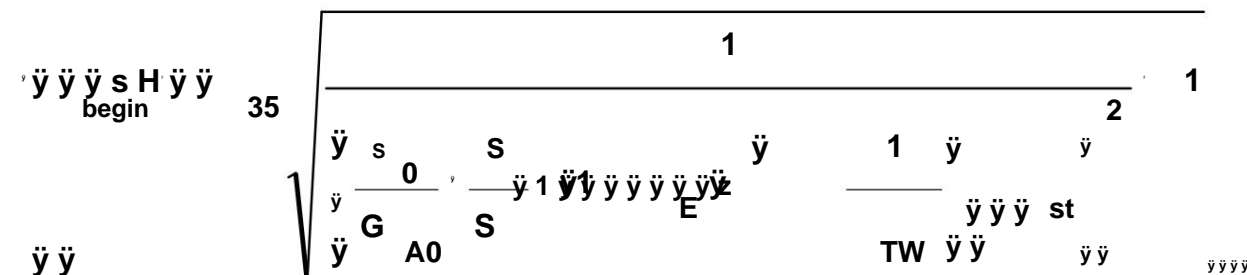
## D Basics of aerodynamic design 1.2 Wing area from take-off distance • Take-off distance

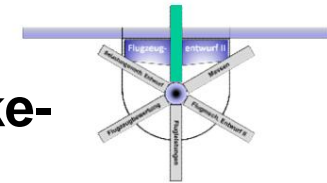
is the sum of take-off roll and climb distance

- The wing loading only contains the term for the rolling distance
- A linear function is obtained between the maximum Wing loading and total take-off distance

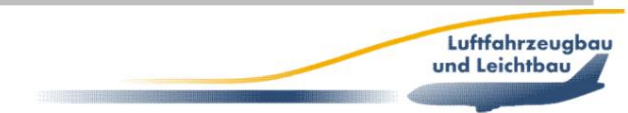
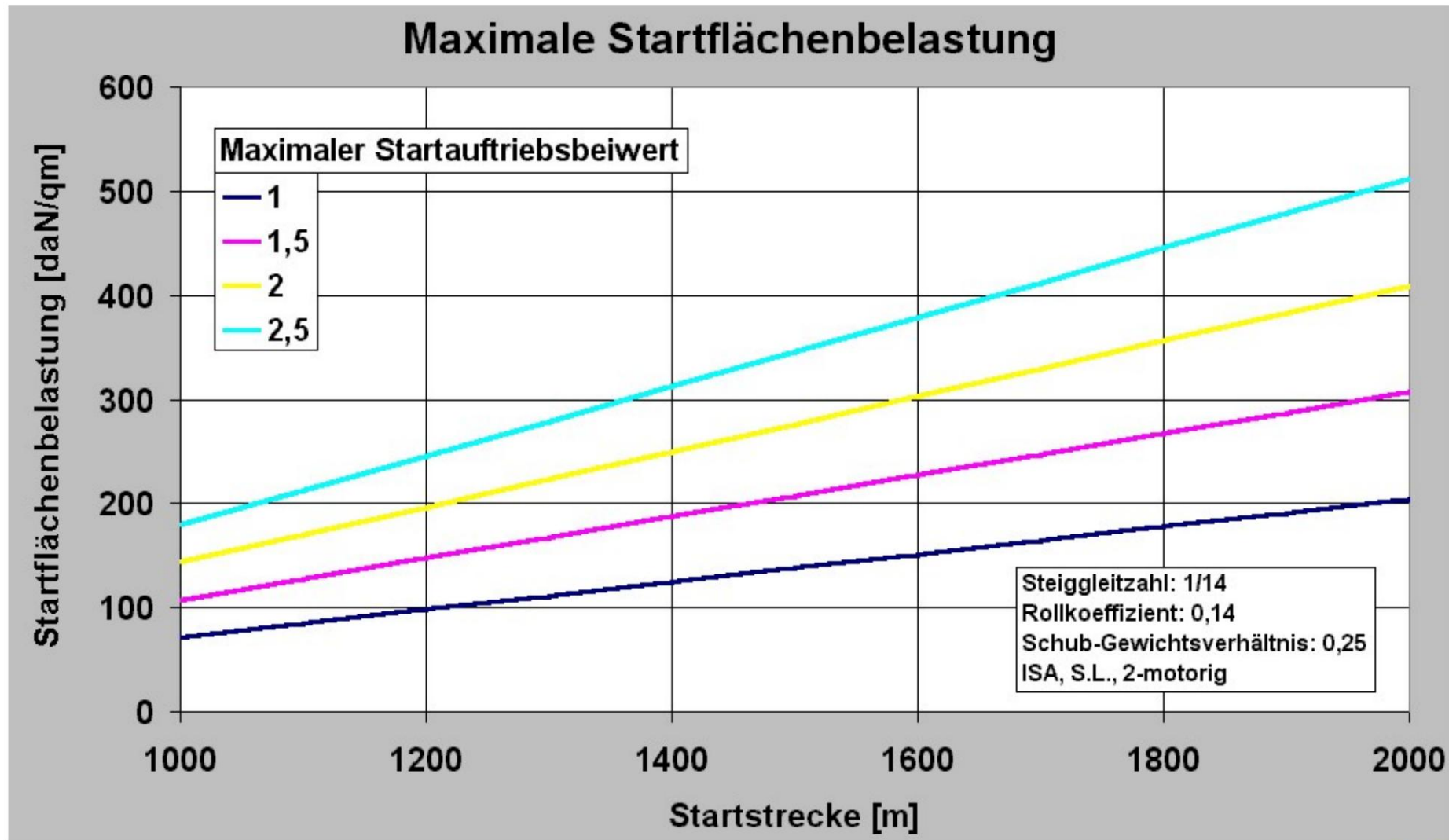
$$\frac{G}{F} = \frac{c_A}{A_{Max}} = \frac{G}{1.32} = \frac{s_0}{\frac{G}{s_0} + \frac{v}{2E}}$$

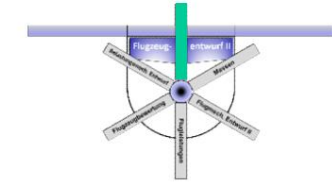
$$y = \frac{1}{TW}$$





## D Basics of aerodynamic design 1.2 Wing area from take-off distance





# D Basics of aerodynamic design

## 1.2 Wing area from range

- For cruising flight, the wing should be set to a minimum glide ratio

- There are two opposing

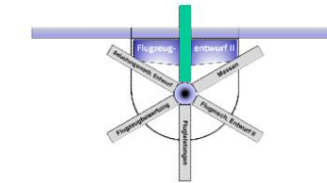
tendencies here:

- As the wing area increases, the air flow around it  
Area larger and the resistance of the wing increases.
  - As the area increases, the cruise lift coefficient also  
decreases and thus the induced drag decreases  
considerably (quadratic dependence!).

- An optimization task must therefore be completed in order to  
determine an optimal wing area for cruising flight.

# D Basics of aerodynamic design

## 1.2 Wing area from range

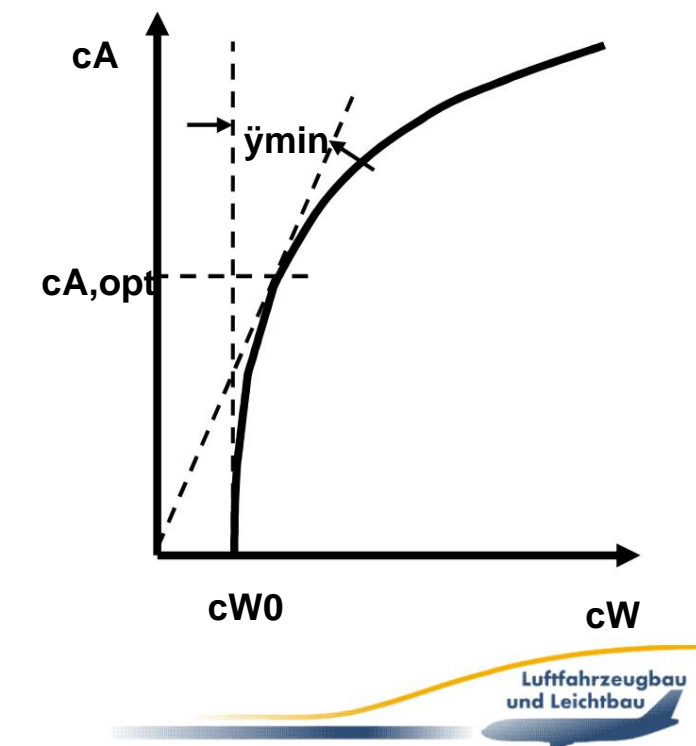


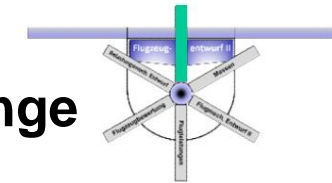
- Assumption: quadratic approach for the resistance polar of the aircraft

- The drag coefficient is

$$\frac{c_A^2}{e} = c_{W0} + \frac{c_W}{c_A}$$

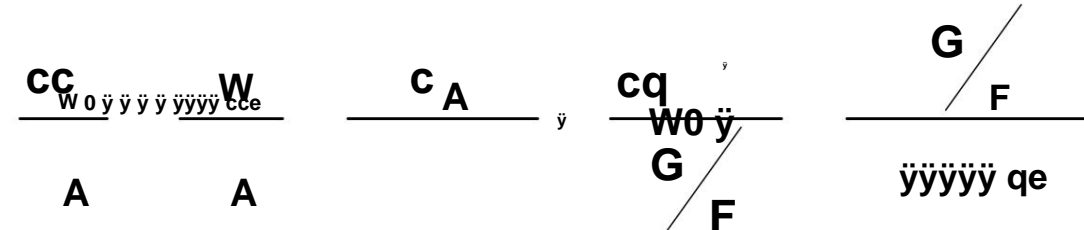
- The zero drag coefficient  $c_{W0}$  describes the  $c_A$ -independent Resistance component
- The second term describes the buoyancy-dependent drag component
- $e$  is the Oswald factor - a correction factor for the influences of a non-elliptical lift distribution, wave resistance and other non-constant components (e.g. interference resistance)





## D Basics of aerodynamic design 1.2 Wing area from range

- Equilibrium of buoyancy and mass forces and extended polar approach with  $cA$  to determine  $\ddot{y}$  result in

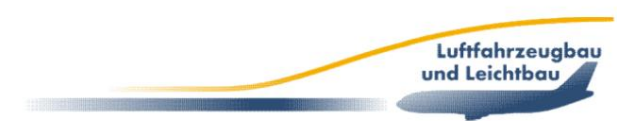


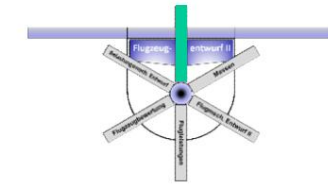
- Zeroing the derivative after the surface loading

$$\frac{\ddot{y} \frac{c_w}{c_A} \ddot{y} \ddot{y} \ddot{y} 0}{\ddot{y} G / F} = \frac{\frac{cq w_0 \ddot{y}}{2}}{\ddot{y} G / F \ddot{y} q} = \frac{1}{\ddot{y} \ddot{y} \ddot{y} e}$$

leads to optimum glide ratio surface loading

$$\frac{\ddot{y} G / \ddot{y} F_{opt}}{2} = \sqrt{\frac{\ddot{y} \ddot{y} \ddot{y} e v_c w_0}{2}}$$





# D Basics of aerodynamic design

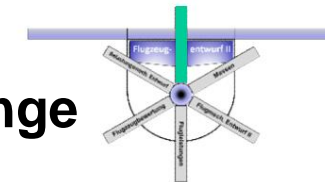
## 1.2 Wing area from range

- Representation over the Mach number  $Ma$  (defined as flight speed  $Ma = v/a$  relative to the speed of sound):

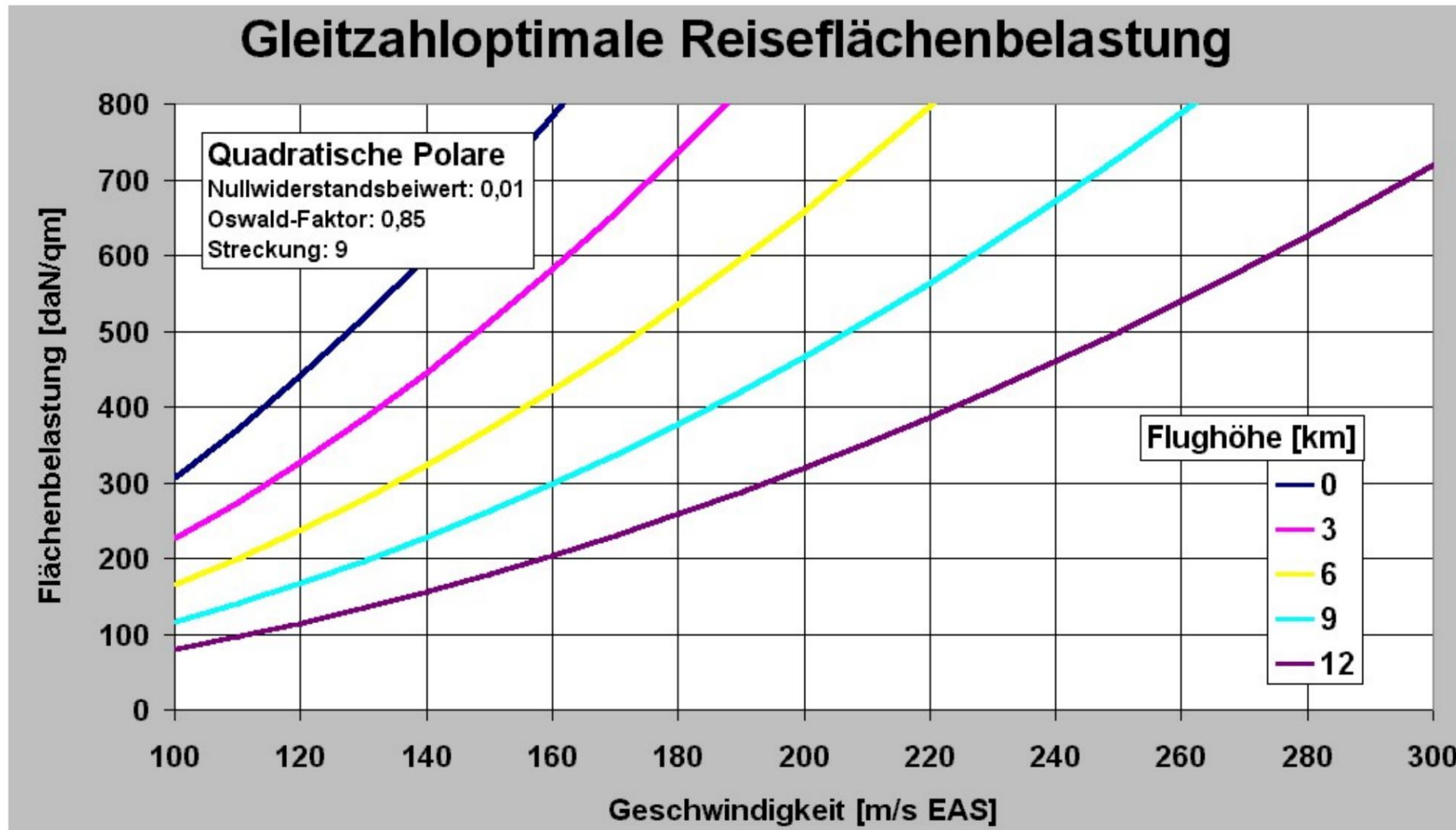
$$\frac{\ddot{y}G}{F_{\text{opt}}} = \frac{\ddot{y}}{2} Ma \frac{ac^2}{w_0} \sqrt{\frac{e}{\ddot{y}G_m}}$$

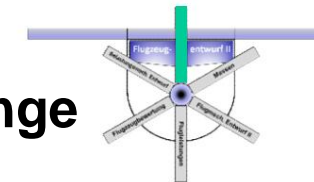
- The surface load derived in this way corresponds to an average Wing loading  $G_m/F$  in cruise flight, which is determined at the mean Flight mass  $G_m$  results in  $\frac{\ddot{y}G_m}{F_{\text{opt}}} = 0.5 \ddot{y}_A G_C$
- The corresponding take-off surface loading  $G_A/F$  is therefore

$$\frac{\ddot{y}G_A}{F_{\text{opt}}} = \frac{\ddot{y}G_m}{F_{\text{opt}}} \cdot \frac{1}{1 + \frac{G_K}{G_A}} = \frac{\ddot{y}G_m}{F_{\text{opt}}} \cdot \frac{1}{1 + 0.5} = \frac{\ddot{y}G_m}{F_{\text{opt}}} \cdot \frac{1}{1.5}$$

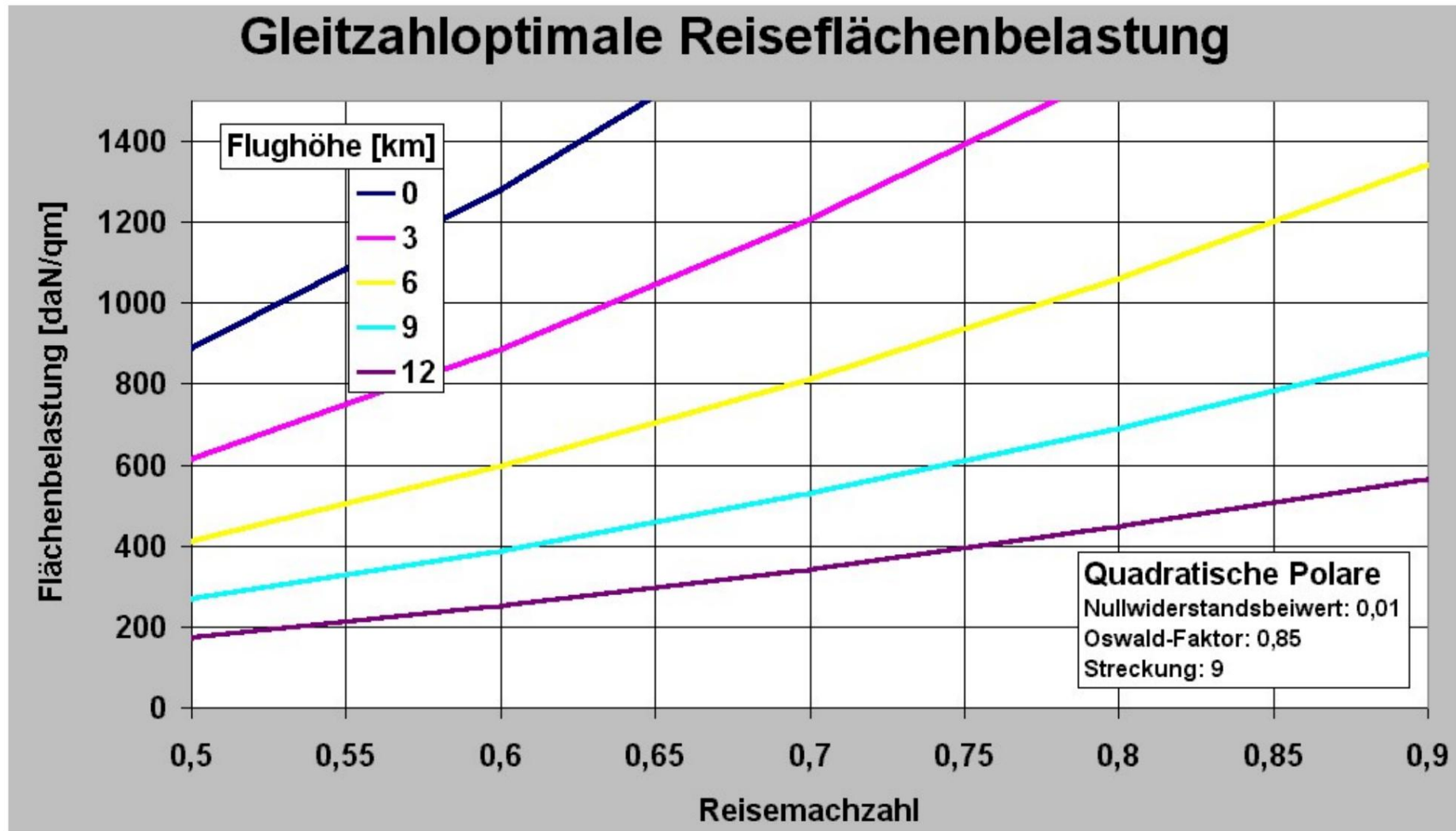


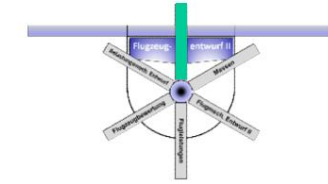
## D Basics of aerodynamic design 1.2 Wing area from range





## D Basics of aerodynamic design 1.2 Wing area from range



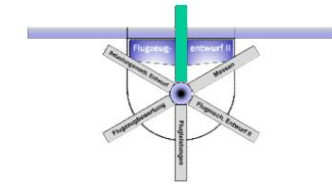


# D Basics of aerodynamic design

## 1.2 Wing area from range

- However, the assumption of a wing design with a minimum glide ratio is only one possible set of meaningful optimization criteria.
- It has been chosen here because of the simplicity of the statement.
- Better here would be, for example, assumptions on a design that minimizes consumption, emissions or operating costs.
- It is now the task of aircraft design to find a compromise for the wing size that – meets all the above requirements and – at the same time leads to a minimum operating cost.

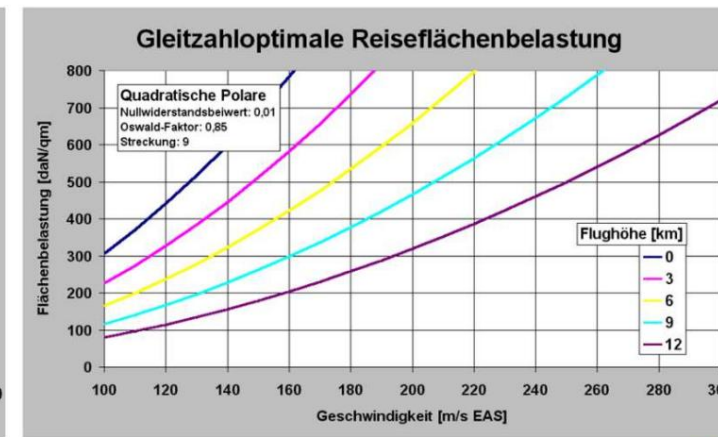
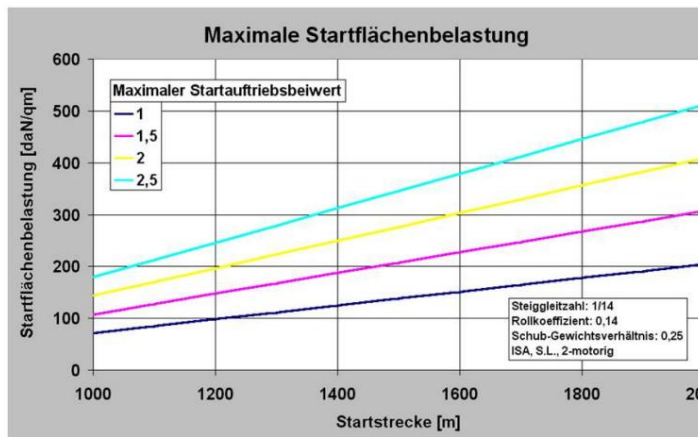
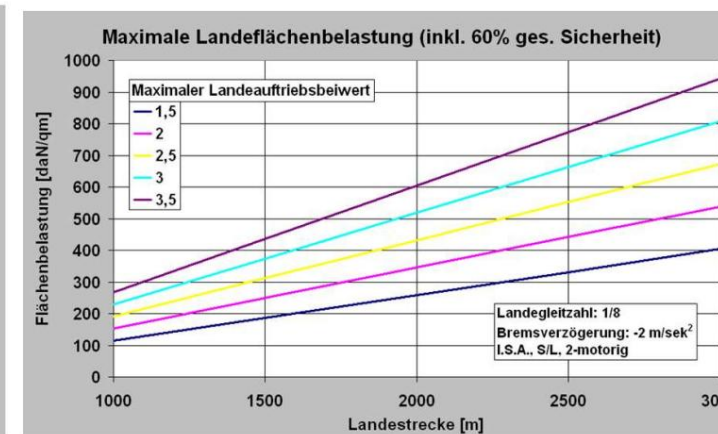
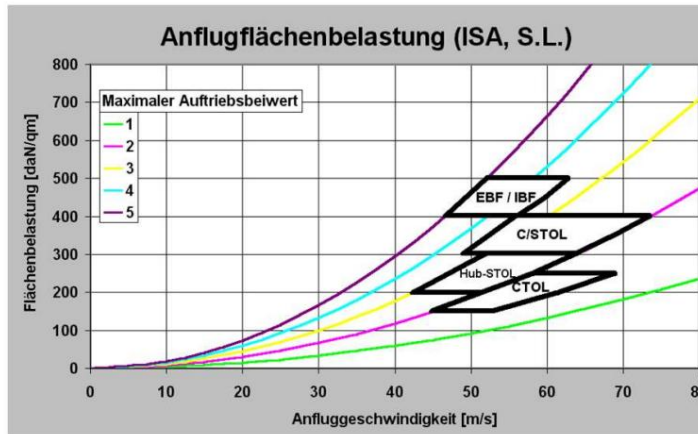


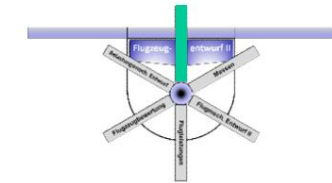


# D Basics of aerodynamic design

## 1.2 Wing area

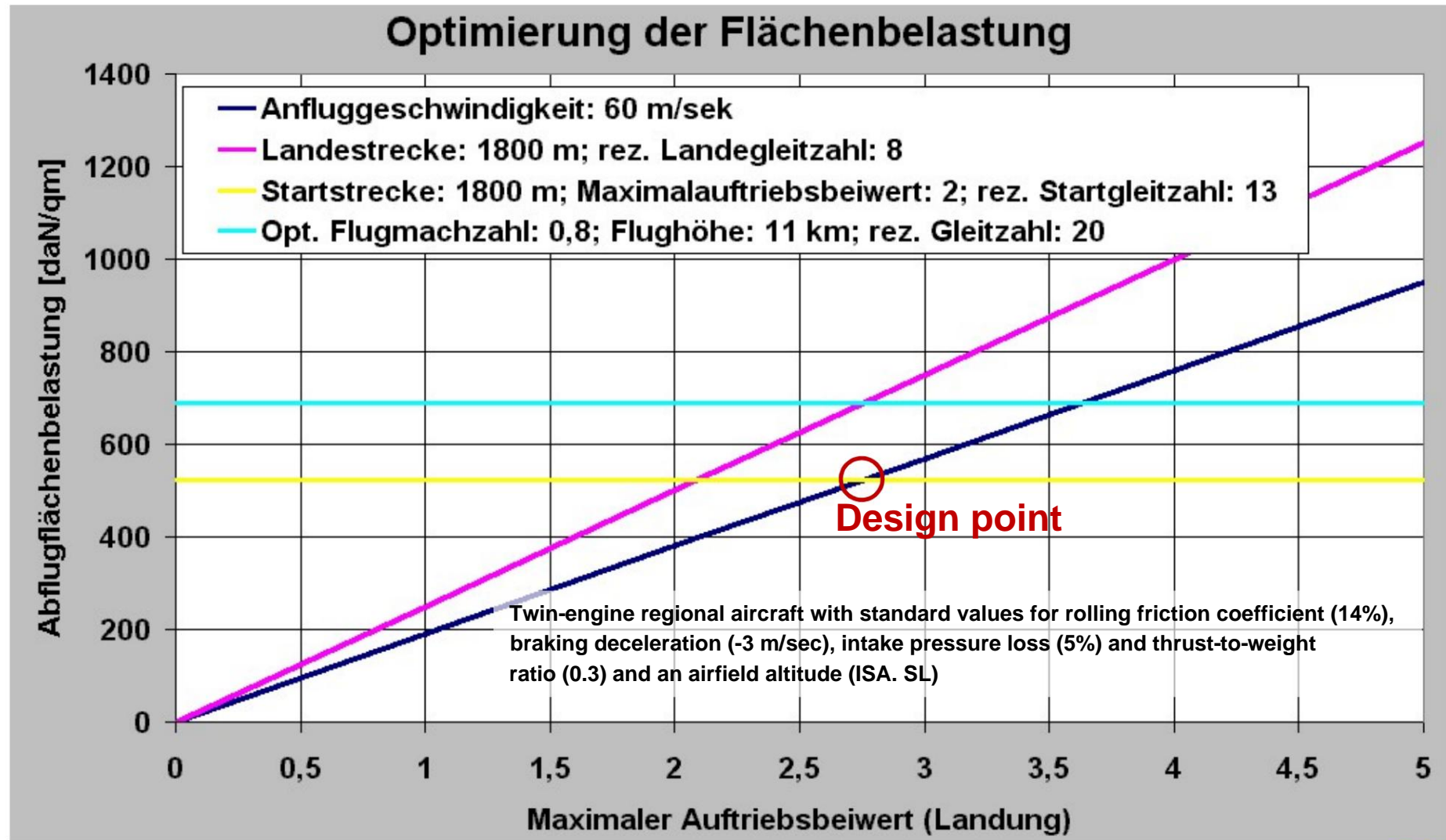
- The different surface loadings based on the Flight surface loading can be compared and the specified design parameters adjusted to compensate.

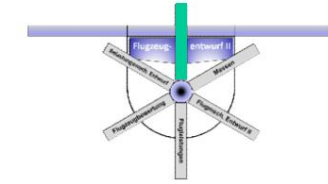




# D Basics of aerodynamic design

## 1.2 Wing area

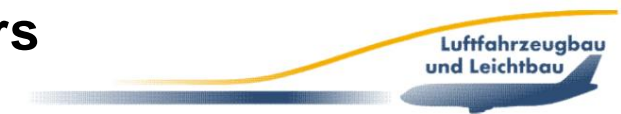


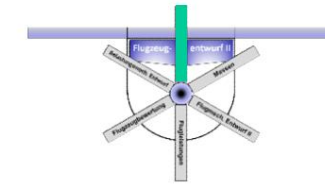


# D Basics of aerodynamic design

## 1.3 Wing profile

- The performance and behavior of the wing are largely determined by the selection of the wing profile.
- First: explanation of the system of basic profile properties for the NACA profile series - statements are largely applicable to modern profile variants.
- The requirements for the sash profile are diverse:
  1. Low drag over a wide lift range with the greatest possible profile thickness ( $\ddot{y}$  minimum wing mass)
  2. Large maximum lift
  3. Low torque
  4. Low pressure point movement
  5. Shock-free operation at the highest possible Mach numbers
  6. Low shock-induced resistance increase
  7. Drag increase only at high Mach numbers



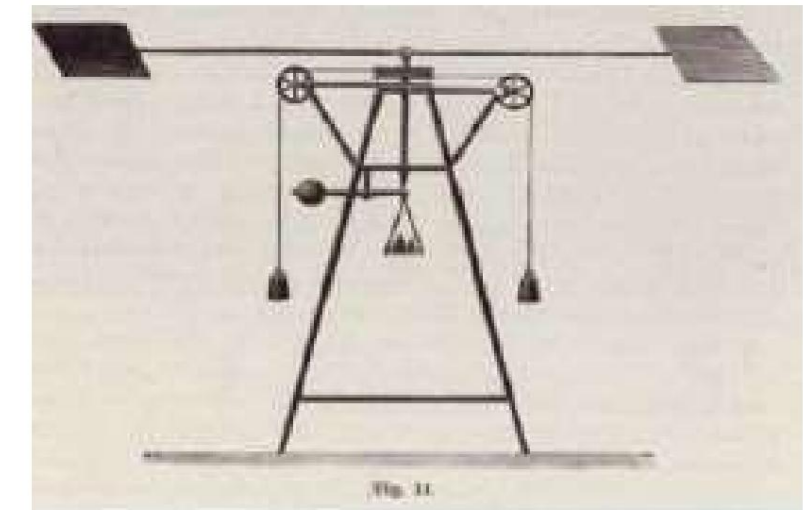
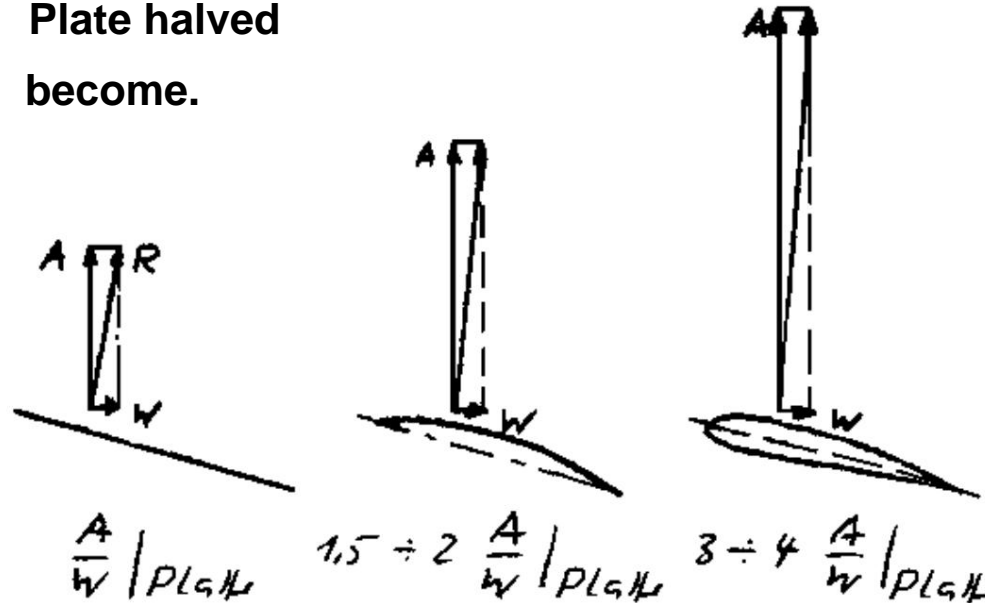


# D Basics of aerodynamic design

## 1.3 Wing profile

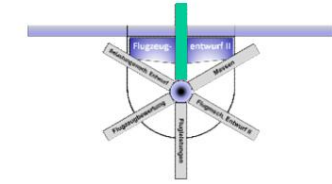
Otto Lilienthal had already recognised the effect of profiling on drag and used curved plates for his first wings. This made it possible to increase the glide ratio compared to a flat

Plate halved  
become.



Lilienthal's measuring apparatus

A further halving could be achieved by thickening the plate to a teardrop profile, whereby at the same time a rounded leading edge and a finite trailing edge angle could be realized and thus the maximum lift could be increased.

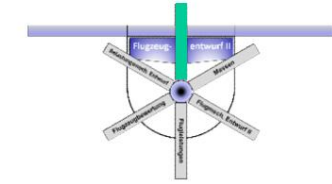


# D Basics of aerodynamic design

## 1.3 Wing profile

- Initially, the wing profiles developed unsystematically table based on the model of nature.
- For the first time, a catalogue with the geometric and aerodynamic descriptions was published in Göttingen, in which they were only numbered according to the date of their experimental creation.
- The first systematic approach was the Joukowsky profiles, whose geometric definition is based on the parameters thickness and camber ratio with a circular skeleton line and a vanishing trailing edge angle is reproducible. Technical utilization was not possible due to the delicate, thin trailing edge.
- The AVA-Göttingen then developed the Göttingen profile system from 1923 to 1927.



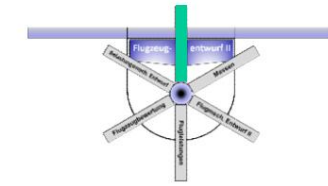


# D Basics of aerodynamic design

## 1.3 Wing profile

- A systematic, parametric study on aerodynamic behavior of profiles was carried out in the 1950s by NACA (predecessor of NASA).
- In a first series of profiles, the 4-digit profiles, the geometric definition was expanded compared to the Joukowsky profiles by the camber offset and the skeleton line composed of two parabolic arches:
- 1st digit of the designation is the curvature in % of the depth
- 2nd digit is the arching reserve in tenths of the depth
- 3rd & 4th digit is the profile thickness in %.
- The profile shape is achieved by overlaying the base profile with a skeleton line.

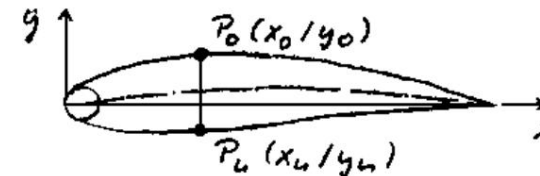




# D Basics of aerodynamic design

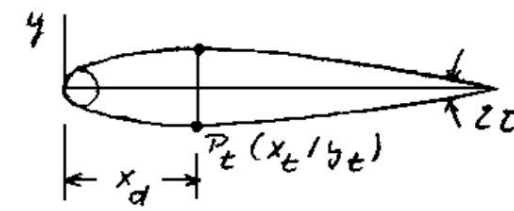
## 1.3 Wing profile

### Profile description NACA 4-digits



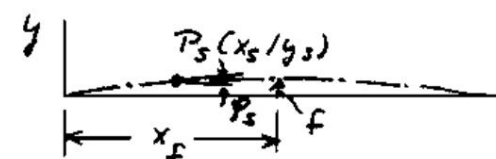
Gewölbtes Profil

=



Basisprofil  
(Dickenverteilung)

+

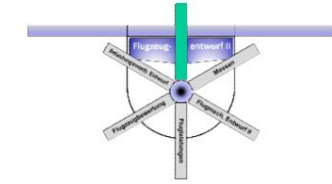


Skelettlinie (mean line)  
aus zwei Parabelbögen  
zusammengesetzt am  
Ort der größten Wölbung  
(für  $a = 1$ )

For profiles with moderate thickness and curvature

$$y_{o,u} \ddot{y} y \ddot{y} y \quad t \quad \text{with} \quad y \ddot{y} \ddot{y} \ddot{\bar{y}} \frac{1}{2} \ddot{y} y \ddot{y} \quad o \quad u \ddot{y} \quad \text{and} \quad 1 \ddot{y} \ddot{y} \ddot{\bar{y}} \frac{1}{2} \ddot{y} \ddot{y} y_{os} \quad us \ddot{y}$$



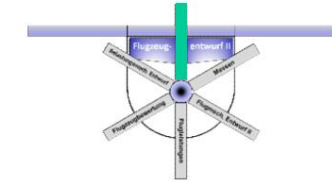


# D Basics of aerodynamic design

## 1.3 Wing profile

- Development was then more focused on specific desired properties:
  - DVL profiles and 8 other NACA series were created
  - Goal: Long laminar running distances, larger critical Mach numbers
  - Approach: large thickness reserve, pressure minimum far back
  - The most important is the NACA-6 series: profile drops and Skeleton line developed according to purely aerodynamic criteria
  - Specification of the desired distribution of the pressure difference between the top and bottom; starting point of the Pressure increase can be set variably over a wide range
  - Determination of the geometry of the skeleton line by calculation

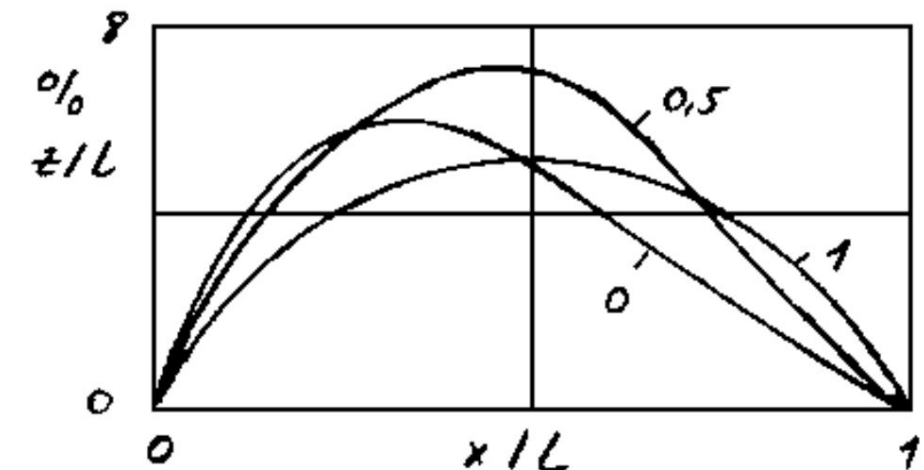
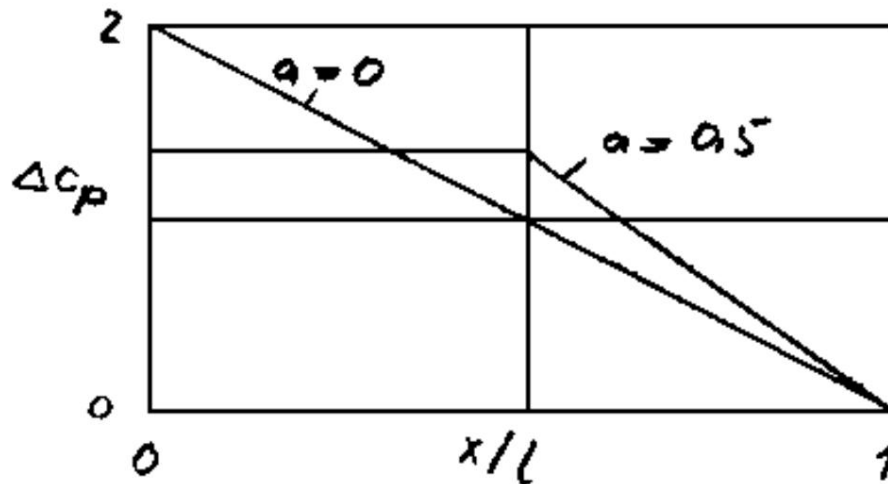


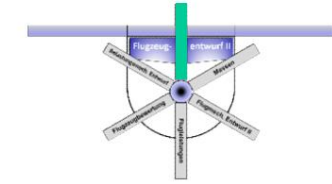


# D Basics of aerodynamic design

## 1.3 Wing profile

- To calculate the skeleton line, desired profile depths  $0 < x/l < a$  can be specified, up to which the velocity distribution of the upper and lower sides should be constant.
- The letter  $a$  in the profile name indicates this Point.  $a = 0.5$  means that up to half the profile depth there is an almost constant differential value of the pressure coefficient, which then drops to 0 up to the trailing edge.





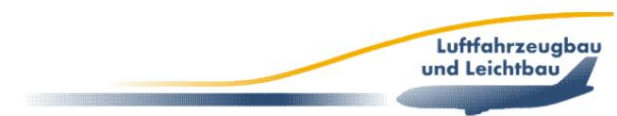
# D Basics of aerodynamic design

## 1.3 Wing profile

- From the designation of the example profile NACA 652 -315,  $a=0.5$   
The following features emerge:

Digit	Value	Meaning
1	6	serial number
2	5	Retention of the pressure minimum of the base profile at $ca = 0$ in tenths of the depth
3	2	$ca$ -range in tenths above and below $ca_{opt}$ , the favorable pressure gradient and low Resistance exists (half the height of the laminar cell)
4	3	$ca_{opt}$ in tenths (middle of the laminardelle)
5.6	15	Maximum thickness in % of depth

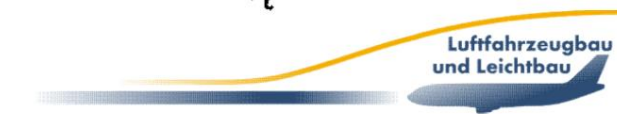
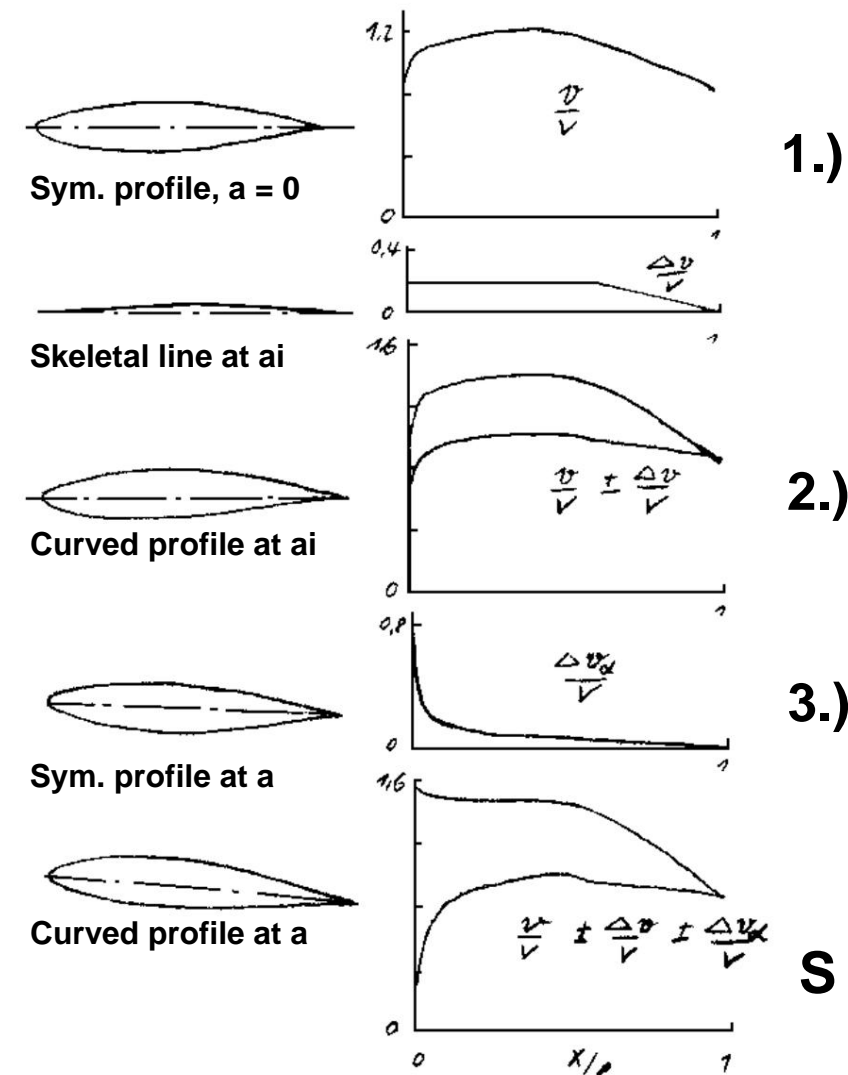
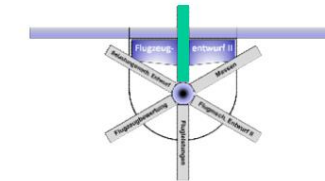
- The NACA profile catalogue (also Abbott/Doenhoff: Theory of Wing Sections) gives tabulated parameterized velocity distributions.

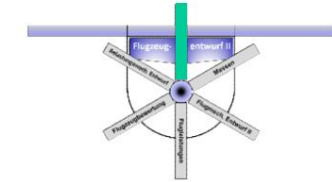


# D Basics of aerodynamic design

## 1.3 Wing profile

- The NACA profile catalogue
- Three speed quotients can be derived for the corresponding profile parameters, which make the speed and thus the pressure distribution calculable through superposition.
- Here,  $a_i$  stands for the ideal angle of attack, which corresponds to the design lift coefficient.





## D Basics of aerodynamic design 1.3 Wing profile

- Knowledge of pressure distribution necessary to assess
  - Lift characteristics of the profile
  - High-speed characteristics of the profile
  - Separation behaviour of the boundary layer
  - Moment behaviour (torsional load of the wing, tail unit size) •

Theoretical calculation is very complex •

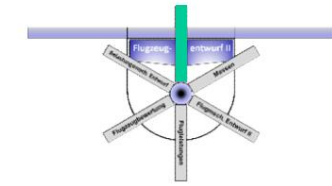
Simpler: Determination of the pressure coefficients  $c_p$  from given Velocity distribution for base profile and additional velocities due to camber and inclination

$$c_p = \frac{p_{\text{total}} - p_{\text{static ambient}}}{q} = \frac{\frac{1}{2} \rho v_x^2}{q}$$

p: local static pressure  $\bar{p}$  :  
static ambient pressure  $\bar{v}$  :  
flow velocity

q: dynamic  
pressure  $v_x$  : local speed





# D Basics of aerodynamic design

## 1.3 Wing profile

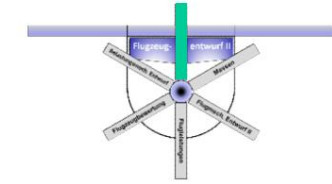
- Speed quotient from profile catalogues (e.g. Abbott, Doenhoff: Theory of Wing Sections) or by means of numerical methods (Computerized Fluid Dynamics - CFD).  
Today mostly numerical methods (e.g. xfoil by M. Drela)
- Determination of the lift coefficient from knowledge of the pressure division
- Lift  $A$  of a wing element of width  $b$  and wing depth  $l$  with the pressure difference between upper and lower sides

$$A = \int_0^l \frac{1}{2} \rho u^2 b dy$$

- Pressure distributions ( $p_o$ ,  $p_u$ ) are obtained using the definition of the pressure coefficient:

$$C_p = \frac{p_u - p_o}{\frac{1}{2} \rho u^2}$$

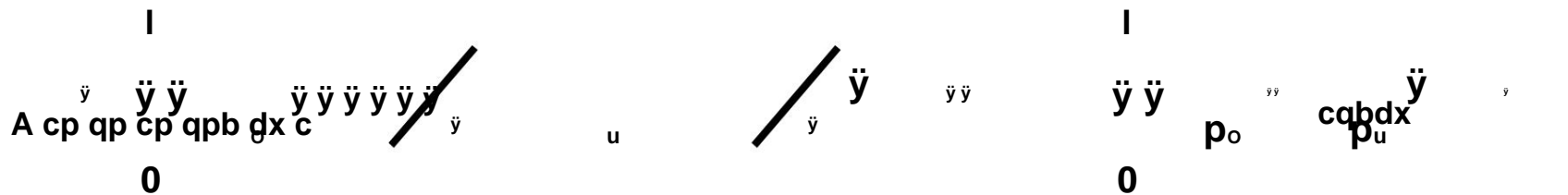




# D Basics of aerodynamic design

## 1.3 Wing profile

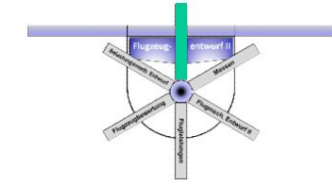
- Lift integral for a wing strip of constant depth (e.g. wind tunnel model!) is then:



- The definition of the lift coefficient follows

$$c_a = \frac{A}{q F} \int_{y_0}^{y_c} \frac{q b y}{y^2 q b l} \left[ \frac{p_o}{p_u} - \frac{c d \ddot{x}}{p_u} \right] dy$$

$$= \frac{C_D}{2} \int_{y_0}^{y_c} \frac{y^2}{y^2 + C_D^2} dy$$



# D Basics of aerodynamic design

## 1.3 Wing profile

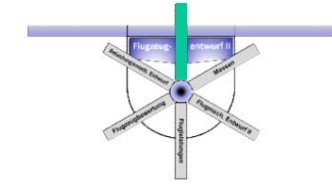
- **Attention:** Strictly speaking, integration only applies to infinitely thin profiles! Actually, the direction cosine of the first contour derivative should be taken into account, since the pressure acts perpendicularly on the local surface.
- The lift coefficient of a profile is obtained by integrating the difference between the pressure distributions on the top and bottom sides:

$$c_a = \frac{1}{l} \int_{x_0}^l \frac{\partial p}{\partial y} dy$$

- The moment coefficient around the profile nose is determined from the multiplying the local pressure force with the effective dimensionless lever arm:

$$m_{x=0} = \frac{1}{l} \int_{x_0}^l \frac{x}{l} \cdot d \frac{\partial p}{\partial y} dy$$





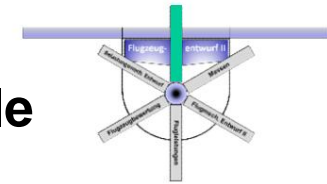
## D Basics of aerodynamic design 1.3 Wing profile • The dimensionless

**position of the resulting lift force**

**(pressure point) results from the center of gravity formation**

**by means of the moment equilibrium around the profile nose ( $x/l = 0$ ):**

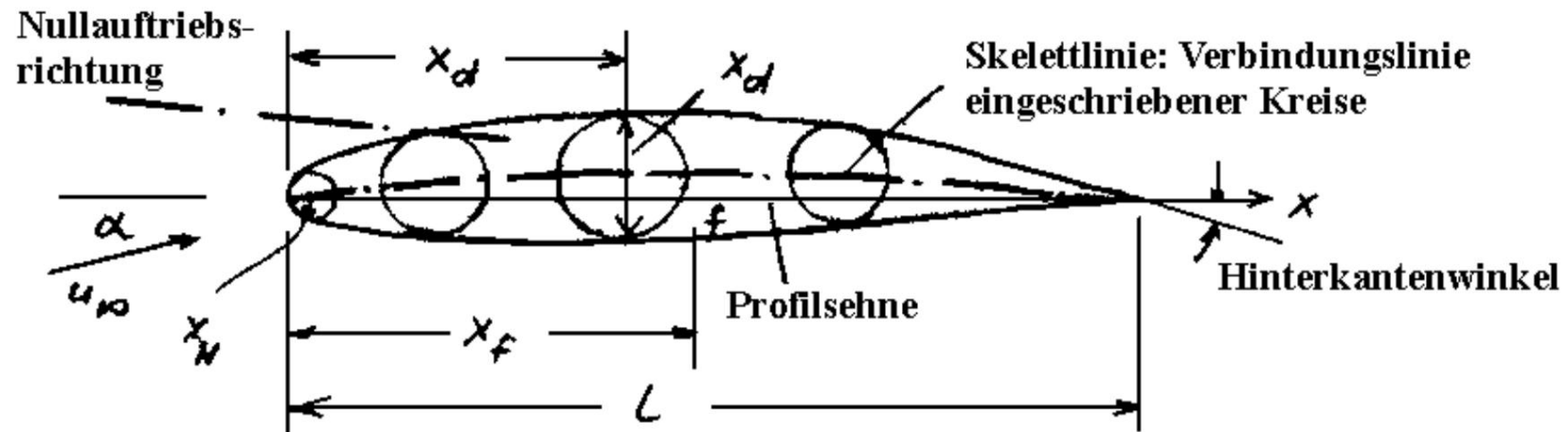
$$\frac{\frac{x_D}{l}}{l} \cdot \frac{x_{0,l}}{l} \cdot \frac{c_m,x,0}{c_a} = \frac{\frac{x_p}{l}}{l} \cdot \frac{d}{l} \cdot \frac{cd}{l}$$



## D Basics of aerodynamic design 1.3 Wing profile • Profile catalogues:

Collection of geometric and aerodynamic data from systematically investigated profile series

- General geometric definition with its terms:



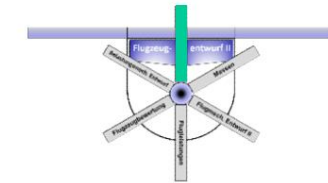
$\frac{d}{l}$  relative film thickness;

$\frac{x_d}{l}$  relative thickness reserve

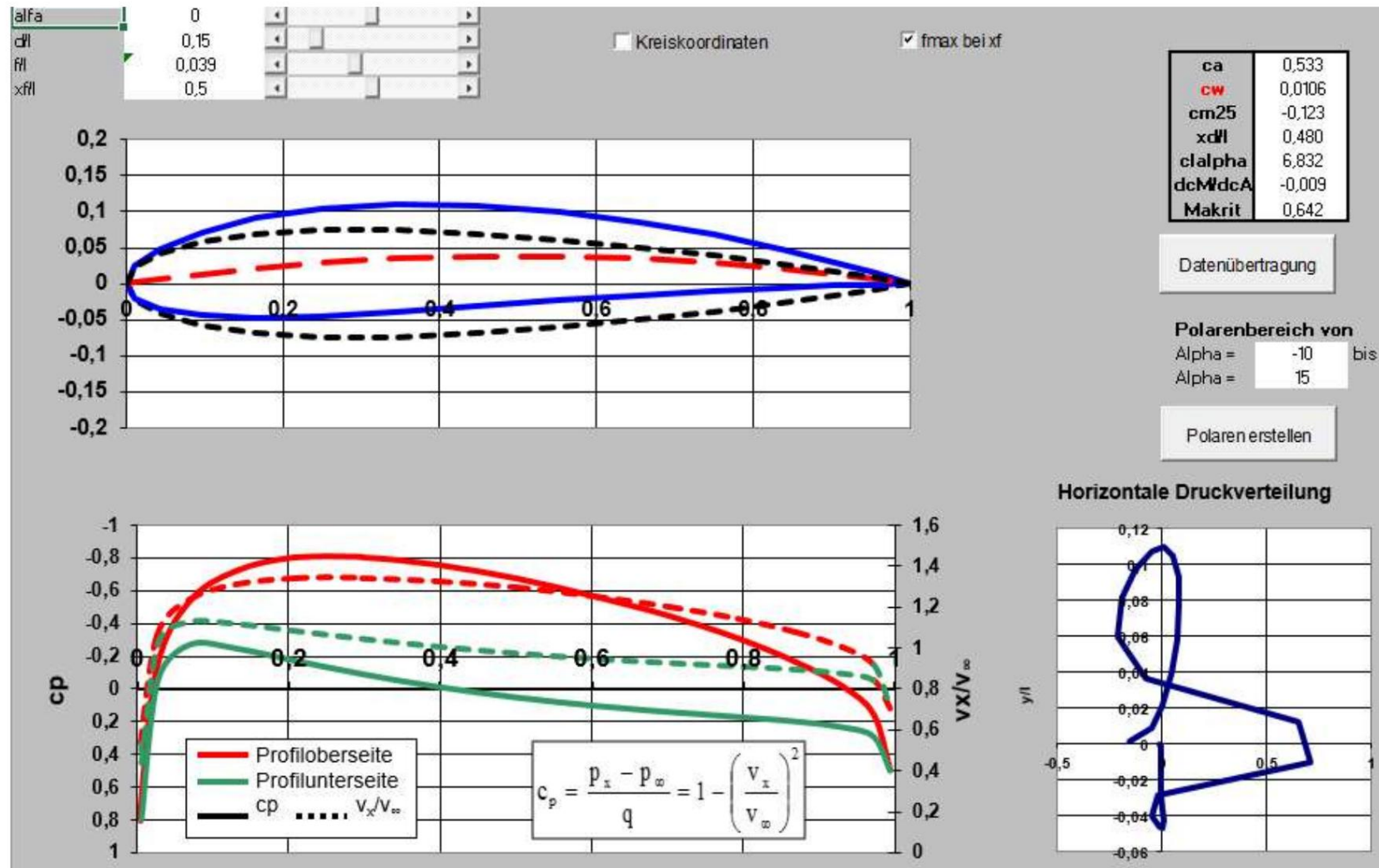
$\frac{f_l}{l}$  relative curvature;

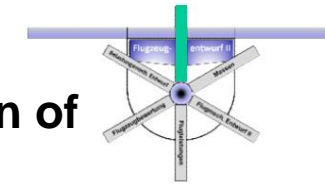
$\frac{x_f}{l}$  relative camber offset



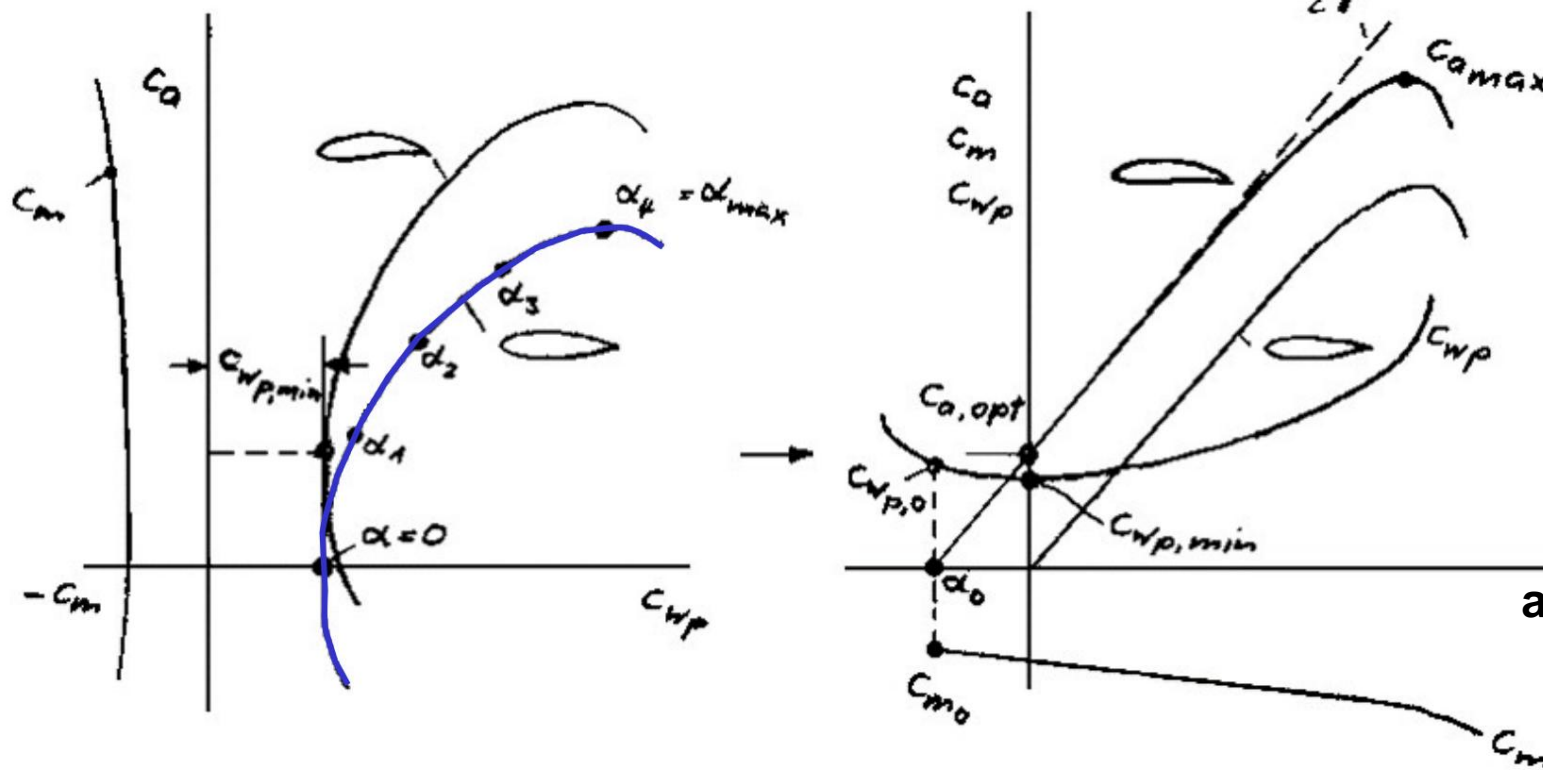


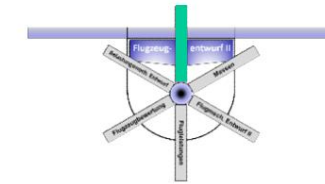
## D Basics of aerodynamic design 1.3 Wing profile





## D Basics of aerodynamic design 1.3 Wing profile • Specification of the most important aerodynamic measurement results in polar form • Examples: symmetrical and curved profile

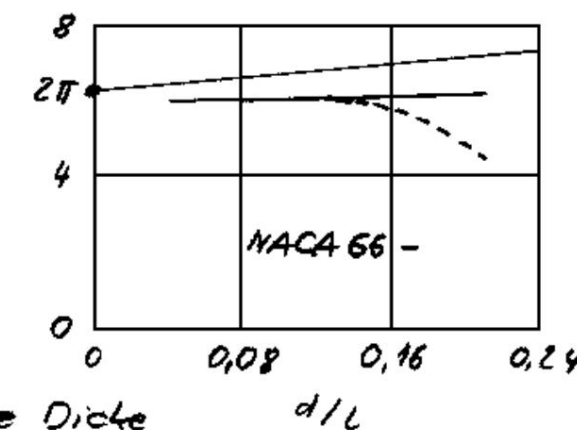
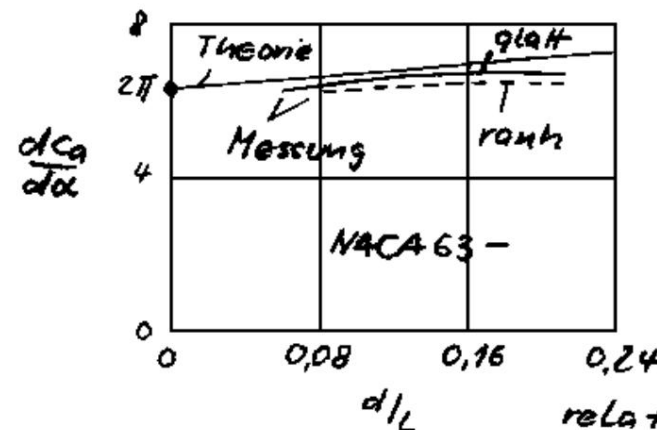


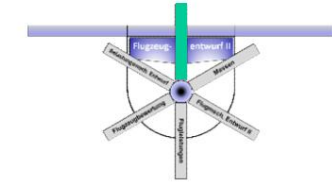


# D Basics of aerodynamic design

## 1.3 Wing profile

- The buoyancy increase approx=  $dC_a / da$  is the slope of the linear region of the resolved polar  $C_a = f(a)$  and depends on – Re number (little)
  - Trailing edge angle (much)
  - Profile thickness
  - Thickness reserve
- Theoretical maximum value is  $2\sqrt{2}$  (flat plate, potential-theoretical value) - is practically only achieved by profiles with a vanishing trailing edge angle.





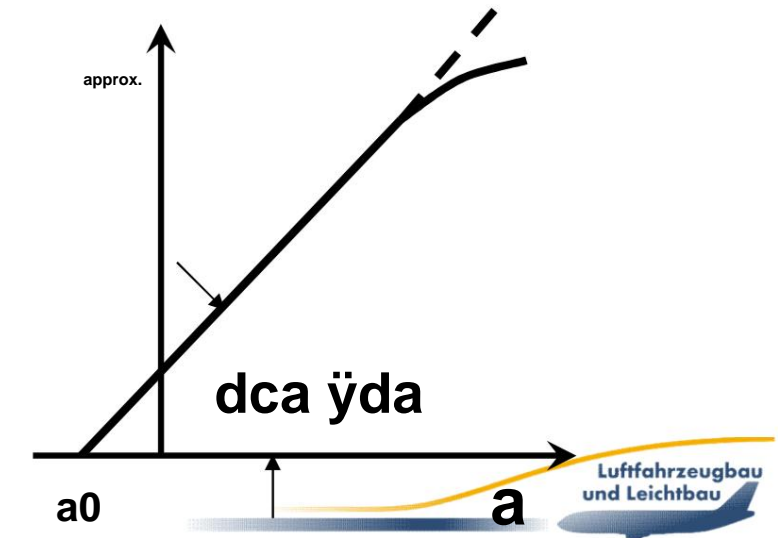
# D Basics of aerodynamic design

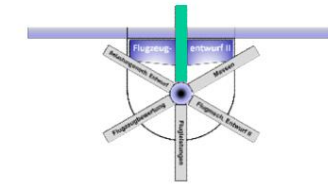
## 1.3 Wing profile

- The maximum lift coefficient  $c_{l\max}$  depends very complexly on the nose radius, the Re number, the roughness, the thickness and the camber, since the separation mechanics of the boundary layer influences the maximum angle of attack.
- The zero angle of attack  $\alpha_0$  is the angle of attack at where the lift disappears. It is 0 for symmetrical profiles and becomes negative for positively curved profiles. Together with the lift gradient, it determines the course of the linear region of the resolved

Polar, because it is

$$c_l \approx \frac{dc_l}{d\alpha} \approx \text{constant}$$

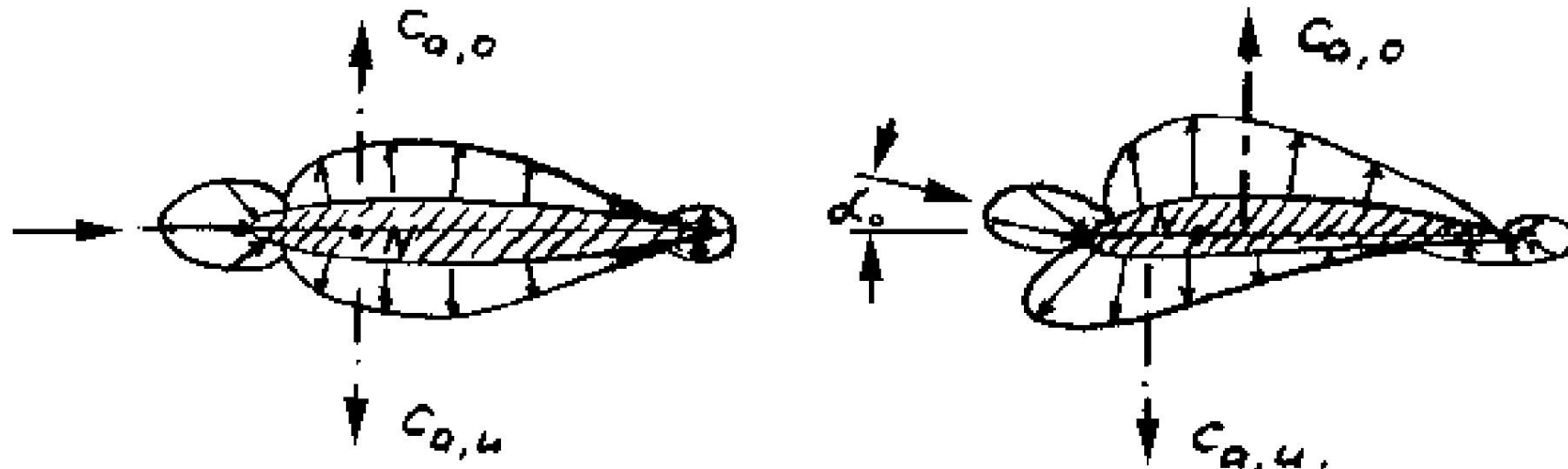




# D Basics of aerodynamic design

## 1.3 Wing profile

- The zero angle of attack results from the pressure distribution, where the resulting lift coefficients of the top and bottom sides are equal.

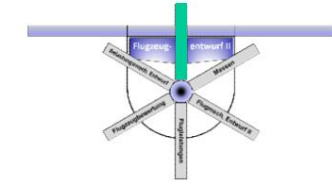


**Symmetrical:**

No resulting moment

**Arched:**

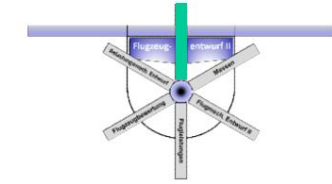
Resulting moment present



# D Basics of aerodynamic design

## 1.3 Wing profile

- The minimum profile drag coefficient  $c_{wp,min}$  denotes the peak of the drag polar.
- It depends on the profile thickness, thickness reserve, Roughness and the Re number.
- This drag coefficient corresponds to the drag-optimal lift coefficient  $c_{aopt}$
- The torque increase  $dcm/da$  indicates the increase in linear region of the moment polars.



# D Basics of aerodynamic design

## 1.3 Wing profile

- The zero moment coefficient  $c_{m0}$  is the moment coefficient at lift  $c_a = 0$  •

**Profile moment coefficient is determined from  $c_{m0}$  and the Torque increase:**

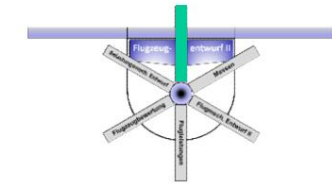
$$c_{m,x,0} = c_{m0,x,0} + \frac{dc_m}{da} \ddot{\gamma} a$$

- By extending with  $dca$  you get the dependency of the moment coefficient of  $c_a$ , because it is initially

$$c_{m,x,0} = c_{m0,x,0} + \frac{dc_m}{da} \ddot{\gamma} a + \frac{dc_a}{da} \ddot{\gamma} a$$

$$c_{m,x,0} = c_{m0,x,0} + \frac{dc_m}{da} \ddot{\gamma} a + \frac{dc_a}{da} \ddot{\gamma} a$$





## D Basics of aerodynamic design 1.3 Wing profile For a,

$$c_a \frac{dc}{a} \ddot{y} \ddot{y} \ddot{y} a$$

there

**write:**

$$a \ddot{y} \frac{dc}{d da} \frac{a}{a}$$

there

**This finally gives the moment coefficient**

$$cc m, x 0 m 0, x 0$$

$$\ddot{y} \frac{dc}{a} \frac{dc}{a} \frac{c}{da} \frac{dc}{a} \ddot{y} a 0$$

there

$$c m 0, x 0$$

$$\ddot{y} \frac{dc}{a} \frac{dc}{a} \frac{c}{da} \frac{dc}{a} \ddot{y} a 0$$

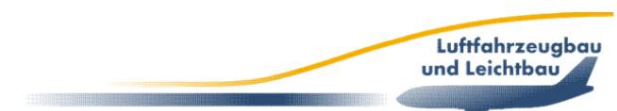
there

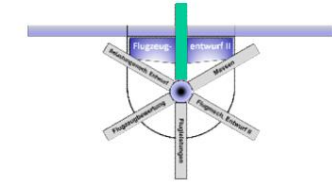
**and for the torque increase**

$$\frac{dc}{m} \frac{cc m, x 0 m 0, x 0}{\ddot{y}} \frac{dc}{a} \ddot{y} a 0$$

there

$$dc_a c_a$$

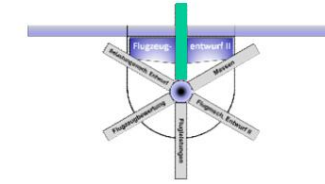




# D Basics of aerodynamic design

## 1.3 Wing profile

- The moment coefficient depends not only on the angle but also on the position of the moment reference point on the profile chord.
- When set in zero lift direction
  - the buoyancy forces of upper (strong suction power in the rear profile area) and underside (strong suction power in the nose area) on each other
  - however, a curved profile creates a resulting top-heavy zero moment, as already proven (see above).

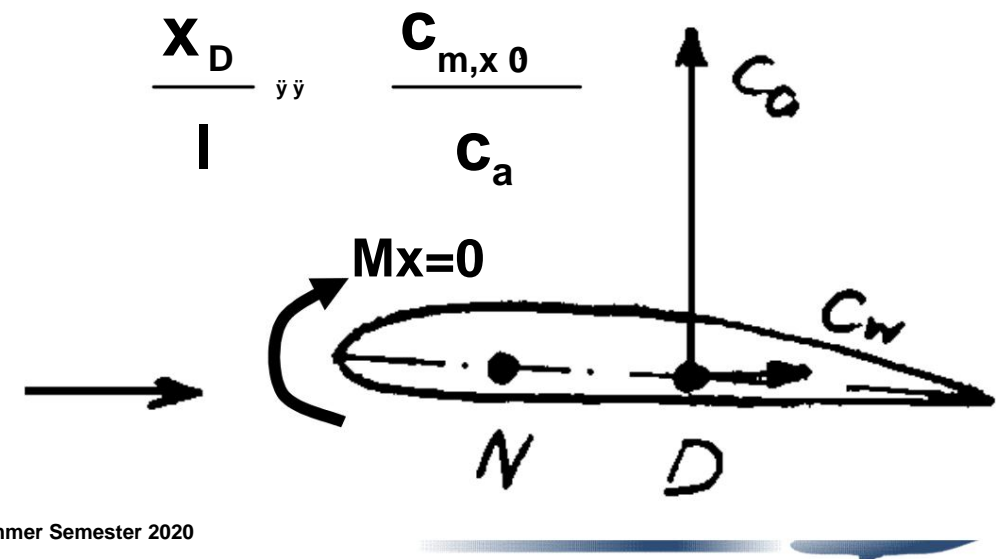


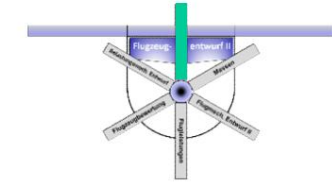
# D Basics of aerodynamic design

## 1.3 Wing profile

- Pressure point D: point of application of the resulting drag and lift resulting force.
- Position of the pressure point changes with the angle of attack – just like Magnitude and direction of the resulting force.
- The profile is moment-free with respect to the pressure point - around every other point on the profile chord there is a resulting moment whose size depends on the air force and the respective lever arm.

- The pressure point is, as shown above, the position of the center of gravity of the distribution of the pressure difference between the top and bottom

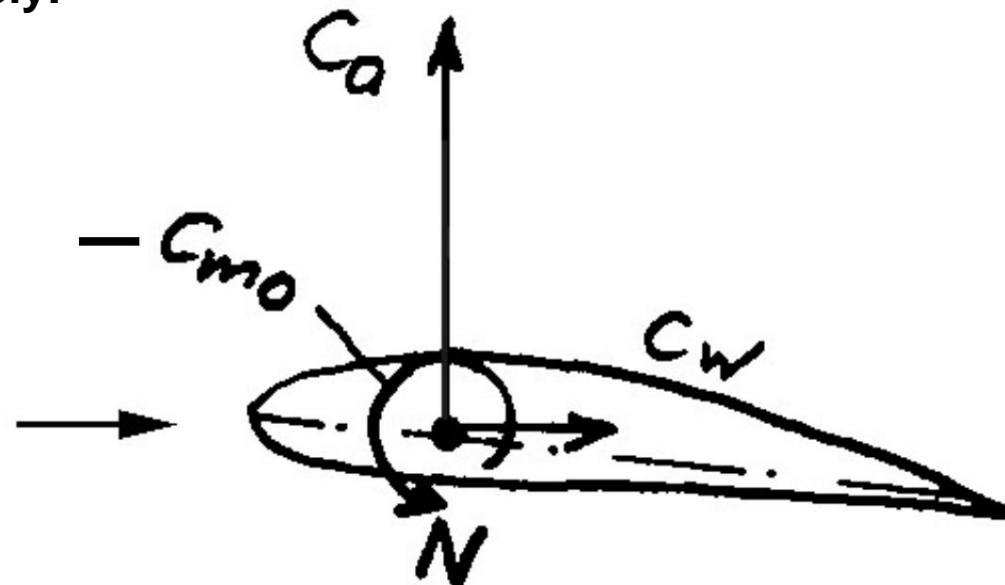


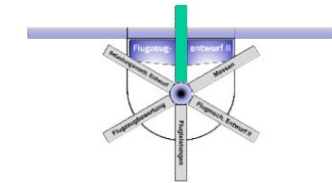


# D Basics of aerodynamic design

## 1.3 Wing profile

- The neutral point N is introduced for reasons of simplification, since the handling of a moving pressure point would be very complex.
- It is a reference point at which the resulting moment becomes independent of the angle of attack, but usually does not disappear completely.





## D Basics of aerodynamic design 1.3 Wing profile

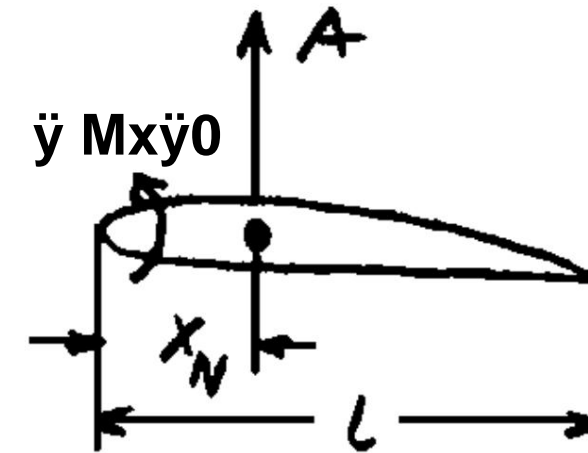
- The neutral point is defined at 25% of the profile depth.
- It is determined from the moment equilibrium around the Profile nose, neglecting the moment resulting from the resistance force and its point of application.
- The moment equilibrium states:

$$\int M \, dA = \int x \, dA$$

and with the coefficients

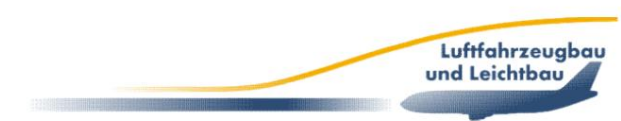
$$\int c_m \, dA = \int x \, dA$$

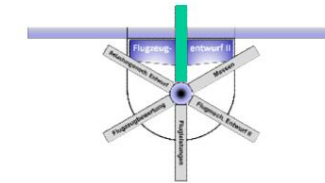
$$\frac{dc_m}{da} = \frac{x_N}{l}$$



or.

$$\frac{x_N}{l} = \frac{\int c_m \, dA}{\int A \, dA}$$





# D Basics of aerodynamic design

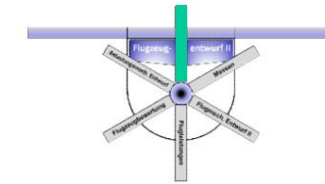
## 1.3 Wing profile

- Measurements on common symmetrical and curved profiles  
confirm: the neutral point is at approx. 25% of the profile depth.
- Therefore, in design practice, a fixed position is assumed  
at 25% of the tread depth.

Profilbezeichnung	E654	NACA 0012	E325	NACA 2412
Profilgeometrie				
Re-Zahl	$2,5 \cdot 10^6$	$9,0 \cdot 10^6$	$7,0 \cdot 10^5$	$8,9 \cdot 10^6$
$\left( \frac{dc_m}{d\alpha} \right)_{(x=0)}$	1,683	1,468	1,647	1,472
$\left( \frac{dc_a}{d\alpha} \right)$	6,303	5,873	6,159	6,016
$x_N/l$	0,267	0,250	0,267	0,245

- The neutral point is also called the aerodynamic center (ac – aerodynamic center).

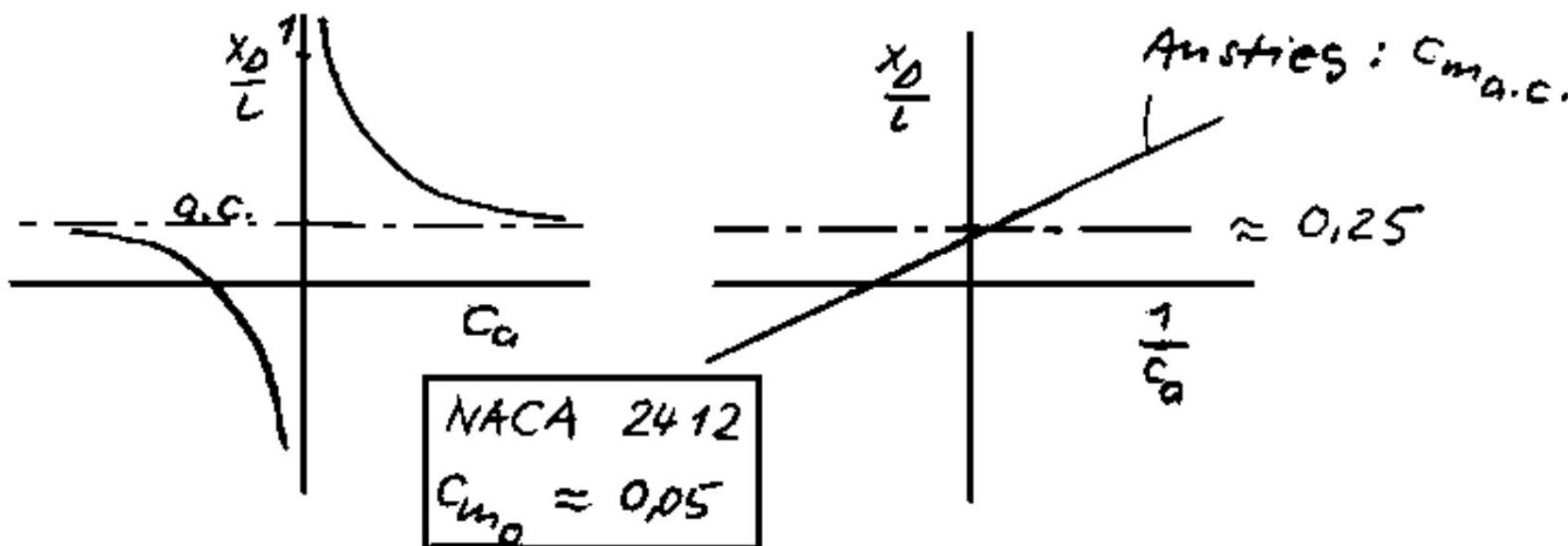


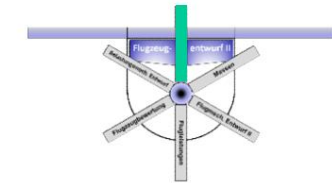


# D Basics of aerodynamic design

## 1.3 Wing profile

- The pressure point moves towards the neutral point as the lift coefficient increases and towards infinity as the lift coefficient disappears.
- The slope of the straight line  $x_D / l$  over  $1/c_a$  corresponds to the moment coefficient in the aerodynamic center



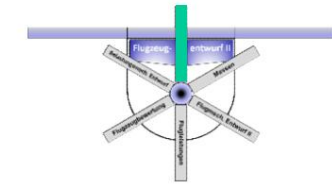


## D Basics of aerodynamic design 1.3 Wing profile

- One can therefore assume that the profile nose-related Moment coefficient also a simplified dependence on the Specify lift coefficient:

$$\begin{aligned}
 & \frac{\frac{\partial c_m}{\partial x_0}}{\frac{\partial c_a}{\partial a}} = \frac{c_{m0}}{c_{a0}} \\
 & \frac{\frac{\partial c_a}{\partial N_x}}{a} = \frac{c_{a0}}{a_0} \\
 & \frac{c_a}{4} = \frac{c_{a0}}{a_0}
 \end{aligned}$$

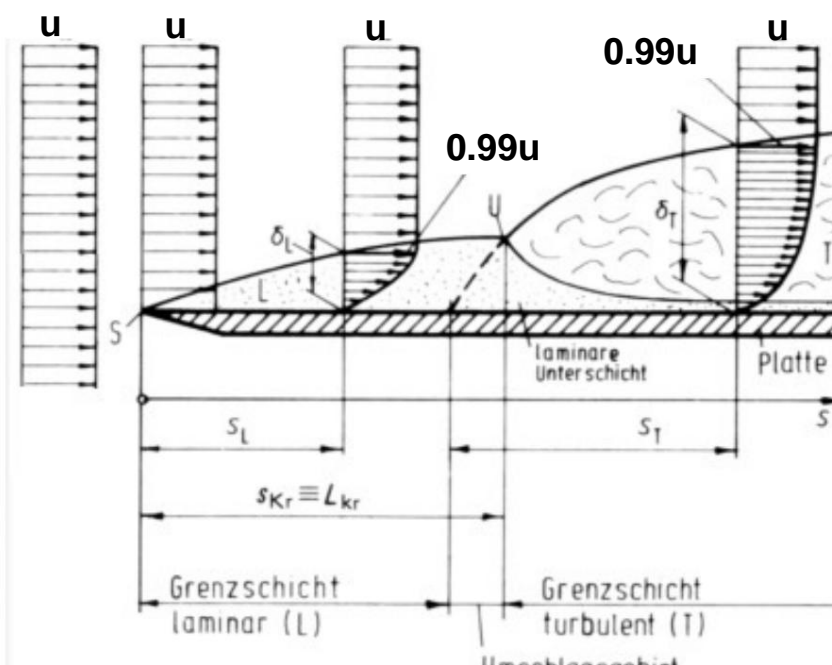




# D Basics of aerodynamic design

## 1.3 Wing profile

- The boundary layer is the area immediately near the wall in which where the velocity increases from standstill (molecules adhere to the wall) to the flow velocity  $u$ .

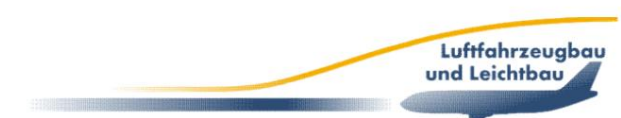


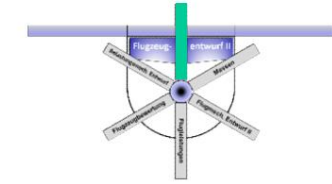
Grenzschichtausbildung an ebener Platte.

S Staupunkt

U Umschlagpunkt

- The boundary layer thickness  $d$  is defined by the distance from the wall at which the local velocity has almost (99%) reached the flow velocity ( $u/d=1$ ) .



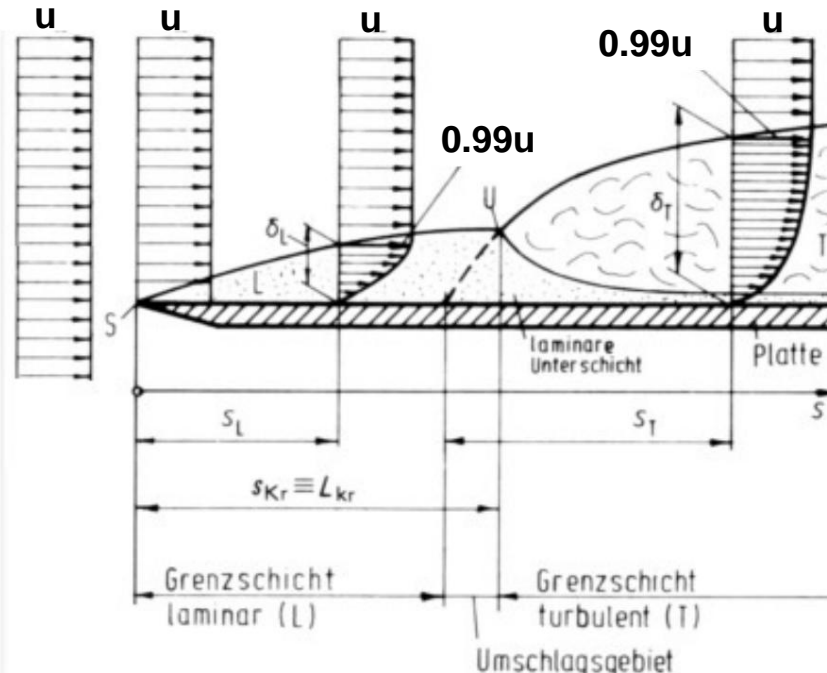


# D Basics of aerodynamic design

## 1.3 Wing profile

There are two different boundary layer qualities:

- Laminar GS: Molecules move on parallel paths
- Turbulent GS: Velocity components in all directions are superimposed on the translational motion.



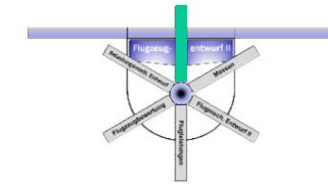
Grenzschichtausbildung an ebener Platte.

S Staupunkt

U Umschlagpunkt

- The wall gradient  $dv/dy(y = 0)$  is a measure of the wall shear stress, which is decisive for the frictional resistance.

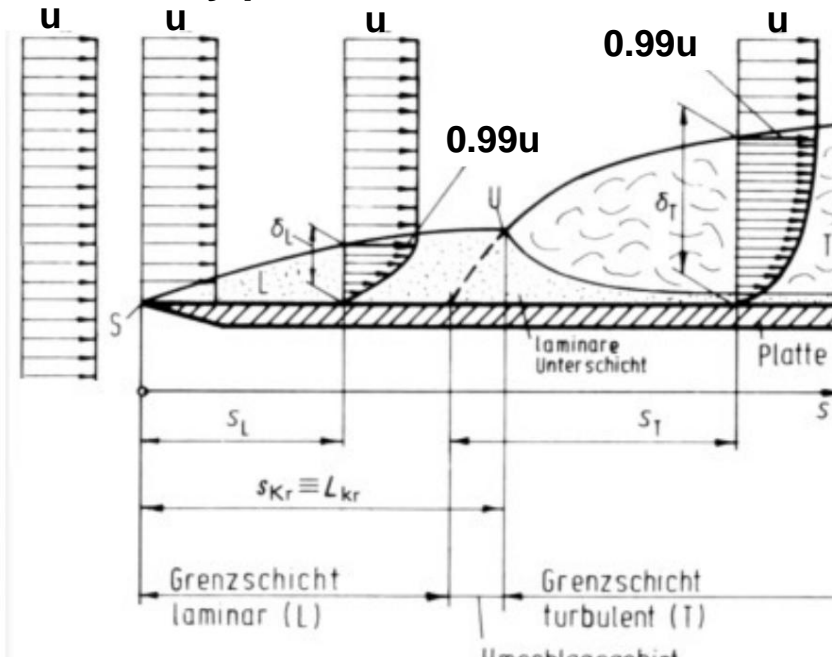




# D Basics of aerodynamic design

## 1.3 Wing profile

- The boundary layer has a vanishing thickness at the stagnation point
- With increasing run length, the boundary layer thickness increases due to wall friction.
- Without any particular disturbance, the boundary layer is initially laminar.



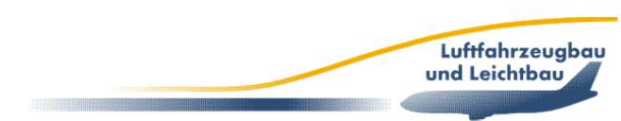
Grenzschichtausbildung an ebener Platte.

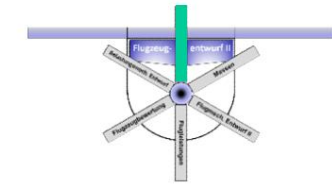
S Staupunkt

U Umschlagpunkt

- Without a pressure gradient (flat plate), a transition region with natural velocity fluctuations occurs at run lengths corresponding to  $Re < 3,000,000$  (Tolmien-Schlichting instability)

- At  $Re = 3,000,000$  the transition to a turbulent boundary layer takes place.

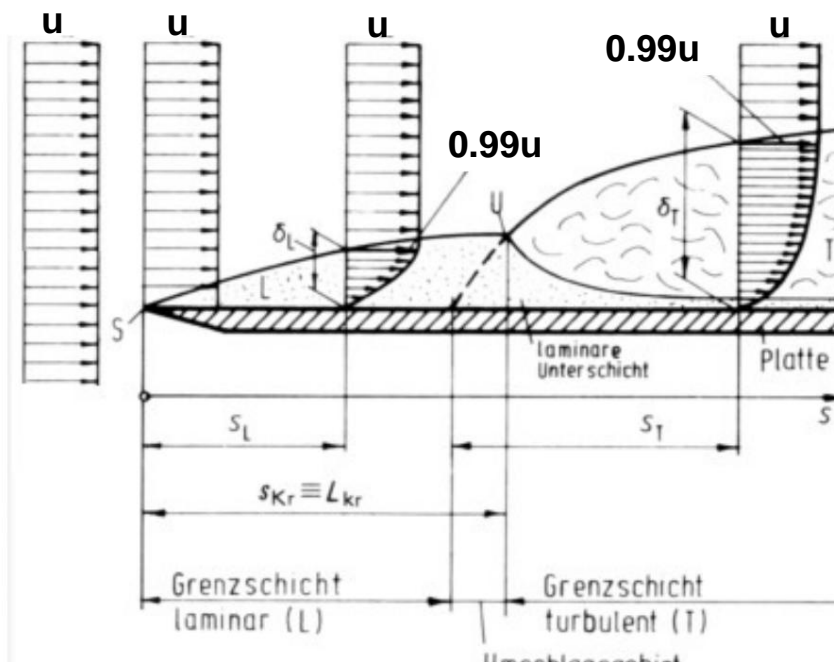




# D Basics of aerodynamic design

## 1.3 Wing profile

- Geometric wall disturbances and pressure increase shift the transition forward; pressure drop backwards.

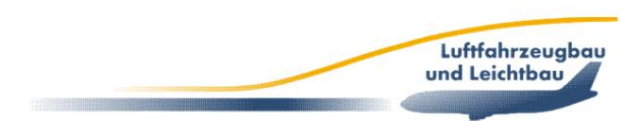


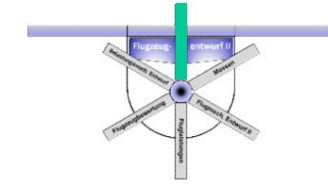
Grenzschichtausbildung an ebener Platte.

S Staupunkt

U Umschlagpunkt

- The thickness of the subsequent turbulent boundary layer increases significantly more with the run length than that of the laminar boundary layer.
- A laminar sublayer forms due to the continuity condition at the impermeable wall.

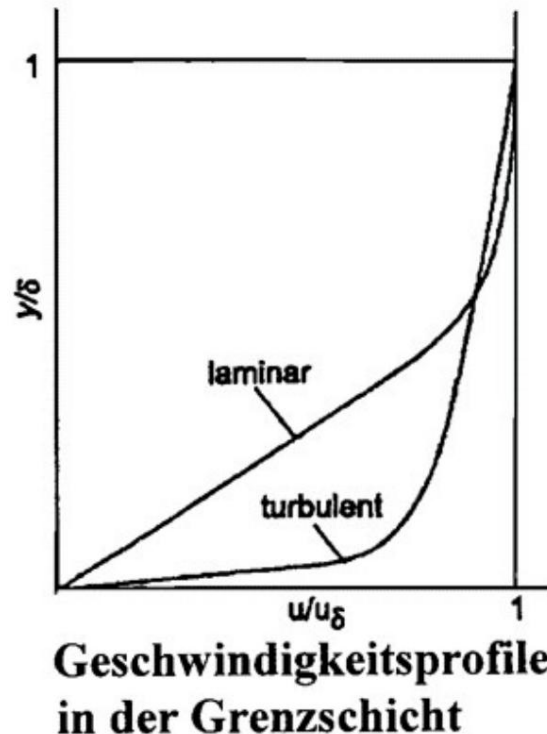




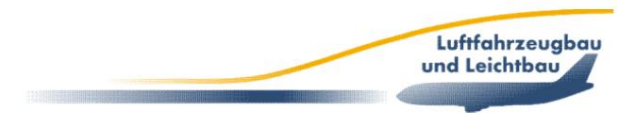
# D Basics of aerodynamic design

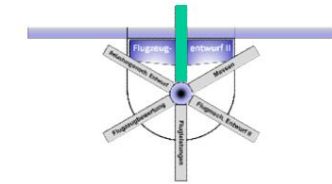
## 1.3 Wing profile

- The frictional resistance results from the surface integration of the wall shear stresses, which are defined by the velocity gradient on the wall and the viscosity of the flowing medium.



- A laminar boundary layer has a smaller gradient than a turbulent boundary layer.
- The frictional resistance of a laminar boundary layer is therefore lower.
- The turbulent boundary layer has a more spherical shape and a higher frictional resistance.

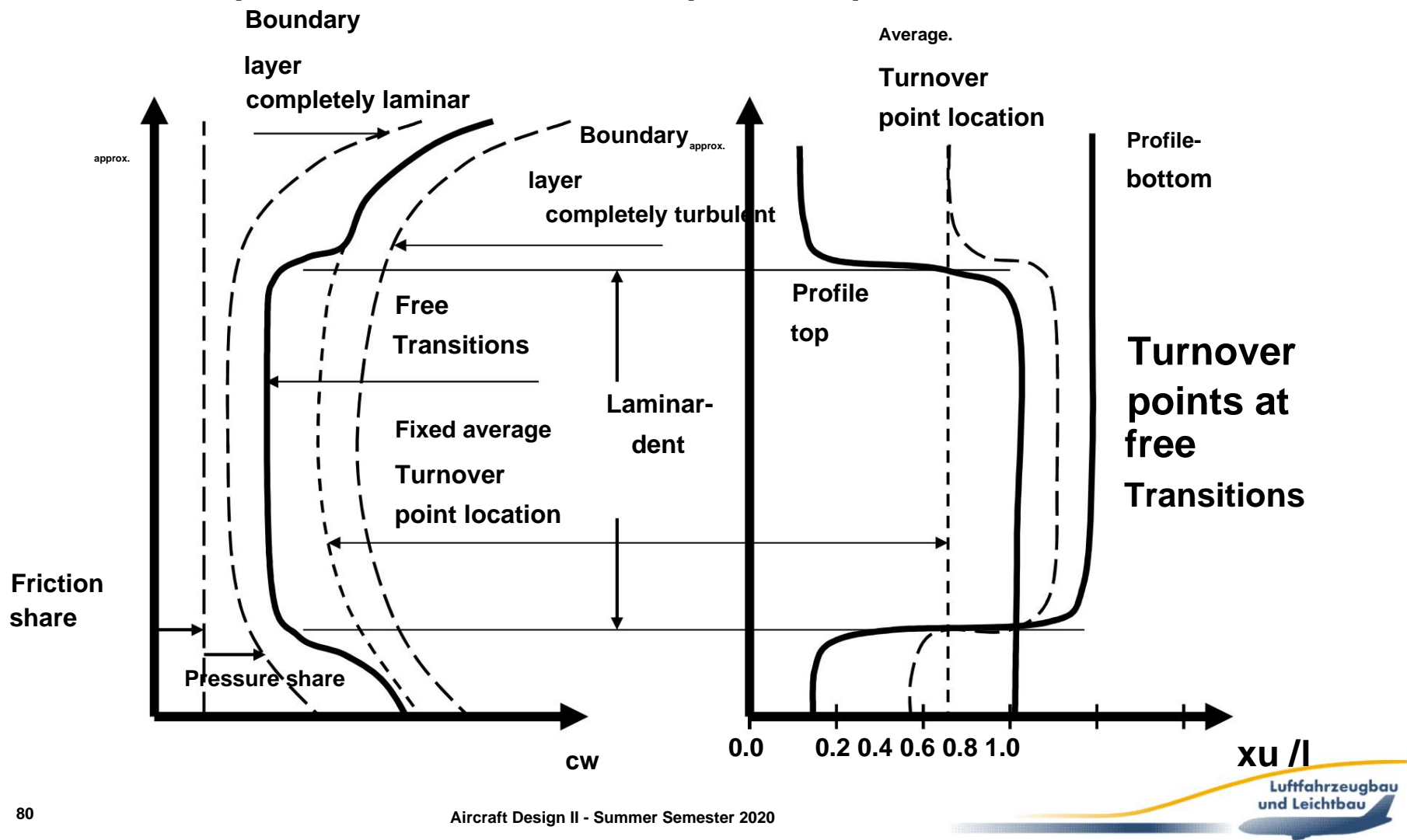


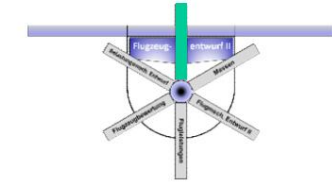


# D Basics of aerodynamic design

## 1.3 Wing profile

### Composition of the resistance polars of profiles



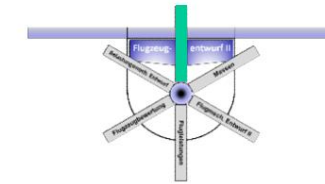


# D Basics of aerodynamic design

## 1.3.1 Influence of profile geometry parameters

- The profile parameters each have their own influence on the aerodynamic properties and, when combined, they are complexly interconnected.
- The nose radius influences the amount of negative pressure at the leading edge of the profile and thus also the separation behavior in a flow with friction. This determines the stall behavior of the wing and thus also significantly the flight characteristics of the aircraft.

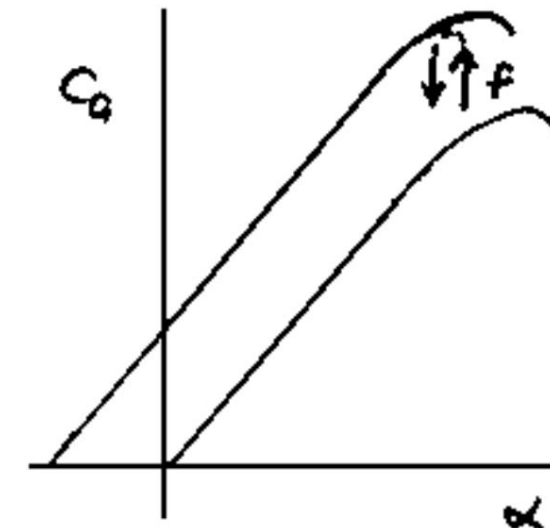
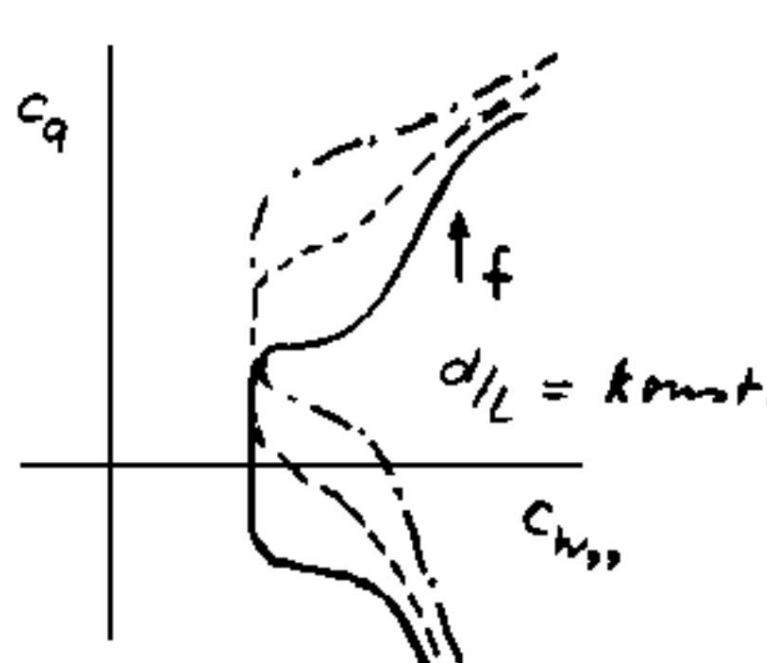


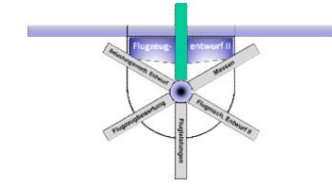


# D Basics of aerodynamic design

## 1.3.1 Influence of profile geometry parameters

- The adaptation of the minimum drag to the lift coefficient is most economically achieved by the camber.
- If the profile thickness remains constant, the width of the area of constant resistance (laminar cell) remains approximately the same

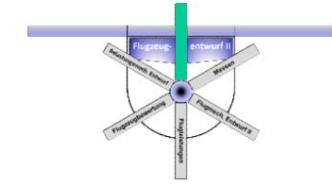




# D Basics of aerodynamic design

## 1.3.1 Influence of profile geometry parameters

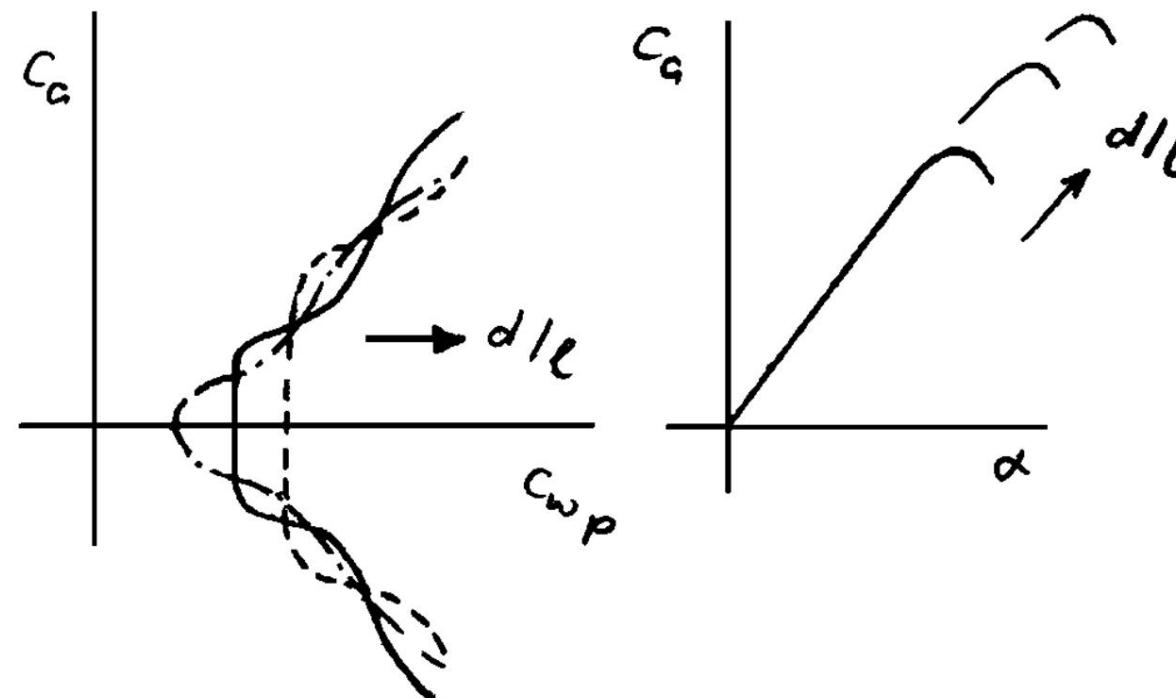
- No general statement can be made about the influence of the camber reserve, since this is defined by the thickness distribution and the skeleton line.
- However, with a larger offset of the camber maximum, the zero moment becomes smaller.
- In addition, with a large camber offset there is a risk of abrupt detachment with increasing angle of attack. flow, which leads to poor flight characteristics

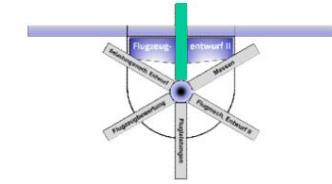


# D Basics of aerodynamic design

## 1.3.1 Influence of profile geometry parameters

- As the profile thickness increases, the minimum drag coefficient increases and the width of the laminar flow increases.
  - As the profile thickness increases, the maximum lift increases.
- This trend only applies to symmetrical or slightly curved profiles.

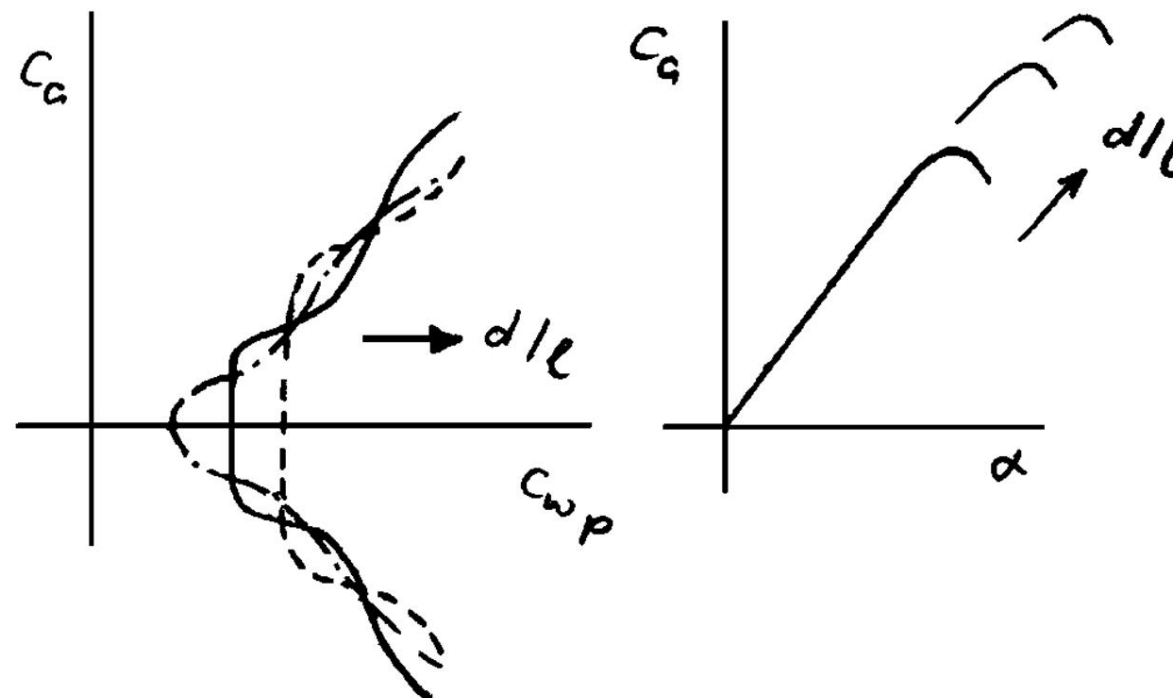


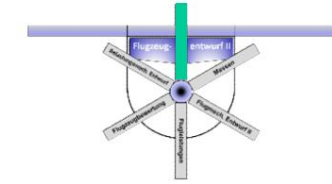


# D Basics of aerodynamic design

## 1.3.1 Influence of profile geometry parameters

- Laminar profiles have a larger thickness offset than conventional profiles.
- As the thickness of the layer increases, the laminar run-up length increases and the minimum pressure coefficient decreases. The laminar cell becomes narrower.



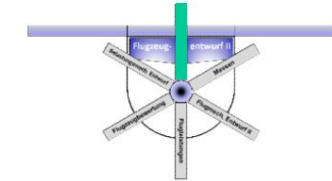


# D Basics of aerodynamic design

## 1.3.1 Influence of profile geometry parameters

- The previous statements apply to smooth wings. • The real wing has a finite roughness and manufacturing inaccuracies such as waviness and structural impacts.
- This means that at large Re numbers the laminar effect is lost and the profile drag increases.

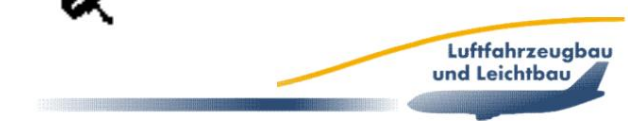
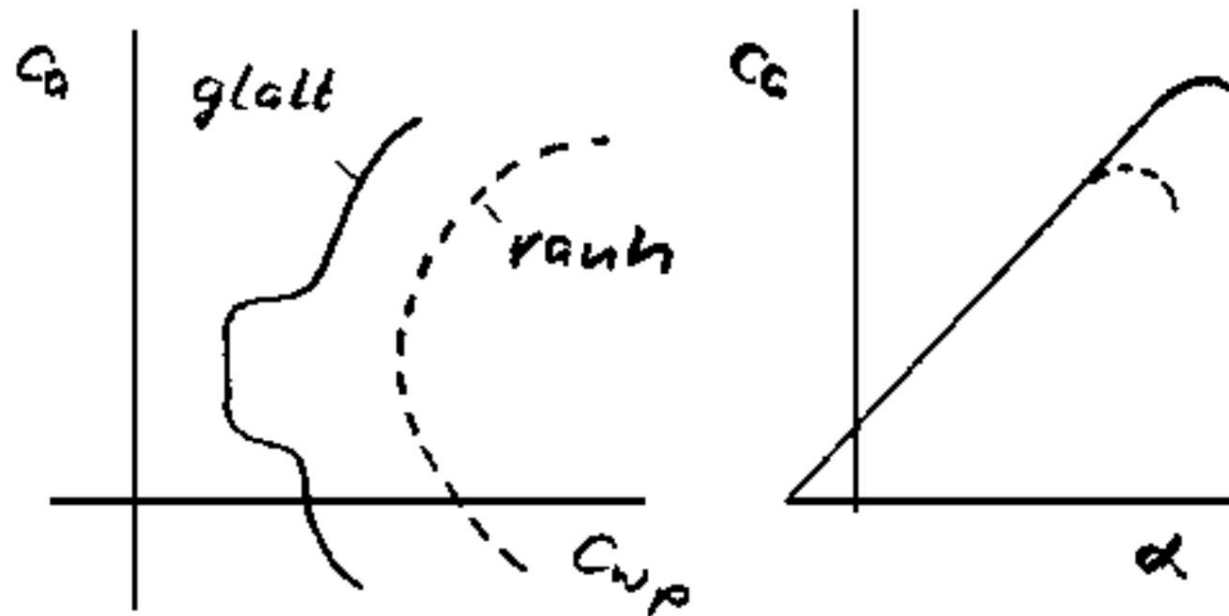


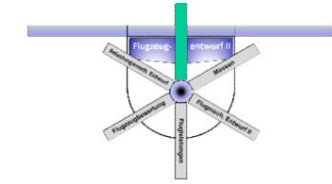


# D Basics of aerodynamic design

## 1.3.1 Influence of profile geometry parameters

- In a turbulent boundary layer, the frictional resistance increases due to roughness, since the increased turbulence near the wall leads to an increase in the wall velocity gradient and thus in the wall shear stresses.
- In addition, due to the energy loss of the boundary layer, the maximum lift is greatly reduced.





# D Basics of aerodynamic design

## 1.3.2 Influence of the Reynolds number

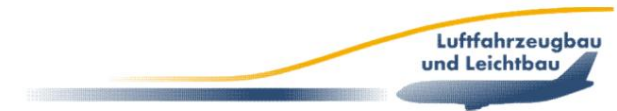
- The Reynolds number also has a significant influence on the aerodynamic behavior of the profiles.
- The Reynolds number  $Re$  is defined as the ratio of mass and viscosity forces and is

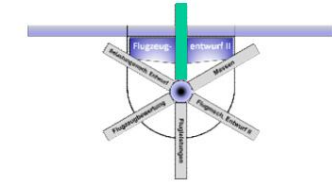
$$re = \frac{v l}{\dot{\gamma}}$$

- The denominator is the kinematic viscosity  $\dot{\gamma}$  as a height-dependent material constant. This is the ratio of the dynamic viscosity  $m$  and the density  $\ddot{\gamma}$ .

$$\dot{\gamma} = \frac{m}{\ddot{\gamma}}$$

- Speed, altitude and size scale determine i.e. the  $Re$  number.





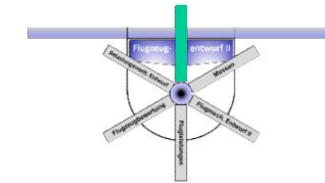
# D Basics of aerodynamic design

## 1.3.2 Influence of the Reynolds number

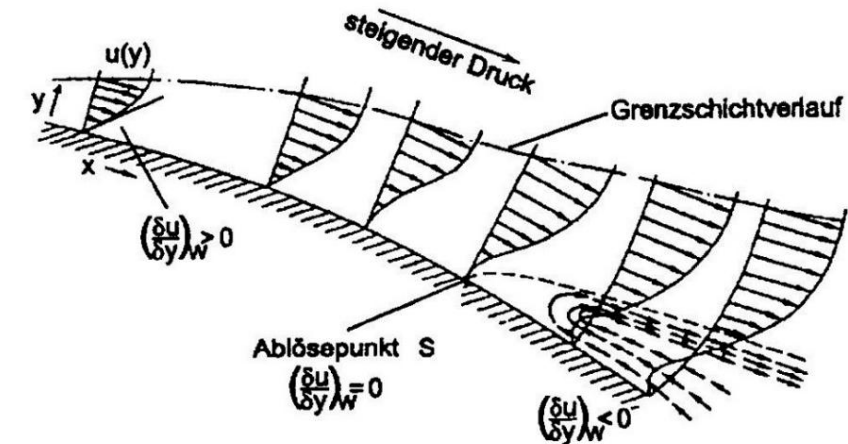
- The above mentioned aerodynamic coefficients are only directly applicable if there is a Reynolds similarity between the results of the profile measurement and the wing.
- Otherwise, the re-influence must be considered separately.
- The Re number has little influence on the buoyancy behavior.
- The Re number influences the boundary layer thickness directly or indirectly via its influence on the transition point position
- With increasing Re number, the boundary layer thickness at the trailing edge decreases and thus increases the circulation.
- Furthermore, as the boundary layer thickness decreases, the momentum loss in the boundary layer and thus the frictional resistance also decreases.

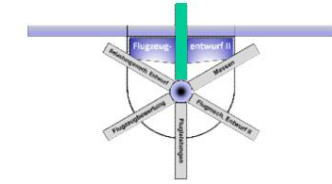
# D Basics of aerodynamic design

## 1.3.2 Influence of the Reynolds number



- Flow separation occurs when the kinetic energy of the fluid near the wall has become so low that it comes to a standstill as a result of increasing pressure.
- Further deceleration leads then to a backflow close to the wall and thus to separation.
- Flow separation defines the stall behavior of the aircraft.





# D Basics of aerodynamic design

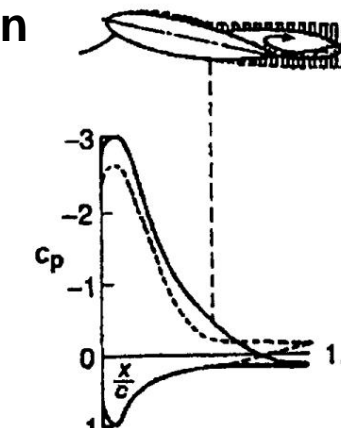
## 1.3.2 Influence of the Reynolds number

- The main influence of the Re number is on the stall behavior, which depends on the profile shape itself due to the different release mechanisms.
- First, one can identify general tendencies for typical profiles notice:
  - At a small angle of attack, the separation point is near the trailing edge and the quality of the boundary layer (laminar or turbulent) has no influence on the lift characteristics, but does influence the frictional drag.
  - As the angle of attack increases, the deflection release point moves forward and the pressure drag increases. Shortly before the lift collapses, the separation point moves rapidly forward. A large turbulent wake area is produced, and thus a very large pressure drag.

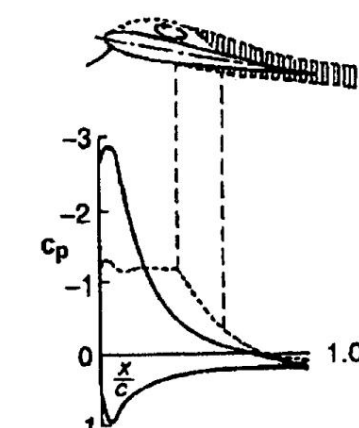
# D Basics of aerodynamic design

## 1.3.2 Influence of the Reynolds number

- At the same pressure gradient, separation occurs earlier in a laminar boundary layer than in a turbulent boundary layer, since in the latter the supply of energy to the area near the wall is made possible by transverse movements.

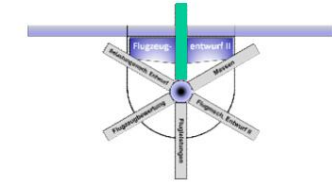


(b): Druckverteilung bei turbulenter Ablösung



(c): Druckverteilung bei laminarer Ablösung

- With a small Re number, the transition point is further back and a stall occurs at lower angles of attack, combined with greater pressure drag than with high Re numbers, which at the same time achieve small drag coefficients at the low angles of attack present in cruise flight.

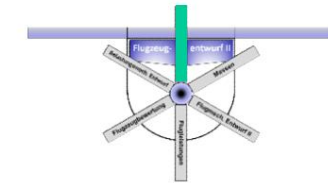


# D Basics of aerodynamic design

## 1.3.2 Influence of the Reynolds number

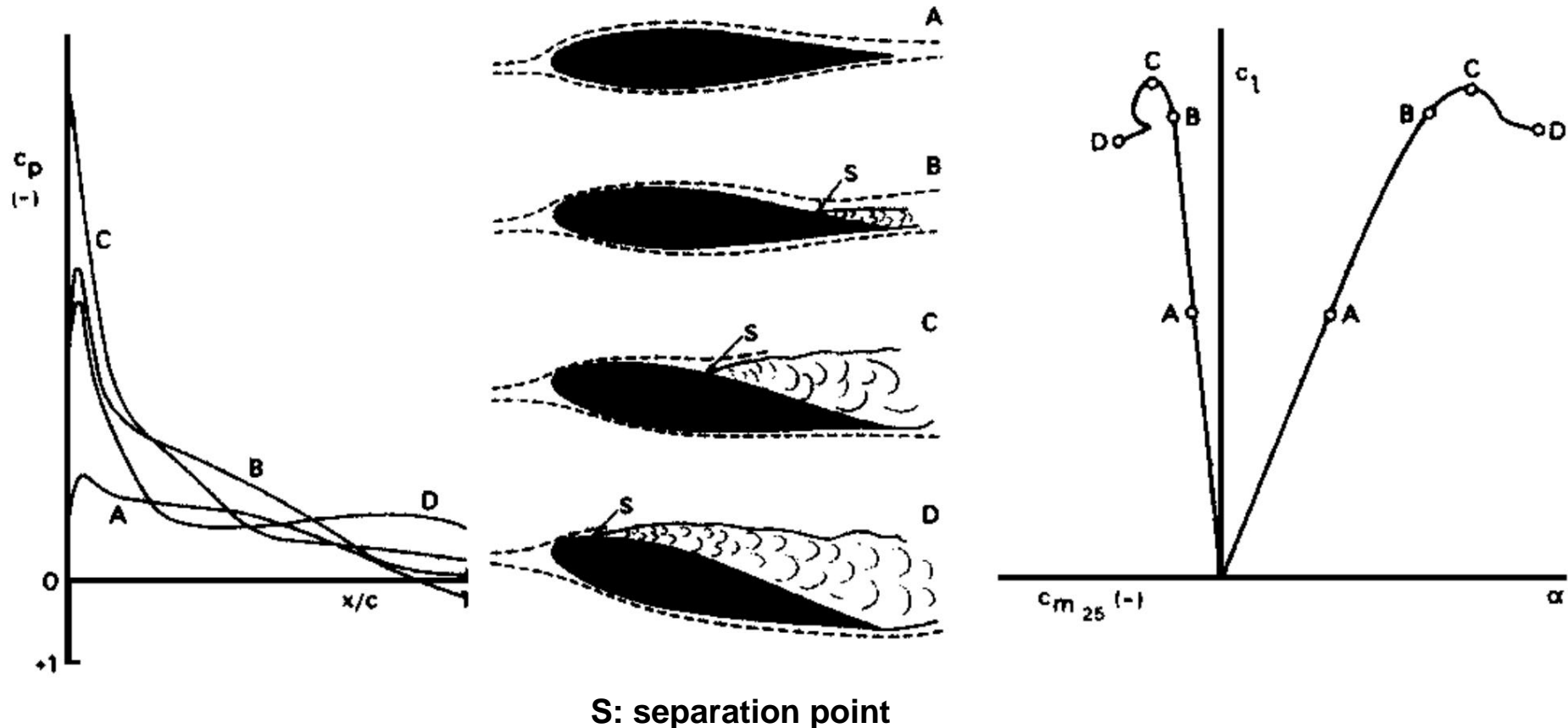
- As the Re number increases, the transition point moves forward and the separation point moves backward. This allows for larger maximum angles of attack, which in turn allow for greater maximum lift. This reduces pressure drag. However, greater frictional drag occurs during cruise flight due to the early transition.

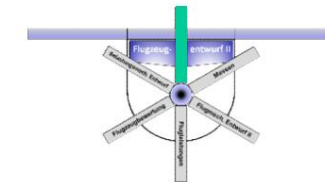
This once again shows the fundamental incompatibility between cruising flight (flight with minimal drag) and take-off and landing requirements (flight at maximum lift) and thus the need for high-lift aids (flaps).



## D Basics of aerodynamic design 1.3.2 Influence of the Reynolds number

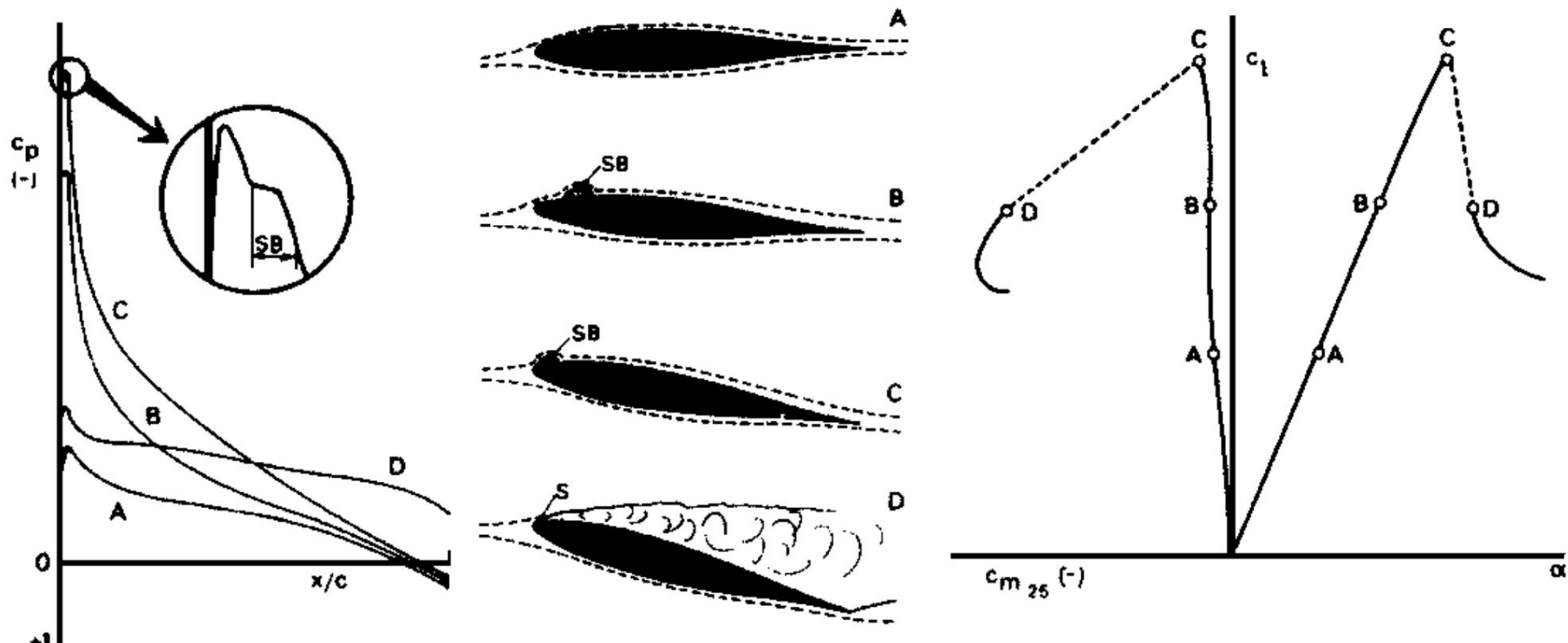
- A thick profile (18%) has good stalling properties





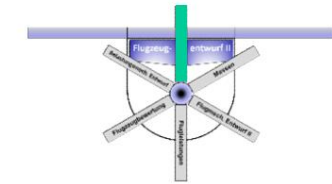
## D Basics of aerodynamic design 1.3.2 Influence of the Reynolds number

- Moderately thin profiles ( $\delta \approx 9\%$ ) have very unfavorable pull-over properties.

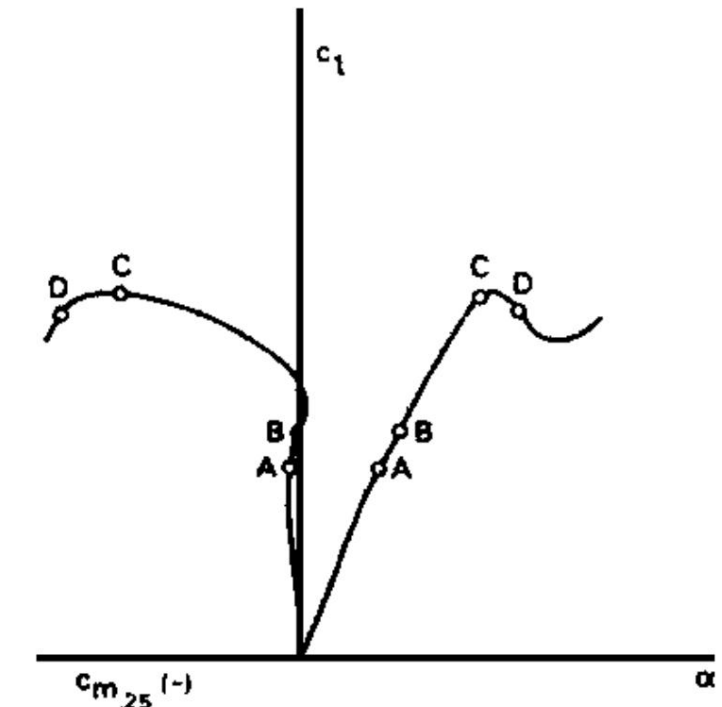
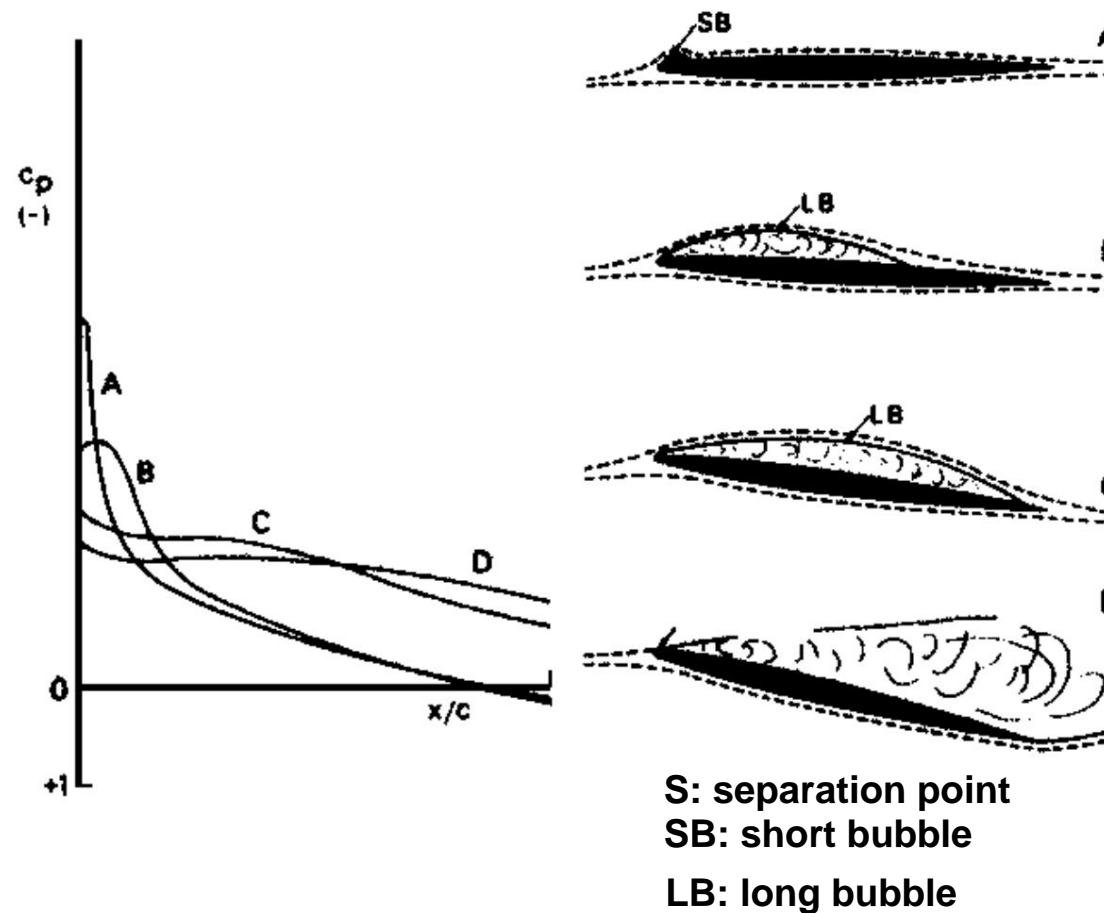


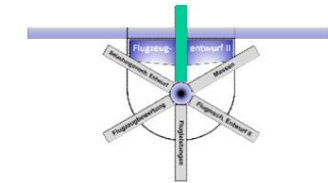
S: separation point  
 SB: short bubble

LB: long bubble



## D Basics of aerodynamic design 1.3.2 Influence of the Reynolds number • Very thin profiles behave more favourably.

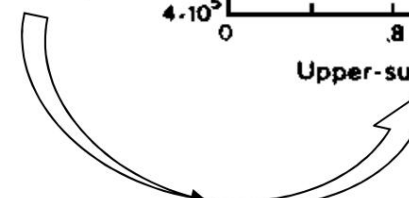
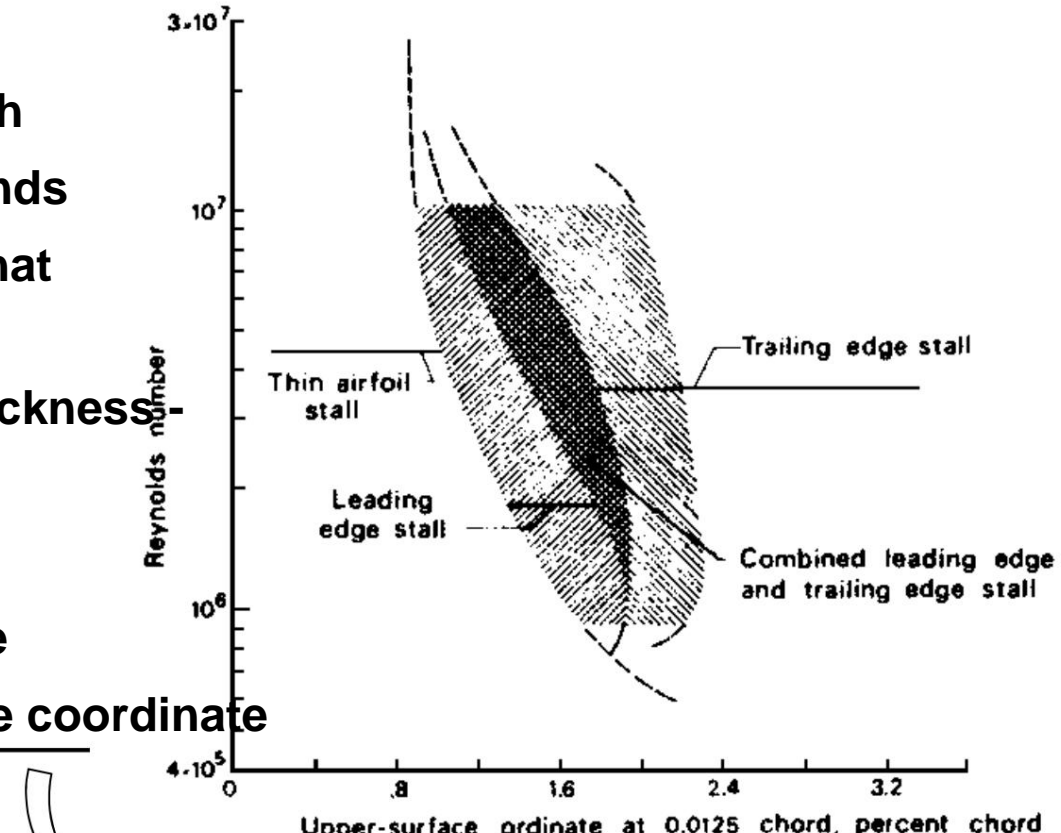


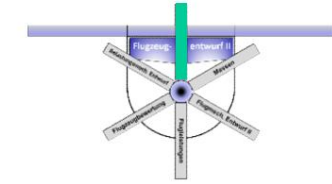


# D Basics of aerodynamic design

## 1.3.2 Influence of the Reynolds number

- The development of the separation mechanisms with the Reynolds number depends on a geometric parameter that determines the - primarily influenced by the profile thickness - Describes the nose radius.
- This radius is not directly measurable and is therefore given in the form of a profile coordinate near the leading edge.

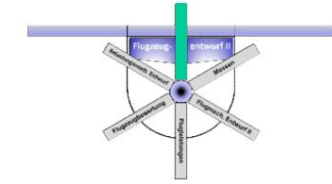




# D Basics of aerodynamic design

## 1.3.2 Influence of the Reynolds number

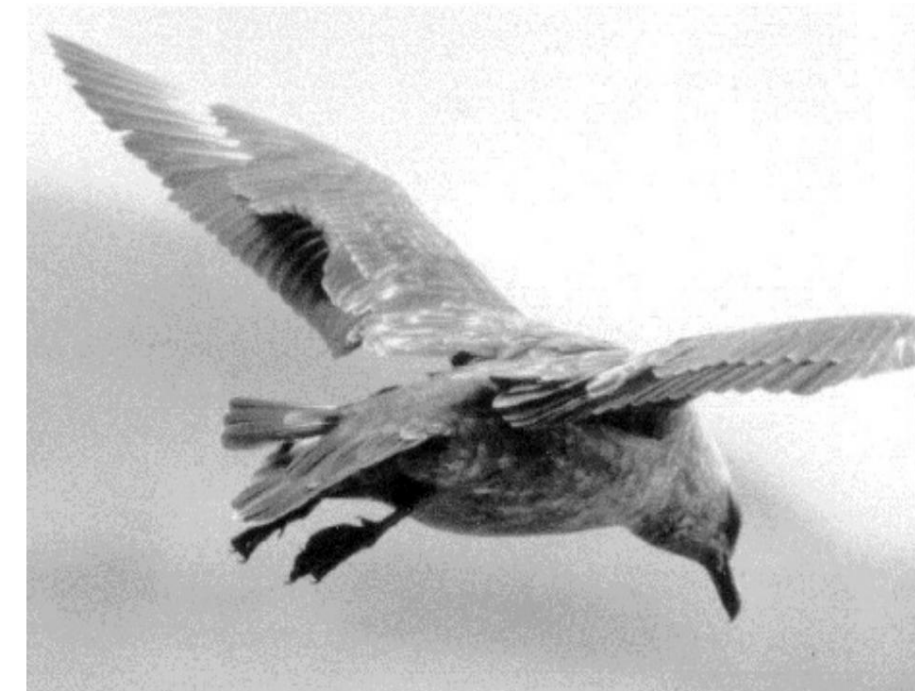
- From the evaluation of the detachment mechanisms described above, there are three prerequisites for a complete capture flow separation:
  1. Strong pressure increase in the direction of flow (pressure distribution)
  2. Thick friction layer (boundary layer)
  3. Possibility of fluid supply into the separation vortex against the flow direction

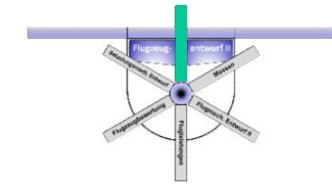


# D Basics of aerodynamic design

## 1.3.2 Influence of the Reynolds number

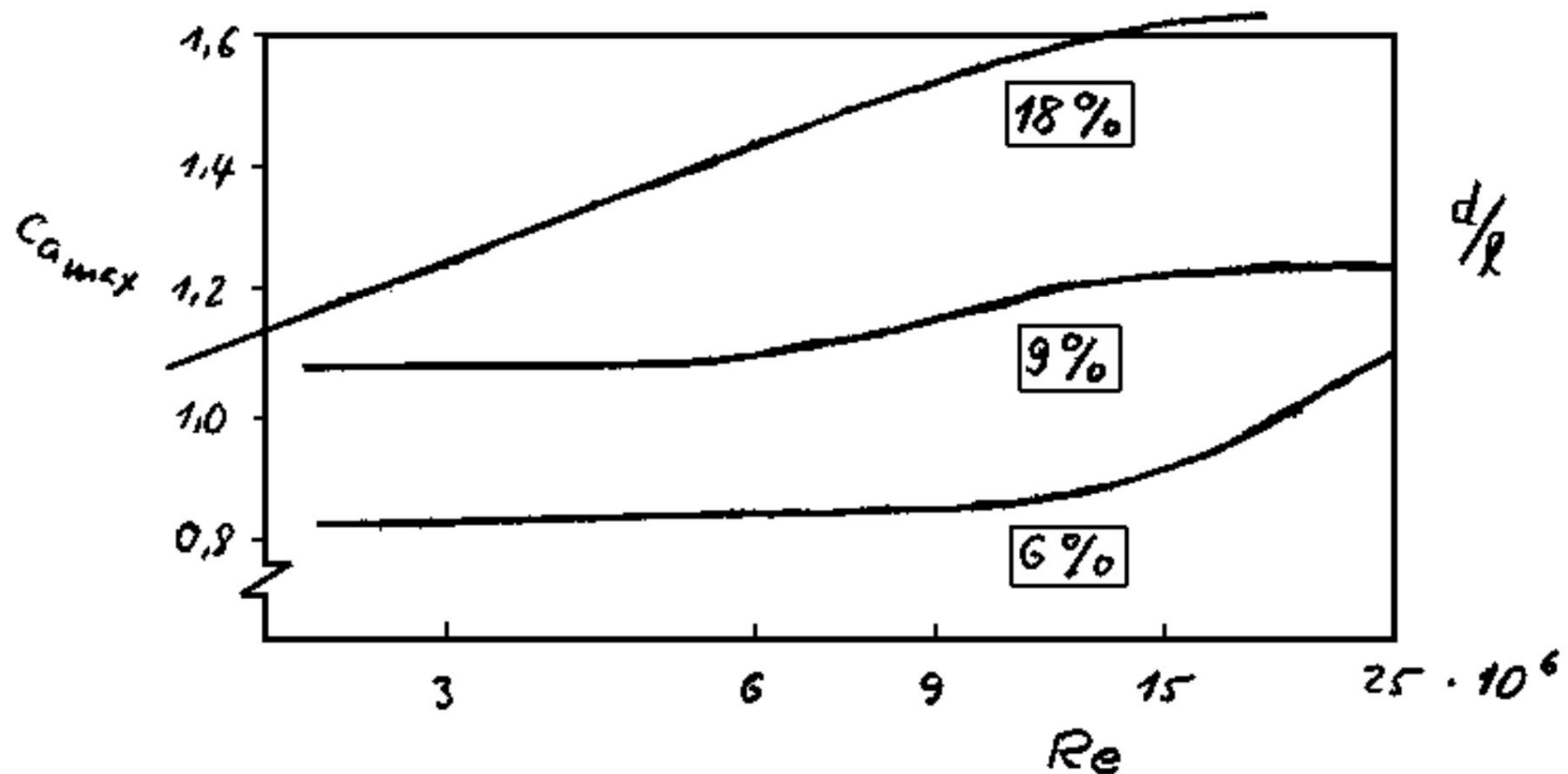
- The first two criteria can be influenced by a suitable choice of geometry parameters or by measures such as boundary layer manipulation (e.g. slats, suction, vortex generators).
- The backflow can cannot yet be prevented by technical means.
- However, the fact that birds raise their feathers when they are in high-lift conditions suggests that this mechanism is also controlled by nature.

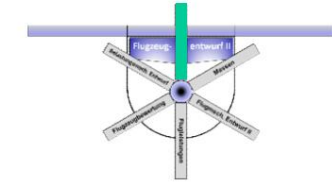




## D Basics of aerodynamic design 1.3.2 Influence of the Reynolds number

- As discussed in relation to the stall characteristics, the Re number has an influence on the maximum lift.

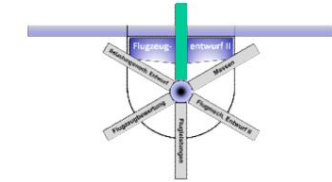




# D Basics of aerodynamic design

## 1.3.2 Influence of the Reynolds number

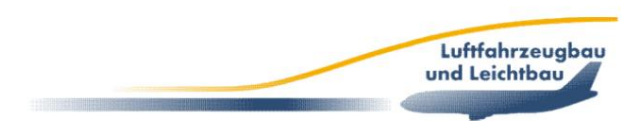
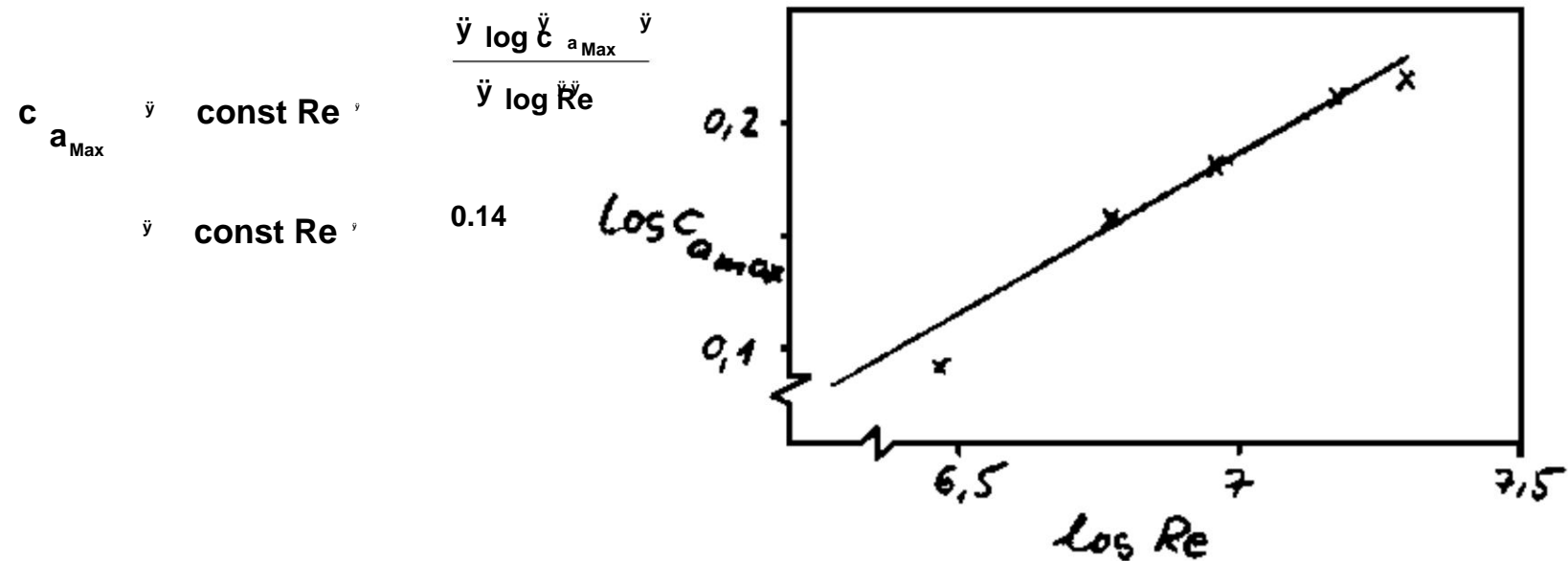
- For thick profiles (18%) the maximum lift coefficient increases with the Re number, since the momentum loss thickness decreases, so that even at larger pressure gradients no separation occurs.
- For medium-thickness profiles (9%), below  $Re = 6,000,000$ , one finds predominantly a long separation bubble, while at  $Re > 6,000,000$ , one tends to find a short separation bubble, which allows a slight increase in the achievable maximum lift.
- For very thin profiles (6%) the Re number dependence is not very pronounced. With increasing Re numbers the occurrence of a long separation bubble is increasingly delayed.

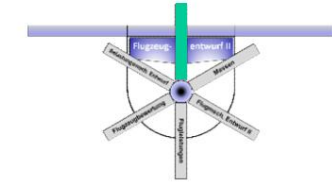


# D Basics of aerodynamic design

## 1.3.2 Influence of the Reynolds number

- In practice, the Re number influence can be simplified by approximate a power law. In limited Re number ranges, a good agreement with the profile behavior is shown.
- For example, for a NACA 633-018 you get the following Dependency from measurements using approximation



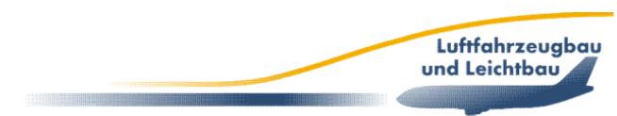


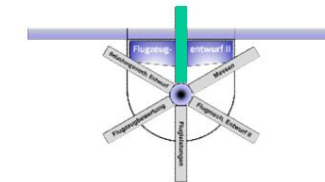
# D Basics of aerodynamic design

## 1.3.2 Influence of the Reynolds number

- Similarly, for certain Re numbers areas, power laws can also be formulated for the drag and moment coefficients.
- This means, for example, that the minimum profile resistance

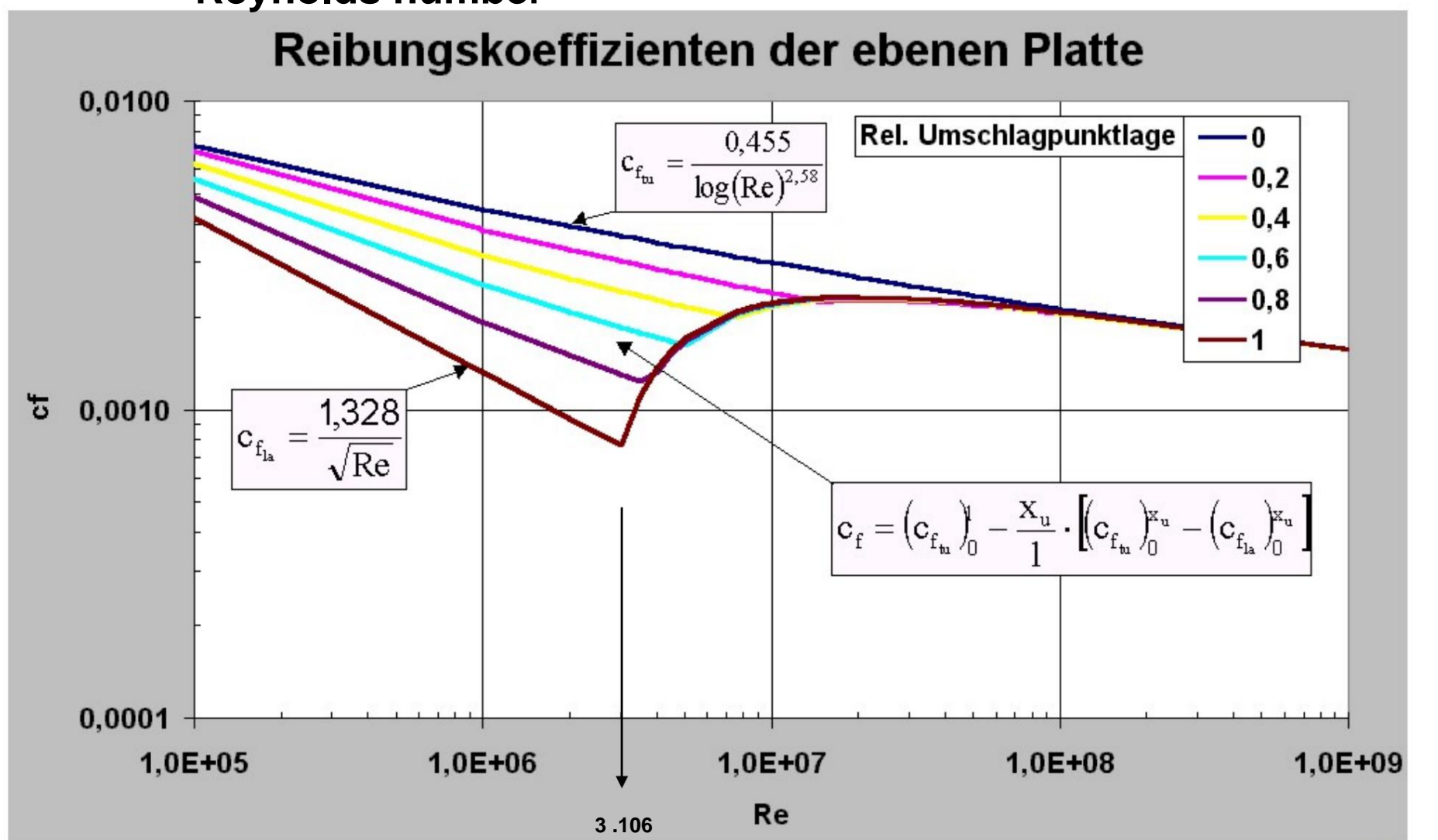
$$c_w \underset{p,\min}{\approx} \frac{\log c_w}{\log Re}$$

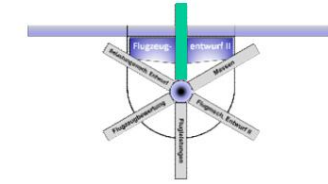




## D Basics of aerodynamic design 1.3.2 Influence of the Reynolds number

### Reibungskoeffizienten der ebenen Platte

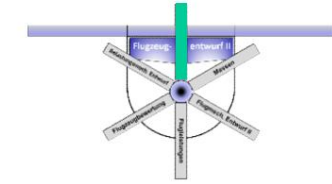




# D Basics of aerodynamic design

## 1.3.2 Influence of the Reynolds number

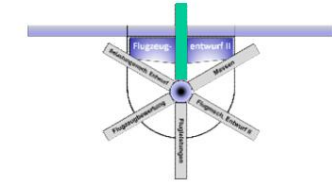
- With increasing run length, the frictional resistance decreases due to the fundamentally decreasing momentum loss thickness of the boundary layer.
- The **upper curve** indicates the fully turbulent water plate, at the **lower one** a free transition takes place at  $Re = 3,000,000$ , as shown by Prandtl's boundary layer theory.
- The curves in between show the influence of a transition forced at the respective transition point position. • A main statement from this is formulated very simply, that a is frequently used in aerodynamics and especially in shipbuilding: “Length matters”.
- The plate analogy can of course be applied to all bodies with flow any contouring, whereby the transition layer depends on the pressure distribution and can only be determined or estimated experimentally.



# D Basics of aerodynamic design

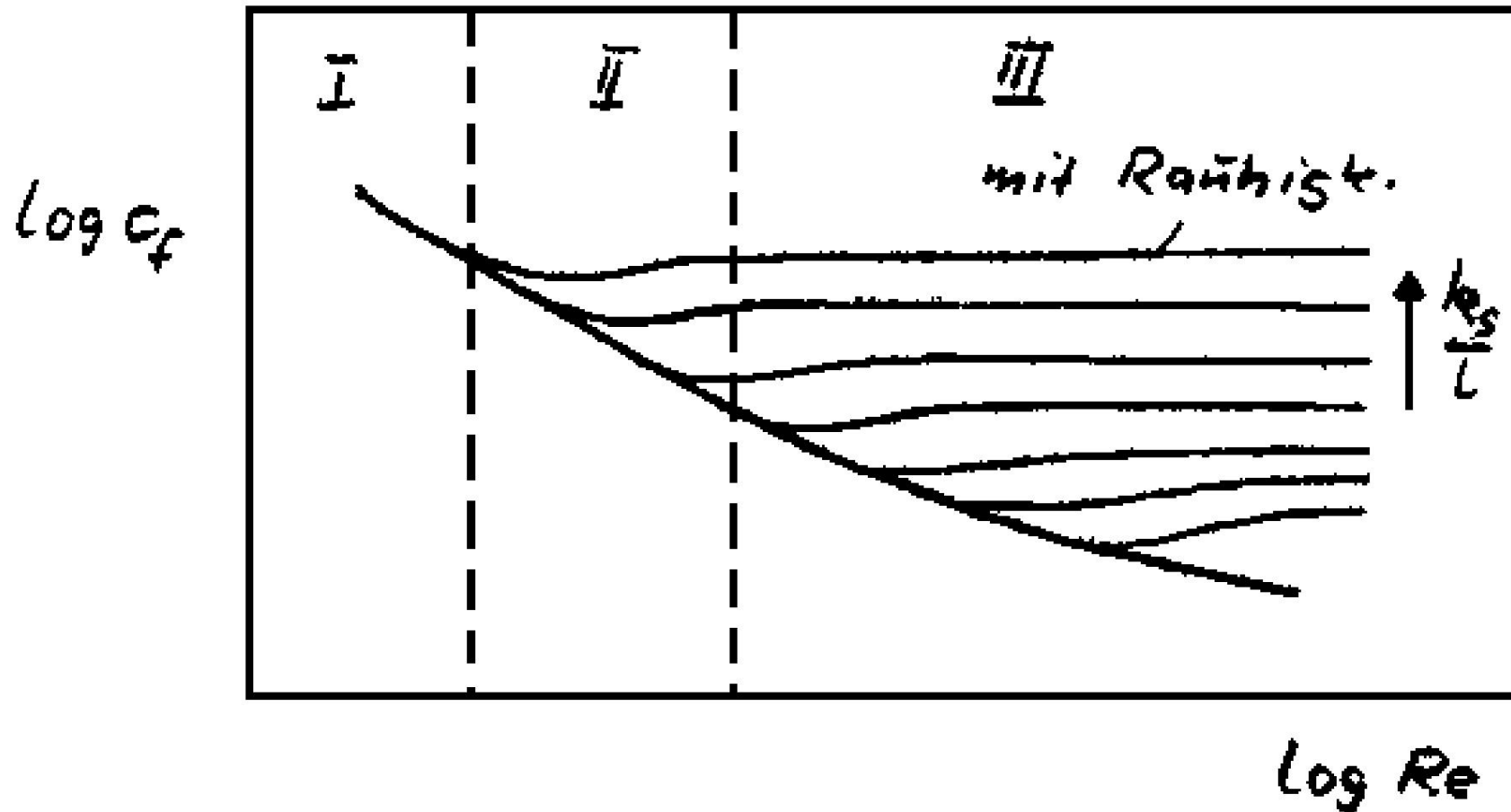
## 1.3.2 Influence of wall roughness

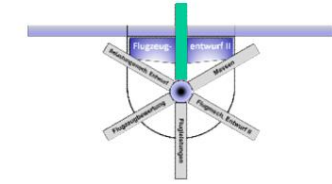
- In practice, the hydraulically smooth surface assumed in the resistance theory of the washed, flat plate will usually not be encountered
- Then the influence of roughness must be considered separately.
- If the roughness value  $ks/l$  exceeds the displacement thickness of a laminar boundary layer, a transition occurs and the friction coefficients increase.
- If the roughness value  $ks/l$  is lower, the roughness has no influence on the frictional resistance of the laminar boundary layer.
- The turbulent boundary layer reacts much more sensitively to roughness.
- As long as the roughness value  $ks/l$  is within the laminar sublayer of the boundary layer, the plate is considered hydraulically smooth and the turbulent friction coefficient is at a minimum. The permissible roughness value must be  $< 100/Re$ .



## D Basics of aerodynamic design 1.3.2 Influence of wall roughness

- Influence of roughness on the friction coefficient

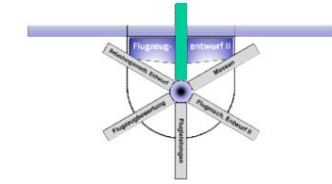




# D Basics of aerodynamic design

## 1.3.2 Influence of wall roughness

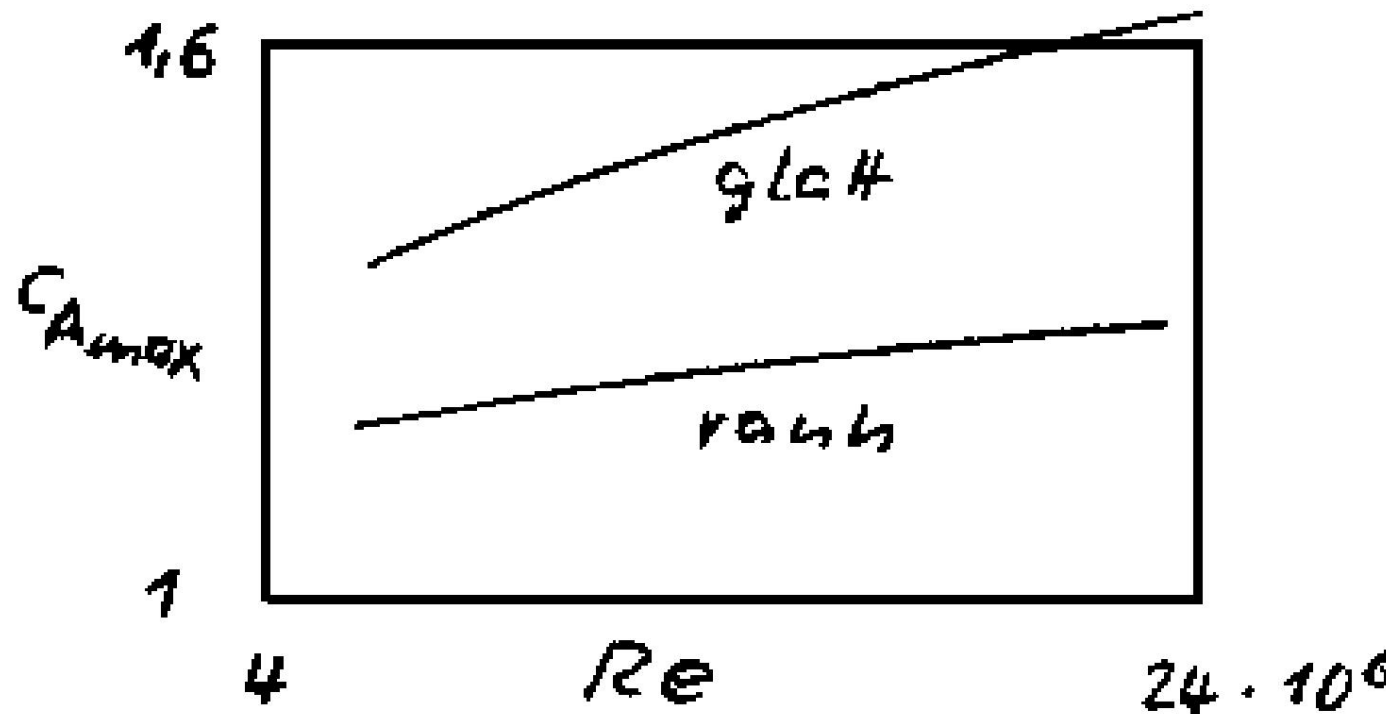
- At the low Re numbers in area I, the roughness has no influence on the coefficient of friction. This is only determined by the Re number.
- In area III only the roughness measure influences the size of the friction coefficient and the Re number influence disappears.
- Area II is a transition area in which both parameters have an influence.
- To illustrate the practical relevance of the influence of friction, the critical roughness depth can be calculated for the flight conditions of a typical commercial aircraft.
- This results in a value of approx. 0.02 mm, which is technically feasible.

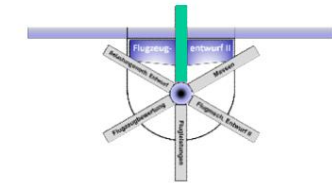


# D Basics of aerodynamic design

## 1.3.2 Influence of wall roughness

- The roughness also affects the maximum lift parts.
- The level of the maximum lift coefficient, which increases with the Re number, decreases significantly by approx. 15 - 20%.





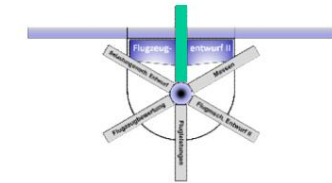
# D Basics of aerodynamic design

## 1.3.2 Influence of wall roughness

- The profile resistance consists of a friction and a pressure resistance component.
- In the coefficient notation, for a profile of finite thickness, which is flowed in the direction of minimum resistance, can be written:

$$c_{w \min p} = 2 c_{\text{profile}} k_y$$

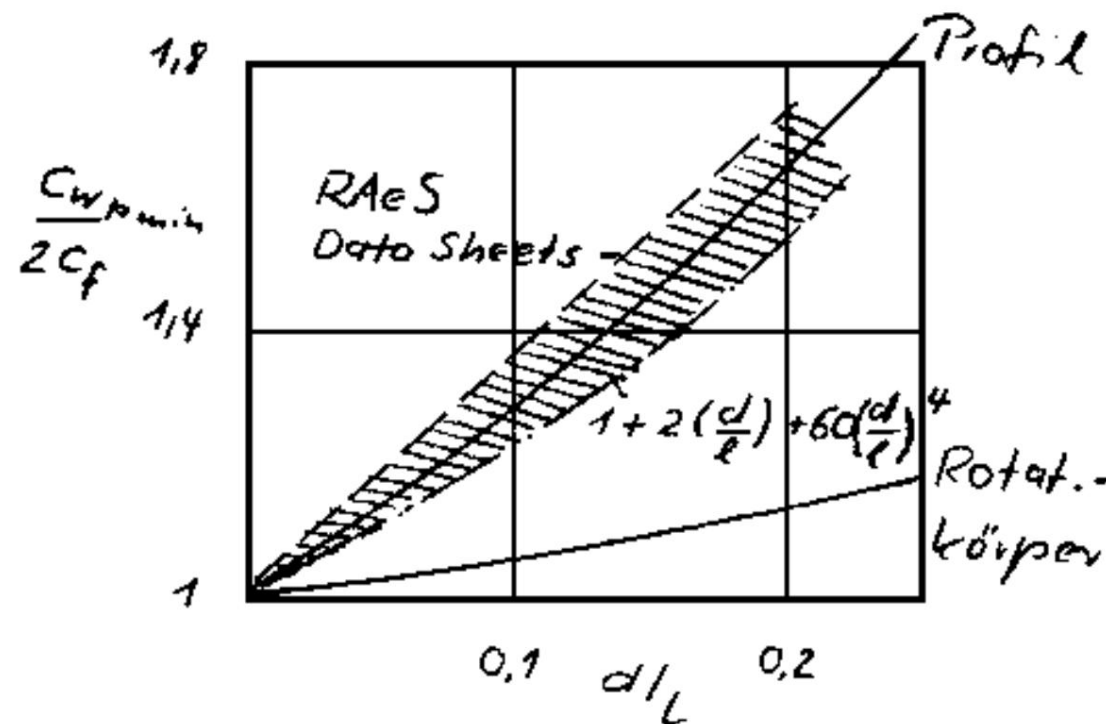
- The factor “2” describes the body with two-sided flow, e.g. a wing •  
The parameter “k”  
stands for the pressure drag coefficient  
which depends to a large extent on the profile thickness as well as  
on the profile type (detachment mechanisms, see above).

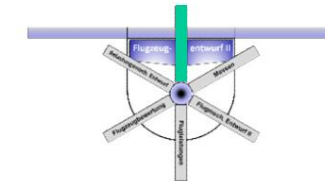


# D Basics of aerodynamic design

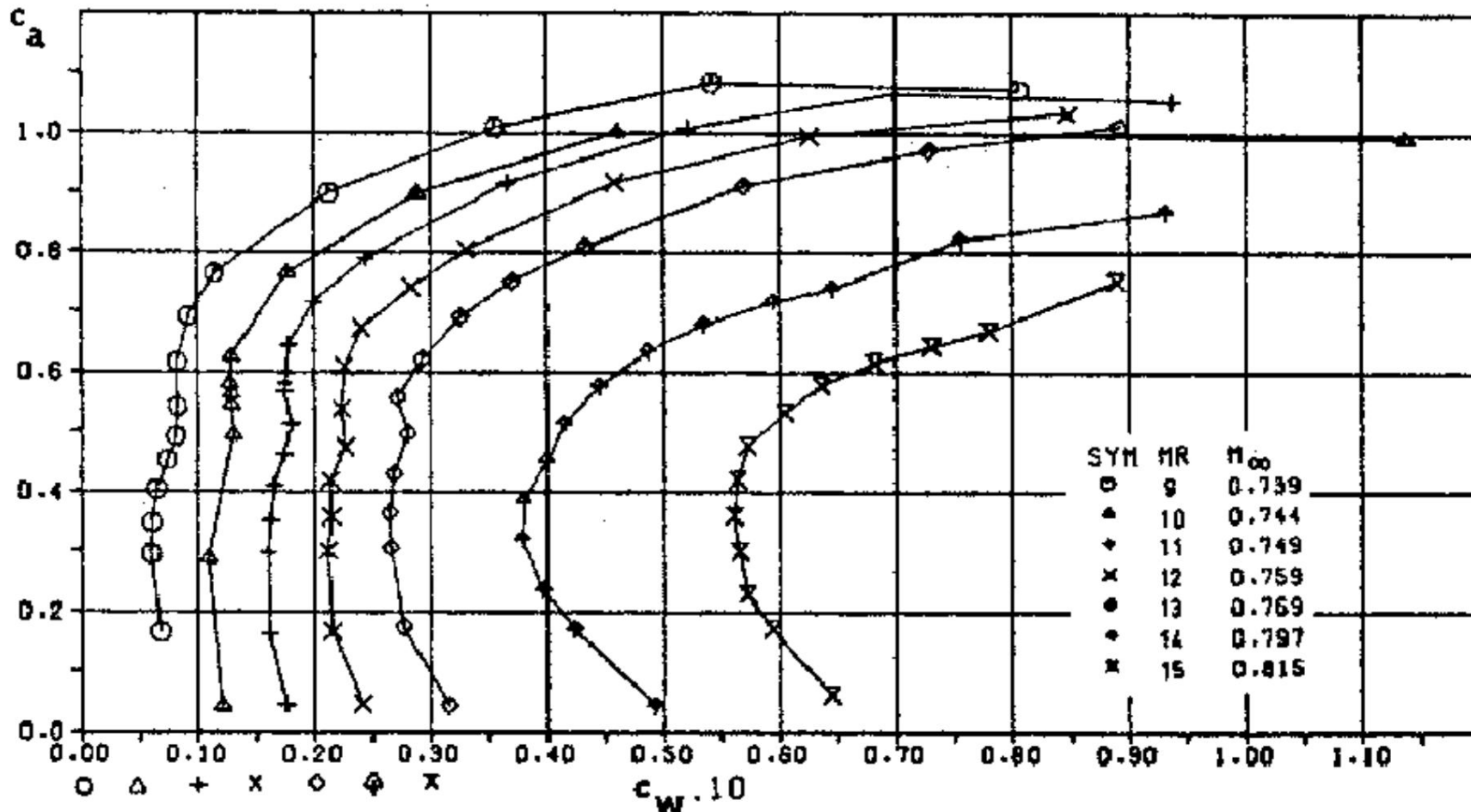
## 1.3.2 Influence of the Reynolds number

- In the additional comparison given here between a profile and a rotating body (e.g. fuselage, nacelle), it becomes clear that the lack of pressure equalization across the third dimension in a planar structure such as a wing leads to the high pressure drag differences.

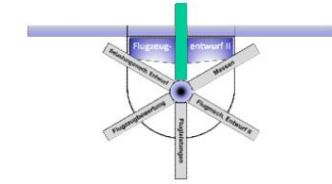




## D Basics of aerodynamic design 1.3.2 Influence of the Reynolds number • Drag polar, profile VA2, $d/l = 13\%$



Attention: Polars have a shifted origin due to small differences.



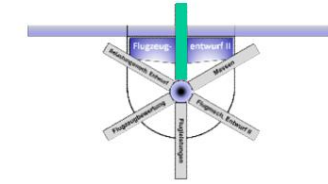
# D Basics of aerodynamic design

## 1.3.2 Influence of the Reynolds number

- A suitable equation for determining the profile polar can only be obtained if an approach for the dependence on the lift coefficient is found that describes the curvature of the drag increase accurately enough.
- For a modern profile (VA2,  $d/l = 13\%$ ), a good result for the incompressible region can be achieved with the approximation

$$C_{\text{yy}} \approx C_{\text{yy}}^{\text{incomp}} + 0.03c^{\frac{k_e}{a}}$$

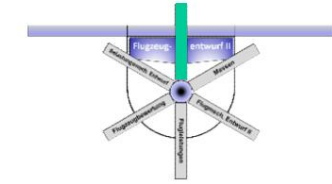
- The specified set of polars for the profile are measured values that were determined for different Mach numbers.
- The almost constant in the lower  $ca$  range, in the upper However, the strongly kinking course of the incompressible polar is well approximated with the exponent  $k_e = 6$ .



# D Basics of aerodynamic design

## 1.3.3 Influence of the Mach number

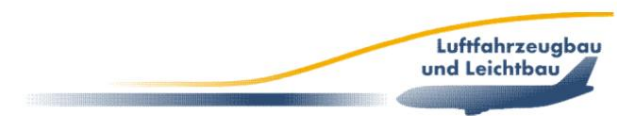
- So far, the interaction of the profile geometry parameters and the Re number with the aerodynamic properties has been discussed.
- It was found that the cruise and the Take-off and landing requirements are contradictory, which is expressed, among other things, by the drag advantage of a thin profile and its poor stalling properties. • If one leaves the area of incompressible flows and looks at the high subsonic range (close to the transonic range) that is of interest to commercial aviation, one must also include the influence of the Mach number in the design considerations.

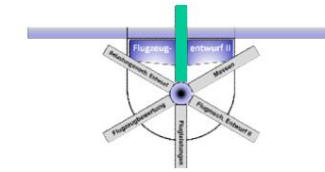


# D Basics of aerodynamic design

## 1.3.3 Influence of the Mach number

- Basically, the local attainment of the speed of sound on the profile is decisive for the dependence of the coefficients on the Mach number.
- The Mach number at which this condition is just reached is the critical Mach number.





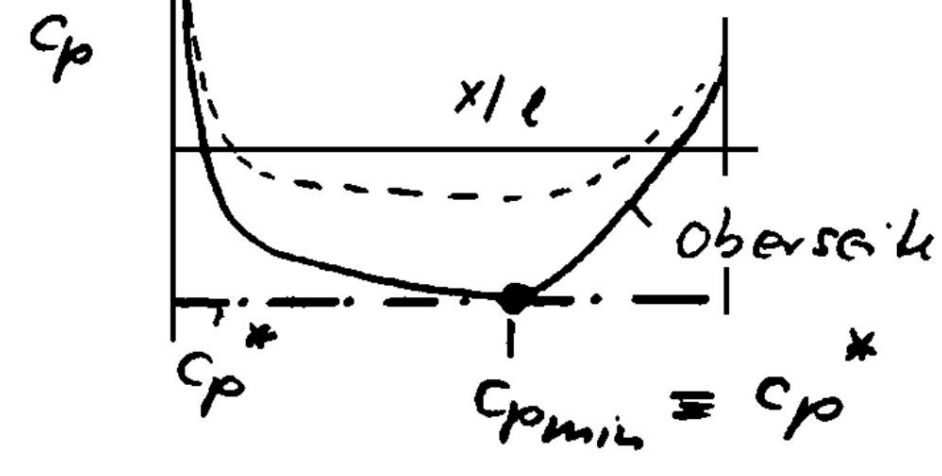
# D Basics of aerodynamic design

## 1.3.3 Influence of the Mach number

- The critical pressure coefficient can generally be formulated for a medium with the isentropic exponent  $k$  (gas constant, for air at ISA: approx. 1.4) as follows:
- ÿ ÿ ÿ ÿ ÿ ÿ

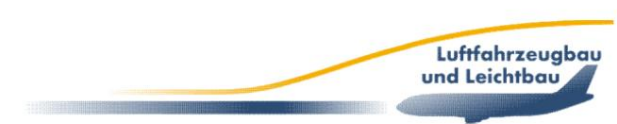
$$c_p = \frac{2}{k + 1} \left( \frac{2}{M^2} - \frac{1}{k+1} \right)^{\frac{1}{k-1}} \quad M = \sqrt{\frac{2}{k+1} \left( 1 - \frac{1}{M^2} \right)}$$

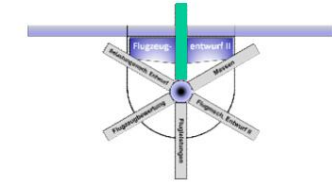
$c_{p, \text{crit}} = c_p^*$



- Is a pressure distribution in incompressible flow possible? known, it can be converted into the compressible pressure distribution using the Prandtl-Glauert factor.

$$c_p = \frac{c_{p, \text{ic}}}{\sqrt{1 + \frac{2}{M^2}}}$$

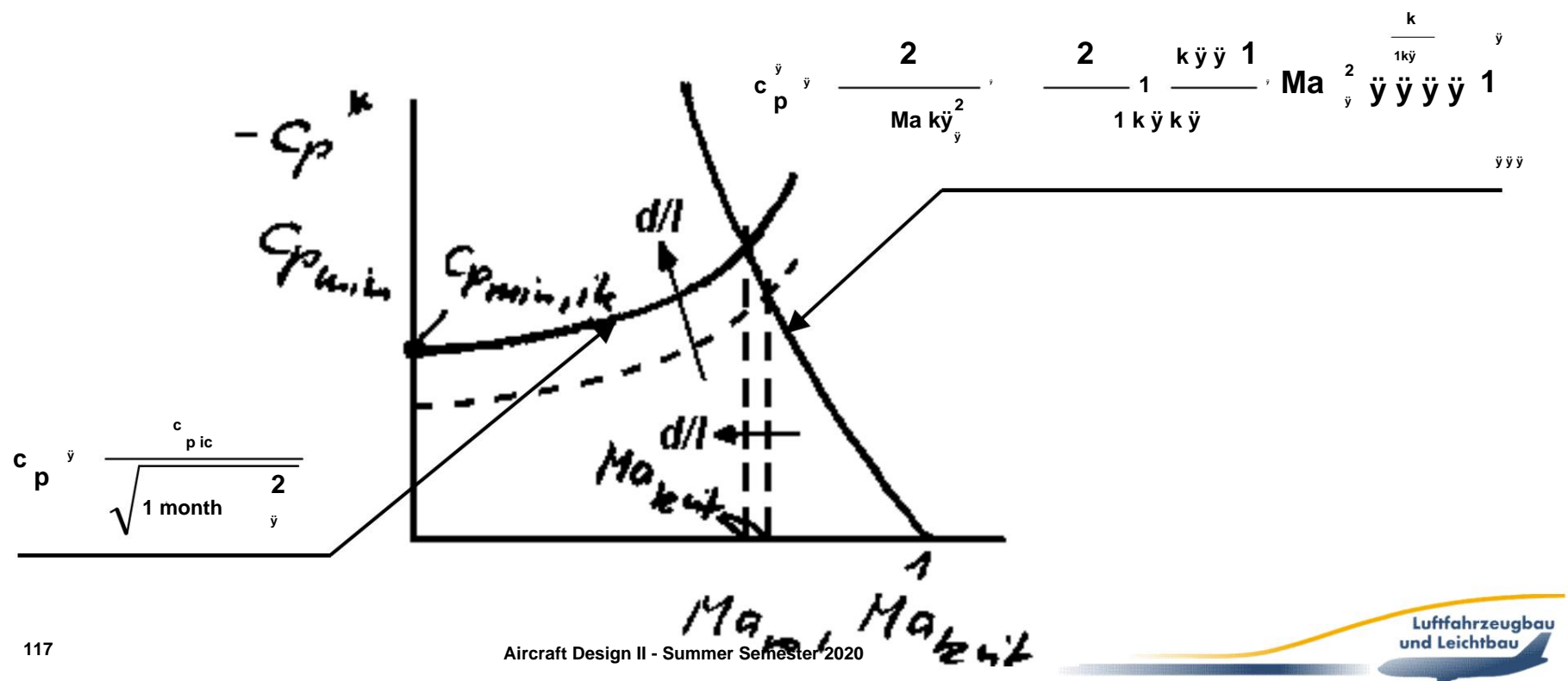


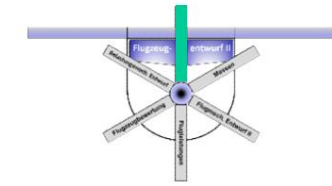


# D Basics of aerodynamic design

## 1.3.3 Influence of the Mach number

- The Mach number therefore causes an increase in the pressure coefficients. Starting from a known incompressible, minimum pressure coefficient, the critical Mach number can now be determined as the intersection point of the compressible profile pressure coefficient with the critical pressure coefficient.



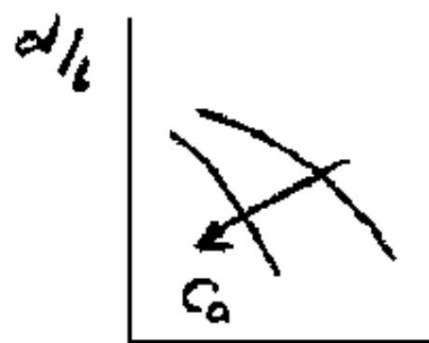


# D Basics of aerodynamic design

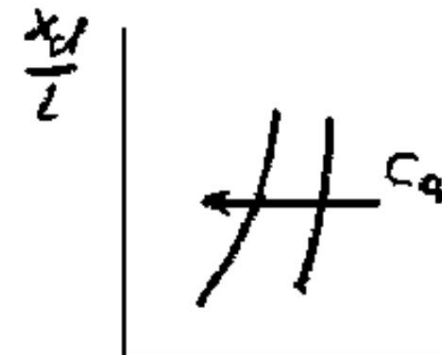
## 1.3.3 Influence of the Mach number

- The minimum pressure coefficient is determined by the profile geometry parameters profile thickness, thickness offset and camber.

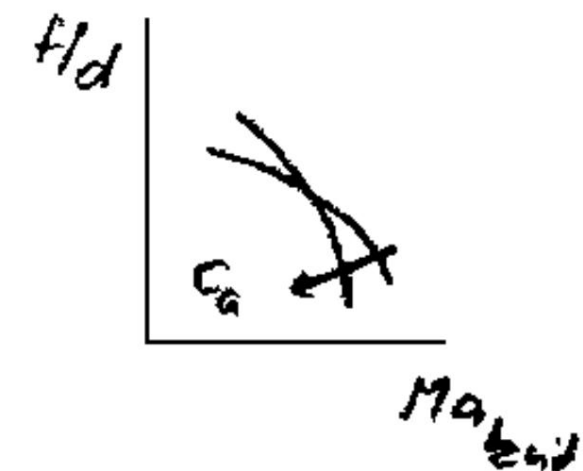
Profilabdrucke

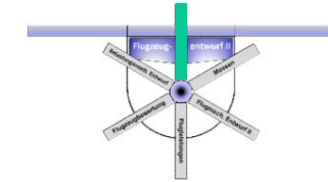


Dickenwindlage



Wölbung

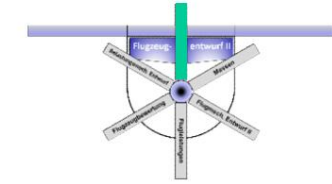




# D Basics of aerodynamic design

## 1.3.3 Influence of the Mach number

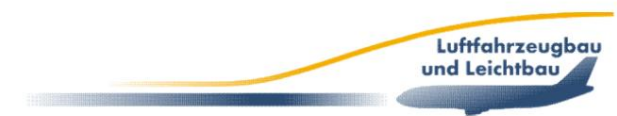
- As the profile thickness increases, the critical Mach number decreases. However, this influence is reduced with increasing angle of attack due to the much greater influence of the suction tip that forms.
- Thickness setback has an increasing influence on the critical Mach number. This trend increases with increasing angle of attack, but at a lower level.
- An increase in the curvature generally has a reduction of the critical Mach number, although the influence of the angle of attack on the pressure distribution causes a shift of the pressure minimum and thus an overlapping characteristic.



# D Basics of aerodynamic design

## 1.3.3 Influence of the Mach number

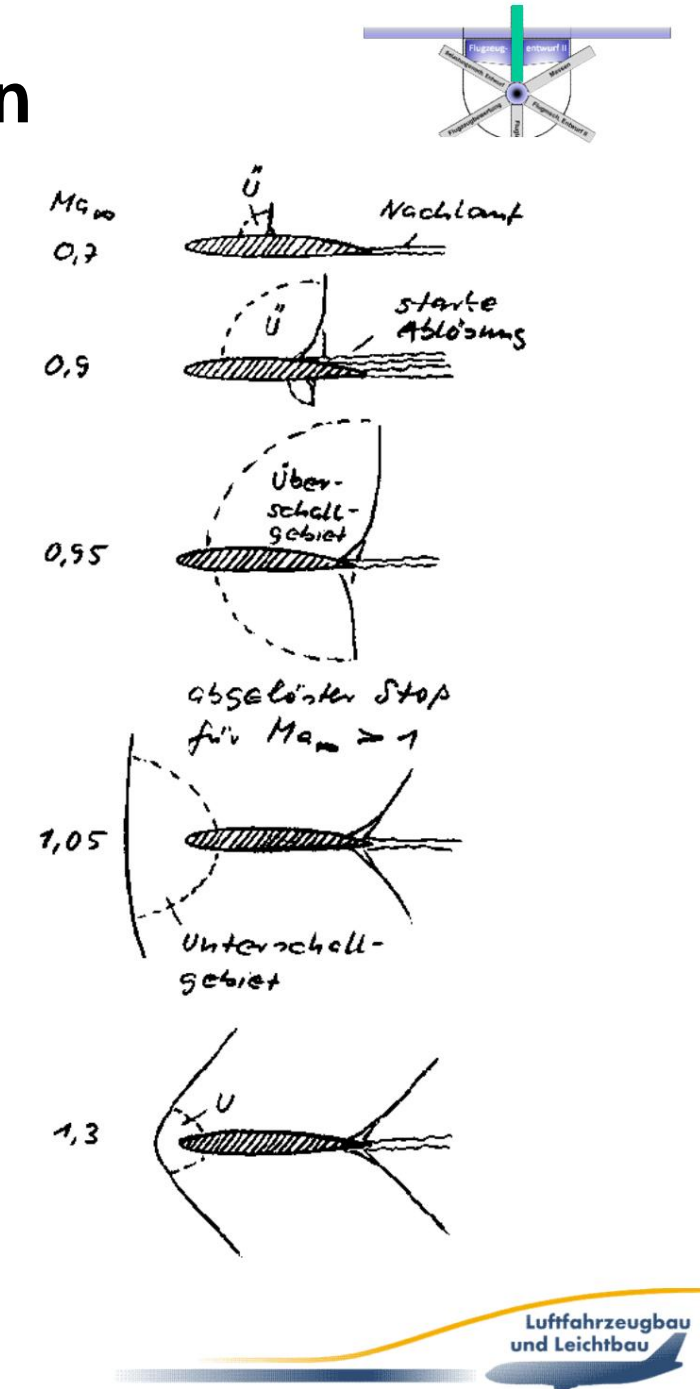
- The existence of supersonic regions on the profile is associated with the occurrence of shock waves.
- The speed decreases spontaneously when passing the shock, the air density and pressure increase and part of the kinetic energy is converted into heat (dissipation).
- In a flow with shock waves, an increase in entropy or a reduction in flow energy will always be observed.
- To form the impact, part of the energy must be converted into a non-exploitable form, the equivalent of which is an increase in resistance.

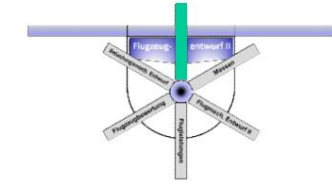


# D Basics of aerodynamic design

## 1.3.3 Influence of the Mach number

- Since the critical Mach number for typical profiles is usually less than  $Ma = 0.7$ , a weak compression shock already occurs at this Mach number.
  - As the supersonic region becomes larger, the shock shifts further and further to behind and is increasing in strength.
  - A strong separation can be seen at  $Ma = 0.9$ . This is associated with a strong increase in drag.
  - Qualitatively, the images in the supersonic range differ only in the Mach angle of the head impact.
- 121

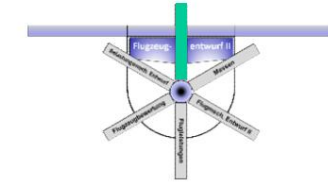




# D Basics of aerodynamic design

## 1.3.3 Influence of the Mach number

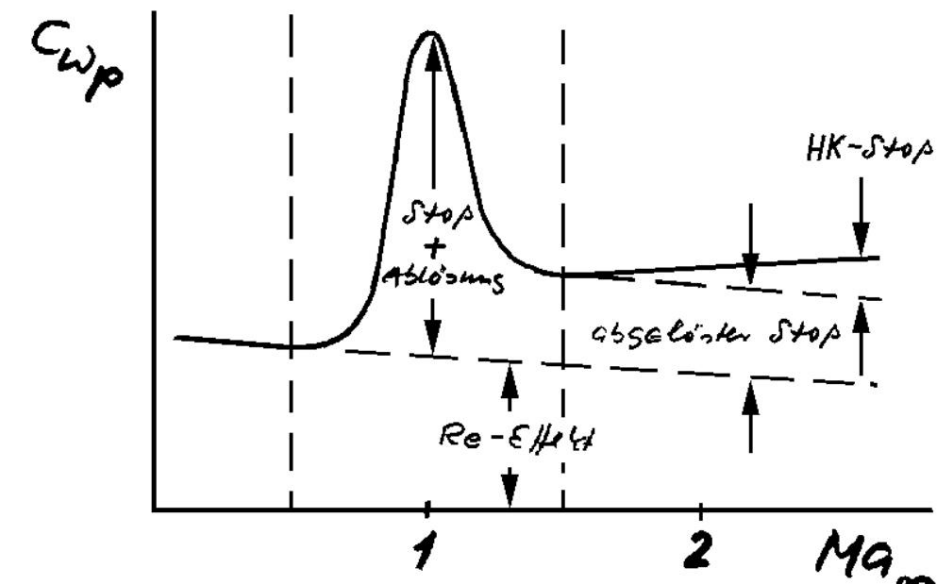
- Measurements of the transonic drag show that the drag is greater than the energy loss due to the shock. The reason for this is the interaction between the shock and boundary layer separation due to the large pressure increase in the shock and the associated backflow near the wall.
- The transonic resistance, also called wave resistance, is composed of
  - the resistance resulting from the formation of the shock wave and
  - the additional drag resulting from boundary layer separation.

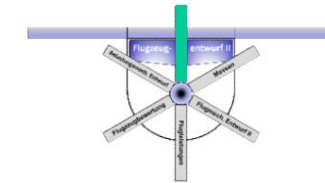


# D Basics of aerodynamic design

## 1.3.3 Influence of the Mach number

- The resistance basis represents the Re number-dependent component, which is effective in the entire speed range.
- In addition, the resistance in the transonic range shock formation and shock-induced boundary layer separation.
- In the supersonic range initially only the energy needed to form a headbutt needs to be applied.
- With further increase in Ma the dissipation due to the collisions increases and the boundary layer separation disappears.





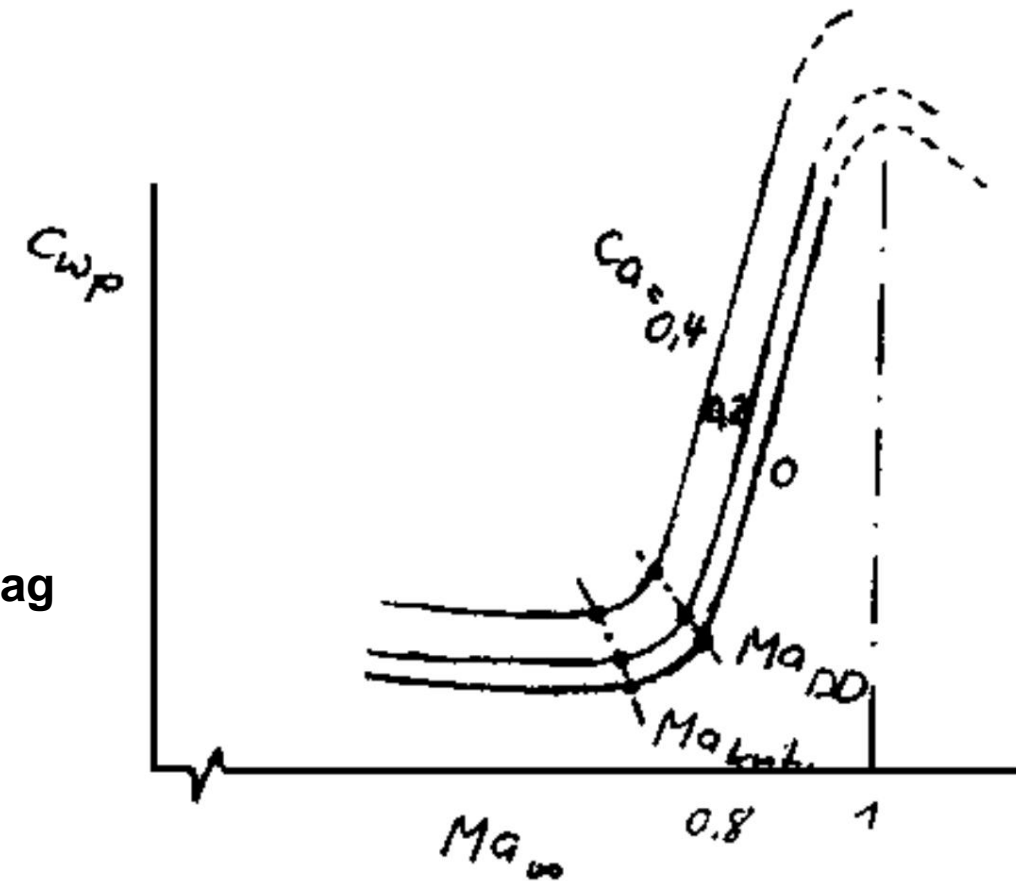
# D Basics of aerodynamic design

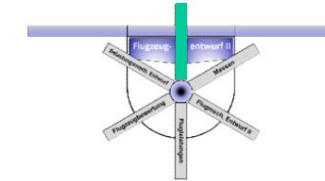
## 1.3.3 Influence of the Mach number

- The critical Mach number is significantly lower than the Mach number of the drag increase

**MaDD**

- MaDD is defined to have a drag increment of 0.002 to the minimum drag coefficient.

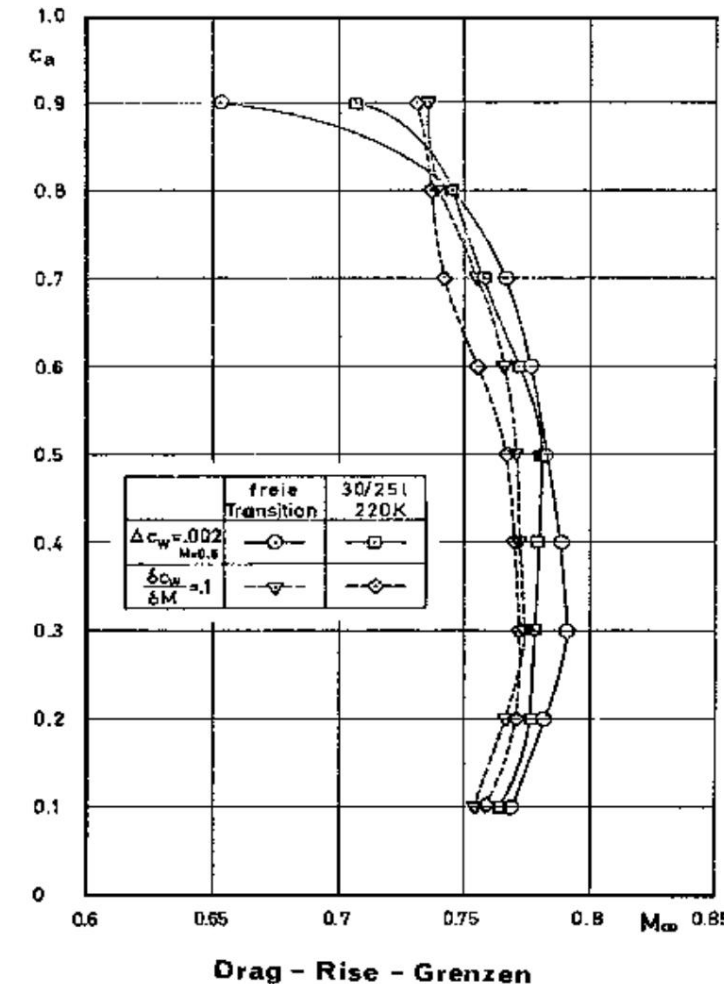




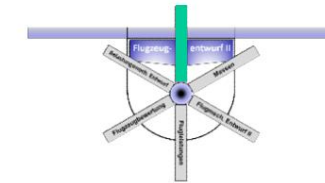
# D Basics of aerodynamic design

## 1.3.3 Influence of the Mach number

- Since the resistance increase also depends slightly on the position of the transition point, this limit is usually given for a realistic transition point and for the free transition, whereby the forced transition is brought about by sanding with a specified grain size (here 220).



**Profile VA2,  $d/l = 13\%$**



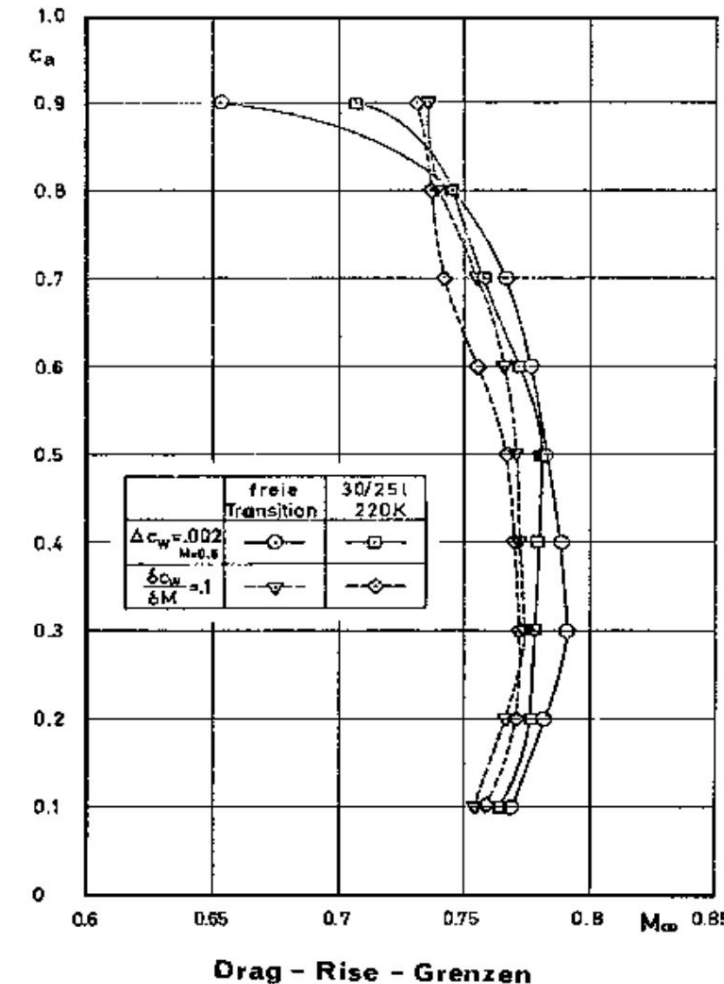
# D Basics of aerodynamic design

## 1.3.3 Influence of the Mach number

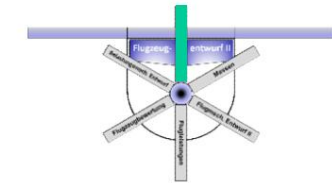
- The definition of the contradiction

The stand rise Mach number with a cw increment of 0.002 is quite arbitrary.

- Another definition used in practice is the resistance gradient of  $dc_w/dM_a = 0.1$ .

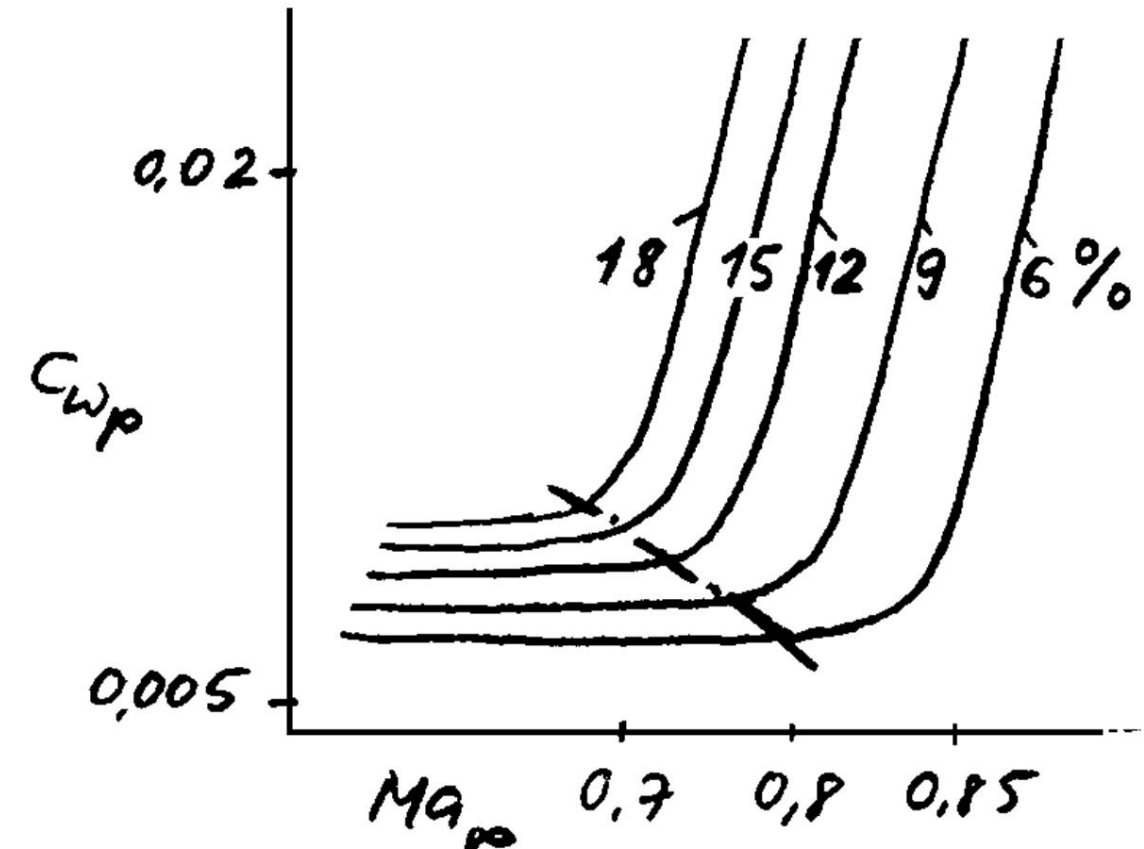


Profile VA2,  $d/l = 13\%$

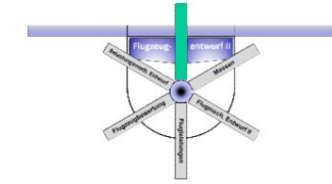


# D Basics of aerodynamic design

## 1.3.3 Influence of the Mach number



- An increased profile thickness not only increases the profile drag, but also shifts the drag increase Mach number to smaller values.



# D Basics of aerodynamic design

## 1.3.3 Influence of the Mach number

- The Mach number also influences the lift behavior of the profile in the same way as the pressure coefficient.
- The incompressible buoyancy increase can be determined using the Prandtl-Glauert transformation can be converted into the compressible value in the same way as the lift coefficient, since both quantities result directly from integration of the pressure curve.

- There

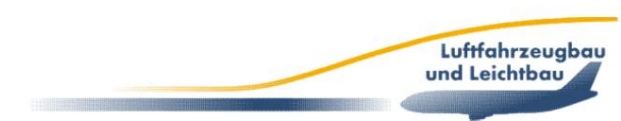
therefore also applies

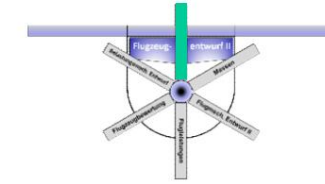
$$c_p \frac{c_{p_{ic}}}{\sqrt{1 + \frac{2}{M^2}}}$$

$$c_a \frac{c_{a_{ic}}}{\sqrt{1 + \frac{2}{M^2}}}$$

as well as

$$c_a \frac{c_{a_{ic}}}{\sqrt{1 + \frac{2}{M^2}}}$$

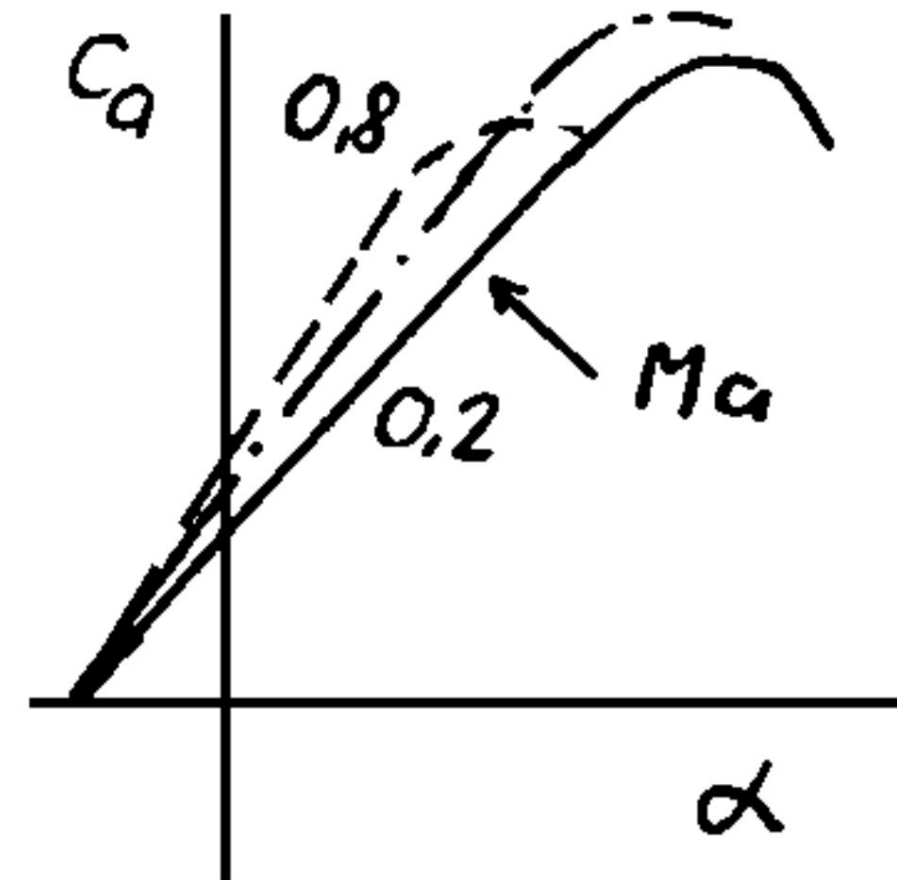


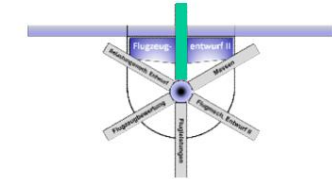


# D Basics of aerodynamic design

## 1.3.3 Influence of the Mach number

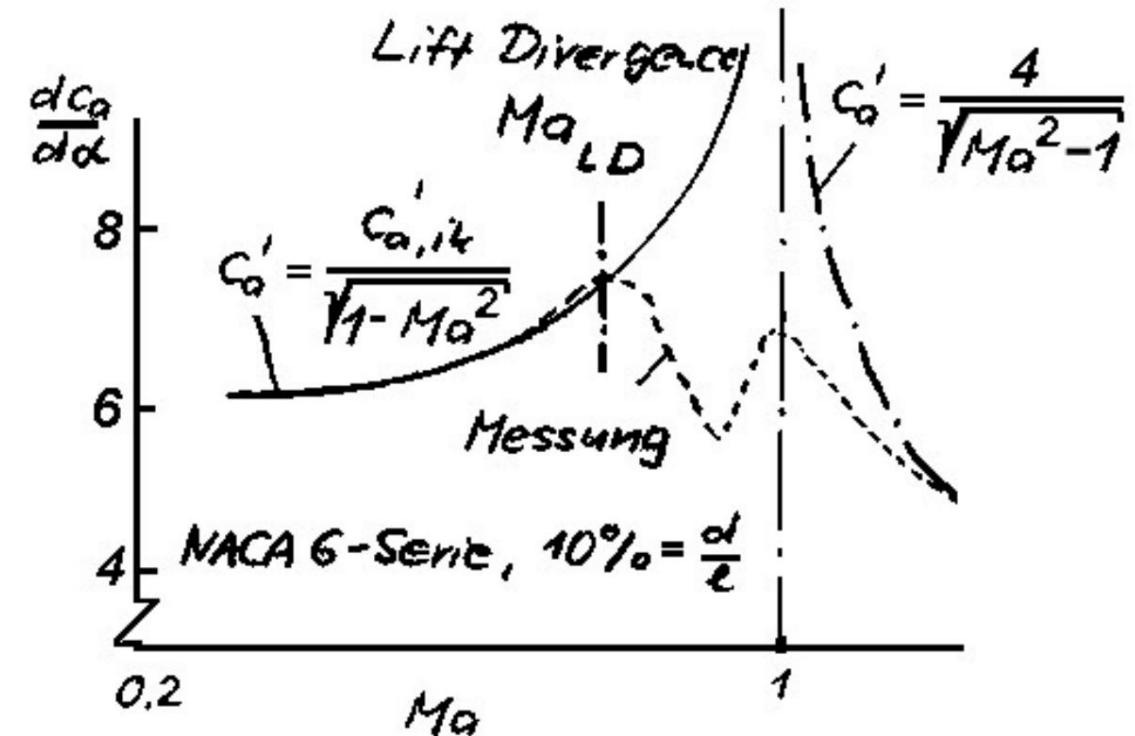
- Based on the resolved Polar can be this  
Influence very clearly recognizable  
nen.
- The polar becomes steeper  
with increasing Mach number.
- The maximum lift initially  
improves as a result of the  
increasing Re number, but  
then decreases again  
significantly due to the  
shock-induced separation.



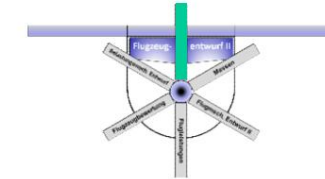


# D Basics of aerodynamic design

## 1.3.3 Influence of the Mach number



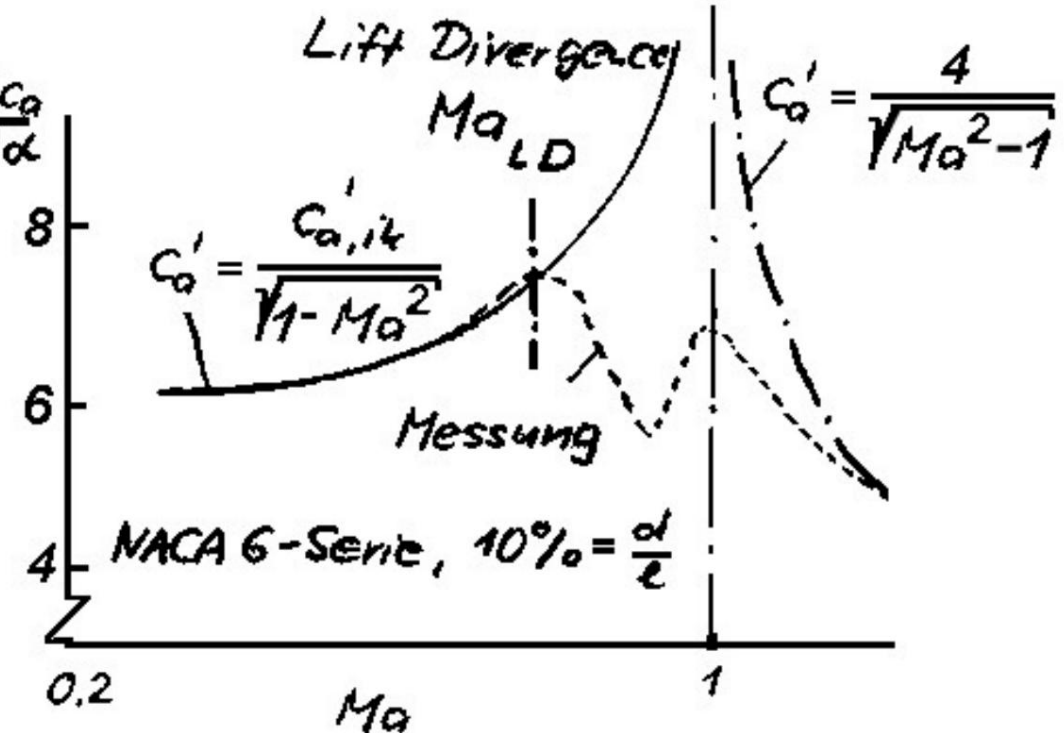
- If the Mach number is kept constant at the angle of attack
- If the aircraft is increased into the transonic region, the lift is initially increased further according to the similarity rule mentioned above until a sudden drop in lift occurs as a result of a shock occurring on the underside.



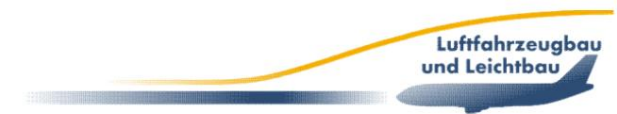
# D Basics of aerodynamic design

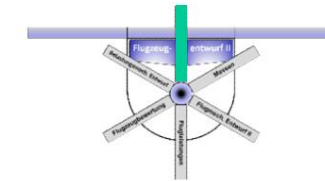
## 1.3.3 Influence of the Mach number

- The Mach number at which this loss of lift occurs (Lift Divergence) represents the boundary between subsonic and transonic ranges.



- In transonics, the change of sign of  $dC_L/dMa$  leads to Longitudinal motion instabilities, which makes it necessary for supersonic aircraft to accelerate through this phase of flight as quickly as possible (afterburner).



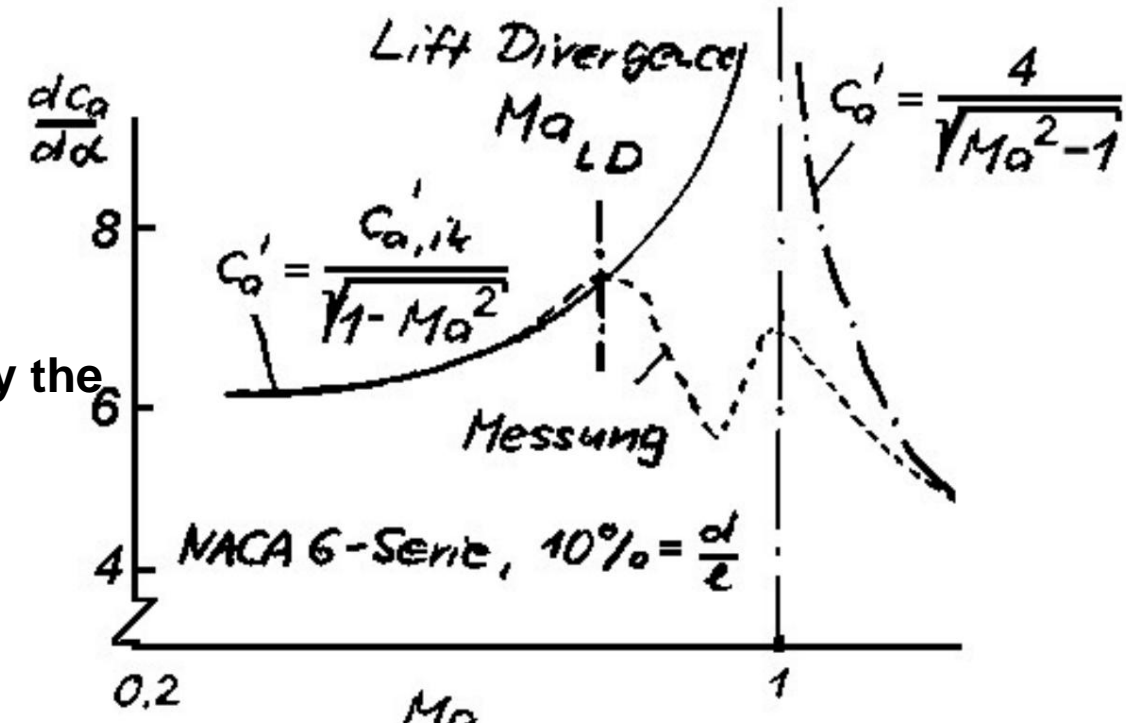


# D Basics of aerodynamic design

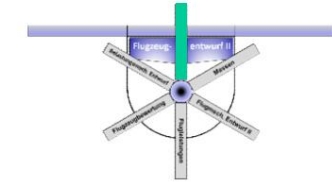
## 1.3.3 Influence of the Mach number

- The falling branch of the lift increase in the supersonic range ( $Ma > 1.2$ ) is sufficiently accurately determined by the Ackeret's relationship described:

$$C_a = \frac{4}{\sqrt{M_a^2 - 1}}$$



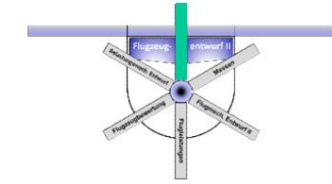
- In the same way as the lift increase, the momentum increase  $\dot{y}_{cm}$  /  $\dot{y}_a$  influenced by the Mach number.



# D Basics of aerodynamic design

## 1.3.3 Influence of the Mach number

- The strong compression shocks and the associated flow separations in the high subsonic range are of great importance for the maneuvering flight of an aircraft and thus for the design point.
- The boundary layer separation results in a wide wake with intensive pressure fluctuations, because shock formation and separation oscillate around a central position, which may lead to high structural loads, but always to shaking of the aircraft.
- The associated limit, the buffet on-set limit, must therefore not be reached in stationary flight, which must be ensured by design (see construction regulations CS 25).



# D Basics of aerodynamic design

## 1.3.3 Influence of the Mach number

Since this phenomenon of the shaking limit is just like

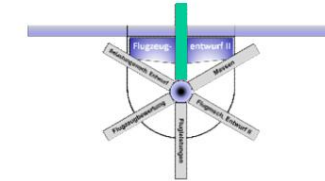
- the critical Mach number,
- the "Lift Divergence" and
- the "drag-divergence" Mach number

with the size of the local pressure coefficients and these are primarily related to

- the angle of attack,
- the profile thickness and
- the curvature,

all these parameters also influence the occurrence of "buffering".



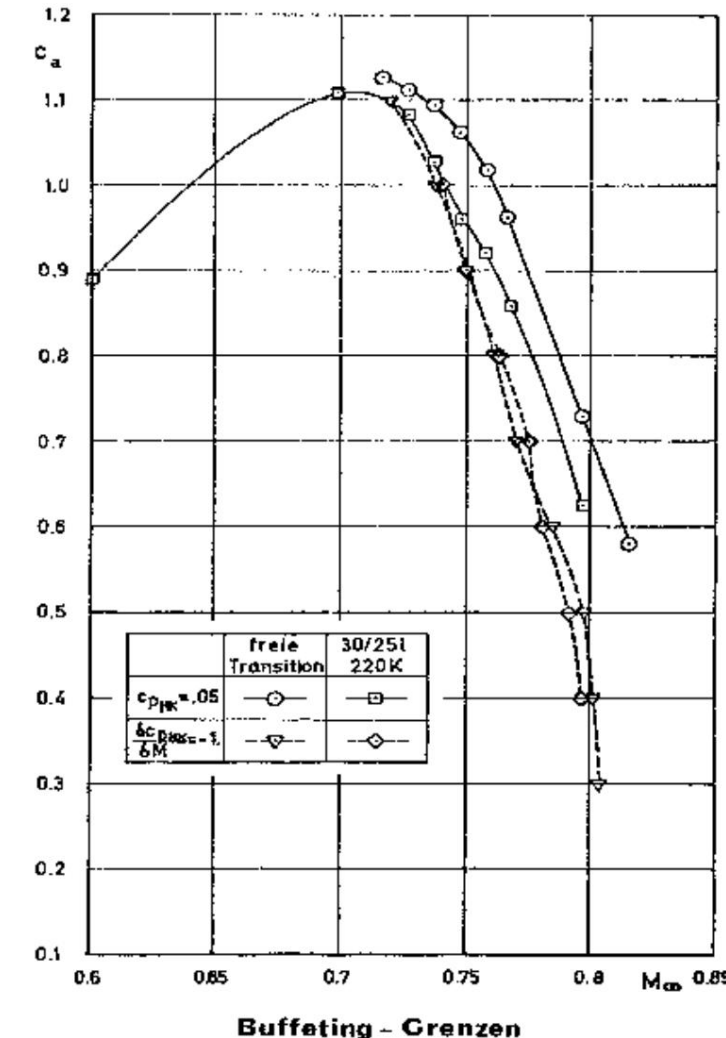


# D Basics of aerodynamic design

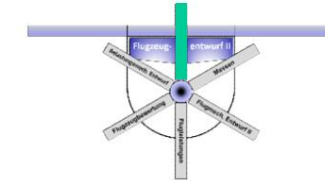
## 1.3.3 Influence of the Mach number

- Since the shaking limit is measurable is technically very difficult to determine, two different measurement values have been agreed upon for its definition. •

This limit is identified as having been reached when the trailing edge pressure coefficient reaches 0.05.



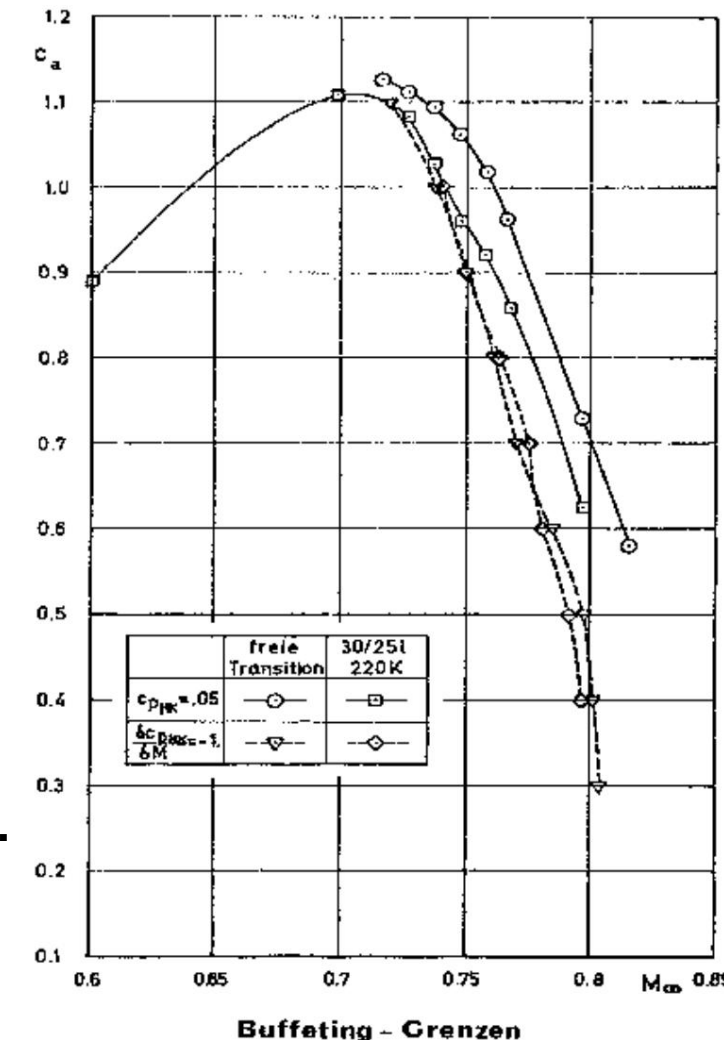
Profile VA2,  $d/l = 13\%$



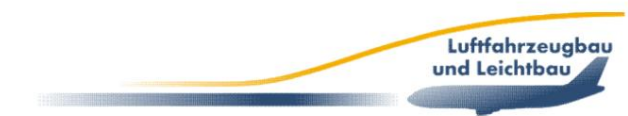
# D Basics of aerodynamic design

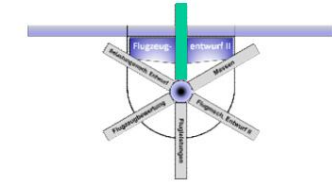
## 1.3.3 Influence of the Mach number

- On the other hand, the change  
Trailing edge pressure  
with the Mach number taken  
as a definition measure.
- If this size has the value -1  
reached, it is called buffet on-set.
- Here, too, the position of the  
transition point plays a role, since  
boundary layer separation can be  
avoided in turbulent boundary layers.



Profile VA2,  $d/l = 13\%$

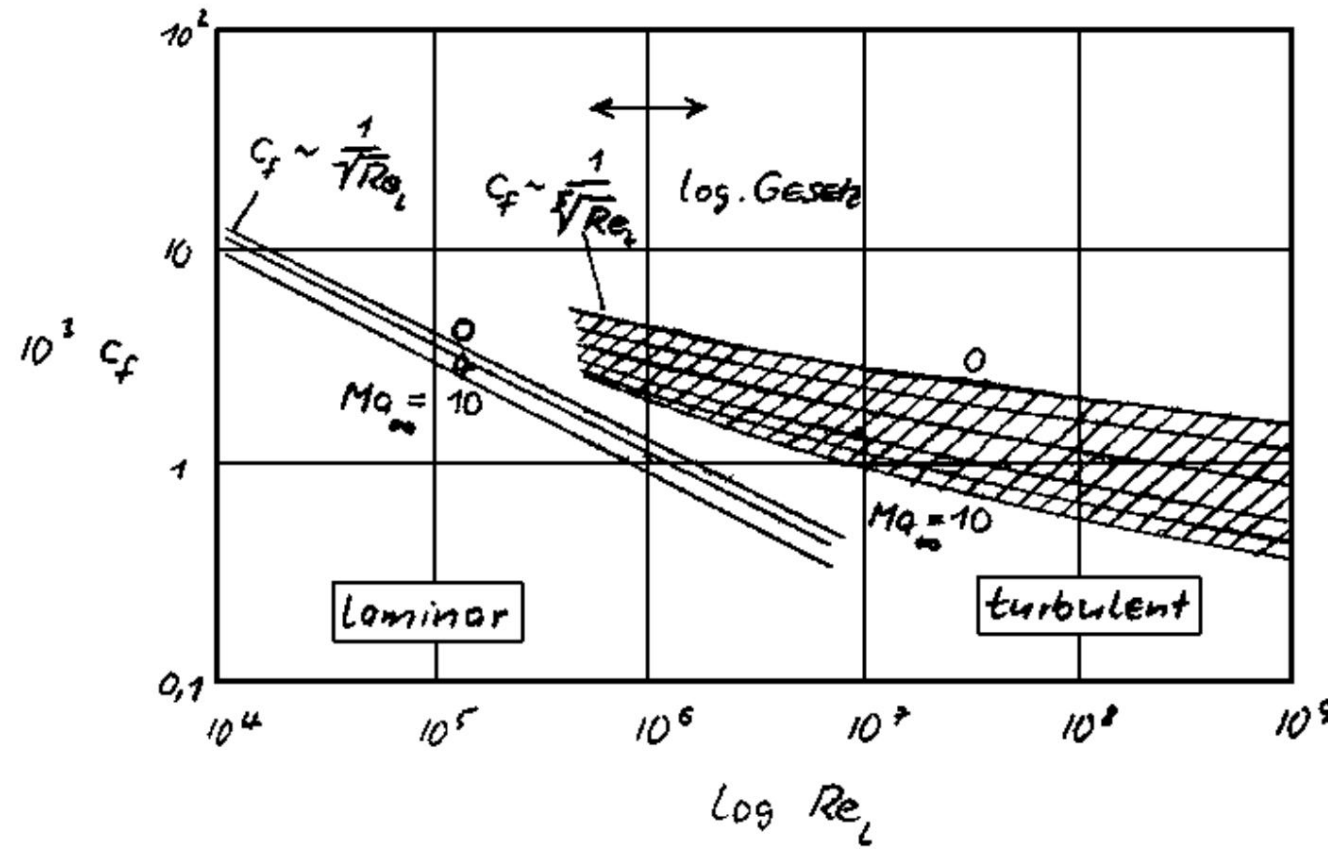


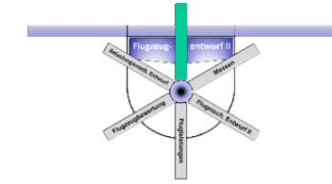


# D Basics of aerodynamic design

## 1.3.3 Influence of the Mach number

- The Mach number also has a not insignificant influence on the friction coefficient when looking at measurement results of a flat plate.





# D Basics of aerodynamic design

## 1.3.3 Influence of the Mach number

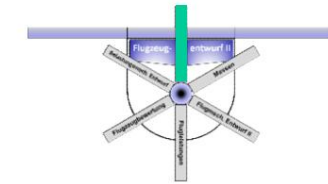
- This assumes a heat-impermeable (adiabatic) wall, i.e. vanishing heat transfer.
- Estimation of the influence in subsonic mode:

$$\frac{c_e}{c_{e_{ic}}} \approx 1 \text{ for } Ma < 1$$

$$\frac{c_e}{c_{e_{ic}}} = \frac{1}{\sqrt{1 + 0.15 Ma^2}}$$

- for  $Ma > 1$ :

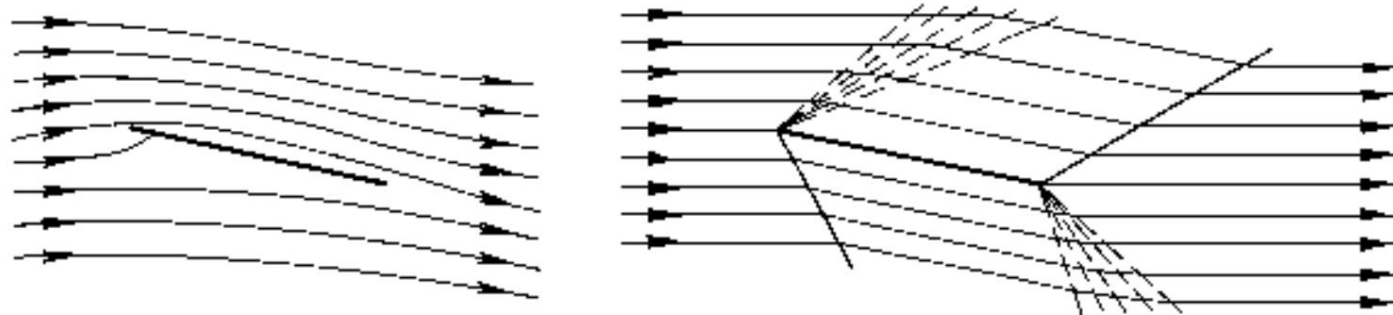
- The reference value in both cases is the incompressible Friction coefficient at  $Ma = 0$ .
- The influence of the Mach number can be changed by heating and cooling the structure (see aero-thermodynamics).



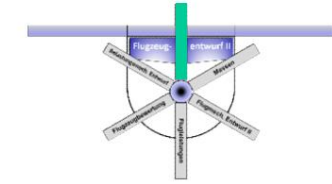
# D Basics of aerodynamic design

## 1.3.3 Influence of the Mach number

- The neutral point position changes only slightly up to the lift divergence Mach number.
- In the higher Mach number range around  $M \approx 1$ , the flow conditions are fundamental.



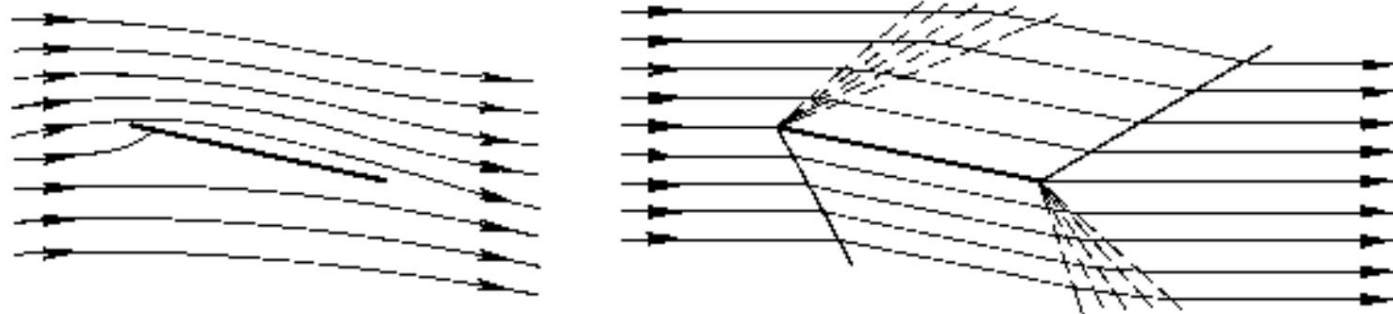
- In supersonic flow, an expansion fan is created at the leading edge at the top and an oblique compression shock at the bottom.
- Both ensure that the flow is diverted in the direction of the plate becomes.
- At the trailing edge, a compression shock on the upper side and an expansion fan on the lower side restore the original flow direction.

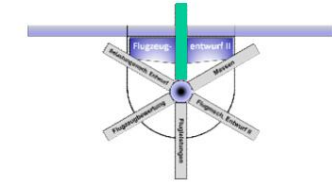


# D Basics of aerodynamic design

## 1.3.3 Influence of the Mach number

- In contrast to subsonic flow, the inflow and outflow directions are therefore exactly the same immediately behind the profile.

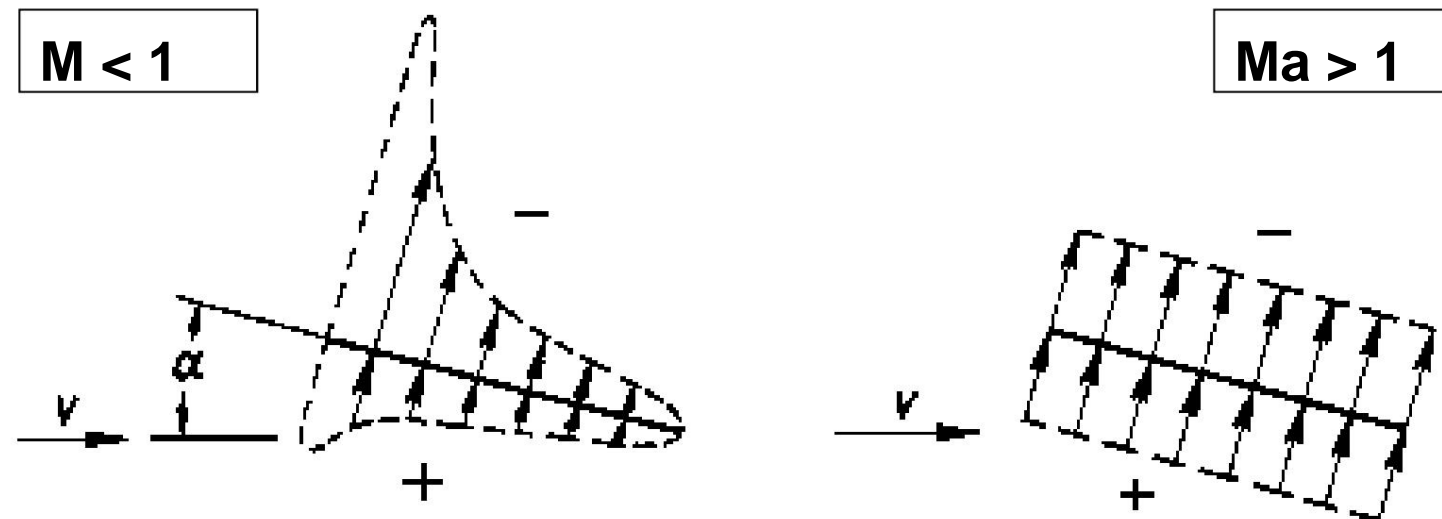


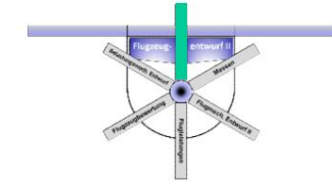


# D Basics of aerodynamic design

## 1.3.3 Influence of the Mach number

- In supersonic flow, there is a constant negative pressure along the profile depth on the upper side of the plate and a constant positive pressure on the underside.
- The constant pressure distribution therefore provides a  
The air force resultant is independent of the angle of attack  
and therefore acts at a fixed pressure point in the centre of the plate.

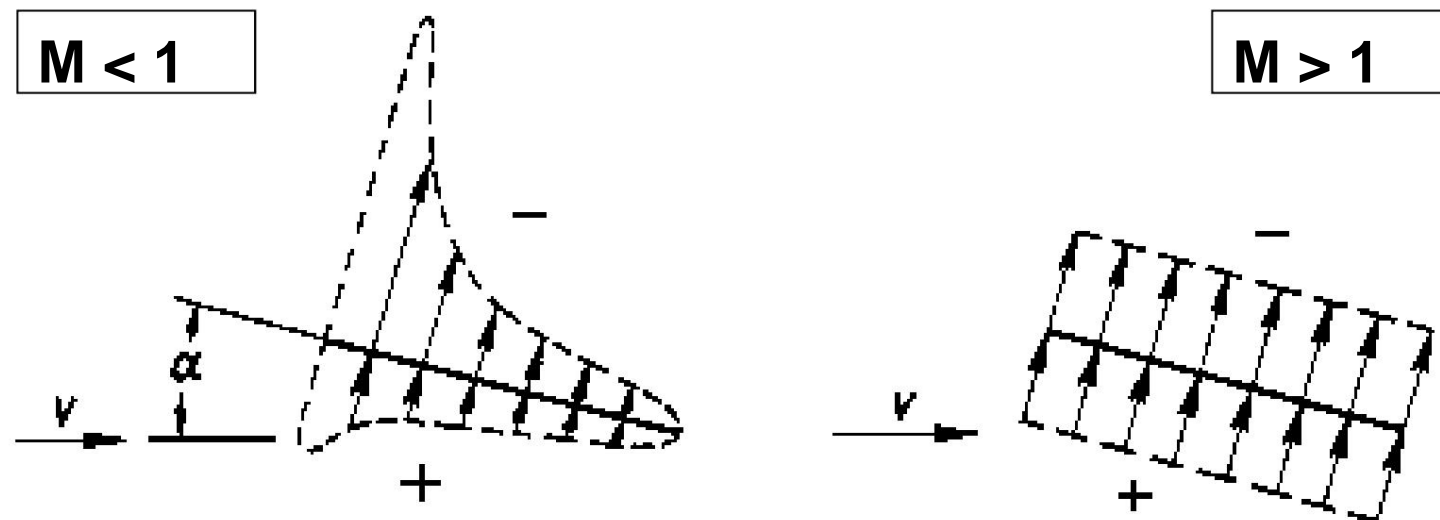


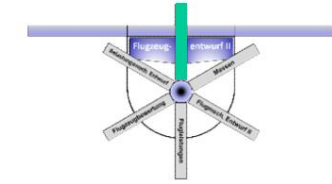


# D Basics of aerodynamic design

## 1.3.3 Influence of the Mach number

- The shift of the neutral point position backwards is many profile shapes can be observed.
- Aircraft flying in the subsonic and supersonic range have larger horizontal stabilizers or trim tanks to trim out the shift in the pressure point.

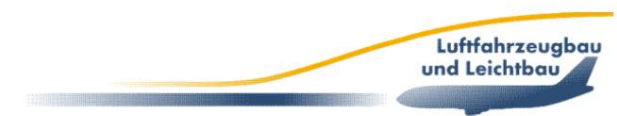


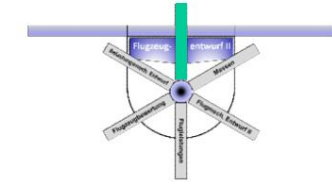


# D Basics of aerodynamic design

## 1.3.4 Profile developments

- For each design case, a suitable profile must be found that optimally meets the requirements. However, the requirements are very different for e.g.
  - Gliders • UAV  
(Unmanned aerial vehicles) •
  - Flying wing aircraft •
  - Ultralight aircraft •
  - Commercial aircraft





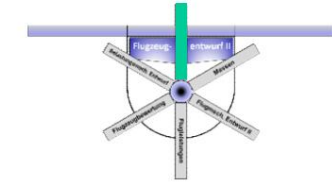
# D Basics of aerodynamic design

## 1.3.4 Profile developments

For each design case, a suitable profile must be found that optimally meets the requirements. For example, a glider needs a laminar profile that, in addition to very low minimum drag and the widest possible laminar flow, should also have good high-lift properties, as the speed range varies greatly (fast forward flight, slow circling in the updraft).

However, it is also important to ensure that the performance does not drop too much in the event of contamination that occurs in practice (mosquitoes in the stagnation point area) and the associated shift of the transition point towards the leading edge.

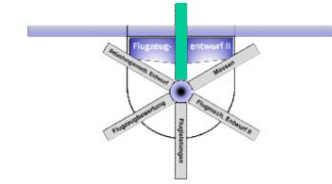
This is especially true for the stall behavior. A suitable nose profile can minimize the "collection" of dirt, as is the case with the HQ profile series from Horstmann and Quast.



# D Basics of aerodynamic design

## 1.3.4 Profile developments

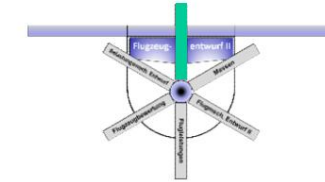
- For aircraft that mainly operate at a constant cruising speed (or  $cA = \text{const.}$ ) (e.g. UAV – unmanned aerial vehicle), the width of the laminar cell is less important than its exact positioning.
- For flying wing aircraft, a vanishing pressure point migration is essential for stabilizing the longitudinal movement. Special profiles with an S-bend on the trailing edge are used here, but their resistance behavior does not match the performance of classic profiles.
- For ultralight aircraft, the wing weight is of paramount importance and it is advisable to work with extremely thick profiles for this aircraft category, which also allow large angles of attack and thus low approach speeds.



# D Basics of aerodynamic design

## 1.3.4 Profile developments

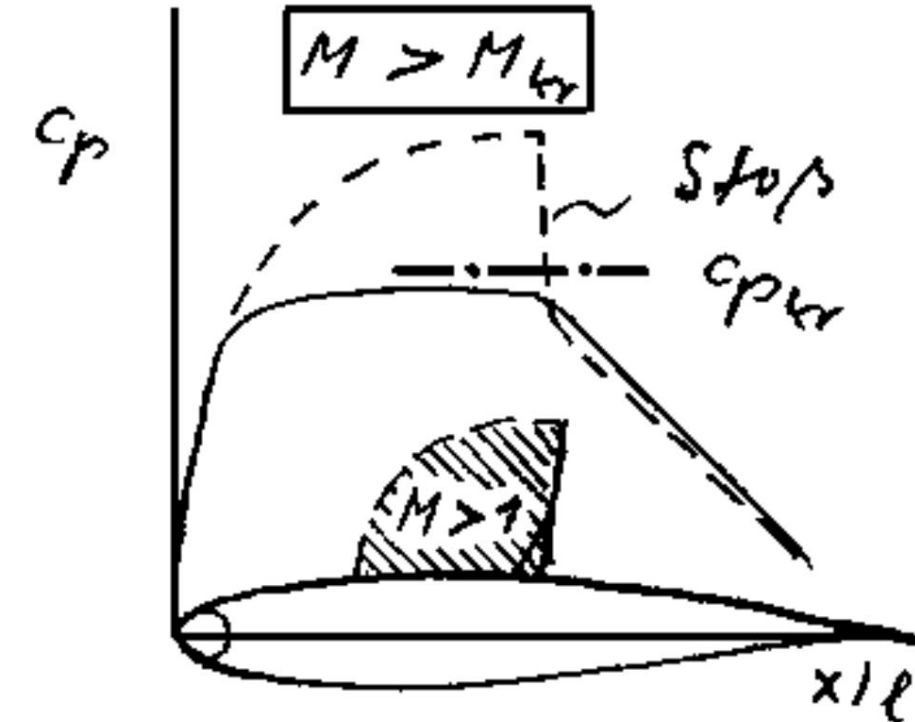
- Especially for high subsonic flight, in which However, in commercial aircraft, a high buffet onset and drag divergence limit is the main deciding factor. • Because of the particular importance, the development of profiles in this application area will be discussed again here.



# D Basics of aerodynamic design

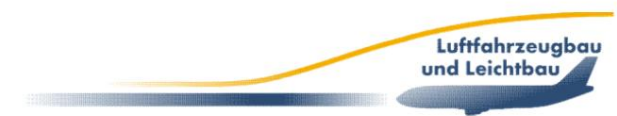
## 1.3.4 Profile developments

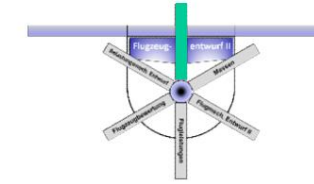
- The "Roof Top Profile" comes from the NACA-6 series



**Application: CARAVELLE**

Shifting the thickness  
reserve from 30 to approx.  
40%, increasing the critical  
Mach number by approx. 0.04



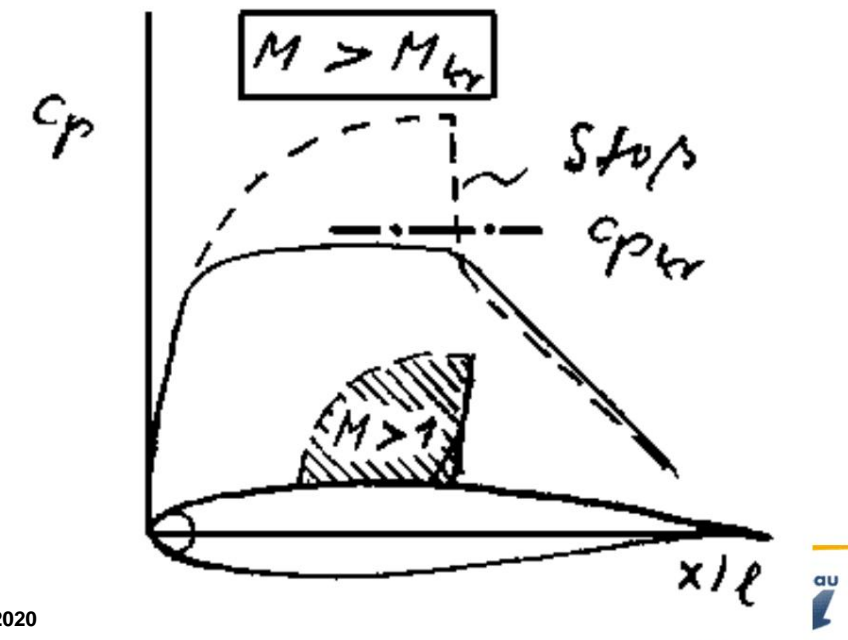


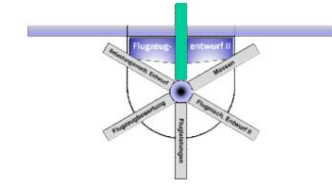
# D Basics of aerodynamic design

## 1.3.4 Profile developments

The profile known as the "Roof Top Profile" comes from the NACA-6 series. The aim of the development was primarily to achieve a late free transition in order to achieve reduced drag. The resulting pressure increase, which is shifted far to the rear, also leads to a more uniform speed distribution, the avoidance of a large supersonic region and thus to an increase in the critical Mach number. As a result, the Ma limits improved accordingly. The broken line in the pressure distribution shows, however, that when the critical Mach number is exceeded, the supersonic region is closed off with a strong shock.

The CARAVELLE is a prominent example of the use of this type of profile. A further optimization was achieved by extending the roof top by shifting the thickness reserve from 30 to approx. 40%, which brought about a further 0.04 Ma points.

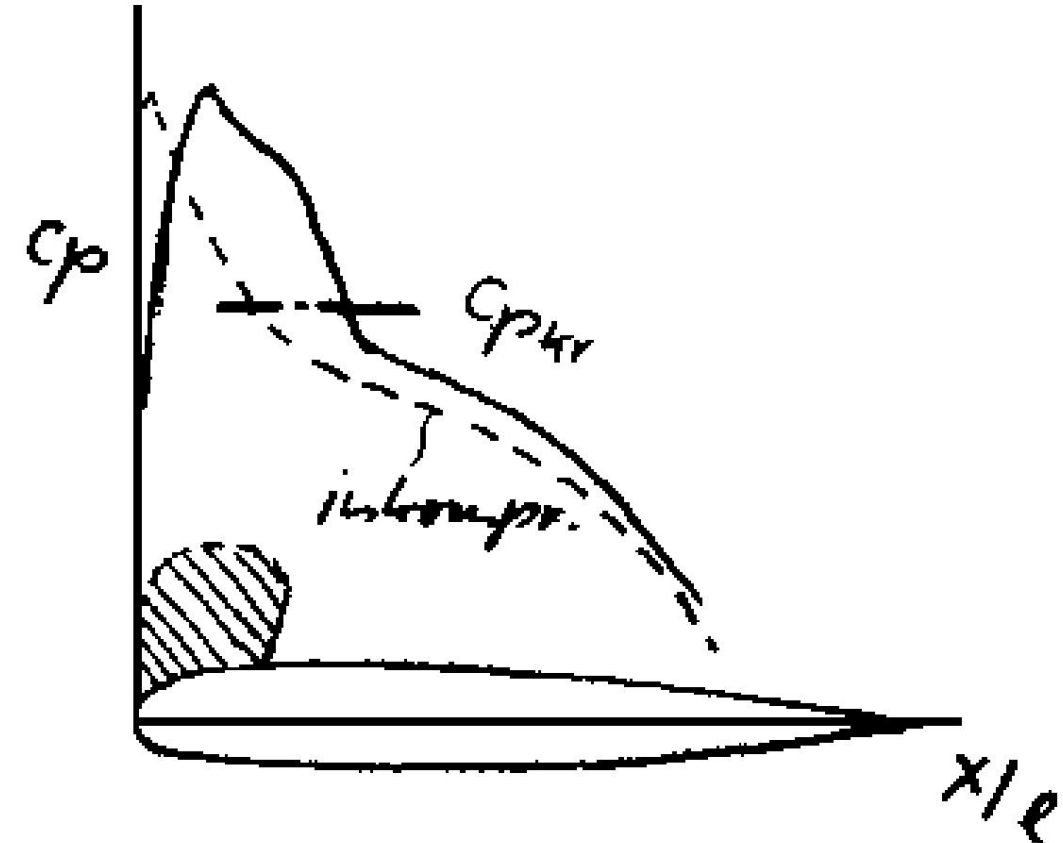




# D Basics of aerodynamic design

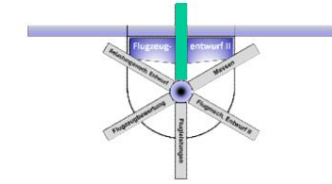
## 1.3.4 Profile developments

- “Peaky Profiles”



**Applications:** DC9 (basis for B717) and BAC 1-11

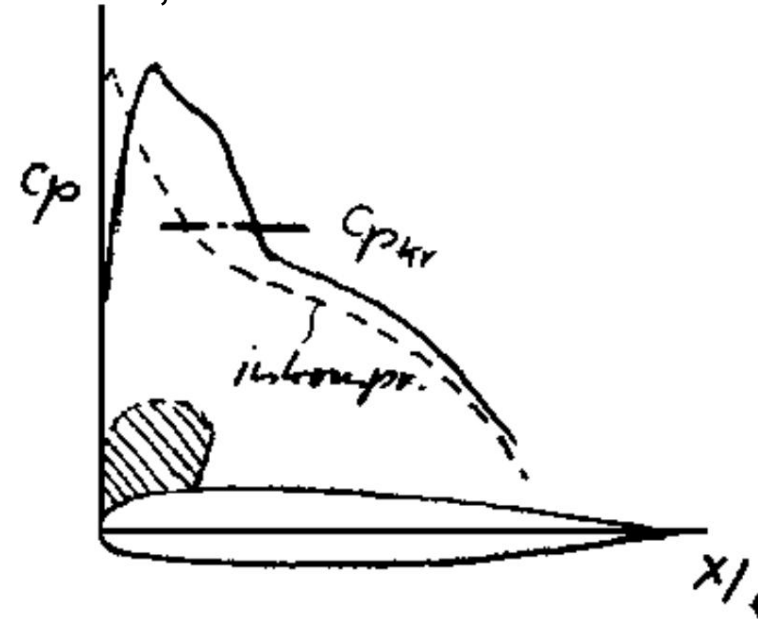
**Increase in drag increase Mach number by a further 0.04 to 0.05 compared to “Roof Top profile”**

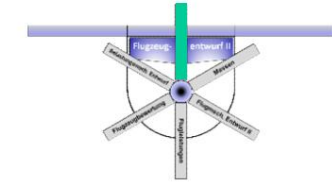


# D Basics of aerodynamic design

## 1.3.4 Profile developments

- With the "Peaky Profiles", a carefully designed profile nose is used to create a targeted suction peak in the nose area, which is initially completed with an almost isentropic compression and a weak shock.
- The drag increase Mach number could be increased by a further 0.04 to 0.05 compared to the roof top profile, thus significantly improving the off-design maneuvering behavior. Examples of applications are the DC9, which is now also operated as a B717 derivative, and the BAC 1-11.



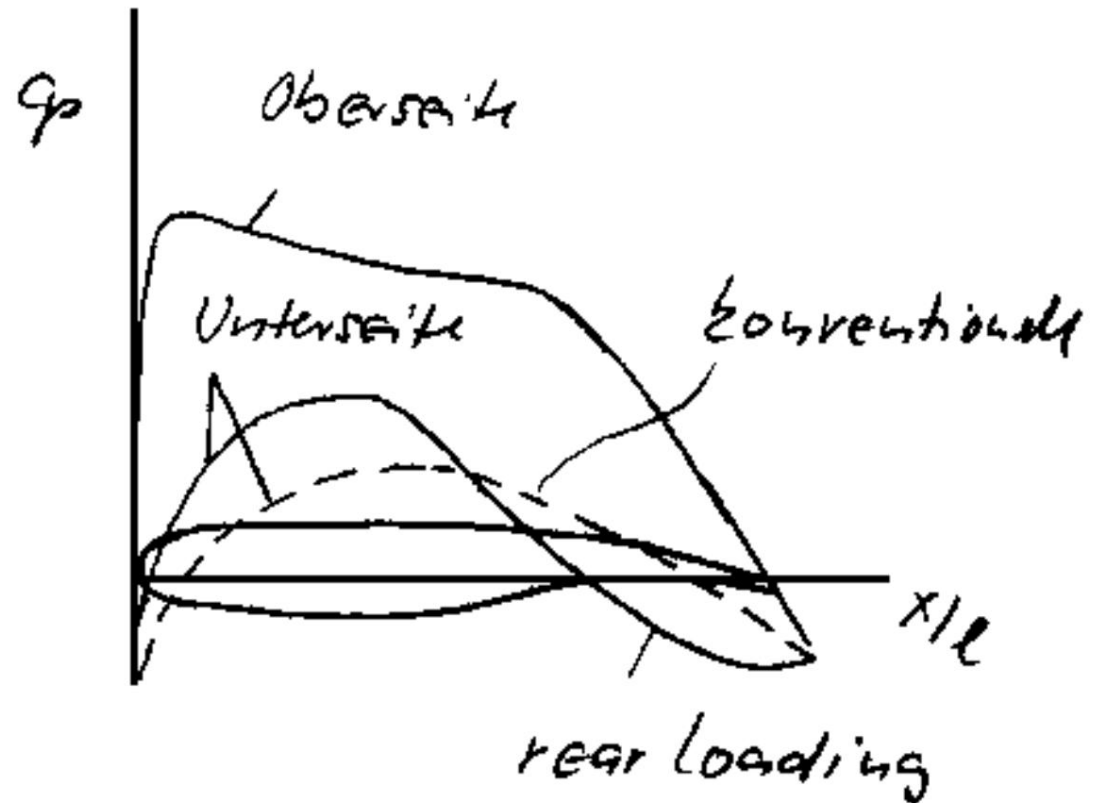


# D Basics of aerodynamic design

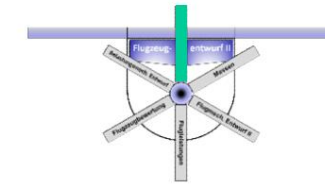
## 1.3.4 Profile developments

- "Rear Loading Profile"

**Applications:** First  
AIRBUS products (e.g. A300-B2/B4) and LOCKHEED TRISTAR.



**Relief of the top surface,**  
**increase of the buffet onset Mach number by about 0.03,**  
**but larger top-heavy moment.**

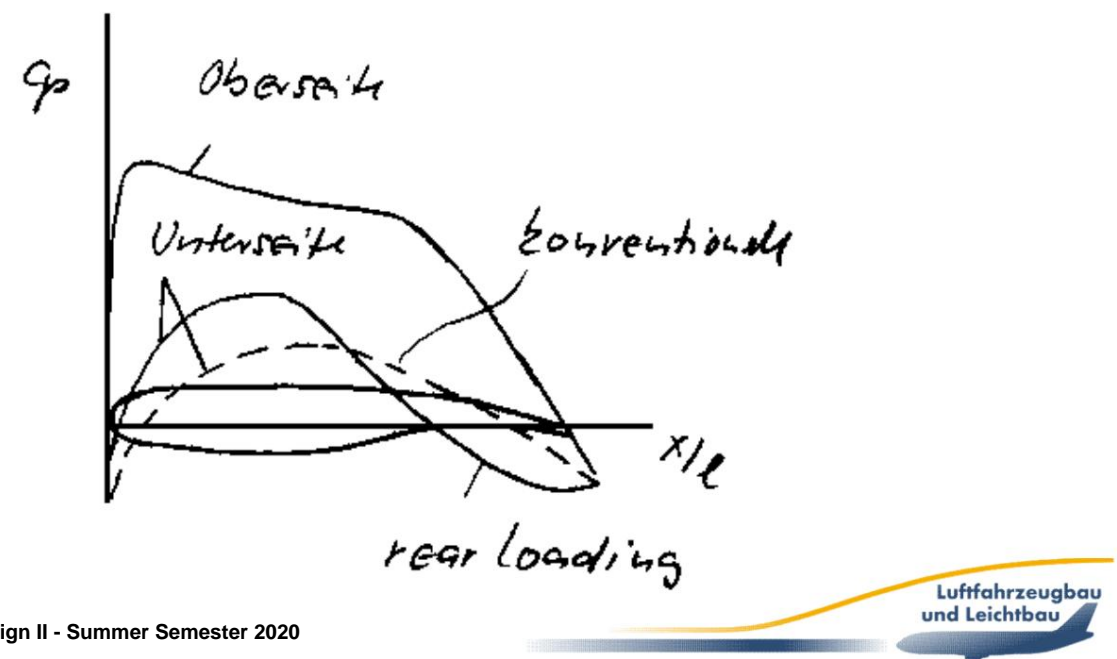


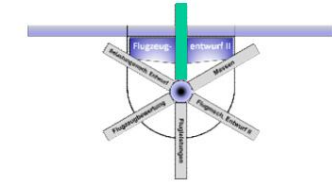
# D Basics of aerodynamic design

## 1.3.4 Profile developments

With the introduction of the "Rear Loading Profile", greater lift was achieved by curving the underside of the profile more than the latter. This made it possible to reduce the load on the top side significantly and thereby increase the critical Mach number. One problem with this type of profile is the slightly larger top-heavy moment due to the greater trailing edge load and the associated greater trim drag. In addition, the reduced height in the end area makes it difficult to install an effective flap system.

This profile was used in the early AIRBUS products (e.g. A300-B2/B4) and the LOCKHEED TRISTAR.



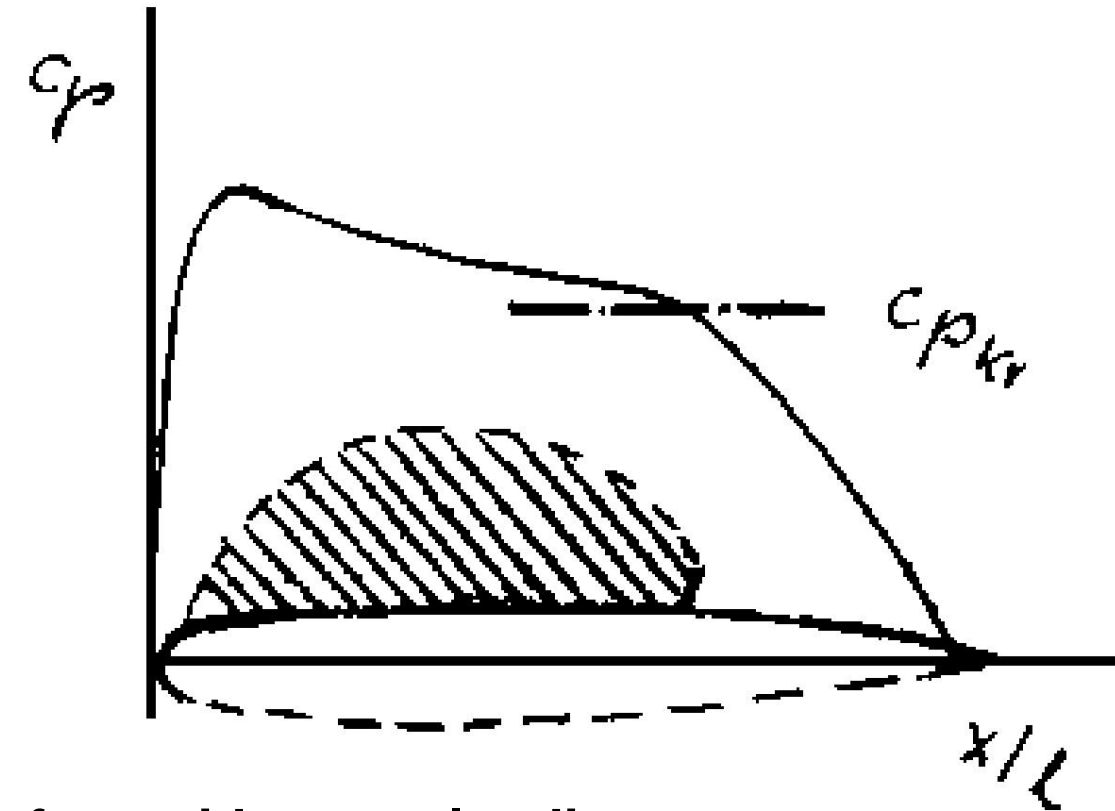


# D Basics of aerodynamic design

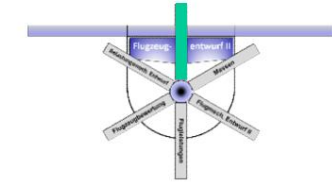
## 1.3.4 Profile developments

- Supercritical profiles

**State of the art,  
First application: A310**



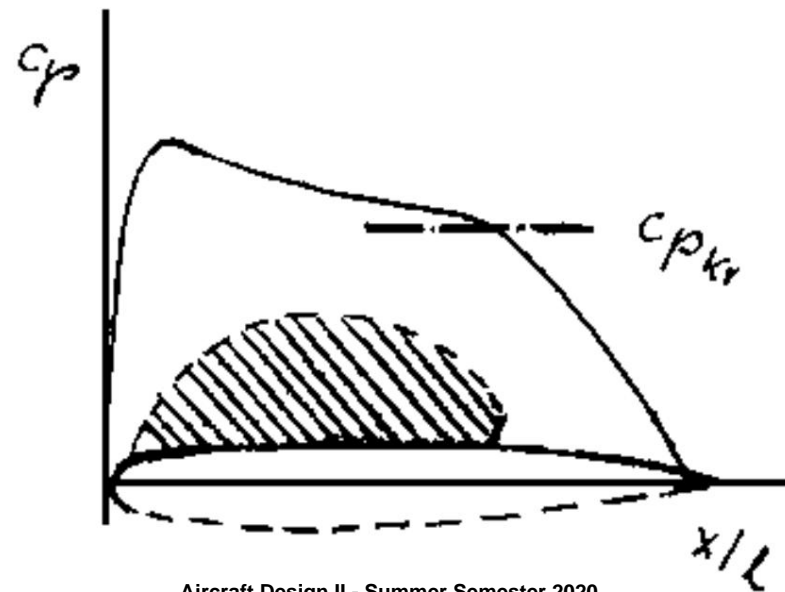
**Combination of a flat surface with a rear loading,  
improved off-design properties**

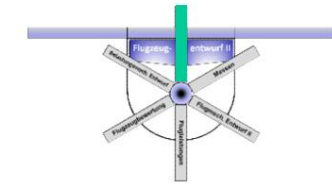


# D Basics of aerodynamic design

## 1.3.4 Profile developments

The supercritical profiles represent the current state of the art. Due to the very flat contour of the upper side, a much larger shock-free supersonic range can be maintained than with the "peaky profiles", but if the flattening is too long, the risk of boundary layer separation becomes high due to the steep pressure increase in the rear area. Particularly good high-speed and off-design properties can be achieved by combining the flat surface with the S-stroke of the "Rear Loading Profile". The first application was with the A310.





# D Basics of aerodynamic design

## 1.3.4 Profile developments

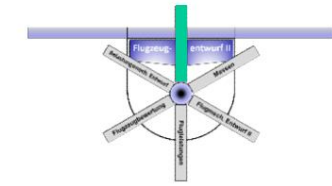
Profile VA2,  $d/l = 13\%$



### Geometrie - Kennzahlen

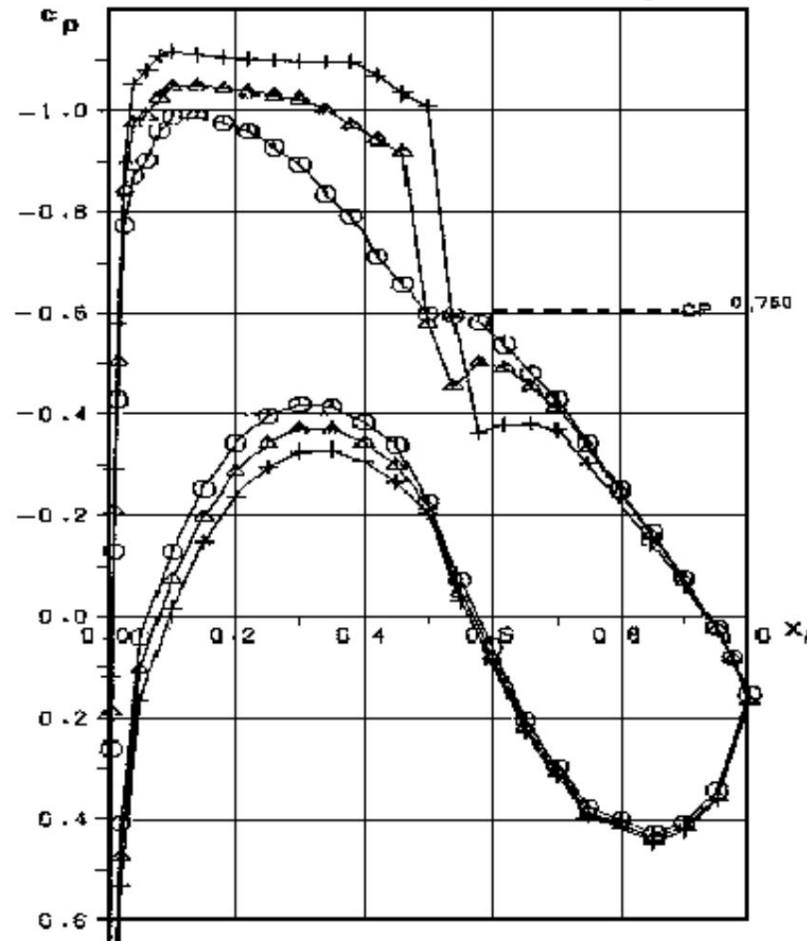
max. Dicke	$(d/l)_{max} = 0.13$
Dickenaufteilung	$(z/l)_{mo}$
Rücklage der max. Dicke	$(z/l)_{max} = 1.065$
Oberseite	$(x/l)_{mo} = 0.42$
Unterseite	$(x/l)_{mu} = 0.3$
Hinterkantendicke	$z_h/l = 0.00522$
Hinterkantenwinkel	$\alpha = 6^\circ$





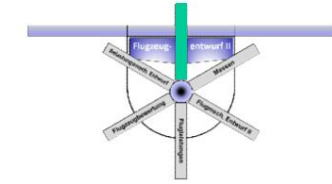
# D Basics of aerodynamic design

## 1.3.4 Profile developments



Profile VA2,  $d/l = 13\%$

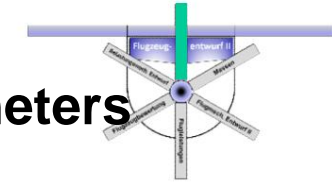
$S_{y1H}$	$M_\infty$	$\alpha^{\circ}$	$c_a$	$c_{vv}$
$\phi$	.75	<b>1.87</b>	.57	<b>.0075</b>
$\Delta$	"	<b>2.28</b>	.64	<b>-0.078</b>
+	"	<b>2.69</b>	.72	<b>-0.100</b>



# D Basics of aerodynamic design

## 1.4 Influence of the wing plan

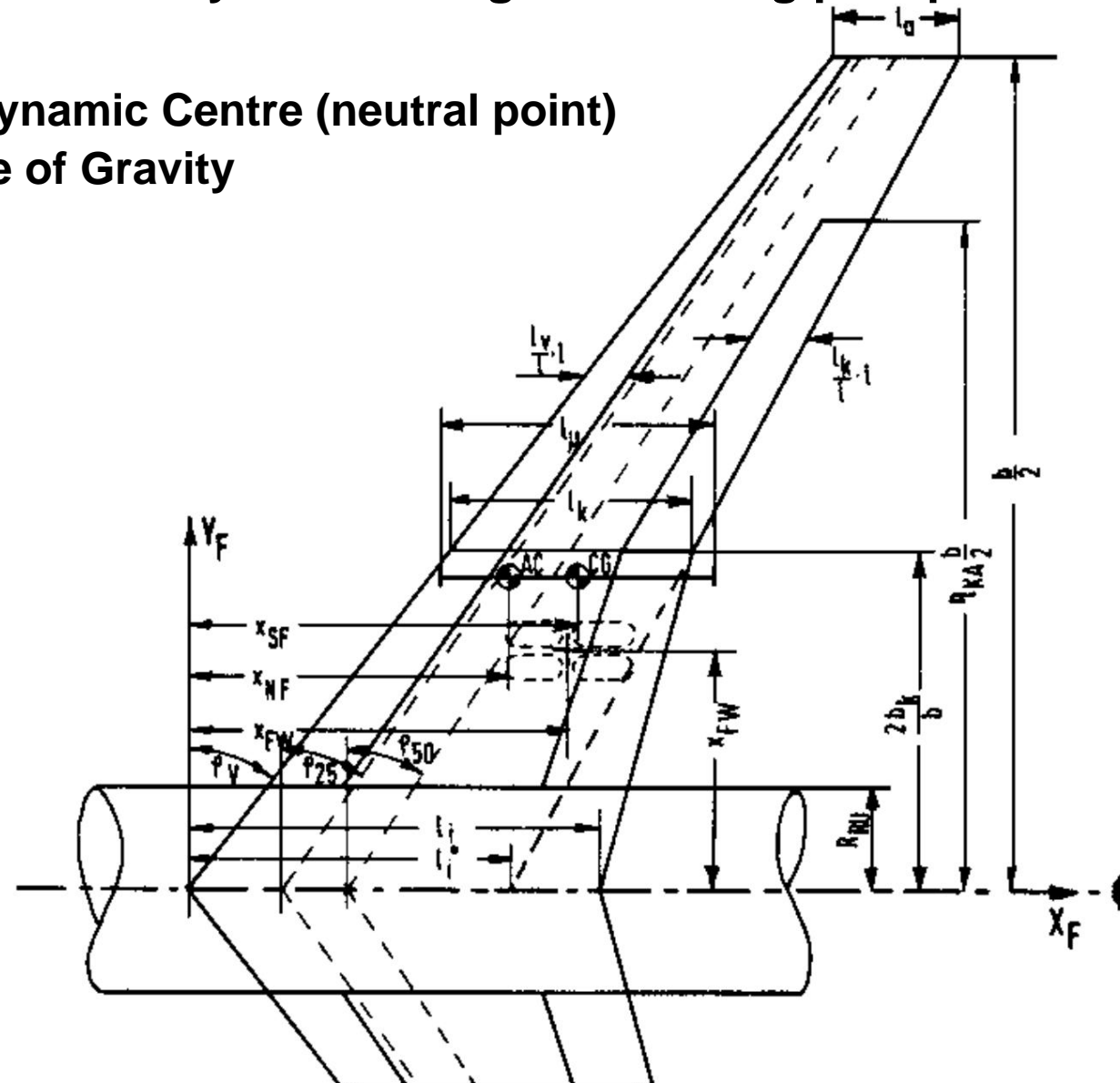
- So far, we have considered the properties of the profile, i.e. the consideration of an infinitely long wing. • On the real, finite wing, there is no constant angle across the span.
- As a result of pressure equalization at the wing tips, a variable, induced angle of attack and lift distribution occurs.
- The floor plan is described by extension, arrowing and depth distribution
- The plan view is particularly important for the distribution of lift, but also for the profile drag of the wing. • These plan view parameters cannot be viewed independently of one another. They are very complexly interrelated.

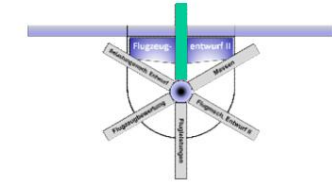


## D Basics of aerodynamic design 1.4.1 Wing plan parameters

**AC:** Aerodynamic Centre (neutral point)

**CG:** Centre of Gravity

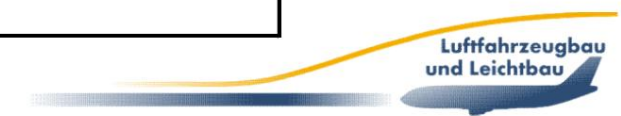


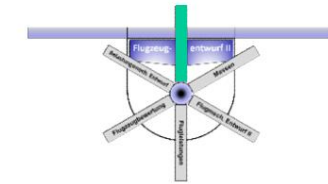


# D Basics of aerodynamic design

## 1.4.1 Wing plan parameters

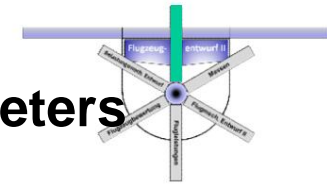
Designation	Generally
Stretching	$\frac{y \ddot{y} \ddot{y}}{F} = \frac{b^2}{I_m}$
Middle deep	$\frac{I_m}{y} = \frac{b F}{\ddot{y} \ddot{y} \ddot{y} \ddot{y} \ddot{y} \ddot{y} \ddot{y}} = \frac{1}{0}$
span	$b \ddot{y} \ddot{y} \sqrt{F} \ddot{y} \ddot{y} \ddot{y} I_m$
Escalation	$\frac{\ddot{y} \ddot{y}}{I_i} = \frac{I_a}{I_i}$
Span coordinate	$\frac{\ddot{y} \ddot{y}}{b} = \frac{2 \ddot{y} y}{b}$





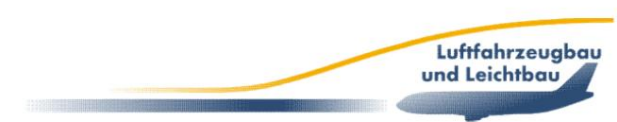
## D Basics of aerodynamic design 1.4.1 Wing plan parameters Trapezoidal wing b

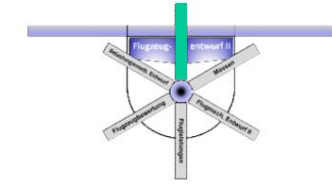
Description General		Double trapezoidal wing
Area	$F = \frac{1}{2} \int_0^1 C(x) dx$	$F = \frac{b}{2} \int_{l_i}^{l_k} \left( \frac{b}{y} + \frac{b}{y} \right) dy$
Escalation	<p>For concave floor plans:</p> $e = \frac{\int_0^1 y dy}{\int_0^1 l_i dy}$ <p>For convex floor plans:</p> $e = \frac{\int_0^1 l_i dy}{\int_0^1 y dy}$	$e = \frac{2(b - l_i)}{b} = \frac{l_a - l_i}{l_i}$
Internal depth	$d = \frac{l_i - l_m}{l_m}$	$d = \frac{2(l_i - l_m)}{l_m}$
Depth gradient	$\frac{d}{l_m} = \frac{l_i - l_m}{l_m}$	$\frac{d}{l_m} = \frac{l_i - l_m}{l_m}$ $\frac{d}{l_m} = \frac{2(b - l_i)}{b}$ $\frac{d}{l_m} = \frac{2(b - l_i)}{b}$



## D Basics of aerodynamic design 1.4.1 Wing plan parameters

Designation General	rel. reference	Trapezoidal	Double trapezoidal wing
depth	$\frac{1}{l_m} \frac{y}{m}$	$\frac{1}{l_m} \frac{4}{3} \frac{1}{y_1} \frac{y}{y_2}$	$\frac{1}{l_m} \frac{1}{3} \frac{y_1}{y_2} \frac{y}{y_1} \frac{y}{y_2}$
rel. reference wing position	$\frac{1}{b} \frac{1}{4} \frac{y}{y_1} \frac{y}{y_2}$	$\frac{2}{b} \frac{1}{3} \frac{1}{y}$	$\frac{1}{b} \frac{1}{6} \frac{1}{b} \frac{2}{b} \frac{1}{3} \frac{2}{b} \frac{1}{6} \frac{1}{b}$
rel. neutral point position	$\frac{x_N}{l_m} \frac{1}{2} \frac{y}{y_1} \frac{y}{y_2}$	$\frac{x_N}{l_m} \frac{1}{2} \frac{y}{b} \frac{y}{y_1} \frac{y}{y_2} \frac{1}{l_m}$	$\frac{x_N}{l_m} \frac{2}{2} \frac{y}{b} \frac{4}{4} \frac{1}{y} \text{ approximately}$ for straight leading edge



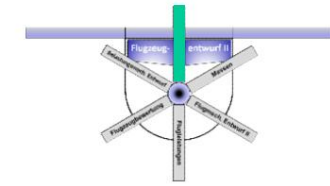


# D Basics of aerodynamic design

## 1.4.1 Wing plan parameters

Description General	Trapezoidal wings	Double trapezoidal wing
Leading edge sweep	$\tan \alpha = \frac{1}{\sqrt{1 - \frac{L^2}{C^2}}}$	$\tan \alpha = \frac{1}{\sqrt{1 - \frac{L^2}{C^2}}} \approx 1$
Centerline arrow	$\tan \alpha = \frac{1}{\sqrt{1 - \frac{L^2}{C^2}}}$	$\tan \alpha = \frac{1}{\sqrt{1 - \frac{L^2}{C^2}}} \approx 1$
General Sweep conversion	$\tan \alpha = \frac{1}{\sqrt{1 - \frac{L^2}{C^2}}} = \frac{1}{\sqrt{1 - \frac{L_m^2}{C_m^2}}} \cdot \frac{\sqrt{1 - \frac{L_m^2}{C_m^2}}}{\sqrt{1 - \frac{L_n^2}{C_n^2}}}$	
Linear geometric Torsion distribution	$\alpha_{lin} = \frac{\alpha_{tip} - \alpha_{root}}{L}$	
Progressive Torsion distribution	$\alpha_{progressive} = \frac{\alpha_{tip} - \alpha_{root}}{L} \cdot \frac{1}{1 + \frac{L}{L_{root}}}$	



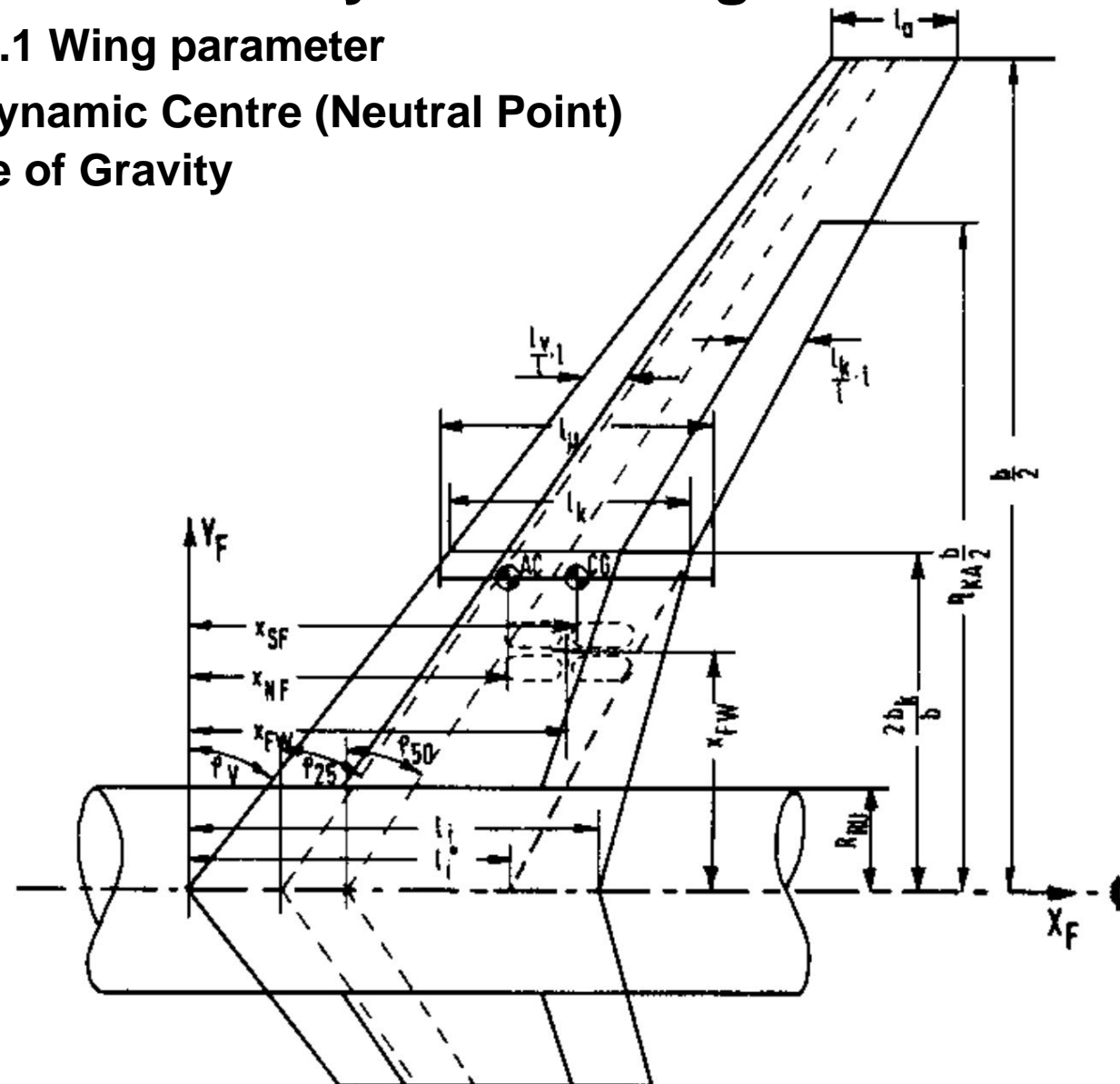


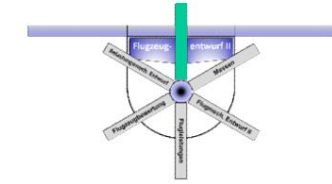
# D Basics of aerodynamic design

## 1.4.1 Wing parameter

**AC:** Aerodynamic Centre (Neutral Point)

**CG:** Centre of Gravity

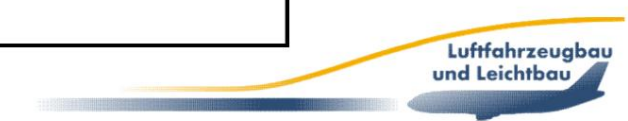


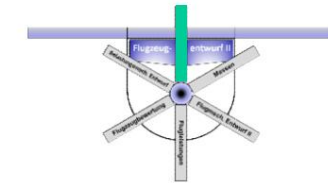


# D Basics of aerodynamic design

## 1.4.1 Wing plan parameters

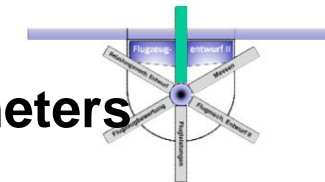
Surname	Calculations
<b>aspect ratio</b>	$\frac{b \cdot b}{F} = \frac{l_m}{l_m}$
<b>average chord length</b>	$l_m = \frac{b \cdot F}{\int_0^1 c(y) dy}$
<b>Chord</b>	$b = \sqrt{F \cdot l_m}$
<b>taper ratio</b>	$\frac{l_i}{l_a}$
<b>relative span</b>	$\frac{2 \cdot y}{b}$





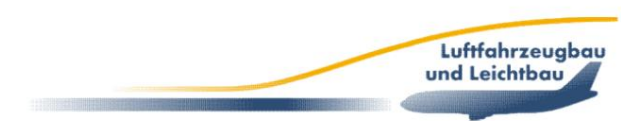
## D Basics of aerodynamic design 1.4.1 Wing plan parameters trapezoidal wing b

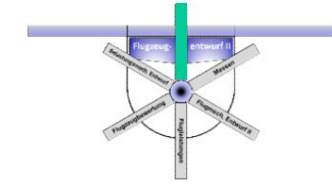
Surname	general		Double trapezoidal wing
<b>Area</b>	$F = \frac{1}{2} \cdot l_i \cdot b \cdot k \cdot 1 \cdot \frac{l_k}{l_i} \cdot \frac{b}{l_i} \cdot \frac{k}{l_i}$	$F = \frac{1}{2} \cdot l_i \cdot b \cdot k \cdot 1 \cdot \frac{l_k}{l_i} \cdot \frac{b}{l_i} \cdot \frac{k}{l_i}$	$F = \frac{b}{2} \cdot l_i \cdot \frac{\ddot{y}_b}{\ddot{y}_b} \cdot \frac{k}{\ddot{y}_b} \cdot 1 \cdot \frac{l_k}{l_i} \cdot \frac{\ddot{y}_b}{\ddot{y}_b} \cdot \frac{k}{\ddot{y}_b} \cdot \frac{\ddot{y}_b}{\ddot{y}_b} \cdot \frac{k}{\ddot{y}_b}$
<b>Taper ration</b>	For concave floor plans: $\frac{l_a}{l_i} = \frac{1}{2} \cdot \frac{l_i}{l_a}$ For convex floor plans: $\frac{l_a}{l_i} = \frac{1}{2} \cdot \frac{l_i}{l_a}$		$\frac{l_a}{l_i} = \frac{2 \cdot b}{b} \cdot \frac{k}{k} \cdot \frac{l_i}{l_i} \cdot \frac{l_a}{l_i} \cdot \frac{l_a}{l_i}$
<b>Inner chord</b>	$l_i = \frac{2 \cdot l_m}{1 + \frac{l_i}{l_m}}$		$l_i = \frac{2 \cdot l_m}{b \cdot \frac{k}{k} \cdot 1 + \frac{l_i}{l_i}} \cdot \frac{l_i}{l_i} \cdot \frac{2 \cdot b}{b} \cdot \frac{k}{k} \cdot \frac{l_i}{l_i} \cdot \frac{l_i}{l_i}$
<b>Chord as function of rel. span</b>	$l_i = \frac{l_m}{1 + \frac{l_i}{l_m}}$		$l_i = \frac{l_m}{1 + \frac{l_i}{l_m}} \cdot \frac{b}{b} \cdot \frac{k}{k} \cdot 1 + \frac{l_i}{l_i} \cdot \frac{b}{b} \cdot \frac{k}{k} \cdot 2 \text{ for } 0 < k < 1$



## D Basics of aerodynamic design 1.4.1 Wing plan parameters

Surname	general	Trapezoidal wing I	Double trapezoidal wing
Mean aerodynamic chord	$\frac{1}{I_m} \frac{1}{m} \frac{2}{0}$	$\frac{4}{3} \frac{1}{2}$	$\frac{1}{I_m} \frac{1}{3} \frac{2}{1} \frac{b}{b} \frac{2}{k} \frac{2}{k} \frac{2}{k} \frac{2}{k}$
rel. span position of MAC	$\frac{1}{2} \frac{1}{b} \frac{1}{0} \frac{1}{4} \frac{1}{0}$	$\frac{2}{b} \frac{1}{3} \frac{2}{1}$	$\frac{1}{b} \frac{1}{6} \frac{2}{2} \frac{1}{b} \frac{2}{k} \frac{2}{k} \frac{2}{k} \frac{2}{k}$
rel. neutral pointposition	$\frac{x_N}{I_m} \frac{1}{y} \frac{1}{0}$	$\frac{x_N}{I_m} \frac{y}{2} \frac{y}{b} \frac{y}{tan} \frac{y}{4}$	$\frac{x_N}{I_m} \frac{y}{2} \frac{y}{b} \frac{y}{approximate} \frac{y}{4}$

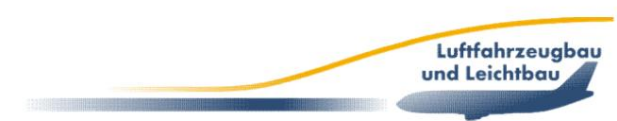


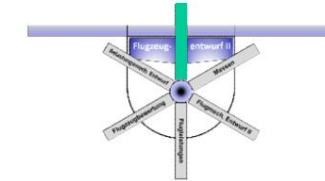


# D Basics of aerodynamic design

## 1.4.1 Wing plan parameters

Description General	Trapezoidal wings	Double trapezoidal wing
Leading edge sweep	$\tan \alpha = \frac{1}{\sqrt{1 - \frac{L^2}{C^2}}}$	$\tan \alpha = \frac{1}{\sqrt{1 - \frac{L^2}{C^2}}}$ approximately for straight leading edge
Centerline arrow	$\tan \alpha = \frac{1}{\sqrt{1 - \frac{L^2}{C^2}}}$	$\tan \alpha = \frac{1}{\sqrt{1 - \frac{L^2}{C^2}}}$ approximately for straight leading edge
General Sweep conversion	$\tan \alpha = \frac{1}{\sqrt{1 - \frac{L^2}{C^2}}} = \frac{1}{\sqrt{1 - \frac{L_m^2}{C_m^2}}} \cdot \frac{\sqrt{1 - \frac{L_m^2}{C_m^2}}}{\sqrt{1 - \frac{L_n^2}{C_n^2}}}$	
Linear geometric Torsion distribution	$\alpha = \alpha_0 + \frac{\alpha_{tip} - \alpha_0}{L}$	
Progressive Torsion distribution	$\alpha = \alpha_0 + \frac{\alpha_{tip} - \alpha_0}{L} \cdot \frac{L}{L + L_{tip}}$	

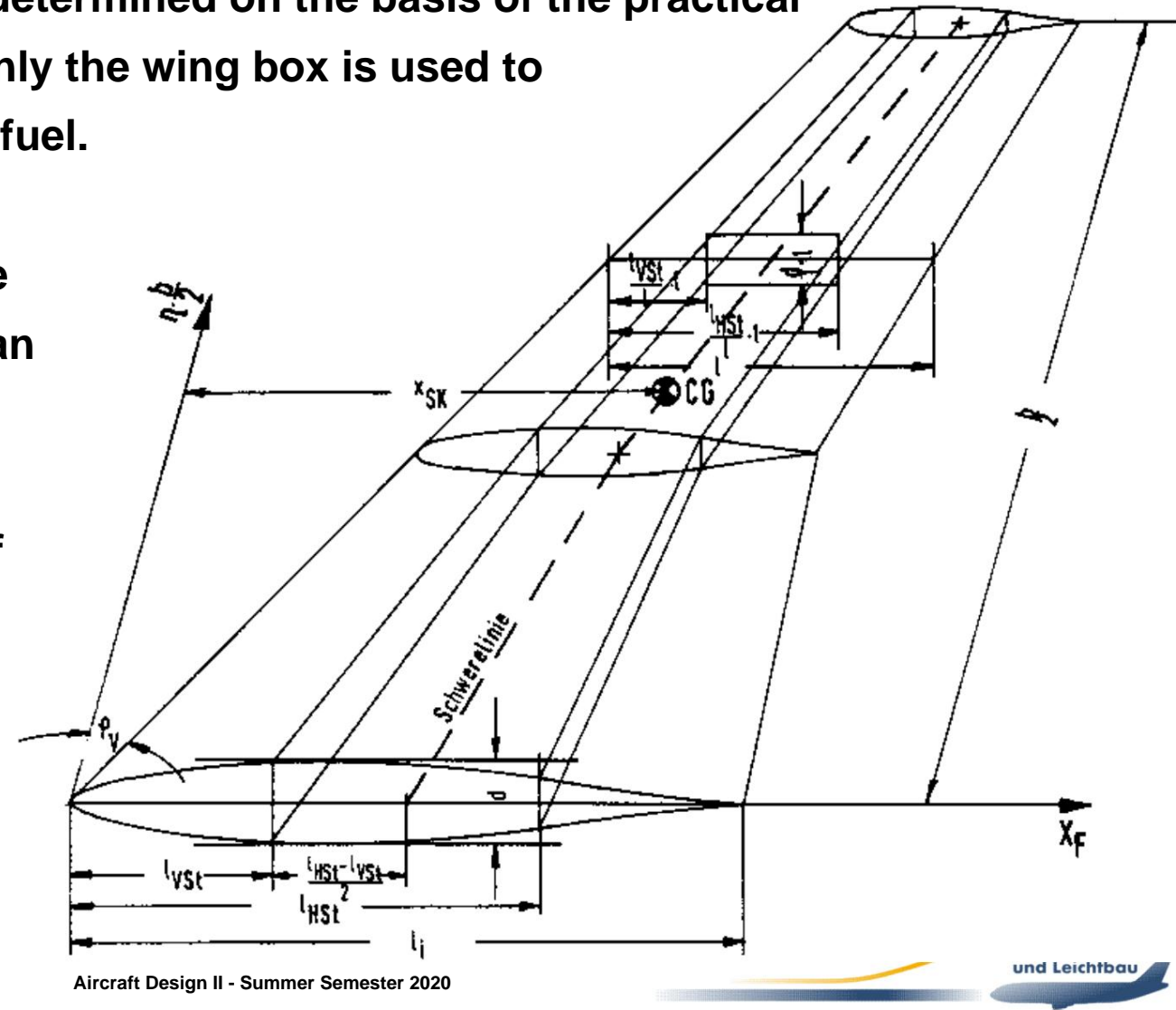


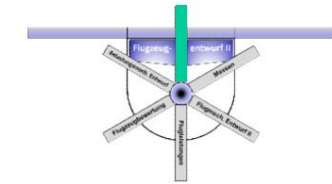


# D Basics of aerodynamic design

## 1.4.1 Wing plan parameters

- The tank volume is determined on the basis of the practical assumption that only the wing box is used to accommodate the fuel.
- If this is done for the entire span, one can use pre-estimated, dimensionless, lateral positions of front and rear web the box volume determine.





# D Basics of aerodynamic design

## 1.4.1 Wing plan parameters

- The box volume is generally

$$V_k = \int_0^{b/2} F(y) dy$$

- If we assume an approximately rectangular wing box, its cross-sectional area is

$$F_k = \frac{1}{2} d \left( \frac{\bar{y}_{HSt}}{\bar{y}_{vSt}} + \frac{\bar{y}_{vSt}}{\bar{y}_{HSt}} \right) \bar{y}_m^2$$

- With dimensionless span coordinates, depth gradients and assuming a constant relative

**Profile thickness applies to the wing with general depth profile:**

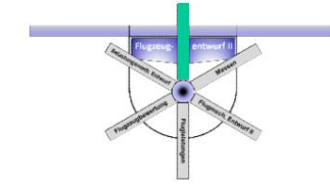
$$V_k = \int_0^1 F(\bar{y}) d\bar{y} = \frac{1}{2} \left( \frac{\bar{y}_d}{\bar{y}_m} + \frac{\bar{y}_m}{\bar{y}_d} \right) \bar{y}_m^2$$

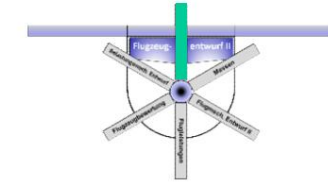


# D Basics of aerodynamic design

## 1.4.1 Wing plan parameters

- A reduction factor of 80 - 90% for the inner structure, mean deviation of the geometry parameters and the vent tank should be applied to reliably estimate the usable fuel volume.

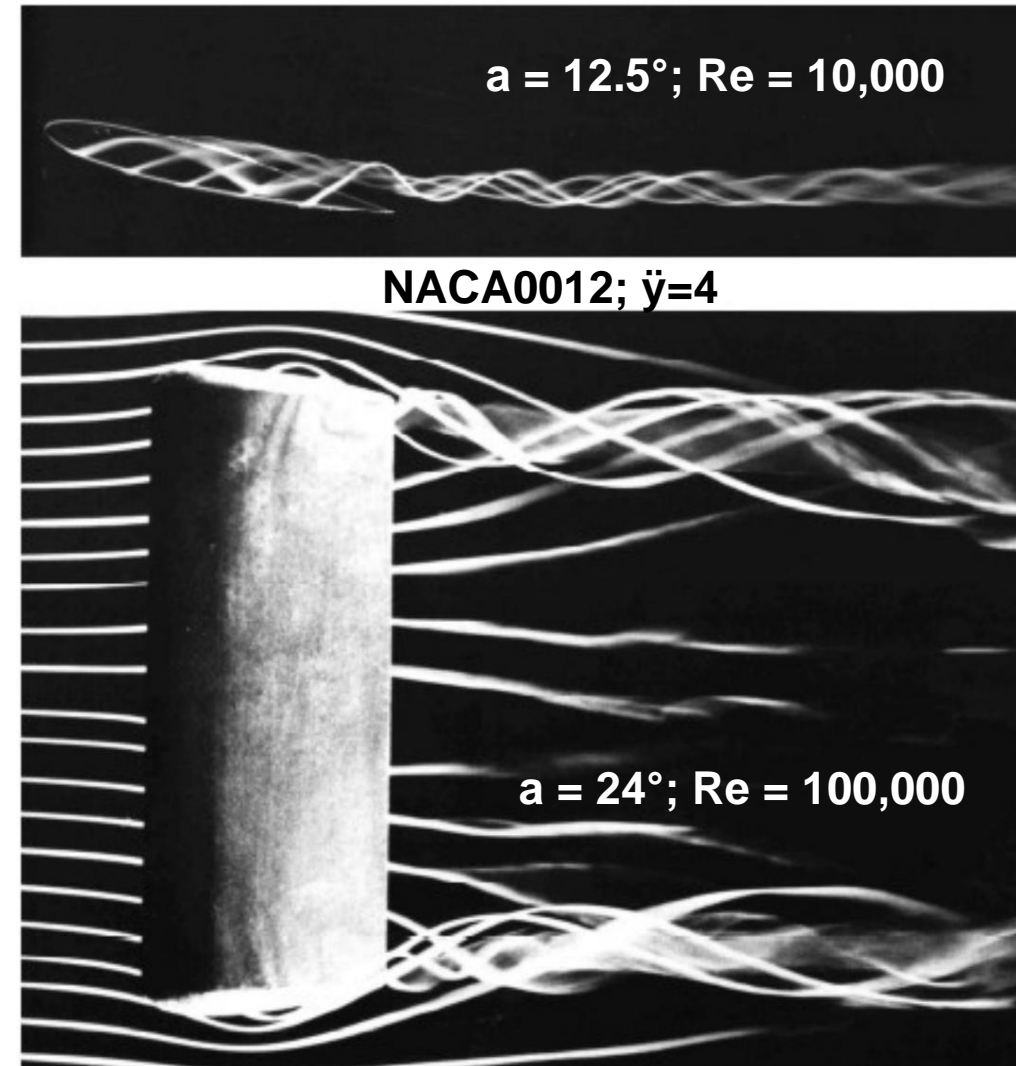


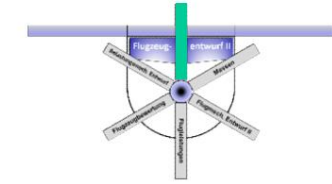


# D Basics of aerodynamic design

## 1.4.2 Lift distribution of the wing

- The infinite wing or a wing clamped between wind tunnel walls has parallel streamlines in the flow around it and only curved in the vertical direction.
- The visualization of the flow around a wing with low aspect ratio shows the phenomenon of “finiteness” particularly well.





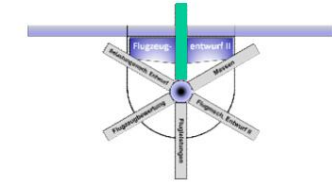
# D Basics of aerodynamic design

## 1.4.2 Lift distribution of the wing

Interpretation of the streamline image

Generation of buoyancy

- The well-known experiment of the circulator (Flettner rotor) proves an equivalence of lift and circulation. The superposition of a translational flow with a rotational flow leads to flow deflection, and the associated change in momentum leads to lift.
- The circulation must be large enough to satisfy the discharge condition at the trailing edge.
- Without friction there is no lift. Since circulation must be maintained, the vortex bound in the wing changes into a horseshoe-shaped free vortex at its edge.



# D Basics of aerodynamic design

## 1.4.2 Lift distribution of the wing

### Formation of induced resistance

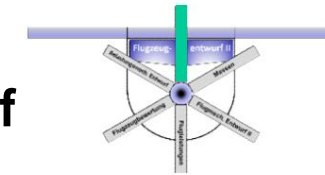
- As a result of the pressure equalization between the upper and lower surfaces, a 3-dimensional flow around the wing tip takes place.
- The flow is deflected towards the wing root on the upper side and outwards on the lower side. This difference in direction results in a separation surface at the wing's trailing edge, which rolls up downstream and merges into two independent, free, conically expanding vortex braids. •

**Energy is required to form and maintain these vortices.**

required because the air must be moved translationally and rotationally be accelerated.

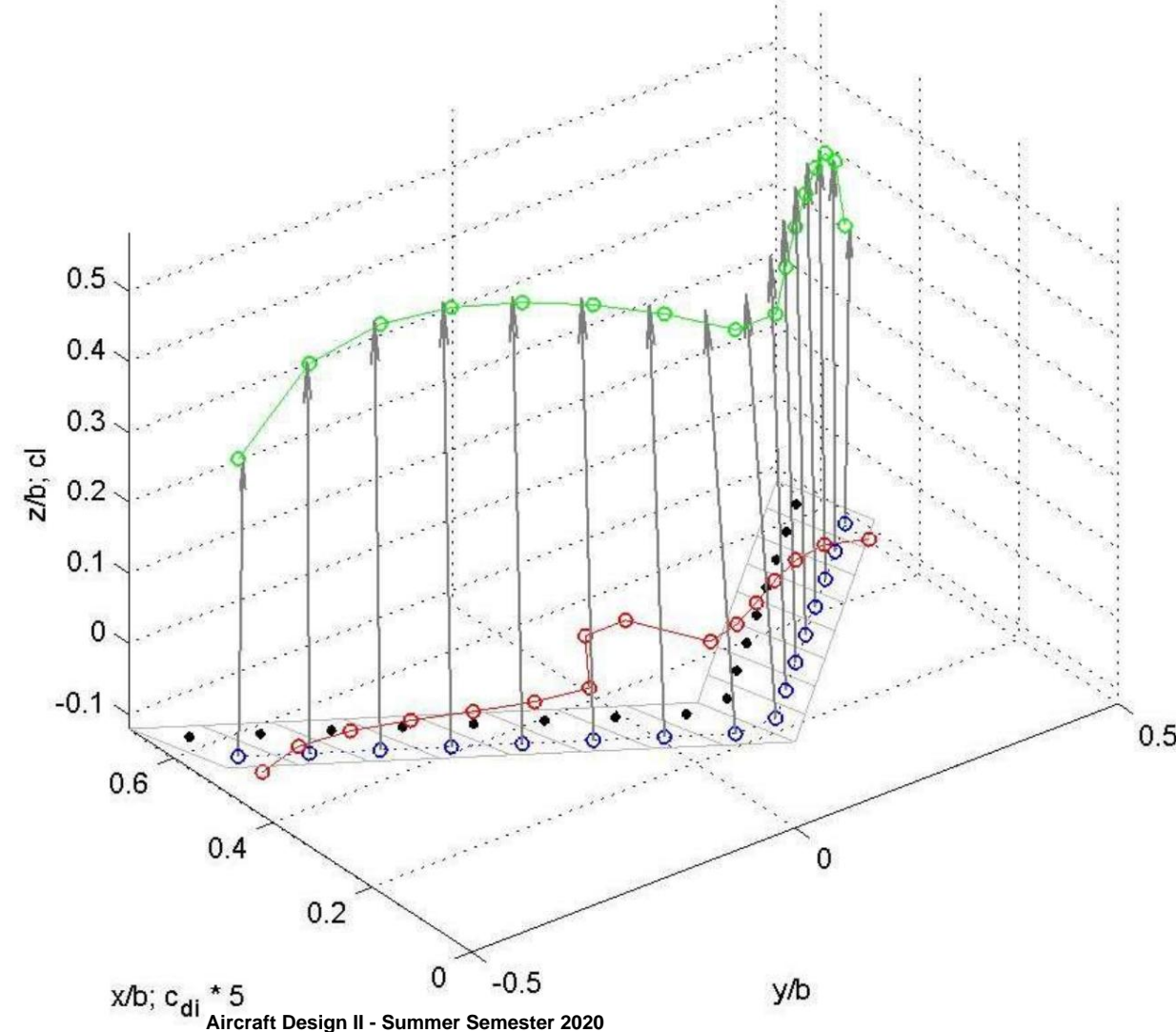
- Even in frictionless flow, work must be done to generate lift on a finite wing.

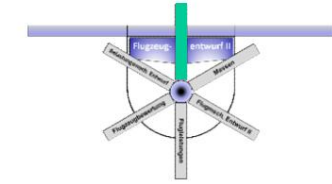
The equivalent of this work is the induced drag.



## D Basics of aerodynamic design 1.4.2 Lift distribution of the wing • Creation of induced drag using the example of a swept rectangular wing

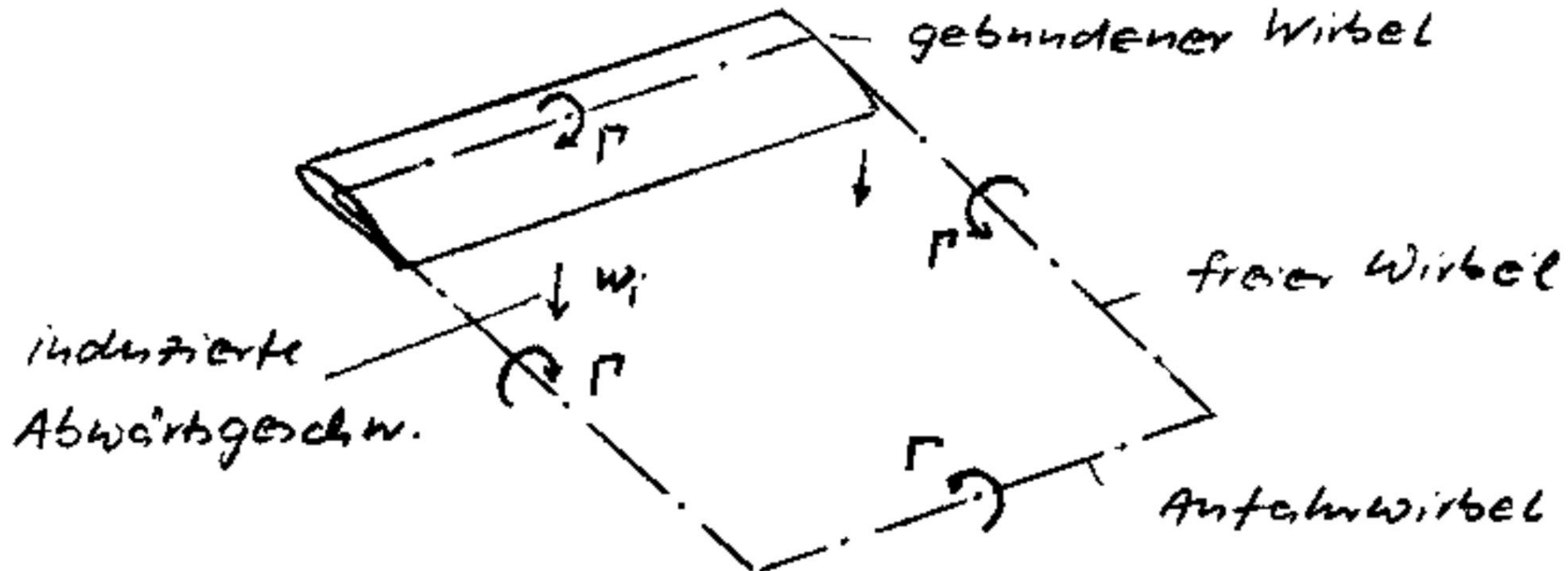
Even a summation of the horizontal force components results in a downstream force, the induced drag!



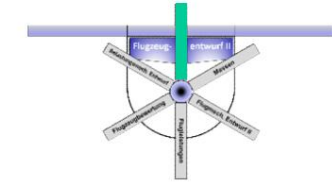


# D Basics of aerodynamic design

## 1.4.2 Lift distribution of the wing



- According to Helmholtz's vortex law, a circulation bound in the wing cannot disappear at the wing tips, but the law of conservation of circulation applies.
- Two free edge vortices are formed, which are in a Close the starting vortex in a ring shape.



# D Basics of aerodynamic design

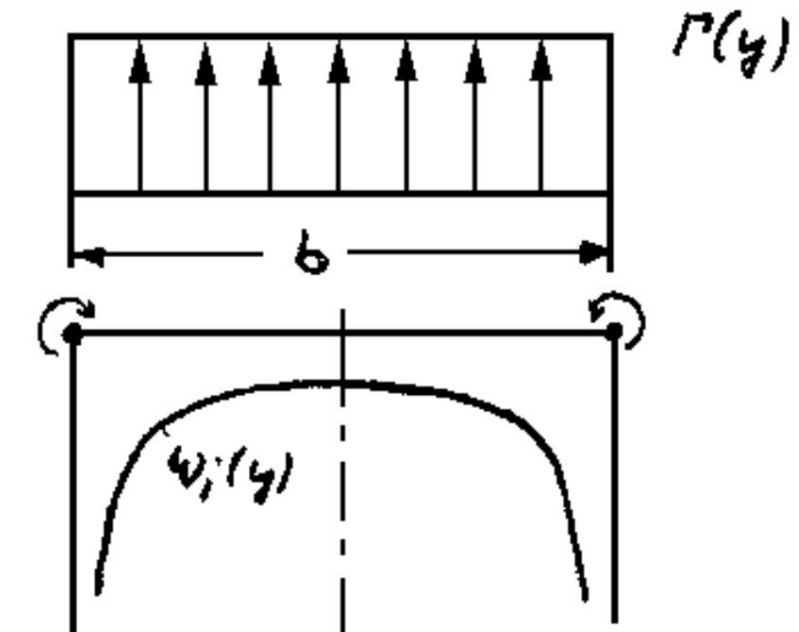
## 1.4.2 Lift distribution of the wing

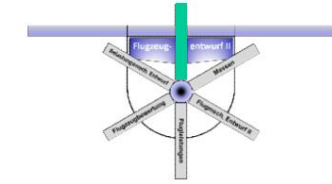
- This starting vortex is created at the moment when the Kutta' cal outflow condition of smooth outflow from the trailing edge is fulfilled and whose circulation reaches the size:

$$\frac{c_A}{2} \frac{A}{b} \frac{\gamma^2}{\gamma_b} = \frac{c_{yl}}{2} \frac{m}{b}$$

- This vortex can actually be measured for a few moments until it disappears due to the air viscosity.
- However, this model has the

**Weakness that the bound circulation does not change with the span.**

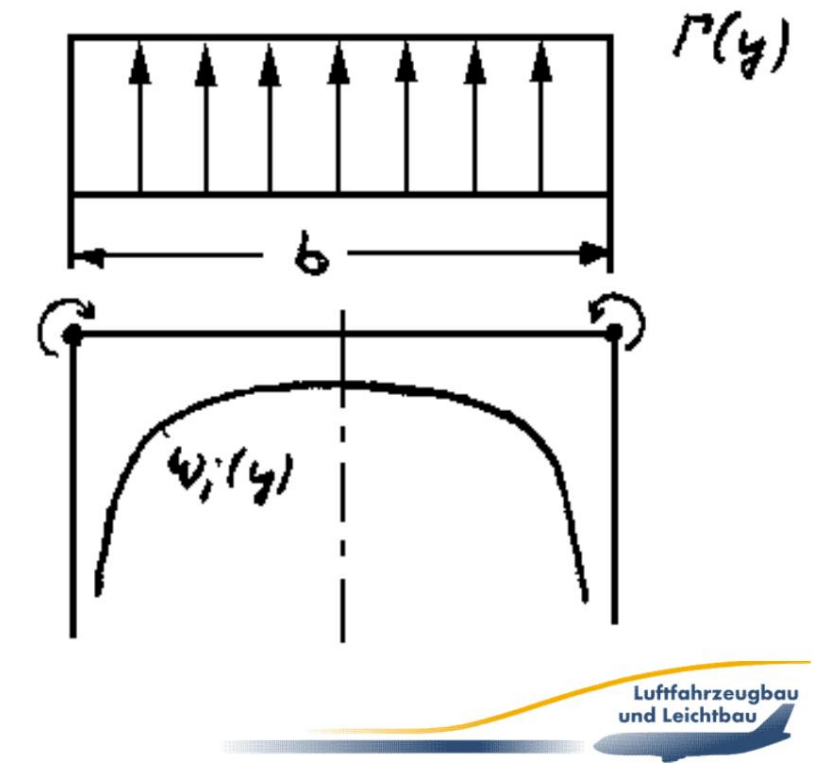


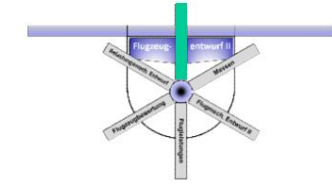


# D Basics of aerodynamic design

## 1.4.2 Lift distribution of the wing

- According to the Biot-Savart law, this condition leads to an infinitely large, downward induced velocity at the wing edge.
- However, it is impossible to reduce the resulting pressure difference between the upper and lower surfaces of the wing.

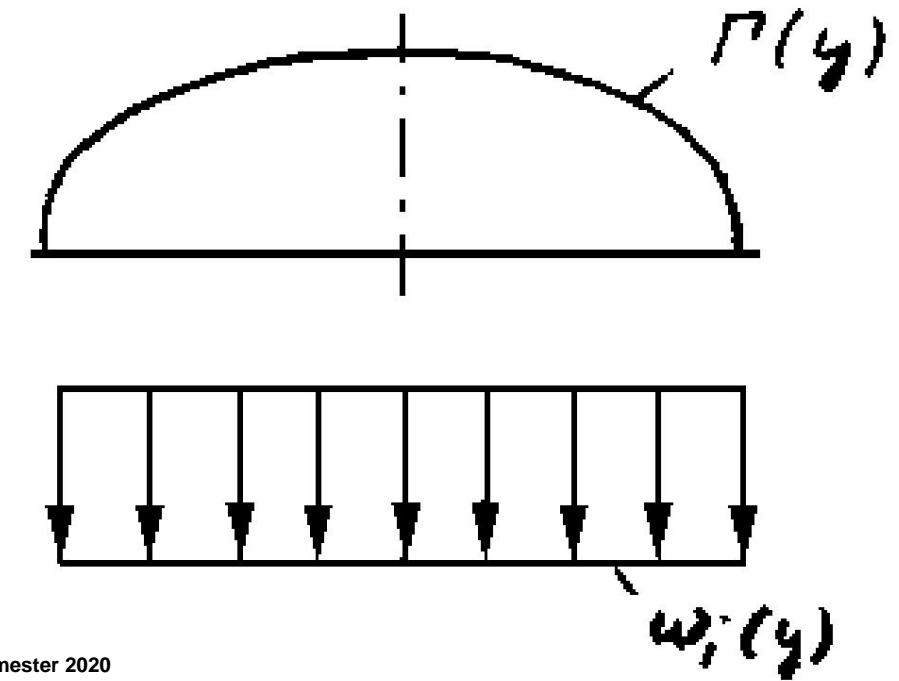


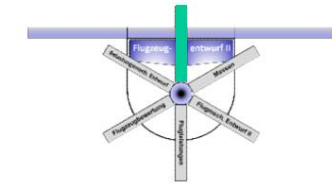


# D Basics of aerodynamic design

## 1.4.2 Lift distribution of the wing

- The pressure equalization that occurs in reality causes the circulation at the wing tips to disappear and consequently a more uniform induced downward velocity is created across the wingspan.
- In case of an elliptical circulation or lift distribution, which can be achieved with an elliptical wing plan, is constant over the span.

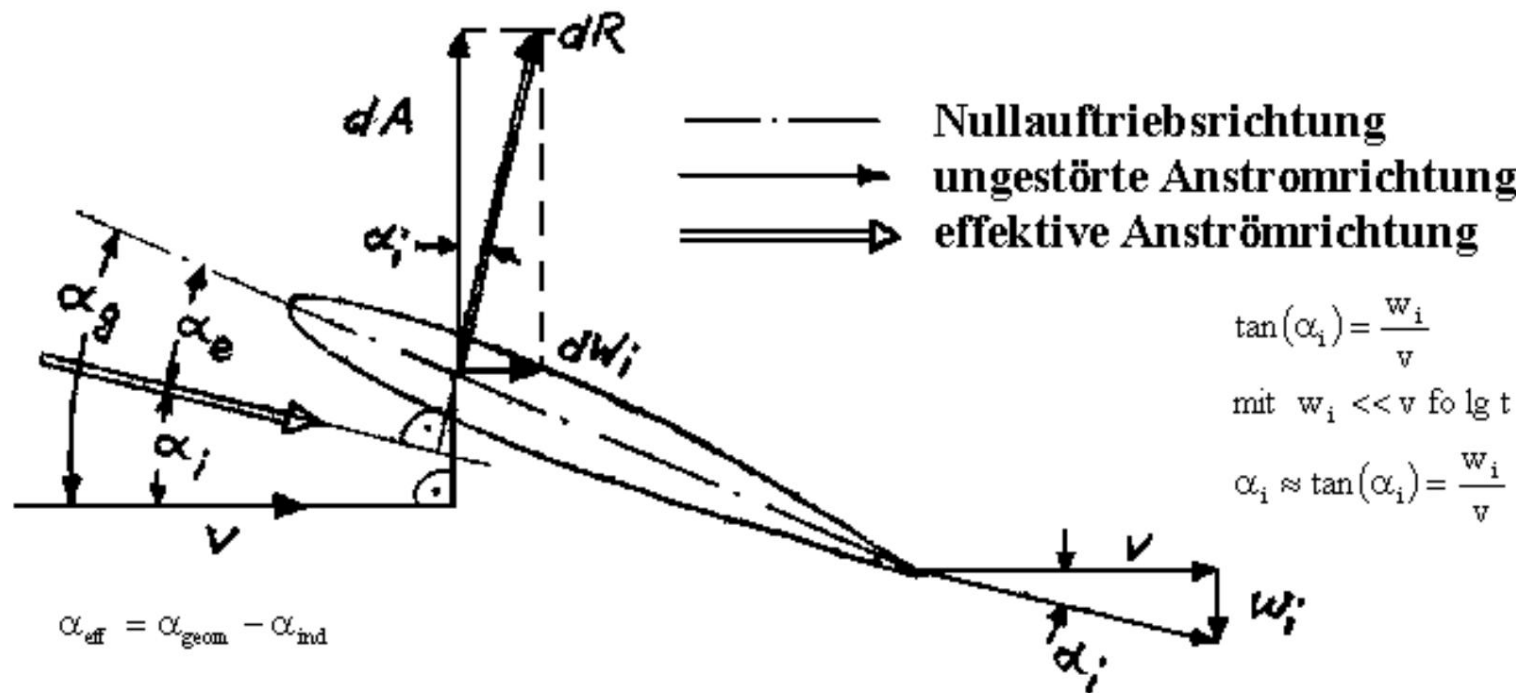


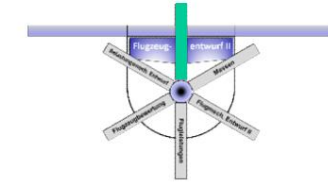


# D Basics of aerodynamic design

## 1.4.2 Lift distribution of the wing

- According to Biot-Savart, the free vortices induce a downward speed, which results in an induced angle of attack distribution by which the resulting flow direction at every location on the wing is inclined downwards compared to the undisturbed flow.

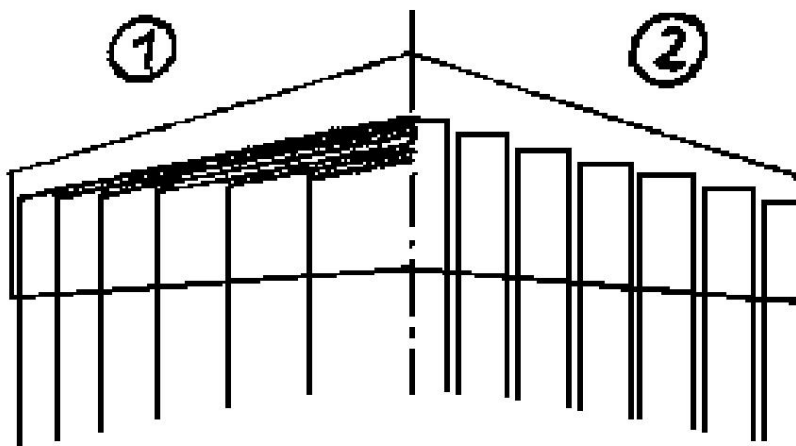




# D Basics of aerodynamic design

## 1.4.2 Lift distribution of the wing

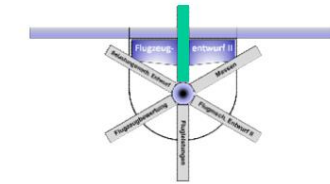
- The above-mentioned inadequacy of the airfoil model for calculating the lift distribution led to the development of extended airfoil methods (e.g. according to Weissinger, Prandtl), which derive the lift distribution with the help of horseshoe-shaped vortex threads staggered in the wing depth, and airfoil methods that use really distributed elementary wings with constant lift distribution as



- ① gebundene und freie Wirbel nach Prandtl-Traglinientheorie**
- ② Ersatz des Flügels durch Elementarflügel**

# D Basics of aerodynamic design

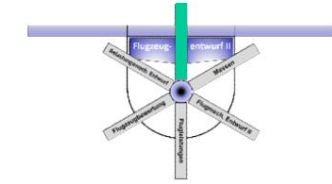
## 1.4.2 Lift distribution of the wing



- The appropriate use of these methods depends on the objective of the analysis. • If a highly aspect ratio, straight, incompressible wing is calculated for a glider, an extended lift line method (eg Multhop) is suitable, depending on the nature of the task.

- The determination of the lift for a commercial aircraft that is to operate at high subsonic speeds with a swept wing will be better done using a compressible wing method (eg panel, vortex lattice method). • The treatment of the problems of transonic and supersonic

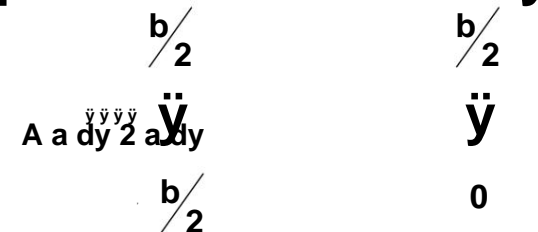
are only possible with non-linear methods. For a description of these methods, please refer to the specialist literature or the courses on fluid mechanics and aerodynamics.



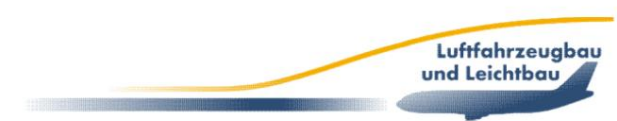
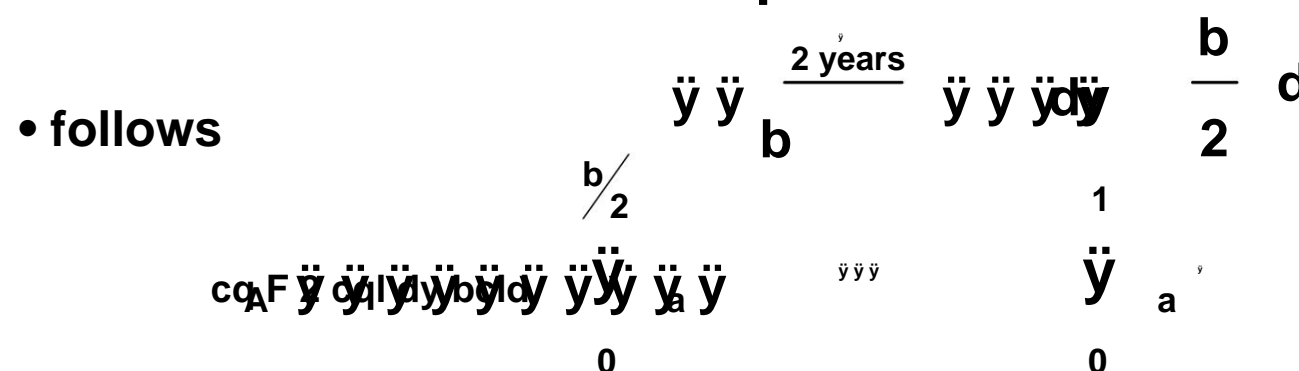
# D Basics of aerodynamic design

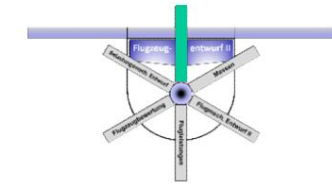
## 1.4.2 Lift distribution of the wing

- Task: Determination of the lift distribution of a wing for a given total lift.
- First: Determine the lift from the integration of the lift contributions  $a$  [N/m] varying over the span of individual differential wing strips with the width  $dy$ :



- With the dimensionless span coordinate





# D Basics of aerodynamic design

## 1.4.2 Lift distribution of the wing

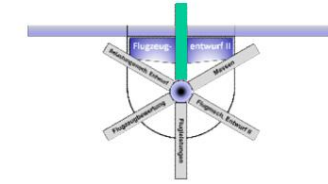
- After solving, the dimensionless wing depth gives and

$$\ddot{y} \ddot{y} c \ddot{y} \frac{I}{I_m}$$

the dimensionless circulation distribution  $\ddot{y}$

$$c_A \frac{b}{F} \frac{1}{\ddot{y}} \frac{c_l d_c}{c_a} \frac{1}{\ddot{y}} \frac{\ddot{y}}{\ddot{y}} \frac{1}{\ddot{y}} \frac{I}{a} \frac{d}{\ddot{y}} \frac{1}{\ddot{y}} \frac{d}{\ddot{y}}$$

- A method for determining the dimensionless circulation distribution  $\ddot{y}$  is presented below.



# D Basics of aerodynamic design

## 1.4.2 Lift distribution of the wing

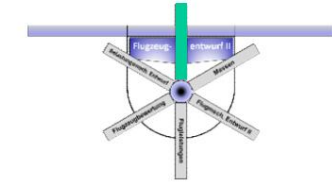
- The semi-empirical wing method according to Diederich has gained practical importance for the design of commercial aircraft.
- It can be used with satisfactory accuracy for swept wings with a general chord profile and moderate aspect ratio up to the high subsonic range.
- The dimensionless circulation distribution is from a buoyancy-dependent component and a base curve It is therefore

$$\frac{4}{\lambda} \frac{1 - \sqrt{\frac{y}{y_0}}^2}{y} \text{C}_2$$

At  $y = y_0$

- The buoyancy-dependent component consists of the weighted Sum of a depth, ellipse and sweep function:

$$C_L = \frac{1}{\lambda_m} \left( C_{L0} + C_{Lc} \frac{1 - \sqrt{\frac{y}{y_0}}^2}{y} + C_{Le} \frac{1 - \sqrt{\frac{y}{y_0}}^2}{y} \right)$$



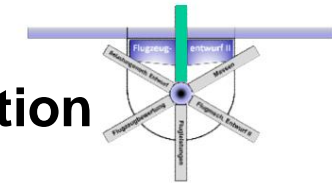
# D Basics of aerodynamic design

## 1.4.2 Lift distribution of the wing

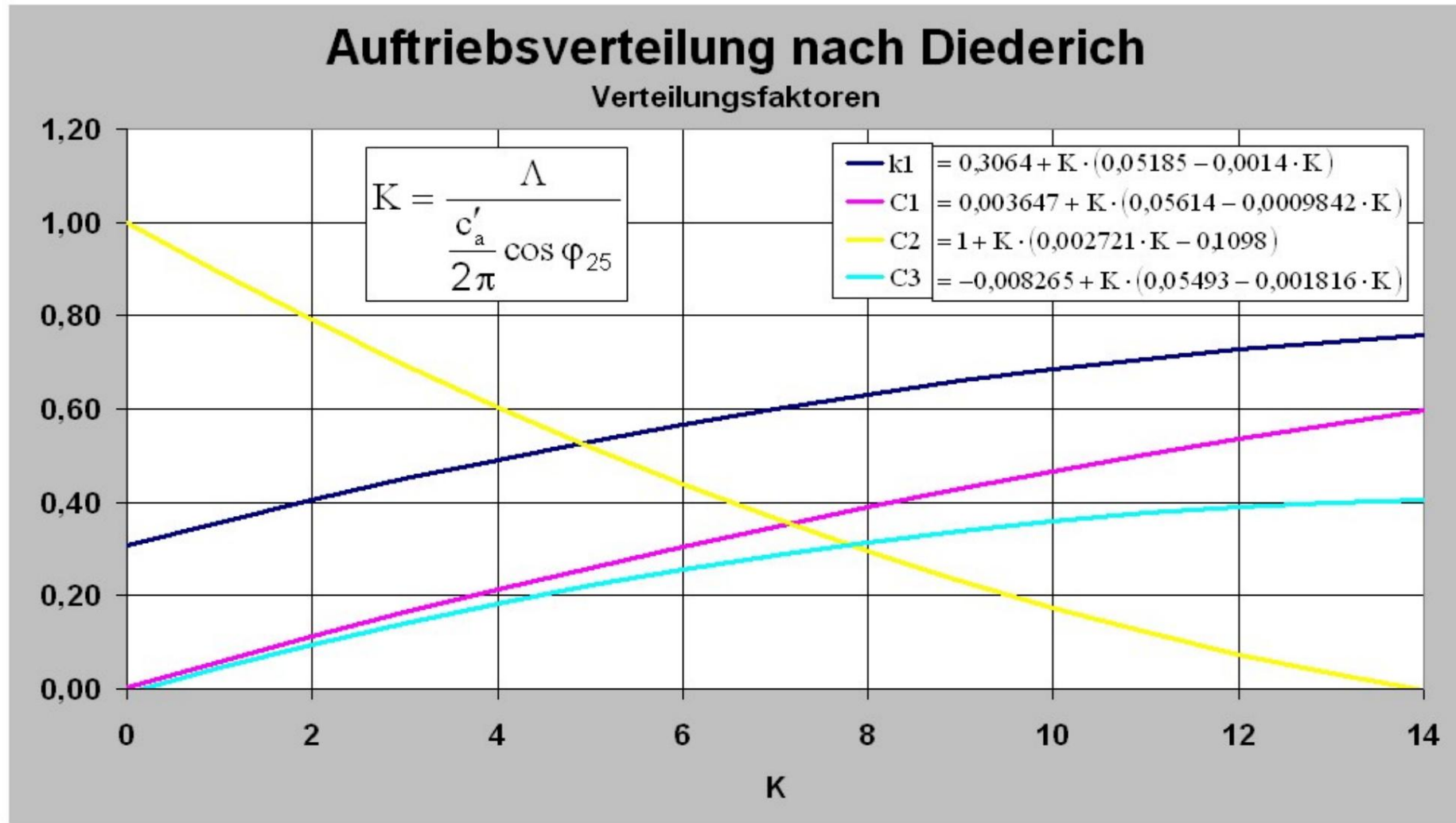
- The base portion describes the effect of the twist and is

$$\ddot{y}_b \ddot{y} \ddot{y} \ddot{y} \boxed{k_c} \ddot{y} \ddot{y} \ddot{y} \ddot{y} \ddot{y} \ddot{y} \ddot{y} \ddot{y} \ddot{y} \ddot{y}$$

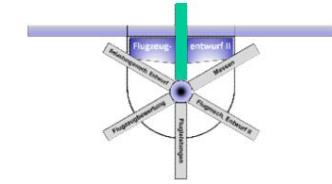
- When numerically evaluating this function, it is important to ensure that the integral value is not dependent on  $\ddot{y}$  but represents a constant mean value for the torsion  $\ddot{y}$  weighted with  $\ddot{y}_a$ , which is subtracted from the torsion curve in the expression in brackets!



## D Basics of aerodynamic design 1.4.2 Wing lift distribution



The sum of the  $c_i$  is always one, so  $K$  only weights the shares!



# D Basics of aerodynamic design

## 1.4.2 Lift distribution of the wing

- The planform factor used here includes aspect ratio, sweep, and the compressible lift increase of the profile used.
- The latter can be determined using the formulas given by Diederich.

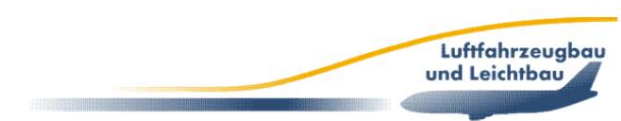
Relationships with

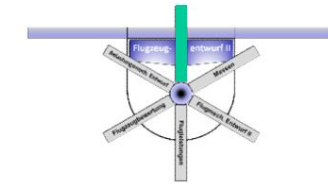
$$c_a^{\ddot{y}} = \frac{2^{\ddot{y}}}{\sqrt{1 + Ma_{Pr \text{ ofile}}^2}}$$

(Based on the load-bearing line theory, Prandtl-Glauert-factor), whereby the effective profile Mach number is

$$Ma_{Pr \text{ ofile}} = \sqrt{\frac{Ma^2 - \dot{y}^2}{1 + \dot{y}^2}}$$

can be estimated with sufficient accuracy.





# D Basics of aerodynamic design

## 1.4.2 Lift distribution of the wing

- The compressible lift increase of the wing can be determined by

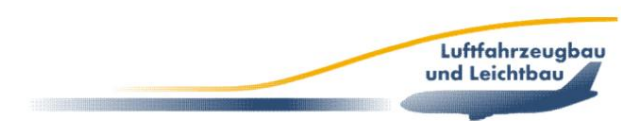
$$\Delta C_L \propto k_0 \cos \alpha$$

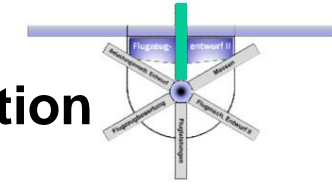
where the factor  $k_0$  is defined as

$$k_0 = \frac{K}{\sqrt{\frac{K^2 - 4}{K^2 + 2}}}$$

- Alternative: The much more convenient formula according to Weissinger (wing theory)

$$C_L = \frac{1}{2} \rho \frac{V^2}{c} \left( 1 + \frac{2}{\pi} \frac{y^2}{L^2} \tan^2 \frac{\alpha}{2} \right)^{-1} \frac{1}{1 - \frac{Ma^2}{2}}$$

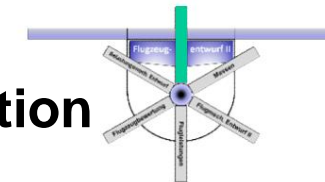




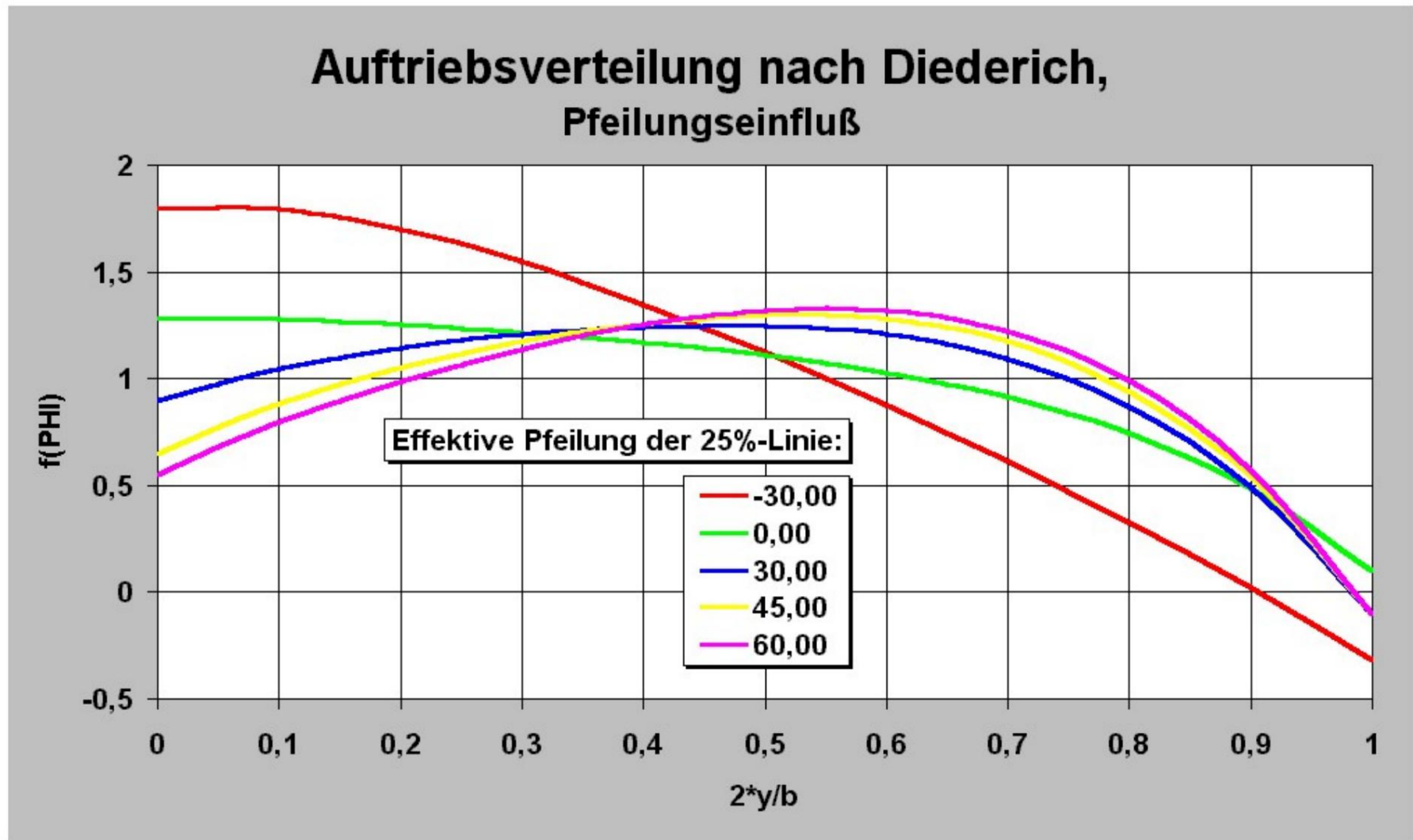
## D Basics of aerodynamic design 1.4.2 Wing lift distribution

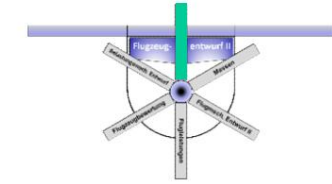
- The sweep functions  $f(\bar{y})$  are available as a function of the effective

$$\bar{y}_e = \arctan \frac{\text{sweep angle, } \bar{y}}{\sqrt{1 - \frac{25}{Ma^2}}}$$



## D Basics of aerodynamic design 1.4.2 Wing lift distribution





# D Basics of aerodynamic design

## 1.4.2 Lift distribution of the wing

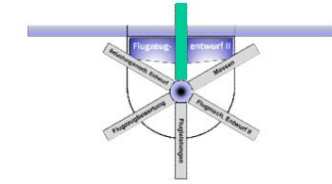
- The curves of the arrow function show very clearly

the fundamental influence of the sweep on the

Detect buoyancy distribution:

- A forward arrow (negative sign) leads to a  
Relief of the outer wing.

- The larger the back arrow (positive sign)  
the more the outer wing is loaded and the further the  
distribution maximum shifts outwards.



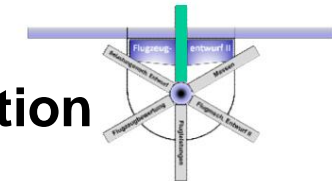
# D Basics of aerodynamic design

## 1.4.2 Lift distribution of the wing

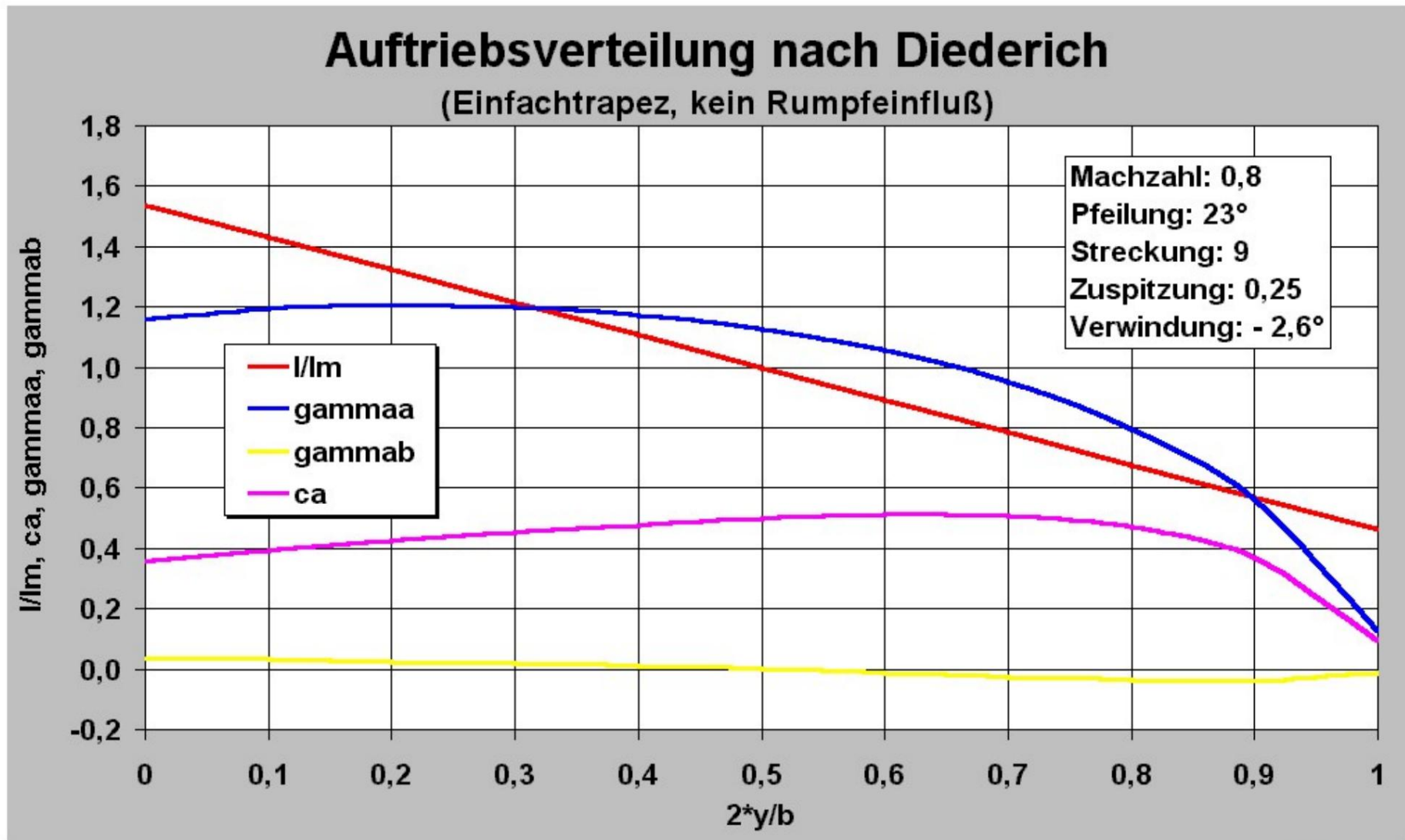
- The distribution of the lift coefficient can now be determined from the dimensionless circulation distribution using the relationship already derived:

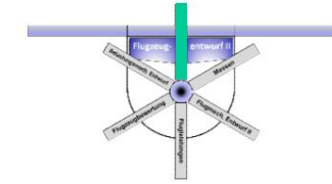
$$c_a \frac{\ddot{y}}{\dot{y}} = \frac{\ddot{y}}{l \ddot{y} / m}$$

- It should be noted that the wing lift coefficient is higher than the lift coefficient that the aircraft has in stationary flight
- To trim the wing moment or center of gravity variations, a downward force on the horizontal stabilizer must also be compensated.



## D Basics of aerodynamic design 1.4.2 Wing lift distribution

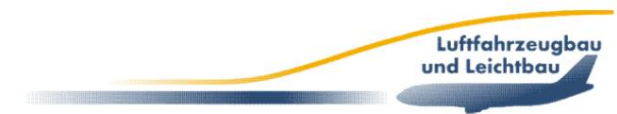


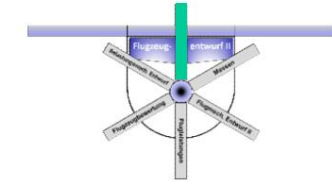


# D Basics of aerodynamic design

## 1.4.2 Lift distribution of the wing

- From this example, it can be seen that, due to the sweep, the wing has its maximum lift coefficient at about 66% of the half span, a range that guarantees sufficient lateral controllability. • However, this position could only be achieved with the help of a drag-increasing twist, as can be seen from the course of the twist-dependent circulation distribution, which has negative values in the outer region.
- The resulting wing lift coefficient is calculated by averaging the  $c_L$  curve and is approximately 0.43, which is the typical value at the design point.
- This method allows the influence of the wing design parameters on the lift behavior to be determined very quickly and effectively.





# D Basics of aerodynamic design

## 1.4.3 Wing moment

- Diederich's method also allows the wing moment to be calculated in a simple manner. •

The moment coefficient around the neutral point can be obtained by adding a base moment and a moment coefficient caused by twisting and sweep:

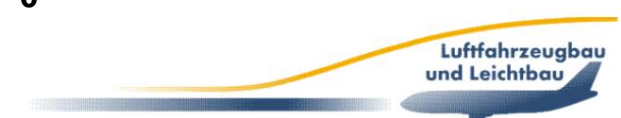
$$\ddot{c}_M \ddot{c}_{M,ac} \text{ Wing} = \ddot{c}_M \ddot{c}_{M,ac} \text{ Basis} + \ddot{c}_M \ddot{c}_{M,ac}$$

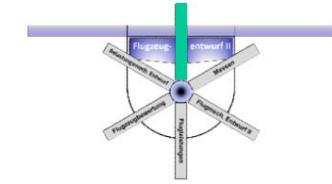
- The base share can be calculated using the relationship:

$$\ddot{c}_M \text{ Base } M_{,ac} = \frac{I_m}{I_m} \cdot \frac{1}{C_{m,ac}} \cdot \frac{\ddot{y} \ddot{y}^2}{\ddot{y} \ddot{y}^2 d}$$

- The twisting component is

$$\ddot{c}_M = \frac{\ddot{y} \ddot{y} \tan \frac{1}{25}}{2 \text{ litres}} \cdot \frac{d}{m}$$

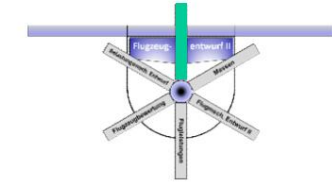




# D Basics of aerodynamic design

## 1.4.3 Wing moment

- The compressible profile moment coefficient  $c_m, ac$ 
  - depends on the local lift coefficient
  - must be subject to a suitably measured or approximately linearly approximated polars



# D Basics of aerodynamic design

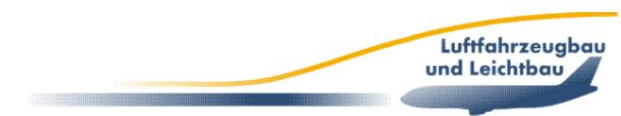
## 1.4.4 Wing drag

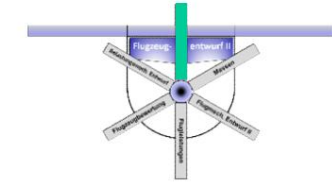
- The resistance of the wing is made up of four parts

together:

1. Frictional resistance
2. (friction-dependent) pressure resistance
3. Wave impedance
4. Induced resistance

- The friction component can be determined with sufficient accuracy and little effort using the theory of the longitudinally flowing, flat plate presented in Chapter D.1.3.2.
- D.1.3.2 also provides a method for taking into account the called surface roughness.
- A Mach number correction method is given in Chapter D.1.3.3.



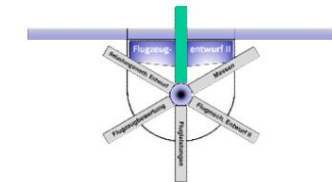


# D Basics of aerodynamic design

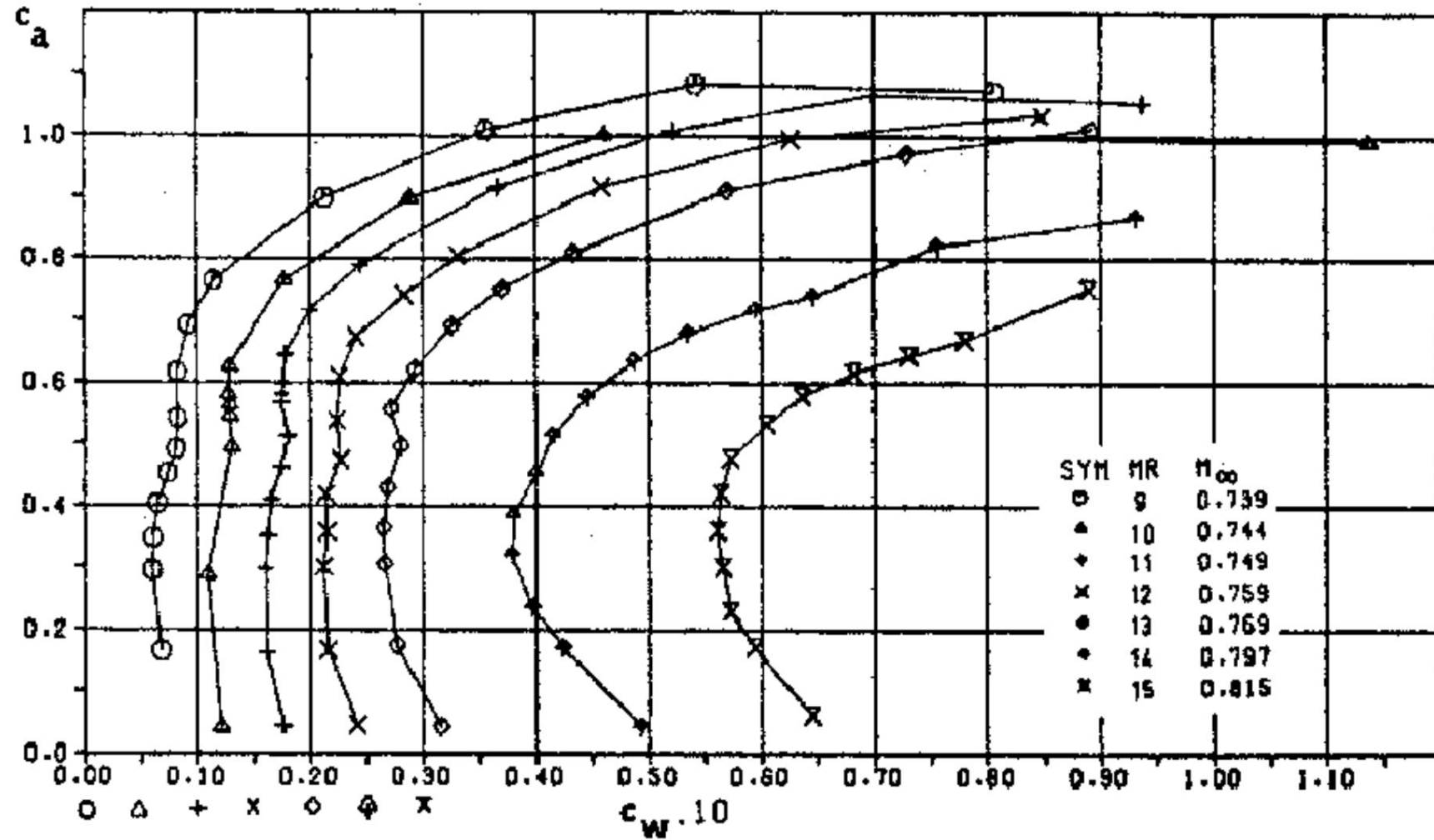
## 1.4.4 Wing drag

- Multiplying the friction coefficient  $c_f$  thus determined with the pressure drag coefficient  $(1+k)$  and adding a term dependent on the lift coefficient  $c_a$  (exponent 6 approximately for profile VA2), one obtains for the incompressible profile polar of the profile:

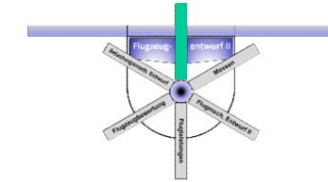
$$C_{w_p} = 2 c_1 k \frac{0.03 C_L^2}{C_a^6}$$



## D Basics of aerodynamic design 1.4.4 Wing drag



Profile VA2,  $d/l = 13\%$

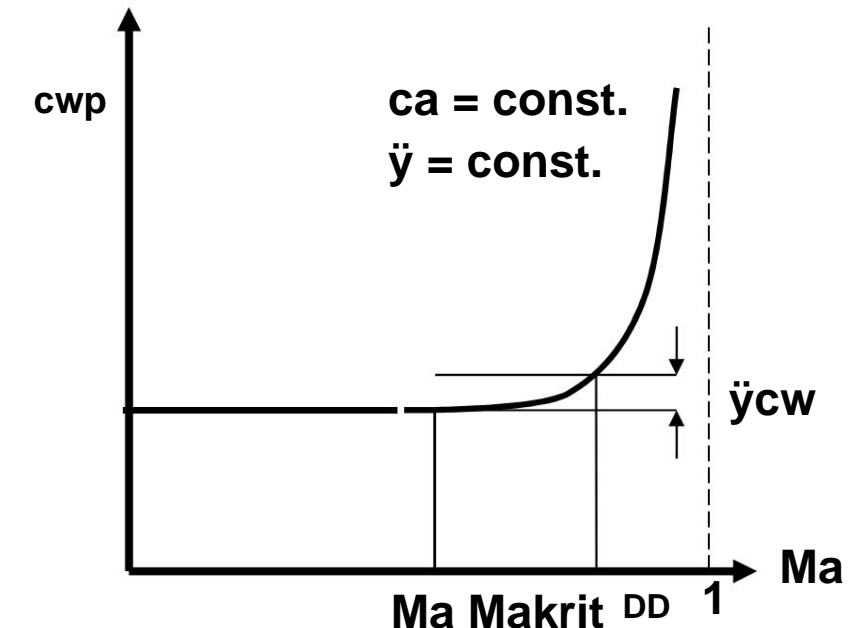


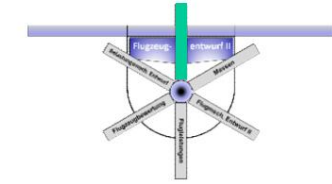
# D Basics of aerodynamic design

## 1.4.4 Wing drag

- The compressible polar also contains the wave resistance was standing.
- This is either determined directly from measurements (see example VA2) or by means of assumptions for the resistance increase
  - Exponential

functions that satisfy the drag-rise point (MaDD) with the defined drag increase (eg  $\ddot{\gamma}_{cw} = 0.002$ ) and at the same time the point of the critical Mach number (Makrit) can be used with good success in the transonic range.





# D Basics of aerodynamic design

## 1.4.4 Wing drag

- After determining the local drag coefficients, the wing drag coefficient is determined by integrating over the span.

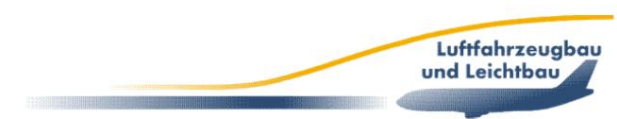
- The following applies to the wing profile drag:

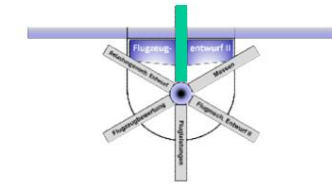
$$\int_0^{b/2} \frac{c_d}{c_l} dy$$

- After inserting the coefficients (analogous to the lift calculation)

$$C_{WP} = \frac{2}{F} \int_0^{b/2} \frac{1}{c_l} \frac{dy}{c_d} = \frac{b}{F} \int_0^1 \frac{1}{c_l} \frac{dy}{c_d} = \frac{1}{I_m} \int_0^1 \frac{I}{y} c_w p dy$$

- This integration of the  $c_d$ -dependent drag coefficients leads to the fact that local coefficient changes (eg the "laminar swell") are only weakly reflected in the wing polar.





# D Basics of aerodynamic design

## 1.4.4 Wing drag

- The total resistance still includes the induced resistance to determine.
- For dilations  $> 4$ , a bi-polynomial approach for  $c_a$  and  $c_d$  is which takes into account the wing plan parameters:

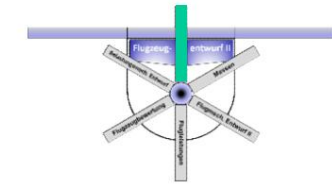
$$c_{w2i} = \frac{c^2}{A} = c_1 + c_2 t^2$$

$$c_1 = 0.0088 + 0.0051t + 1.6t^2 - 10t^4 + 2t^6$$

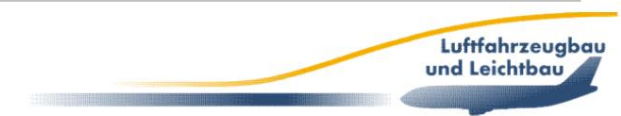
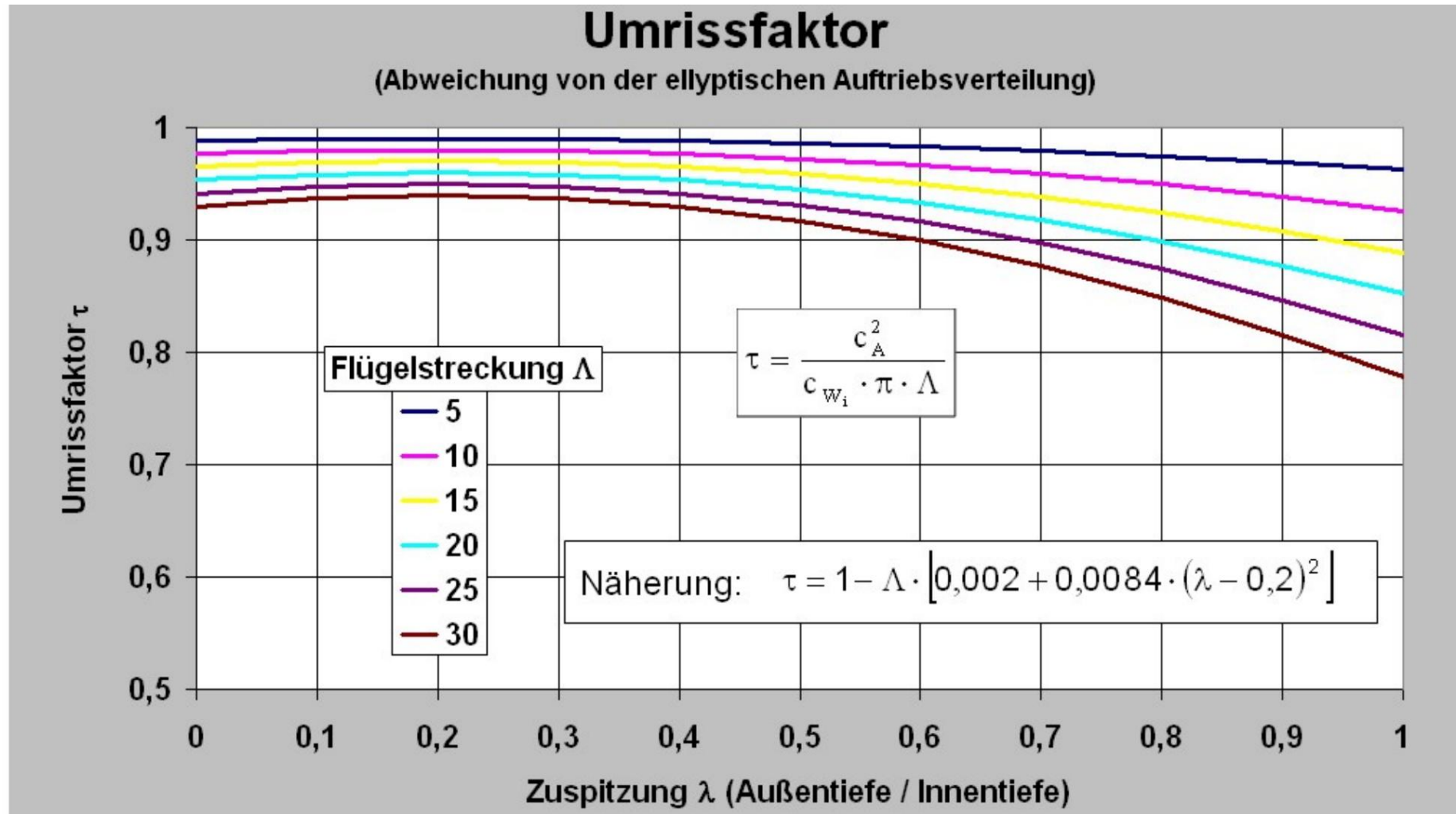
$$c_1 = 0.0134 + 0.3t + 0.0037t^2$$

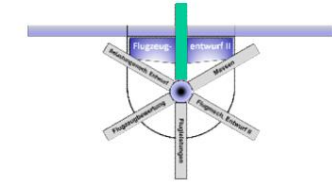
$$c_2 = \frac{1.5t^6}{t^3}$$





## D Basics of aerodynamic design 1.4.4 Wing drag

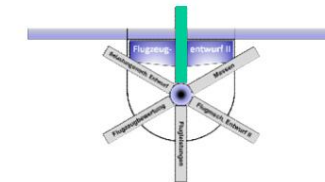




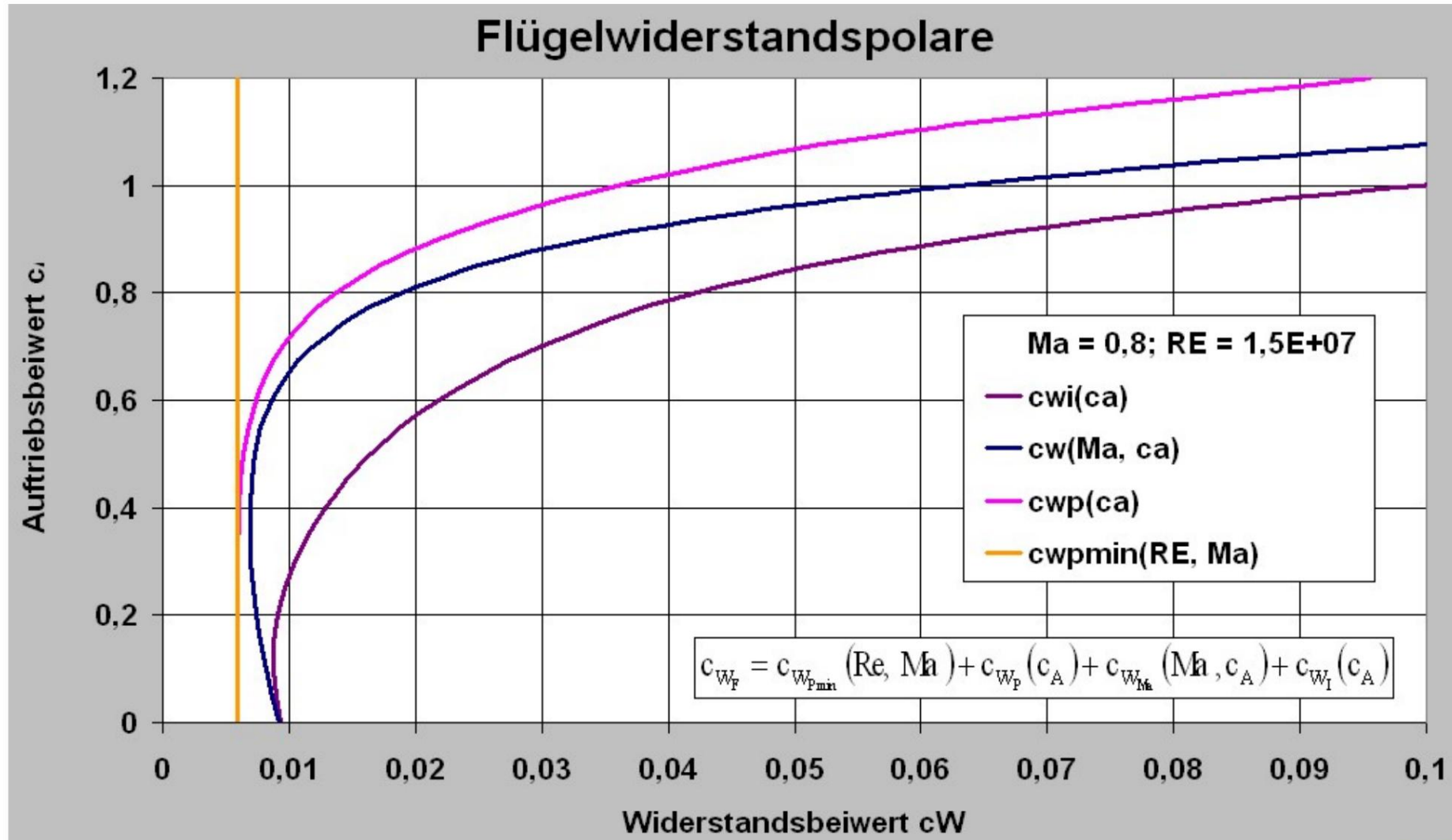
# D Basics of aerodynamic design

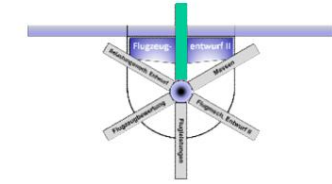
## 1.4.4 Wing drag

- When calculating the induced drag, a linear geometric twist is assumed.  
 $\delta_t$  denotes the difference between the profile setting angle at the wing edge and that at the wing root.
- The sum of the above mentioned shares in the shown  
The drag polar of the wing formed in this way is also called the “design polar” of the wing because the design conditions are assumed to be constant regardless of the angle of inclination.
- The equivalence of lift and weight, which is the basis for free flight,  
does not apply here, but it is treated as if “a massless model in  
the wind tunnel” is being investigated.



## D Basics of aerodynamic design 1.4.4 Wing drag





# D Basics of aerodynamic design

## 1.4.5 Influence of wing extension

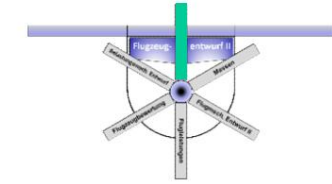
- The aspect ratio is a "slenderness measure" of the wing and is related to the span  $b$  and the mean wing depth  $l_m$ :

$$\text{Aspect Ratio} = \frac{b}{l_m}$$

- Since the wing area also depends on the span and the wing depth, the following formulation is usually used for the stretch:

$$\text{Stretch} = \frac{b^2}{F}$$

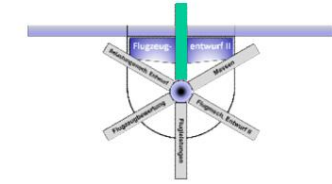
- Values for the aspect ratio range from 3 - 5 (fighter aircraft) to 8 - 10 for commercial aircraft and up to 45 (high-performance gliders).



# D Basics of aerodynamic design

## 1.4.5 Influence of wing extension

- It is obvious that, for a constant area, the height of a wing decreases with increasing aspect ratio.
- This is associated with an increase in weight.
- In addition, the tank volume of the wing box decreases, which can lead to range problems.



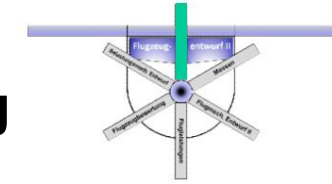
# D Basics of aerodynamic design

## 1.4.5 Influence of wing extension

- While the infinite wing only has a profile drag, the finite wing has a significant additional drag component, the induced drag.
- This drag is calculated using potential theory for the straight wing with elliptical lift distribution as:

$$c_{w_i} = \frac{c^2}{\pi A}$$

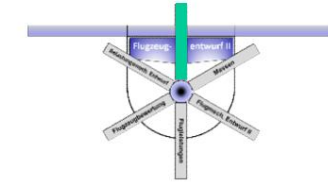
- The induced drag decreases with increasing aspect ratio and increases significantly with increasing wing loading (increasing lift coefficient).



## D Basics of aerodynamic design 1.4.5 Influence of wing aspect ratio

- For real wings, the deviation from the elliptical  
Consider buoyancy distribution
- Using the contour factor  $\ddot{y}$ , the induced  
Resistance

$$c_{w_i} \ddot{y} \frac{2c_A}{\ddot{y}\ddot{y}\ddot{y}\ddot{y}\ddot{y}}$$



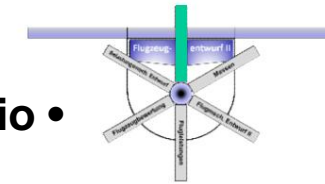
# D Basics of aerodynamic design

## 1.4.5 Influence of wing extension

- The phenomenon of stretching influence on resistance

The following consideration can clarify:

- If you compare wings of the same area but different aspect ratios  
If the air mass is deflected downwards per second, then, using the principle of momentum and with the same lift, the product of the air mass deflected downwards per second times the downward speed must be equal.
- Since the wing has a low aspect ratio and therefore also lower lift coefficient  
Since it can only deflect a smaller mass over a larger wingspan, it must generate a greater downward velocity and thus larger induced angles of attack.
- As has been shown, an increase in the induced angle of attack is accompanied by an increase in induced drag.

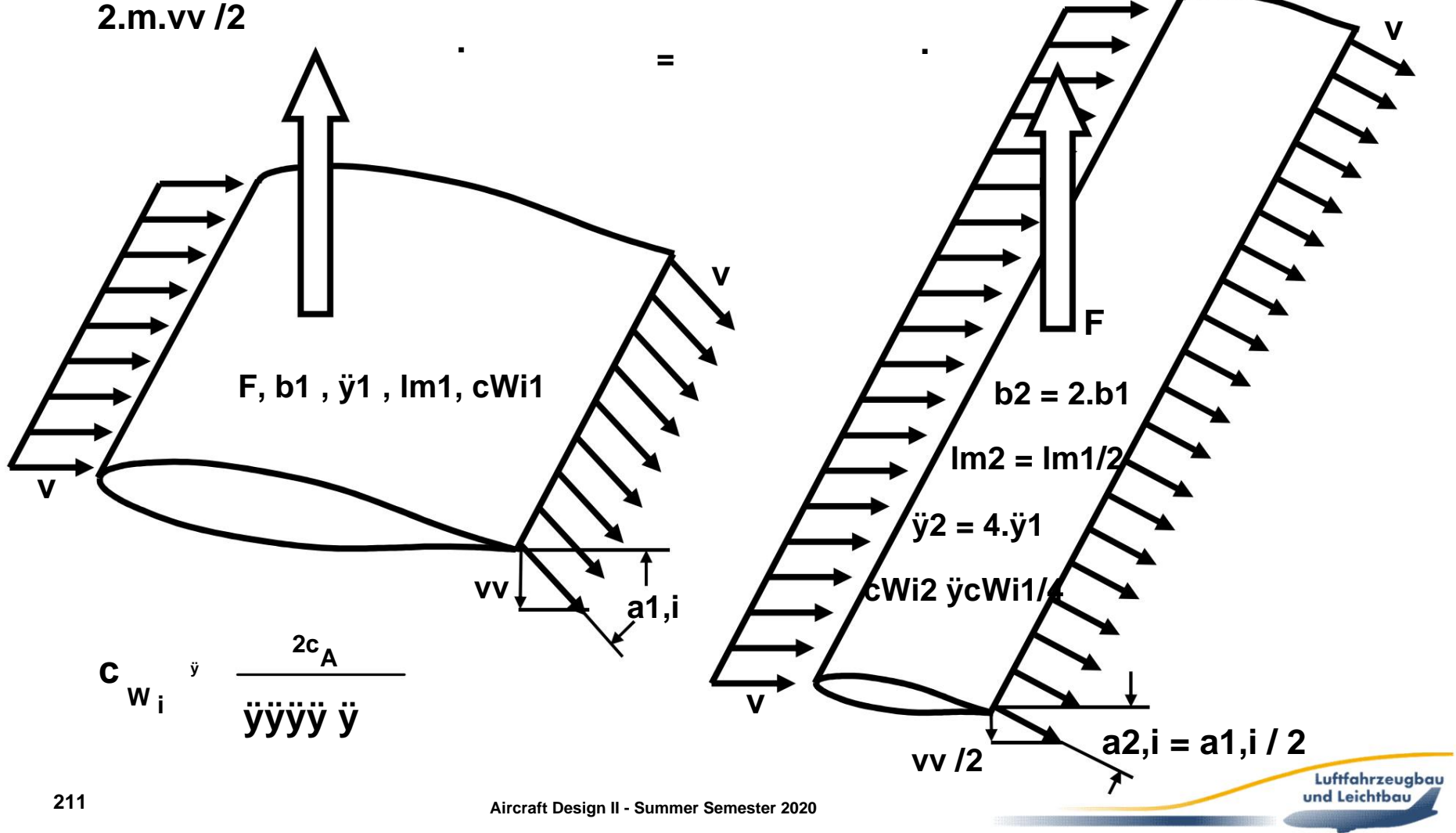


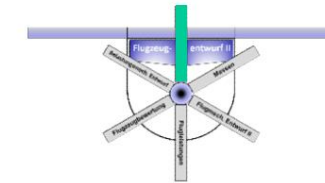
## D Basics of aerodynamic design 1.4.5 Influence of wing aspect ratio •

### Explanation of the influence of aspect

ratio on the induced drag using the momentum theorem  $A = m.vv A =$

$$2.m.vv / 2$$





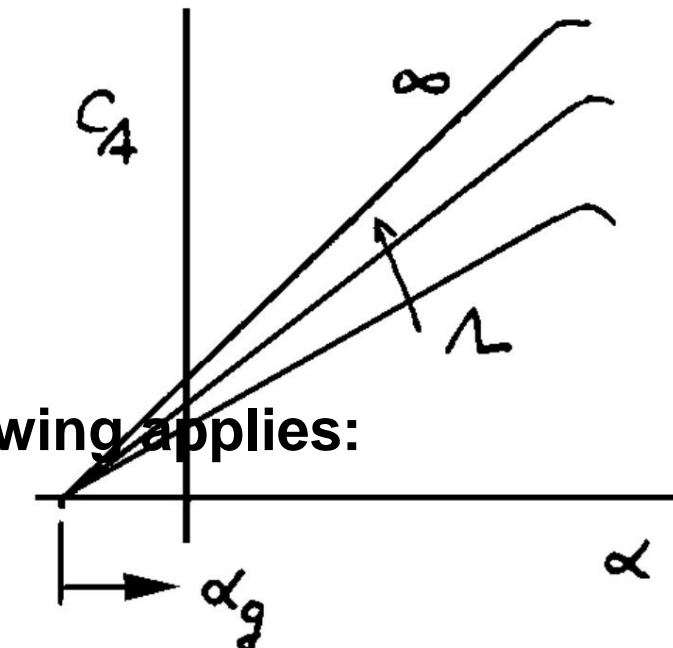
# D Basics of aerodynamic design

## 1.4.5 Influence of wing extension

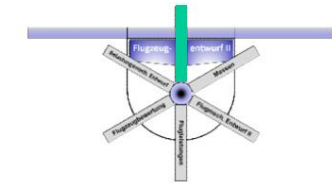
- The high aspect ratio wing is much more efficient in generating lift because it requires a smaller geometric angle of attack than the low aspect ratio wing to generate the same lift.
- The influence of the aspect ratio on the lift gradient for the wing with elliptical lift distribution can be directly derived from the lift line theory. In potential theory, the following applies:

$$c_A \frac{dc}{dy} = \frac{c_a}{1 + \frac{c_a}{2}} \quad \text{for } y=0$$

$$c_A \frac{dc}{dy} = \frac{2}{y+2} \quad \text{for } y \neq 0$$



$$c_A = \frac{c_a}{1 + \frac{c_a}{2}}$$



# D Basics of aerodynamic design

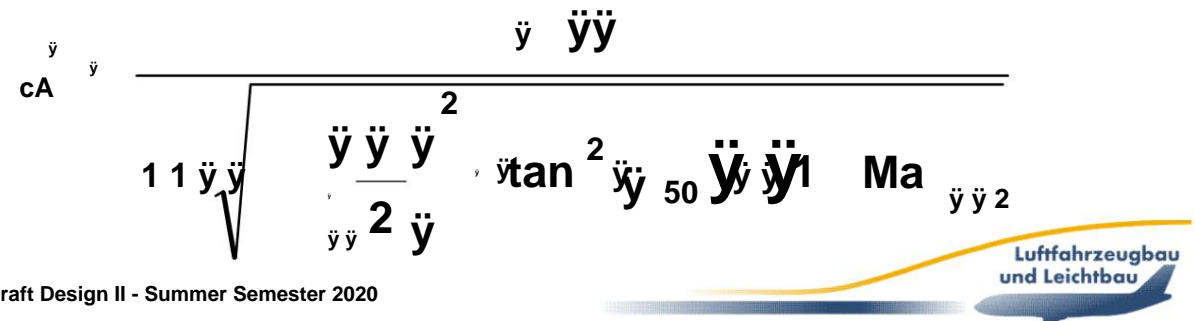
## 1.4.5 Influence of wing extension

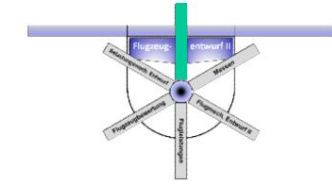
- **Real wing:**

- Measured lift increase is smaller than theoretically expected.
- **Reason:** Elliptical lift distribution can only be achieved with an elliptical floor plan. However, common wing floor plans are rectangular, trapezoidal or double trapezoidal → deviation!
- **Correction:** Use the outline factor  $\bar{c}_A$  to take into account:

$$\bar{c}_A = \frac{\int c(y) dy}{\int A(y) dy} = \frac{\bar{c}_a}{\frac{\int A(y) dy}{\int c_a(y) dy}}$$

- Weissinger formula allows progressive connection with the Recognize wing extension even better:

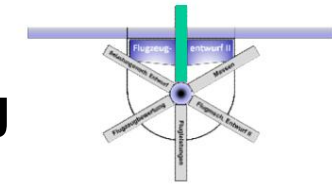




# D Basics of aerodynamic design

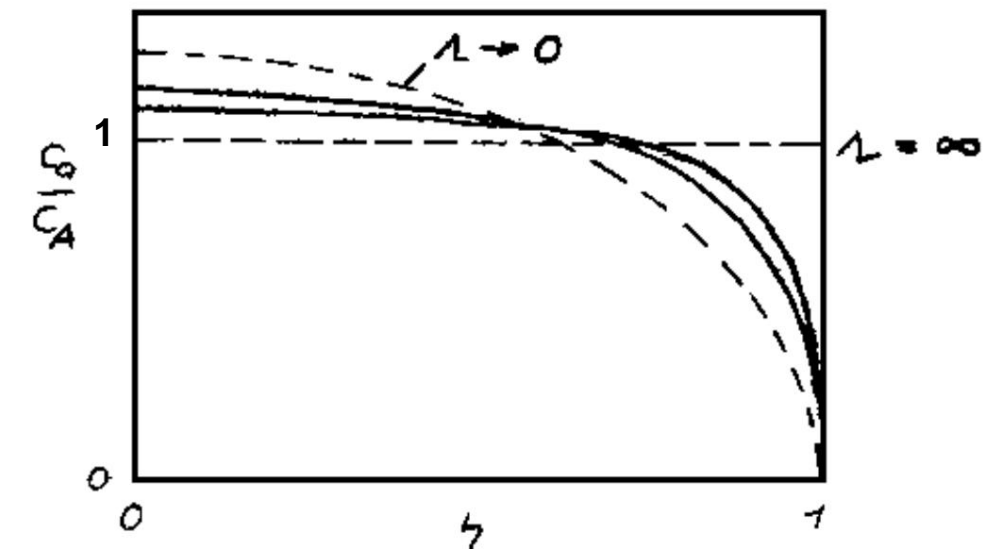
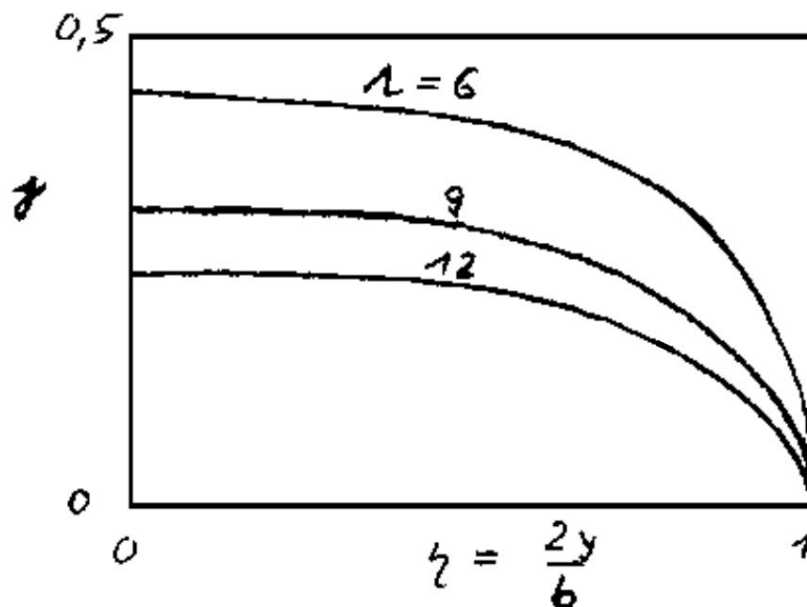
## 1.4.5 Influence of wing extension

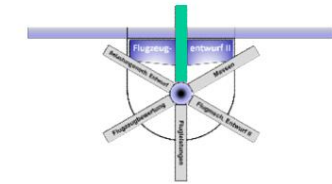
- This phenomenon leads to two flight practical Effects: With increasing stretch
  - the gust sensitivity of the wing increases, as a Increase in angle of attack leads to increasing lift and
  - the change in angle of attack with flight speed becomes smaller, which leads to more demanding landing characteristics.
- However, the lower bending stiffness of a highly stretched wing reduces the effects of gust sensitivity noticeable, which has a positive effect on gliders.



## D Basics of aerodynamic design 1.4.5 Influence of wing aspect ratio

- Influence of stretching on the distribution of coefficients of Circulation  $\gamma$  and lift  $c_a$  of an unswept rectangular wing

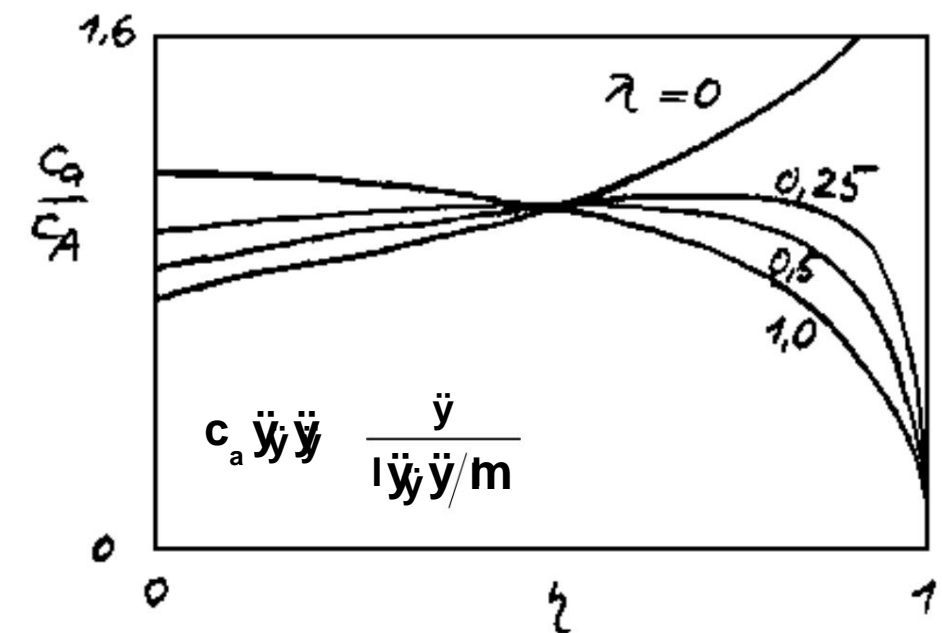
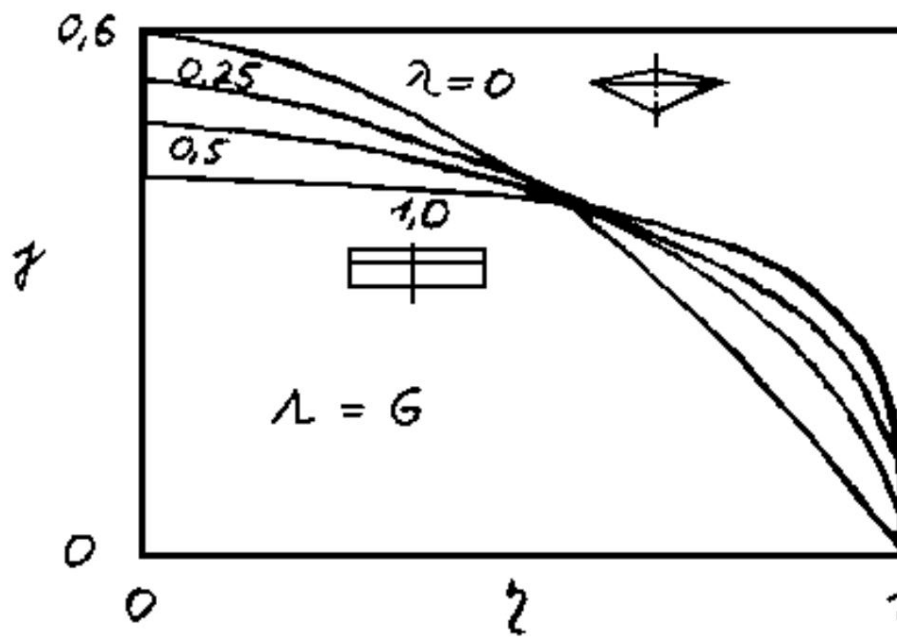


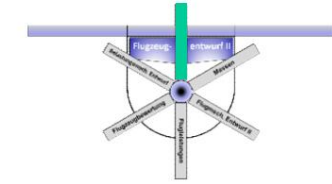


# D Basics of aerodynamic design

## 1.4.6 Influence of escalation

- In addition to the aspect ratio  $\lambda$  and the outline factor  $\lambda$ , the taper  $\lambda$  is another important measure for describing the floor plan.
- The taper  $\lambda$  is 1 for rectangular wings and 0 for delta wings with vanishing external depth.

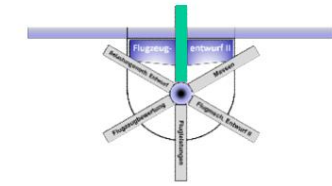




## D Basics of aerodynamic design

### 1.4.6 Influence of escalation

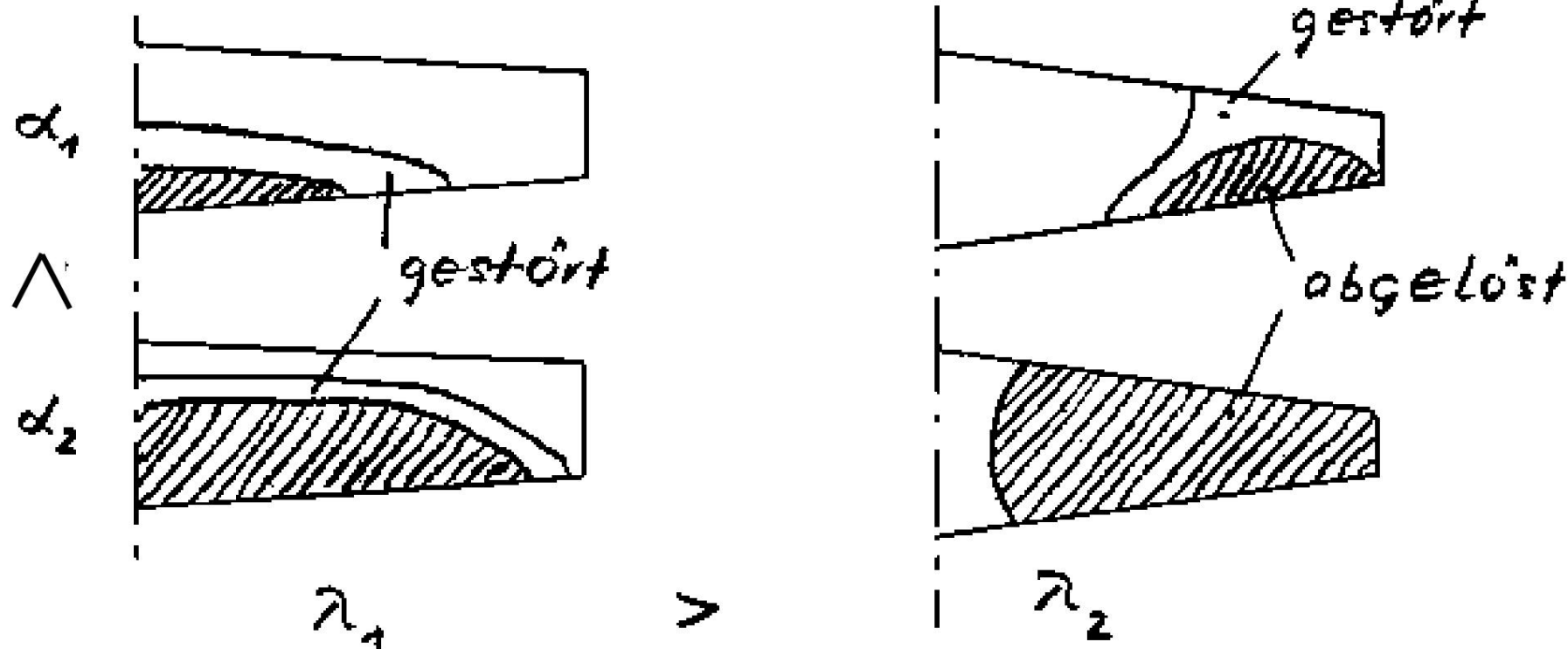
- The local lift coefficient  $c_a$  is inversely proportional to the local wing depth  $\delta$  low taper  $\delta$   
leads to large  $c_a$  values in the outer area of the wing.
- An optimum for  $\delta$  can only be determined together with other geometry parameters (sweep and twist).
- Typically:  $\delta$  is approx. 0.3 to 0.4 for unswept wings and approx. 0.25 to 0.35 for swept wings.

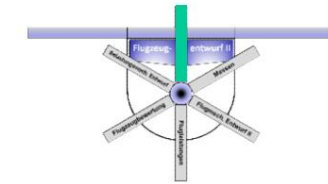


# D Basics of aerodynamic design

## 1.4.6 Influence of escalation

- Influence of tapering on stall behavior

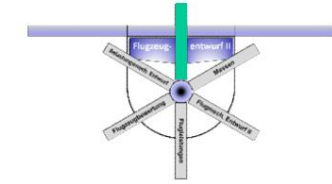




# D Basics of aerodynamic design

## 1.4.6 Influence of tapering

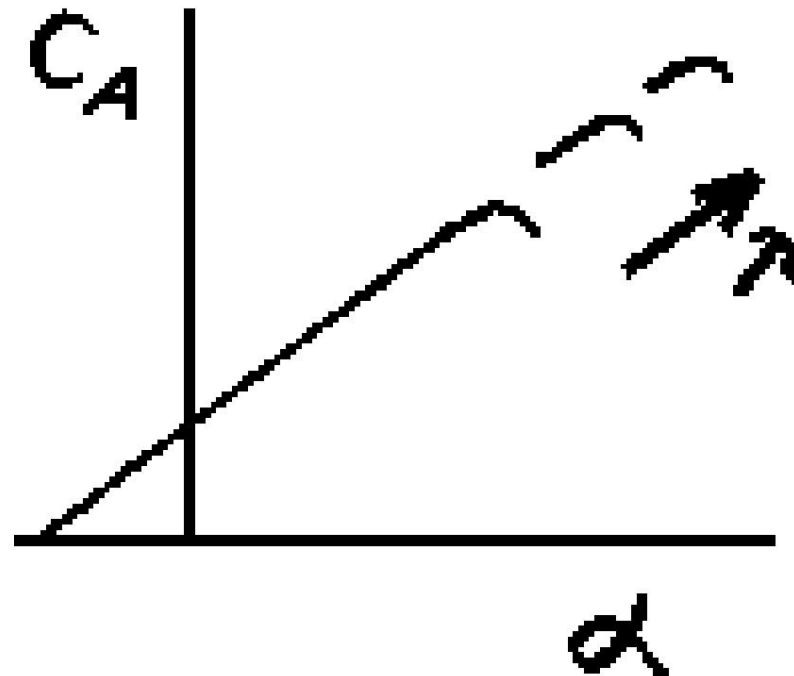
- While the wing with a low taper causes flow separation at the wing root, the strongly pointed wing in the critical outer area detaches first.
- This is not desirable because the only control element for controlling the rotation around the longitudinal axis, the aileron, becomes ineffective in slow flight and at the same time large, uncontrollable moments occur due to the highly unsteady nature of this separation.
- The residual lift (approximately non-hatched area) is on the wing ringer tapering is significantly larger, ie the maximum lift is greater.
- The behaviour of the wing in the high angle of attack range is strongly dependent on the taper, because the onset of boundary layer separation depends on the achievement of the local maximum lift.

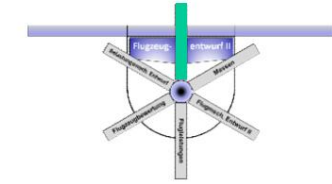


# D Basics of aerodynamic design

## 1.4.6 Influence of escalation

- The behaviour of the wing in the high angle of attack range is therefore sensitively dependent on the taper, because the onset of boundary layer separation depends on the achievement of the local maximum lift.

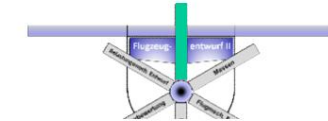




# D Basics of aerodynamic design

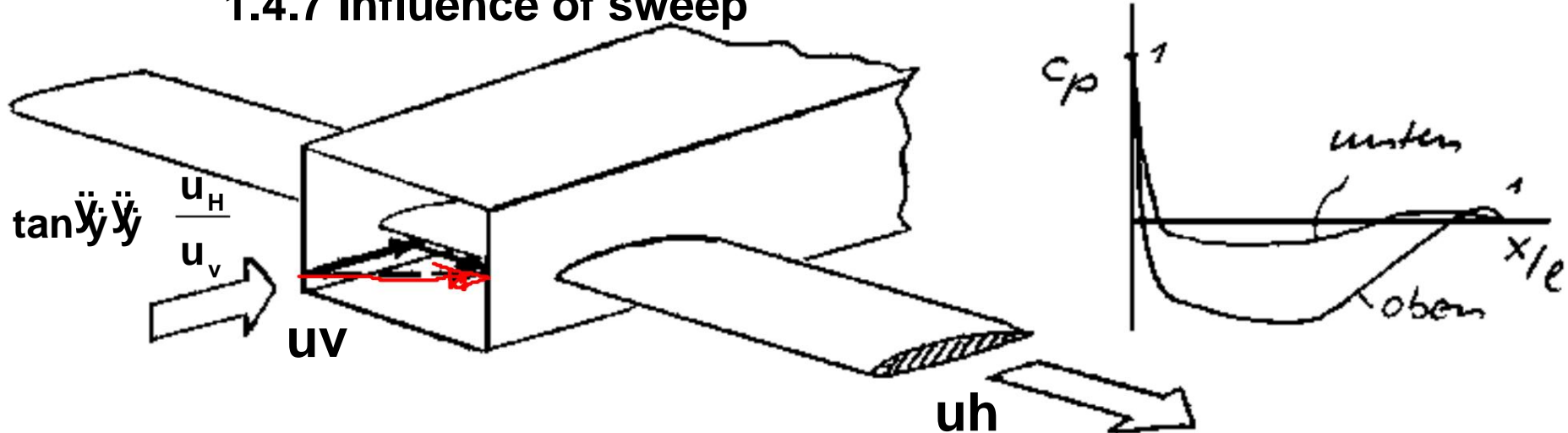
## 1.4.7 Influence of sweep

- Aircraft operating in the high subsonic range usually have a swept-back wing. • A swept-back wing has structural disadvantages because of the torsion of the wing box, which acts in addition to the profile moment and in the same top-heavy direction.
- This causes an increase in weight, which is only justified if there are expected advantages in aerodynamic behavior. • In fact, the sweep causes a shift in the critical Mach number to higher values and thus a corresponding shift in the buffet onset and drag divergence Mach numbers. This is what makes economical cruising at high altitudes possible.

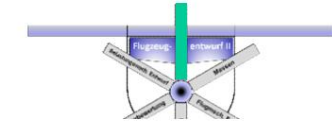


# D Basics of aerodynamic design

## 1.4.7 Influence of sweep

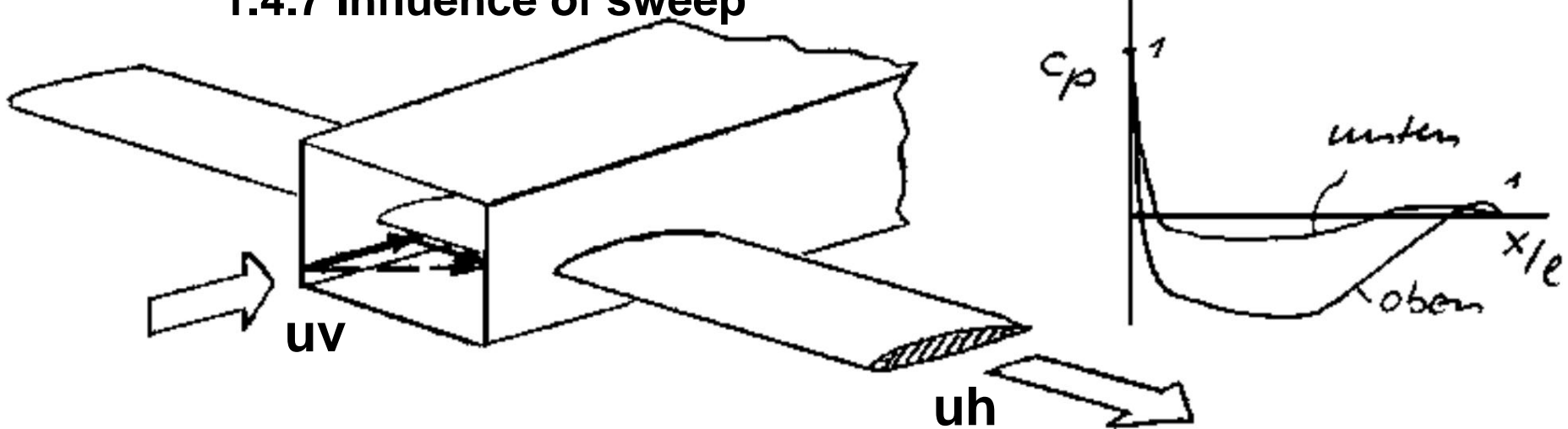


- If an infinitely long wing is pushed longitudinally through a running wind tunnel at a certain speed, the vectorial flow velocity increases and the flow direction rotates by the virtual sweep angle  $\ddot{\gamma}$ .
- $u_v$  is the speed component perpendicular to the wing leading edge (here the channel speed) and  $u_h$  is the sliding speed.



# D Basics of aerodynamic design

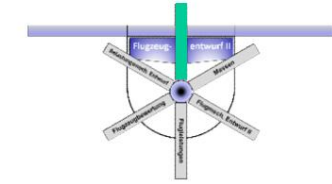
## 1.4.7 Influence of sweep



- The resulting higher speed does not change the Pressure distribution of the sliding or swept wing:

$$u \quad \frac{u_v}{\cos \gamma}$$

- Only the boundary layer with the wing movement.

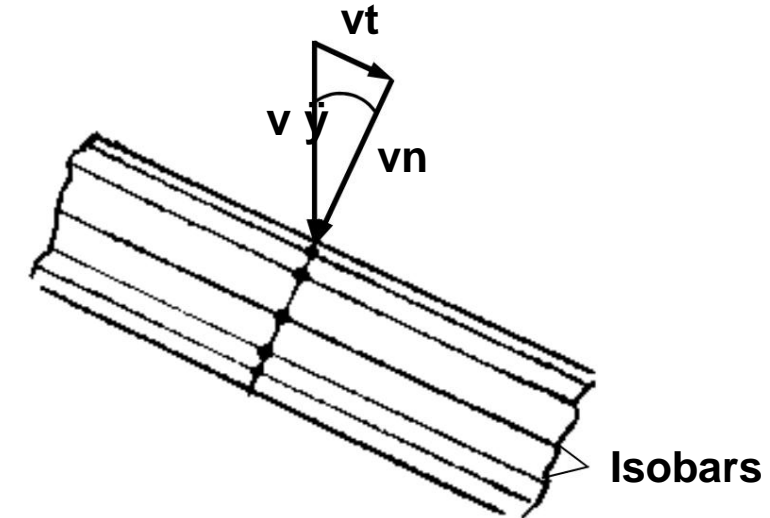


# D Basics of aerodynamic design

## 1.4.7 Influence of sweep

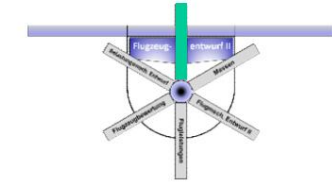
- This means that a swept wing has higher critical Mach numbers by the reciprocal cosine of the sweep angle for the same critical Mach number of the profile, since only the vertical

Speed share for the Pressure distribution becomes effective, and therefore:



$$\frac{Ma_{kr}}{\cos \gamma}$$

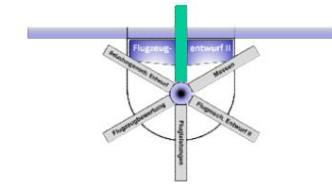
- This fact also means that while the structural thickness of the wing remains the same, the aerodynamic thickness decreases due to the sweep.



# D Basics of aerodynamic design

## 1.4.7 Influence of sweep

- This effect not only affects the critical Mach number, but also the associated limiting Mach numbers (buffet onset, drag divergence, lift divergence) as well as the lift increase and the profile drag.
- The sweep can therefore be used to increase the critical and all limiting Mach numbers based on it.



# D Basics of aerodynamic design

## 1.4.7 Influence of sweep

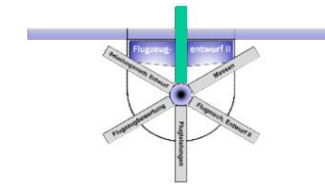
- In D.1.3.3, the critical Mach number was determined as the intersection point of the minimum pressure coefficient transformed into the compressible range using the Prandtl-Glauert factor and the curve of the critical pressure coefficient.
- The same procedure can be followed for the swept wing.
- The minimum pressure coefficient occurs at the vertical Mach number acting to the leading edge  $\frac{\partial}{\partial}$  Transformation:

$$c_{p_{min}} = \frac{c_{p_{min,ik,0}} \cos \frac{\partial}{\partial} \frac{\partial}{\partial}}{\sqrt{1 + Ma \cos^2 \frac{\partial}{\partial} \frac{\partial}{}}}$$

- The critical pressure coefficient is accordingly

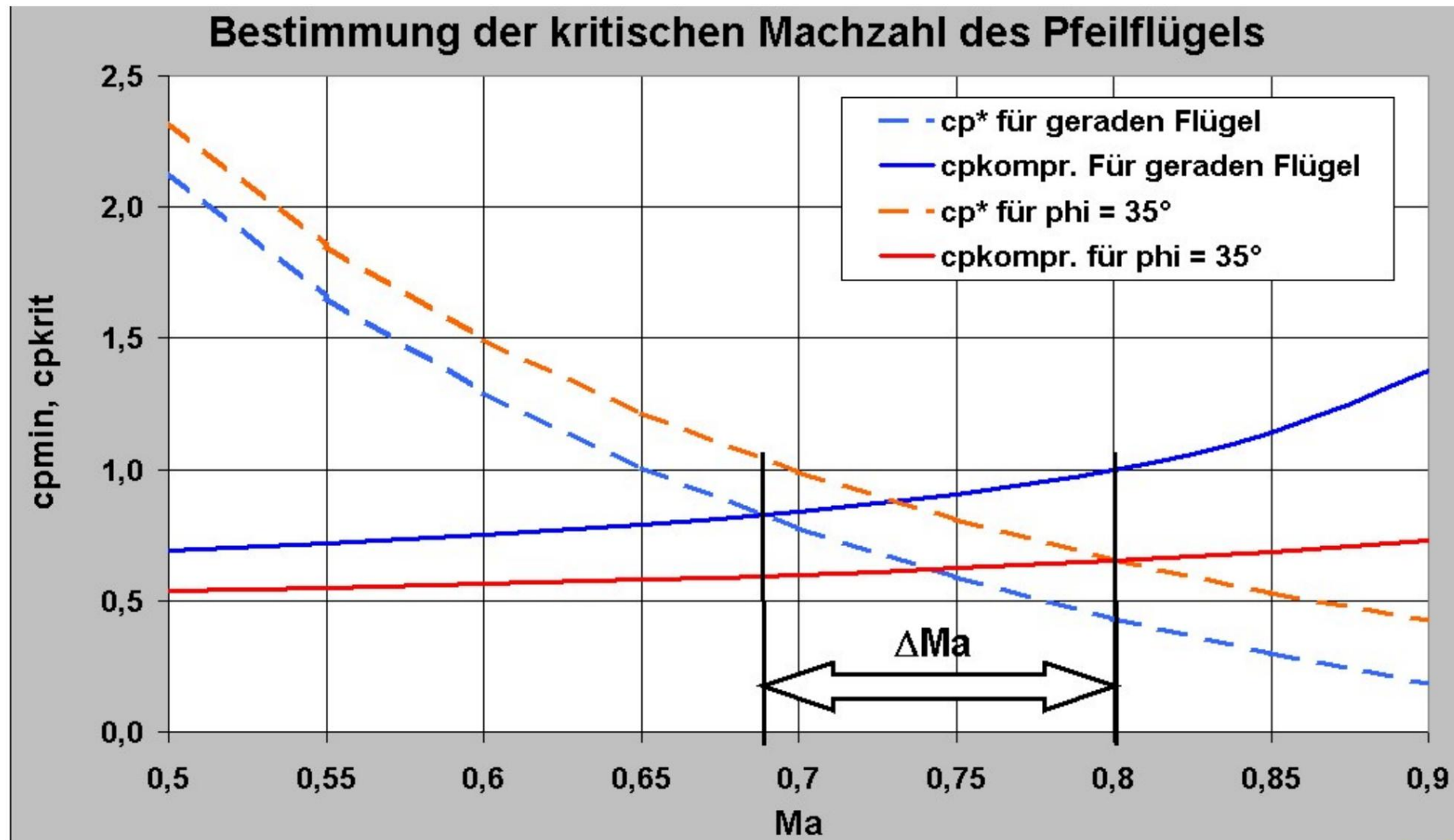
$$c_{p_{ik}} = \frac{2}{k \frac{\partial}{\partial}} \frac{\partial}{\partial} \frac{2}{\frac{\partial}{\partial} \frac{\partial}{}}, \quad \text{But } \frac{2}{\frac{\partial}{\partial}} \cos \frac{\partial}{\partial} \frac{\partial}{} \frac{k \frac{\partial}{\partial} - 1}{k \frac{\partial}{\partial} - 1}, \quad \text{But } \frac{2}{\frac{\partial}{\partial}} \cos \frac{\partial}{\partial} \frac{\partial}{} \frac{k \frac{\partial}{\partial} - 1}{k \frac{\partial}{\partial} - 1}$$

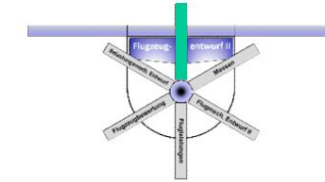
Luftfahrzeubau  
und Leichtbau



# D Basics of aerodynamic design

## 1.4.7 Influence of sweep

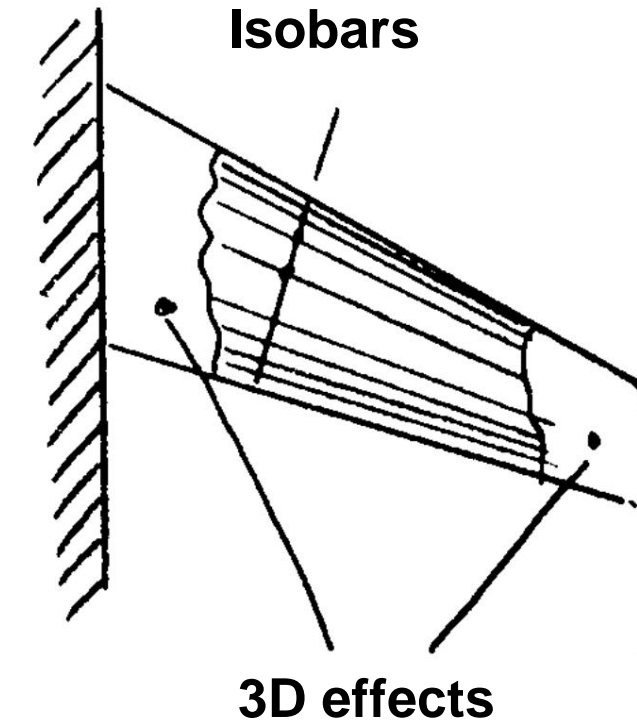


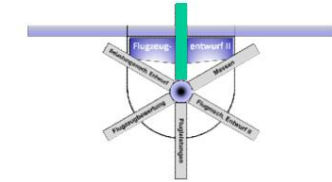


# D Basics of aerodynamic design

## 1.4.7 Influence of sweep

- This consideration assumes that the isobars are parallel across the wingspan, so that no 3-dimensional effects (e.g. edge influence) occur.
- In practice, this is not to be expected for a tapered, finite wing, since fuselage, engine nacelle, boundary layer and edge effects come into play.
- The span range with pronounced parallel isobar progression is usually limited.

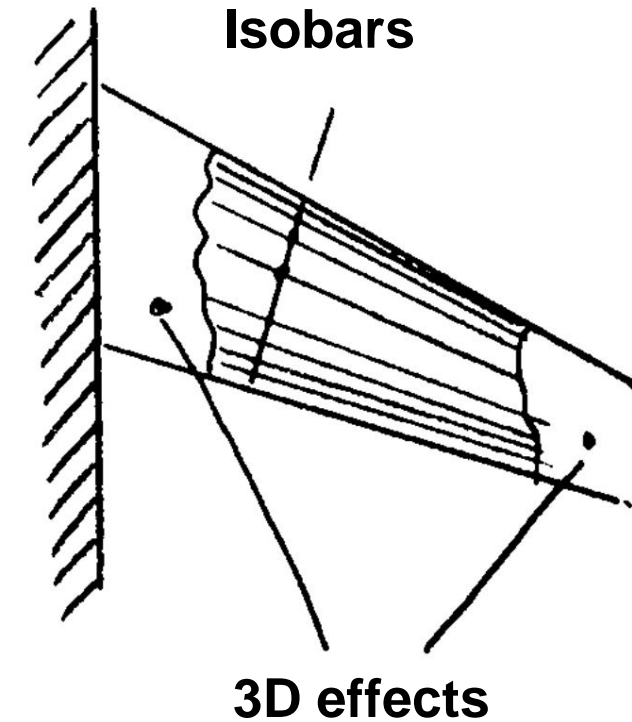


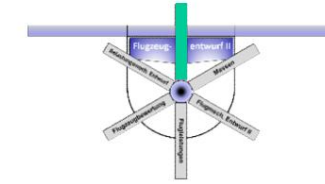


# D Basics of aerodynamic design

## 1.4.7 Influence of sweep

- Measurements have shown that for the real wing, the shift in the Mach numbers cannot be determined with sufficient accuracy using the cosine function of the sweep angle, but that a sweep effect reducing function ~~leads to~~ to more realistic results.
- A good design of the wing plan can ensure that the curvature of the isobars in the fuselage area is kept within limits.



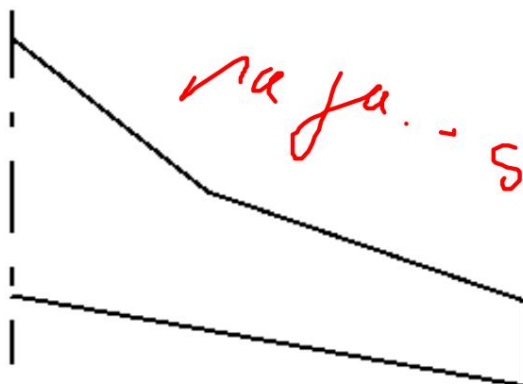


# D Basics of aerodynamic design

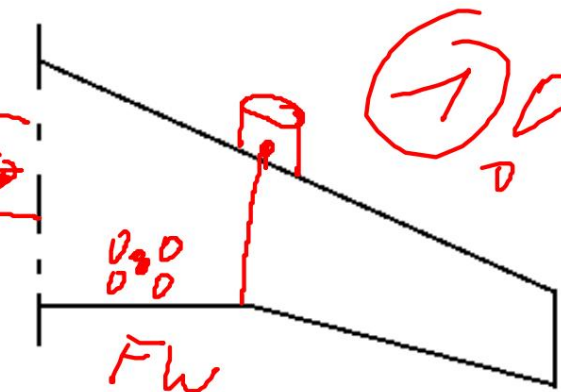
## 1.4.7 Influence of sweep

- The task is to use the sweep effect on the shift of the limiting Mach numbers as effectively as possible.
- For the double trapezoidal wing, which represents the general wing plan, the question arises as to the sweep distribution over the span.
- The following variants are possible in borderline cases:

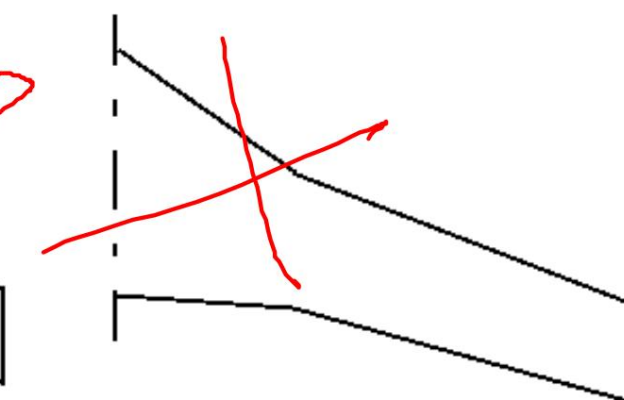
Straight trailing edge

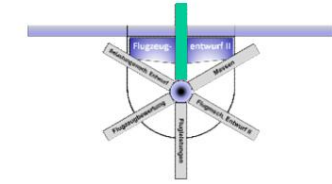


Straight leading edge



Straight quarter point line

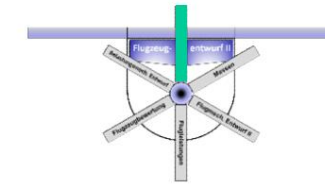




# D Basics of aerodynamic design

## 1.4.7 Influence of sweep

- The results of 3-dimensional flow analyses determine which configuration will produce the best results. In any case, a kink in the leading or trailing edge will result in increased construction costs, as the corresponding high-lift aids will also have to be interrupted at this point.
- Another aspect concerns the accommodation of the landing gear on the wing. Since there must be sufficient height behind the wing box for this, today's double trapezoid wings on commercial aircraft are always equipped with a straight leading edge. For this reason, the relative profile thickness is also often increased in the root area.
- With “body mounted gears” this aspect is not relevant and therefore these aircraft are usually fitted with shoulder wing configurations with the aerodynamically better and structurally less complex single trapeze variant.

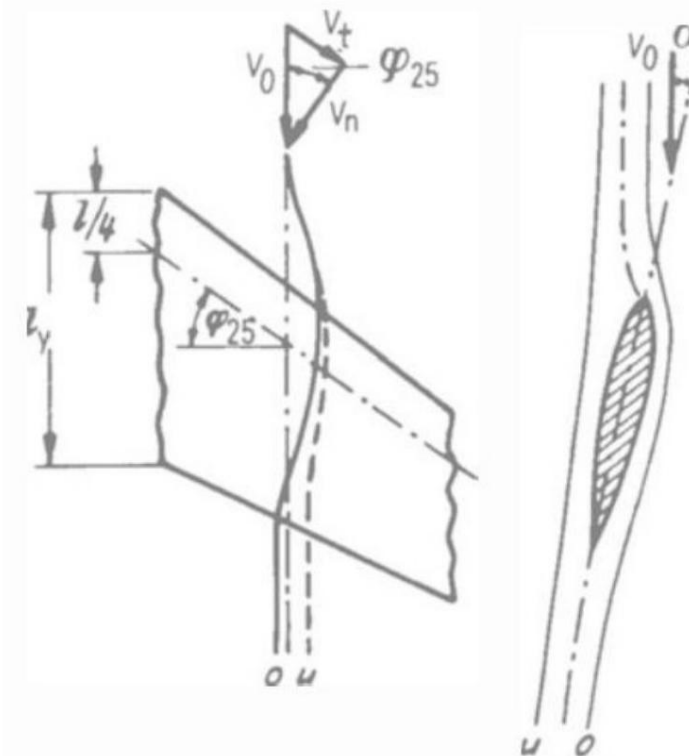


# D Basics of aerodynamic design

## 1.4.7 Influence of sweep

### “Out Wash”

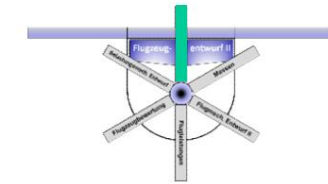
- The arrowed isobar curve basically leads to the effect that the streamlines are deflected.
- In the area of pressure drop, the positively swept The streamline is initially bent outwards in the wing, before turning inwards again in the subsequent region of pressure increase.



Source: F. Dubs, Aerodynamics of pure subsonic flow, Fig. 137, Springer, 1979

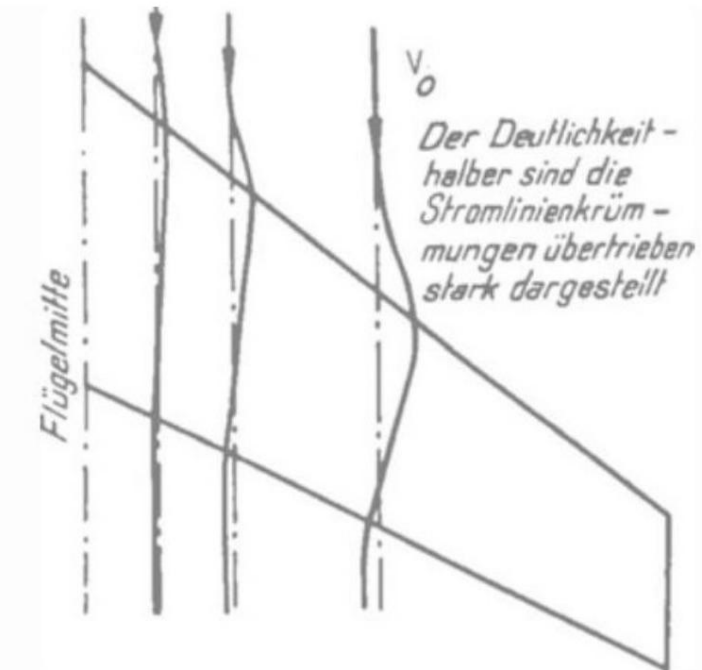
# D Basics of aerodynamic design

## 1.4.7 Influence of sweep

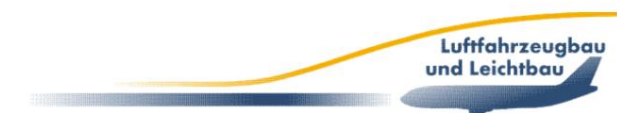


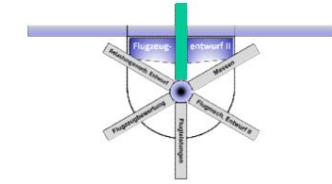
### “Out Wash”

- The effect disappears as you approach the center of the wing
- The final streamline is obtained when, in addition to the arrow effect, the deflection by the Edge flow is taken into account
- The effect is more pronounced in the area close to the wall than outside the boundary layer, since there the mass inertia forces are smaller in relation to the pressure forces.



Source: F. Dubs, Aerodynamics of pure subsonic flow, Fig. 138, Springer, 1979



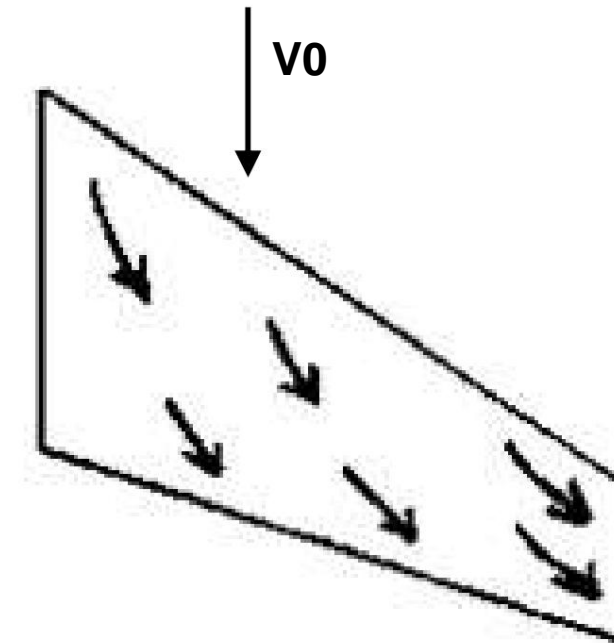


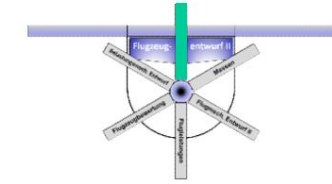
# D Basics of aerodynamic design

## 1.4.7 Influence of sweep

### “Out Wash”

- This is known as “Out-Wash”  
This effect leads to a tendency for the flow to be deflected towards the wing tip.
- Since this effect is a  
Since the boundary layer thickens in the direction of deflection, there is also an increased risk of separation on the outer wing.

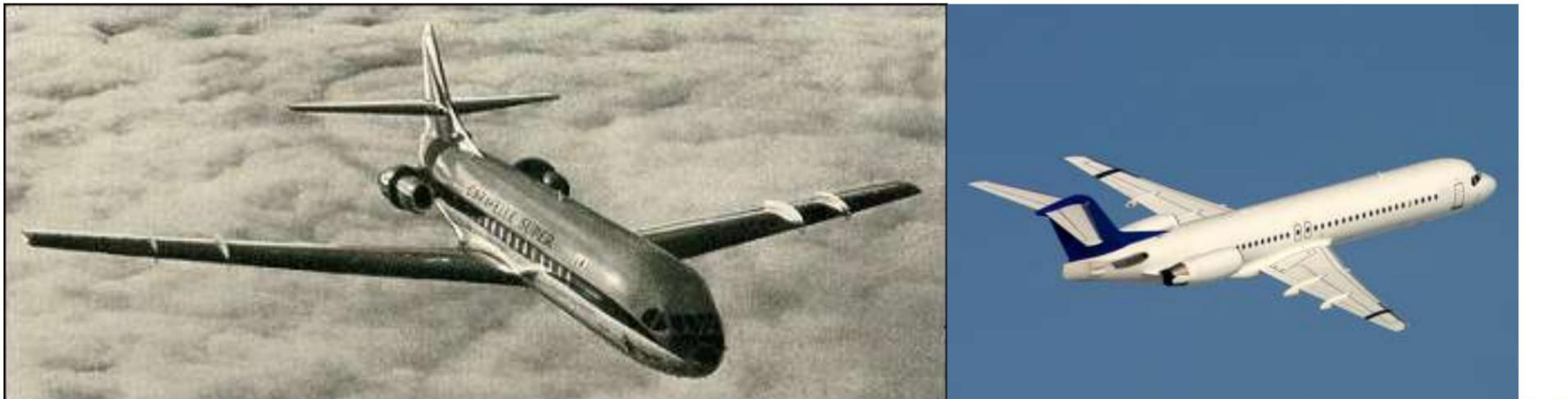


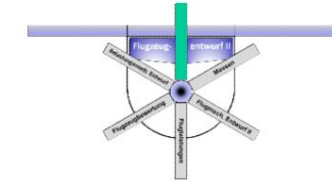


# D Basics of aerodynamic design

## 1.4.7 Influence of sweep

- Boundary layer fences, vertical sheets aligned around the profile nose in the direction of flow, which prevent outward flow.
- The same applies to a swept wing for the deflection of the streamlines towards the fuselage.
- The following picture shows such an aerodynamic measure  
Example of the Aerospatiale Caravelle & Fokker 100:



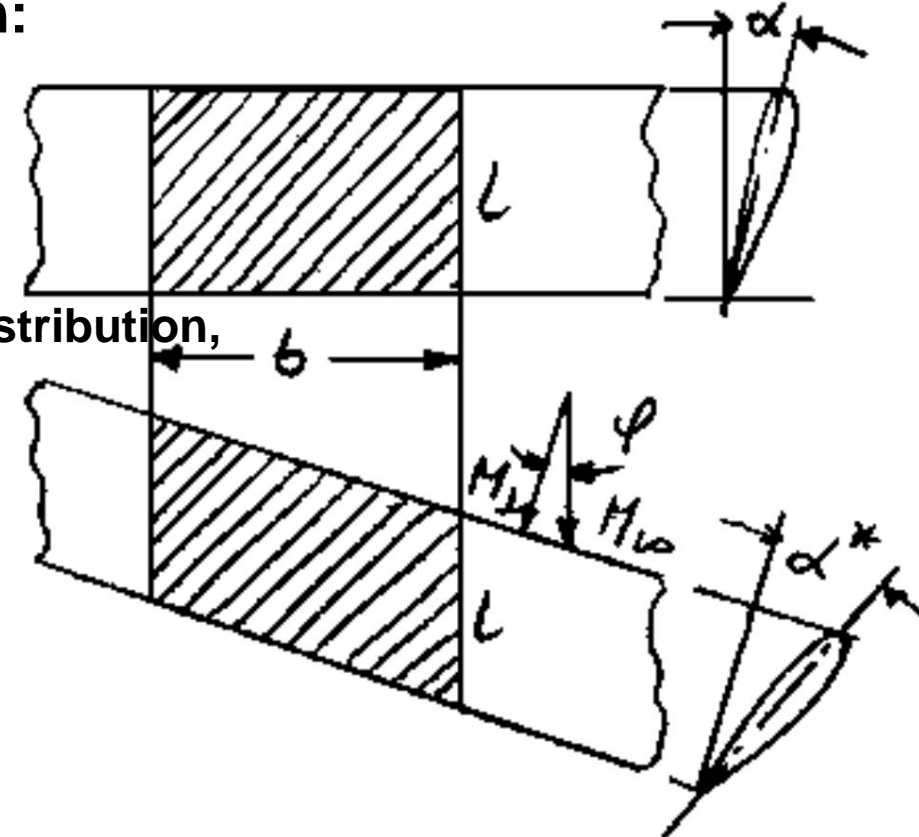


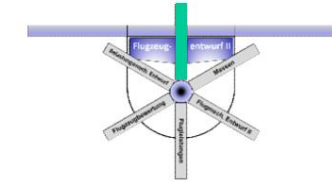
# D Basics of aerodynamic design

## 1.4.7 Influence of sweep

- The influence of the sweep on the angle of attack, the lift coefficient and the lift increase can be determined using the following consideration:

- The setting force acting perpendicular to the leading edge, which is decisive for the formation of the pressure distribution, is larger than the angle of attack to the resulting flow direction





# D Basics of aerodynamic design

## 1.4.7 Influence of sweep

- This fact can be used to calculate the buoyancy of the swept wing writing

$$A \frac{\dot{y}}{2} \cdot \dot{y} u \cos \dot{y} \dot{y} \dot{y}^2 F c_{A0\ddot{y}}$$

- However, the lift of the unswept wing is

$$A c \ddot{y} \frac{\dot{y}}{2} u^2 F$$

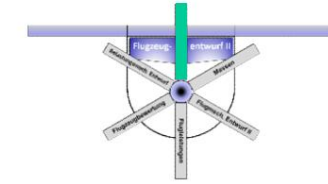
- For the same buoyancy ( $A^* = A$ ) the ratio the lift coefficients

$$\frac{\frac{A}{2} \cdot \dot{y}^2 u^2 \cos \dot{y} \dot{y} \dot{y}^2 F c_{A0\ddot{y}}}{A c_A \frac{\dot{y}}{2} u^2 F} = \frac{c_{A0\ddot{y}}}{c_A} \cdot \cos^2 \dot{y} \dot{y} \dot{y}$$

- and thus

$$c_{A0\ddot{y}} = c_A \cos^2 \dot{y} \dot{y} \dot{y}$$





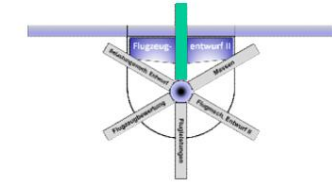
# D Basics of aerodynamic design

## 1.4.7 Influence of sweep

- The unswept profile section must therefore be designed for a lift coefficient that is  $\cos^2(\alpha)$  larger than the coefficient of the swept, infinitely long rectangular wing.
- Furthermore, the above considerations for the buoyancy increase

$$\frac{c_A}{\alpha} = \frac{c_A}{\alpha_0} \cos^2(\alpha)$$

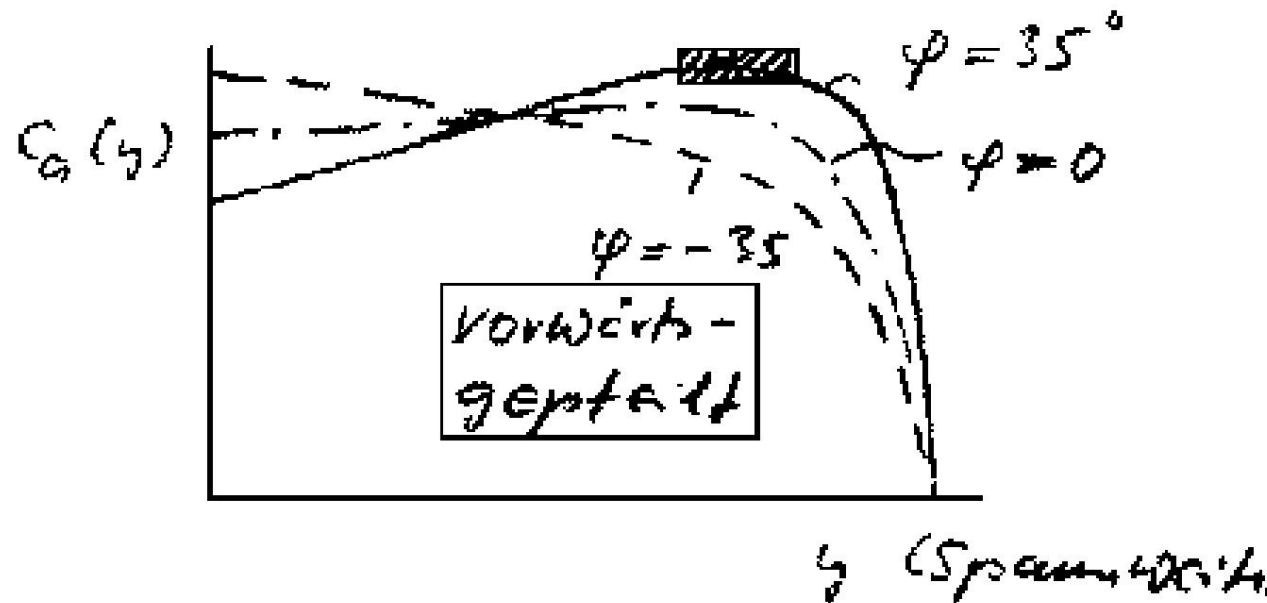
- The increase in lift therefore decreases with the cosine of the sweep angle, which in practice means, among other things, that the gust sensitivity of a swept wing is much lower than that of a straight wing.

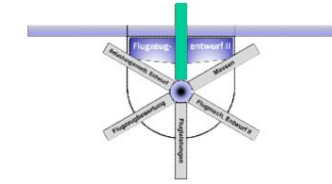


# D Basics of aerodynamic design

## 1.4.7 Influence of sweep

- In chapter D.1.4.2, a method for calculating the lift distribution on the wing was presented, which described the influence of the sweep using a sweep function.
- Characteristic here is the increasing return  
The area of maximum lift coefficients is shifted outwards by the sweep.

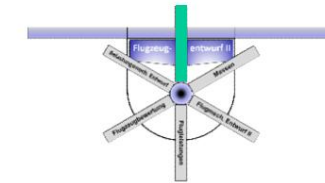




# D Basics of aerodynamic design

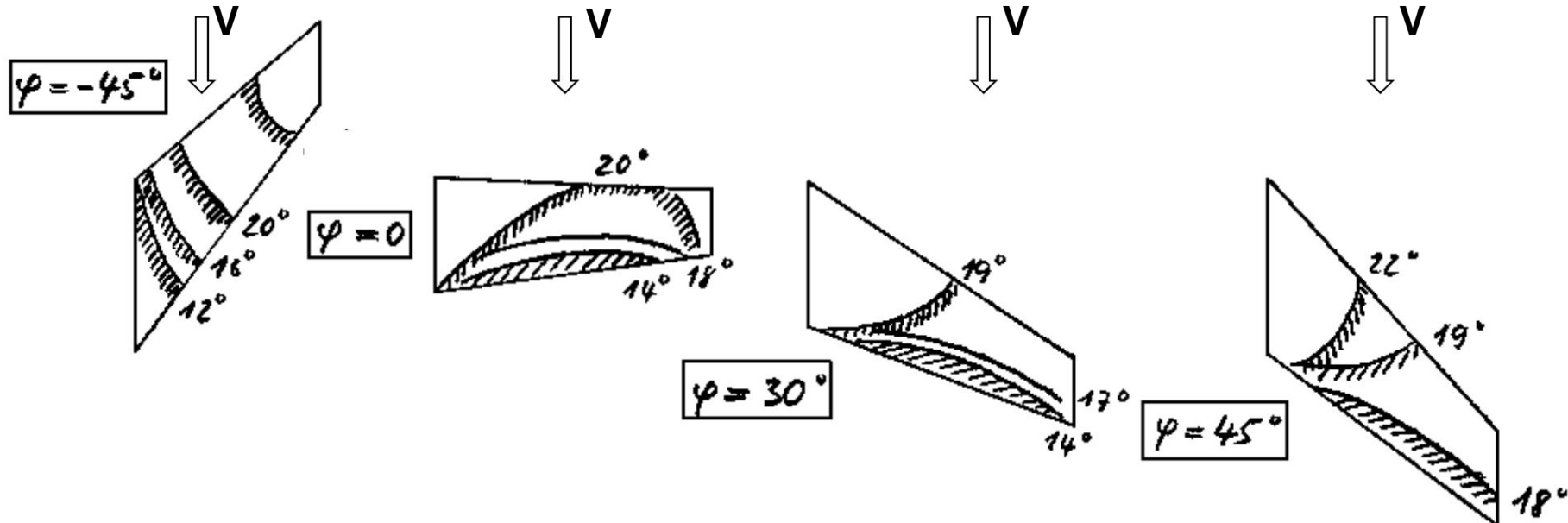
## 1.4.7 Influence of sweep

- If you integrate the  $ca$  distributions over the span coordinate and divide by the span, you get the total lift coefficient of the wing  $c_A$ .
- Comparing the mean values of the above curves, it can be seen that there is a sweep for which the lowest local lift increase and thus the maximum overall lift coefficient is achieved.
- For higher and lower sweep angles this maximum total lift coefficient decreases.

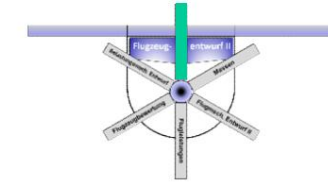


# D Basics of aerodynamic design

## 1.4.7 Influence of sweep



- As you can see, the swept wing has the most benevolent behavior: The buoyancy breaks, starting from the wing root, increasingly outwards and even in the extreme high angle of attack range there remains a sufficient controllability around the longitudinal axis.



# D Basics of aerodynamic design

## 1.4.7 Influence of sweep

- With an unswept wing, the flow initially tears at the trailing edge in the middle of the wing.

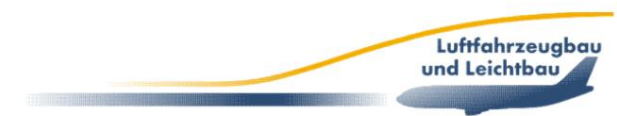
- The increasing separation extends towards the leading edge.

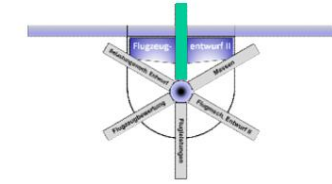
There are large areas inside and outside the wing where the airflow is still present even in the stalled flight condition.

• As the sweep increases, the first separation shifts further and further outwards and the separation area increases in size over the outer edge inwards, which severely impairs controllability right from the start of the stall.

- The loss of buoyancy in the outer area is also associated with associated with greater tail-heavy moments (danger of super-stall or pitch-up).

- What has been said about the influence of the wing taper also applies to the sweep. Here too, the maximum lift is greatly reduced as a result of the cA - superelevation with increasing sweep.



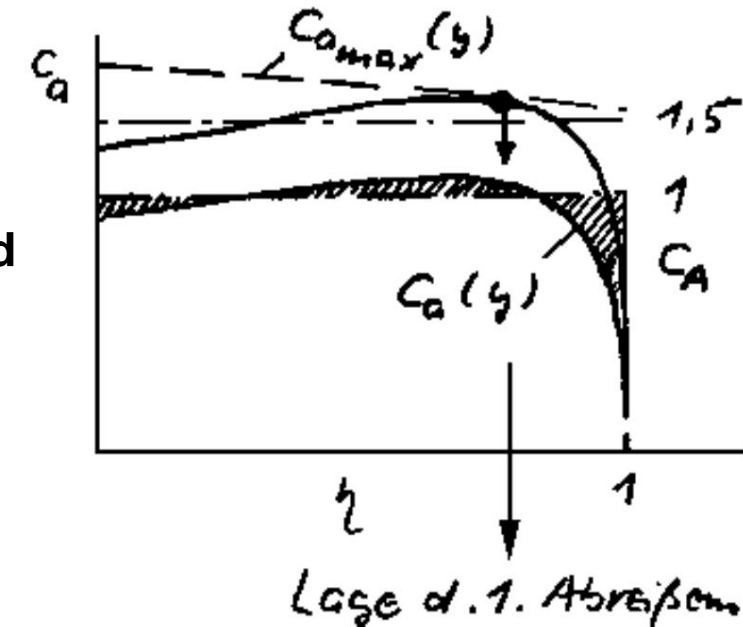


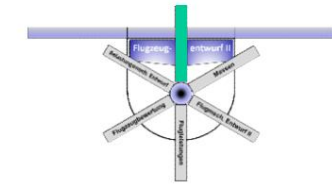
# D Basics of aerodynamic design

## 1.4.7 Influence of sweep

- Therefore, when designing the wing, tapering, sweep and twisting must be considered together as possible measures to avoid the disadvantageous lift distribution.

- Where the maximum lift coefficient (Re number effect) of the profile, which depends on the wing depth and therefore decreases towards the outside, tangent to the  $c_a$  distribution, is the separation point of the incipient stall (here as an undesirable "tip stall").

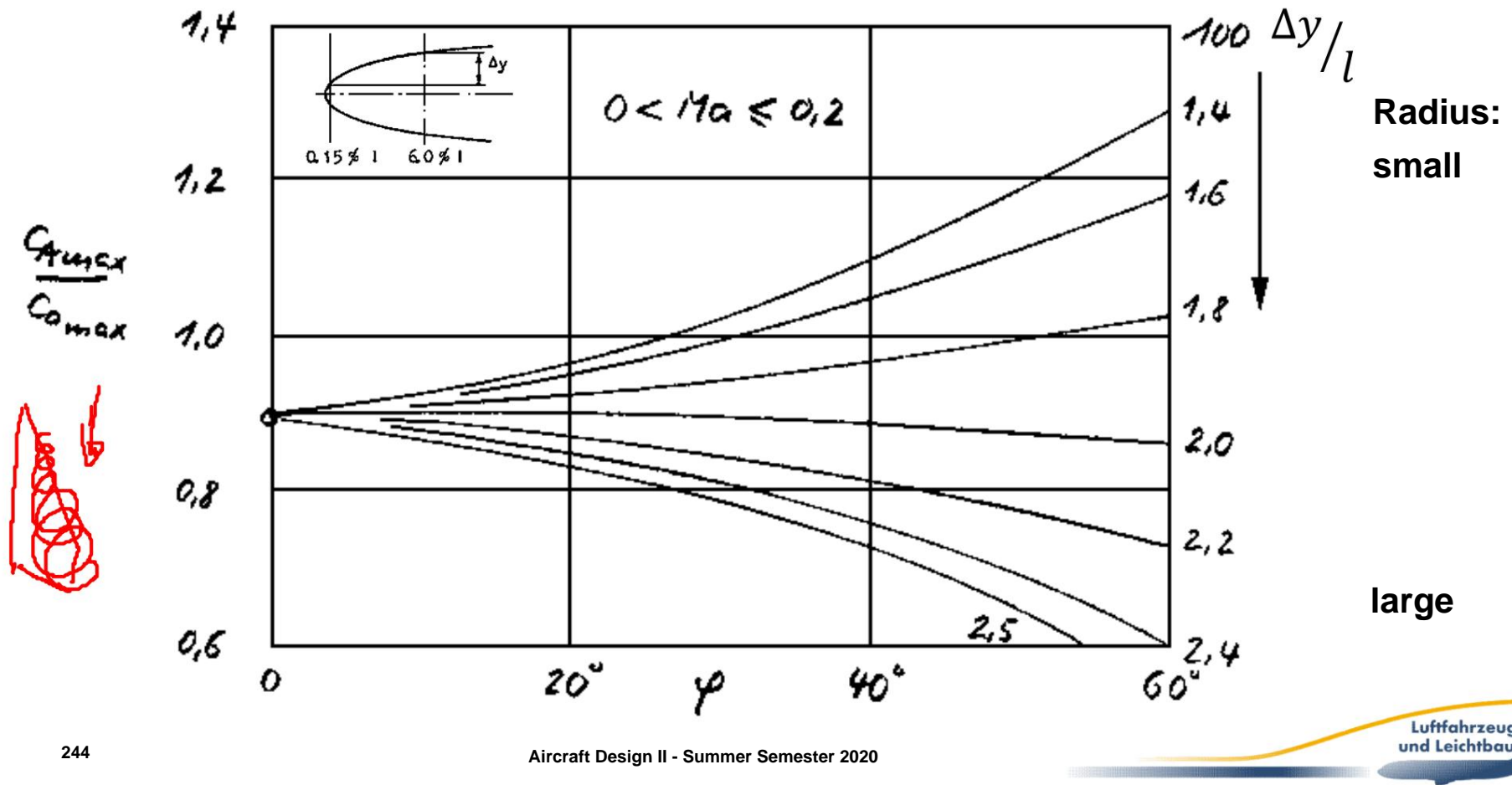


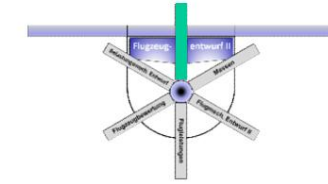


# D Basics of aerodynamic design

## 1.4.7 Influence of the sweep •

The lift increase and the separation behavior of the wing profiles together determine the stall behavior of the wing. • The influence of the nose radius ( $\Delta y/l$ ) must also be taken into account:

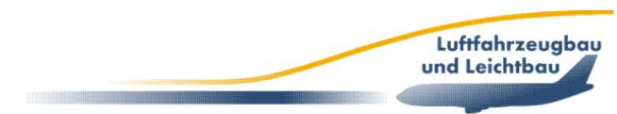


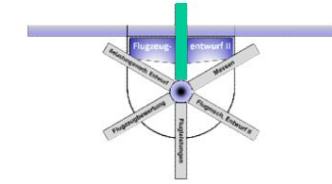


# D Basics of aerodynamic design

## 1.4.7 Influence of sweep

- As already mentioned in the discussion of the replacement modes of different profiles  
As explained, the nose radius plays an important role here. • The nose radius can be described with the characteristic geometric size  $\ddot{y}y/l$ .
- The transition of the stall behavior of swept wings from a classic trailing edge separation ( $\ddot{y}y/l > 0.02$ ) to a leading edge vortex flow can be seen.
- This is promoted by a sharp front edge and causes an increase in maximum lift with increasing sweep.
- In this case, the wing lift does not break when the local lift maximum, but rather a defined vortex forms on the upper side of the wing along the leading edge (leading edge vortex flow), which generates a correspondingly large negative pressure. The linear wing theory is abandoned in this case.

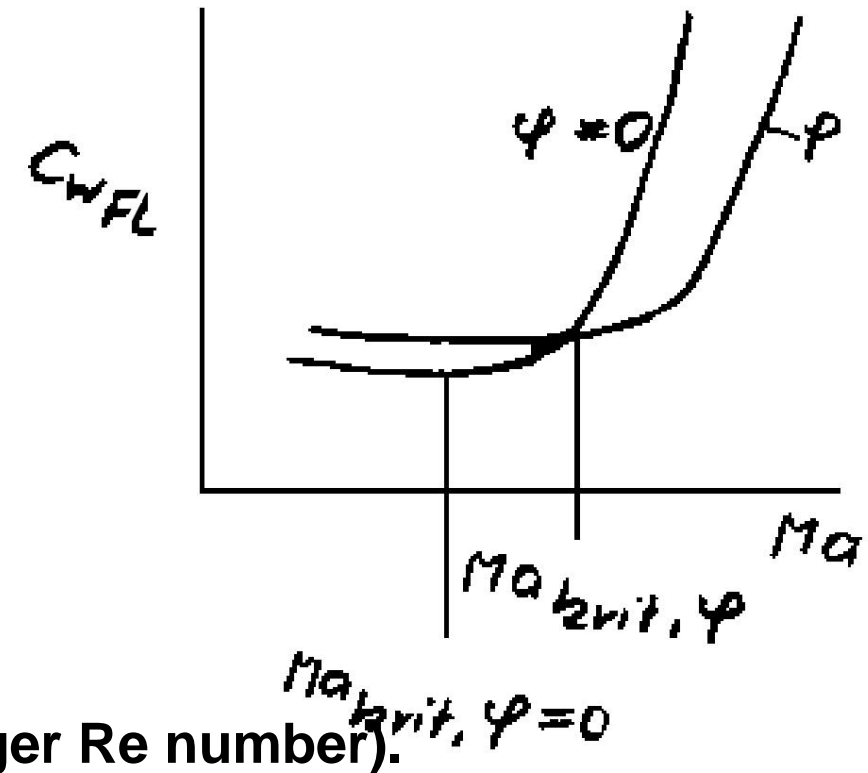


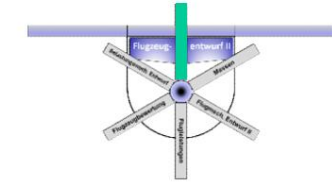


# D Basics of aerodynamic design

## 1.4.7 Influence of sweep

- As has been shown, the drag-divergence Mach number can be increased by means of the sweep, whereby the law is applied with sufficient precision.
- However, it is not only a shift of the limit curve to the right, but also a shift upwards
- The reason is the increase in induced drag, because pressure and frictional drag tend to decrease as a result of the larger wing depth (smaller relative thickness, larger Re number).

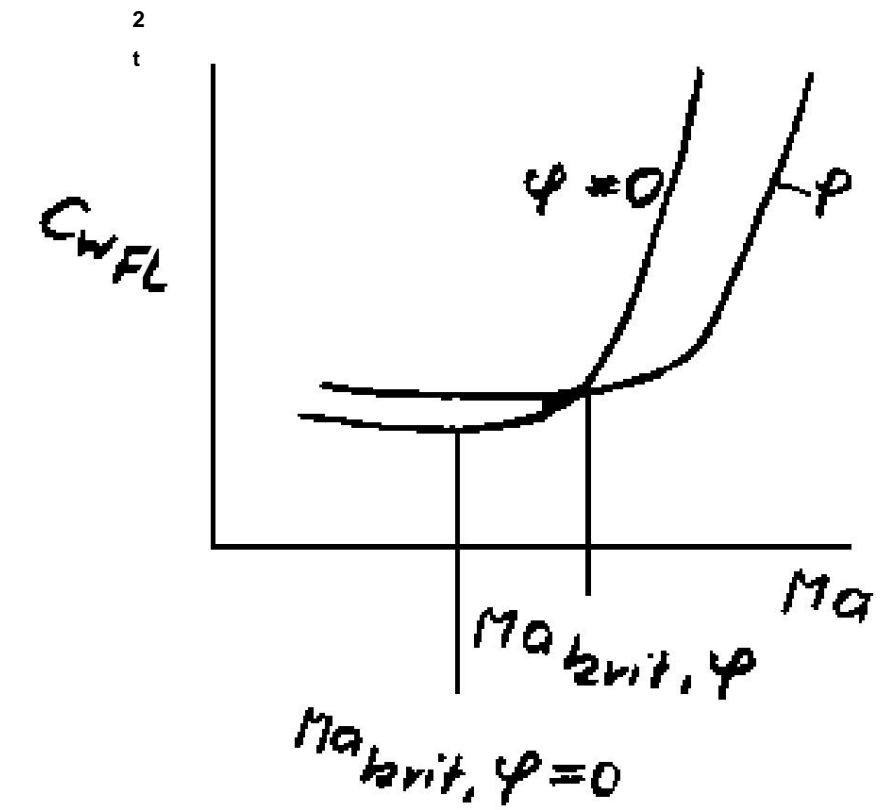
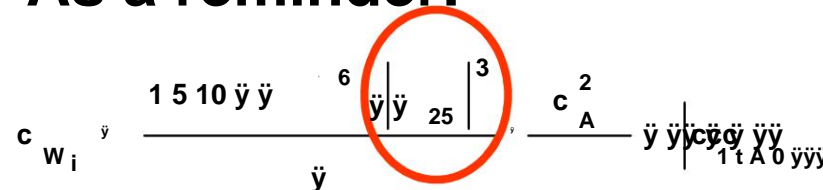


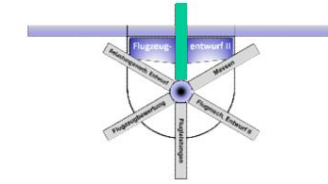


# D Basics of aerodynamic design

## 1.4.7 Influence of sweep

As a reminder:





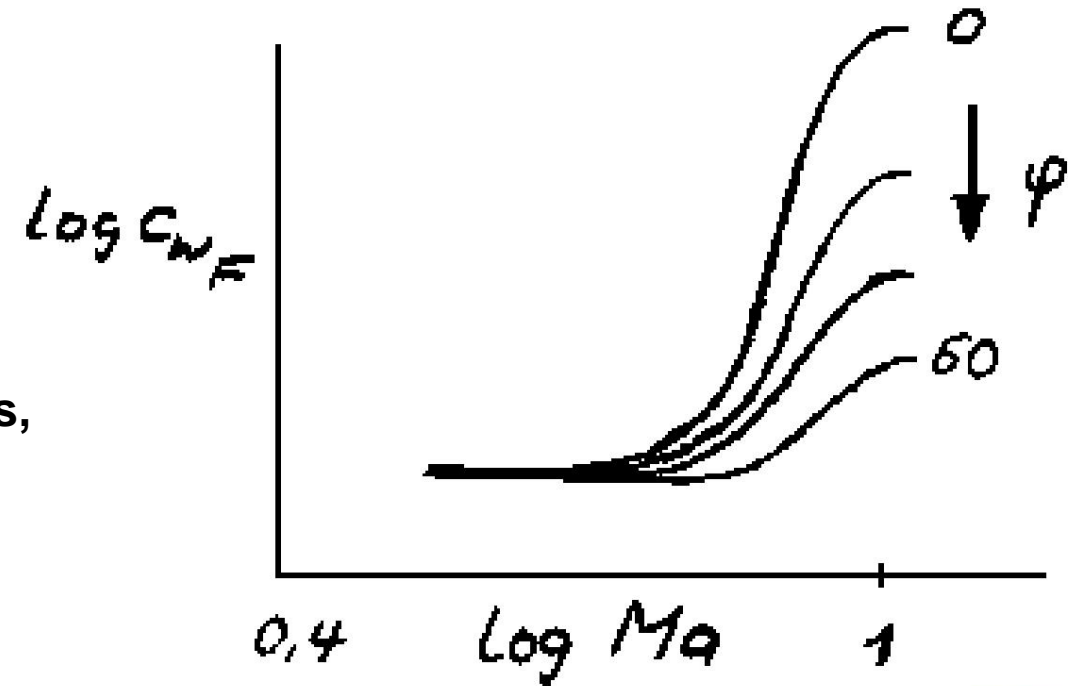
# D Basics of aerodynamic design

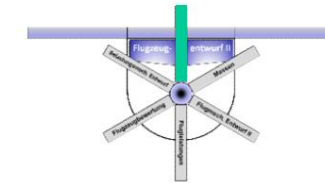
## 1.4.7 Influence of sweep

- The trend flattens out, as can be seen in the graph due to the logarithmic representation.
- The curve near the speed of sound shows that a significant reduction in the transonic drag can be achieved by sweeping the flow.

- Above Mach 1

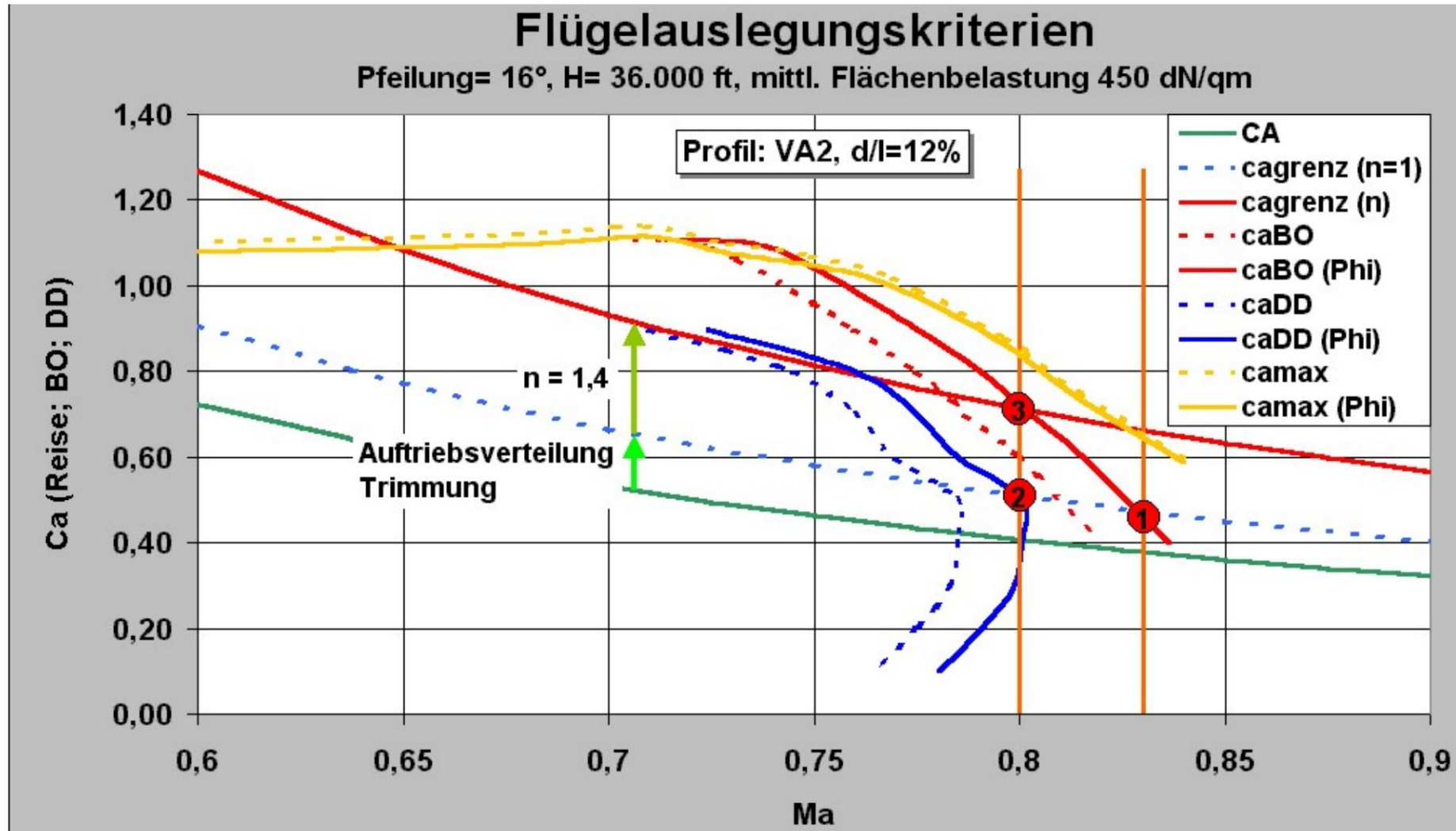
As already shown, the drag coefficient decreases, whereby the influence of the sweep almost disappears, but the subcritical level is no longer reached.

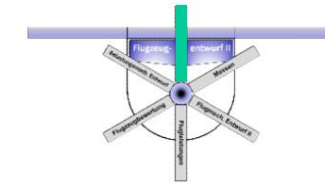




# D Basics of aerodynamic design

## 1.4.7 Influence of sweep





# D Basics of aerodynamic design

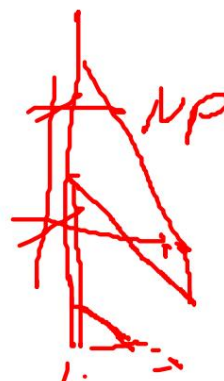
## 1.4.7 Influence of sweep

- Using the Diederich method, the chapter

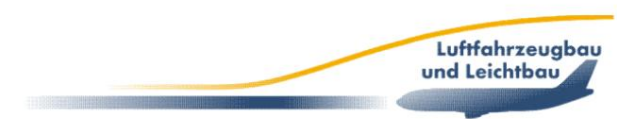
D.1.4.2 In addition to the lift distribution, the moment coefficient is also determined.

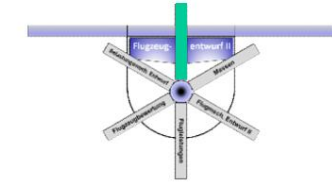
- The influence of the sweep is considered as a moment increase which links the twist (basic lift distribution) and the sweep and is as follows:

$$\frac{\frac{M_{ac}}{c} \tan \alpha}{2 \text{ litres}} = \frac{1}{I_m} \frac{C_l}{C_m}$$



250

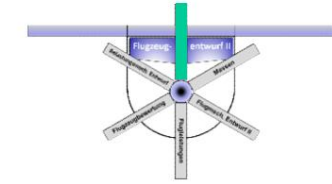




# D Basics of aerodynamic design

## 1.4.7 Influence of sweep

- The centre of lift of the wing, which is shifted backwards as a result of the sweep, causes an additional top-heavy moment, which increases the trim drag and at the same time has a major influence on the torsional load of the wing structure and thus on the weight.
- It is also possible to overcome problems with the aeroelastic behaviour by using a swept-back wing.
- The torsional moment of the swept wing, which acts on the angle of attack in a reducing manner, leads, for example, to a natural reduction in the angle of attack and, as a result, the bending loads during gusts and thus to a loading-mechanically convergent behavior.

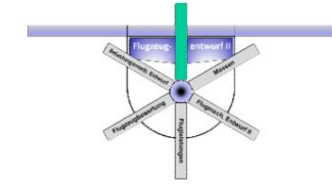


# D Basics of aerodynamic design

## 1.4.7 Influence of sweep

- The opposite is the case with a swept wing.
- A slight increase in the angle of attack due to the rearward torsion of the wing box leads to a further increased angle of attack and thus to an increased load, which corresponds to a divergent load-mechanical behavior.

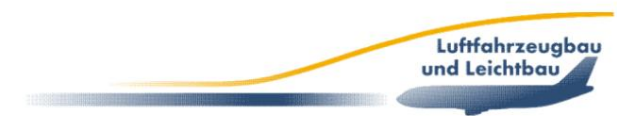


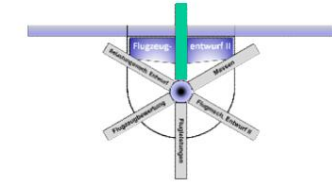


## D Basics of aerodynamic design

### 1.4.8 Influence of torsion

- As already mentioned in connection with the wing floor plan parameters meters of stretch, taper and sweep, their partially unfavorable effects on the course of the lift distribution can be compensated by a targeted measure: With the help of torsion.
- This refers to the change in the local effective angle of attack compared to the angle of the root profile.



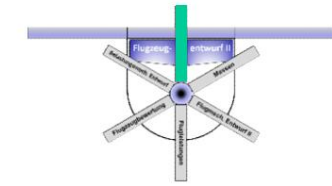


# D Basics of aerodynamic design

## 1.4.8 Influence of torsion

- There are several options for this:
  - The geometric distortion (change of setting each profile section),  $\varepsilon_i$
  - the aerodynamic twist (change in Zero lift direction of each profile section due to camber or changed profile shapes) or
  - the combined twisting.
- The number of these possibilities is increased even further when one considers the different torsion patterns, which further underlines the complexity of this measure.



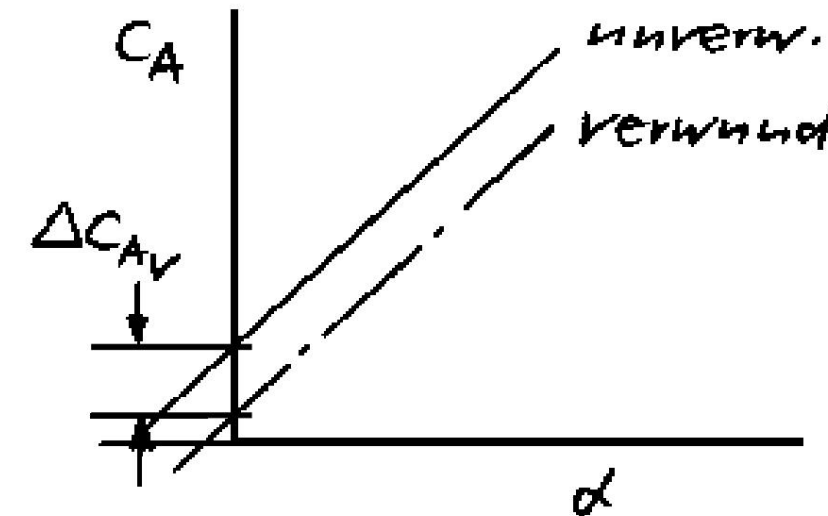
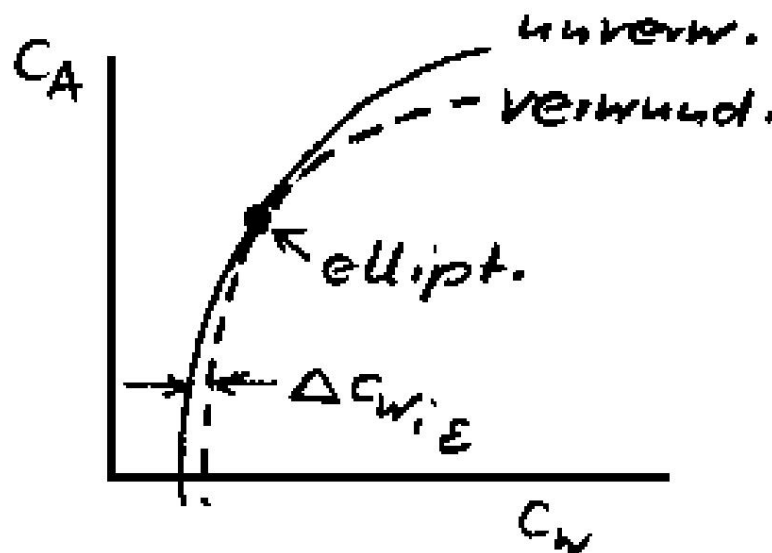


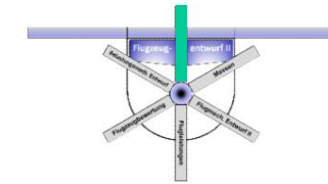
# D Basics of aerodynamic design

## 1.4.8 Influence of torsion

- Basically, a distortion results in increased construction costs  
Result → tool more complicated.
- In addition, twisting always leads to increased induced resistance.

$$C_{W2i} = \frac{C_A^2}{\frac{1}{tA_0} + \frac{\Delta C_{A,V}}{C_A}}$$

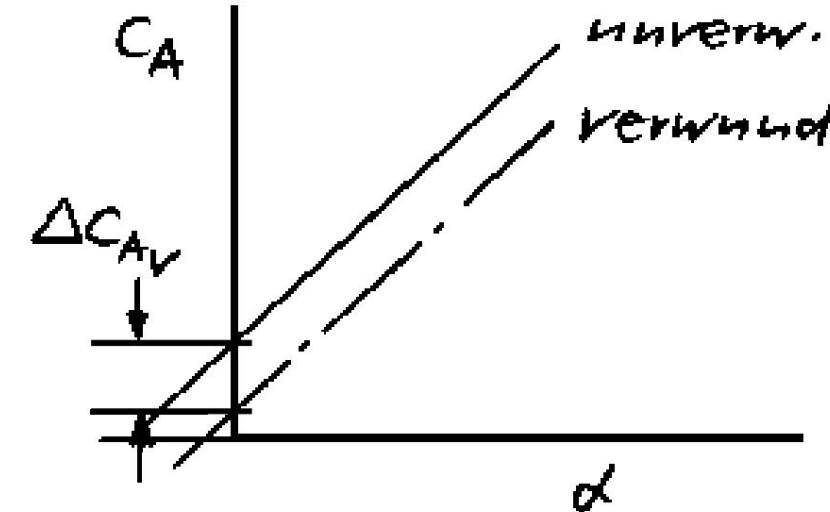
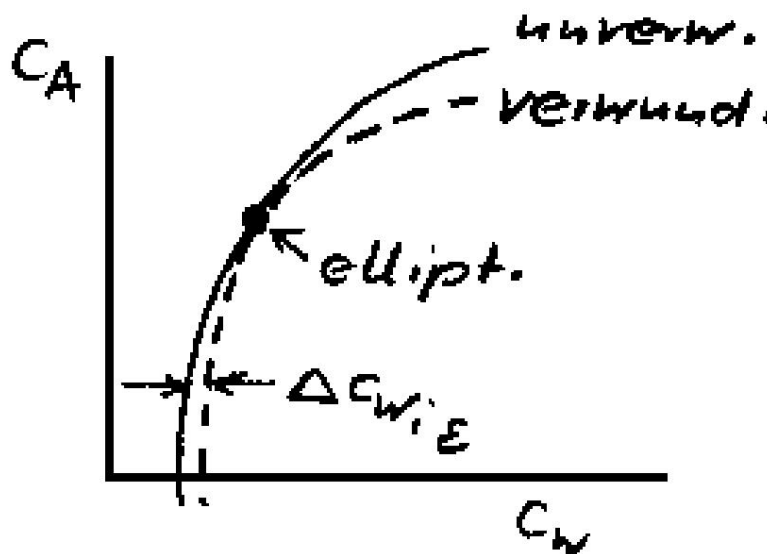


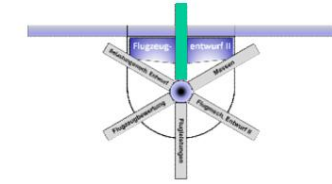


# D Basics of aerodynamic design

## 1.4.8 Influence of torsion

- Here, the term describes the induced resistance  $\Delta C_{A,V}$  condition of a wing with elliptical circulation distribution. • With a twisted wing, an approximately elliptical circulation distribution can only be achieved for a cA. • If this is deviated from, the induced drag always increases.

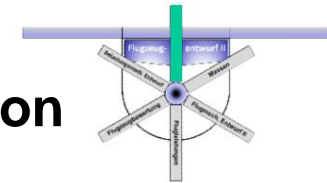




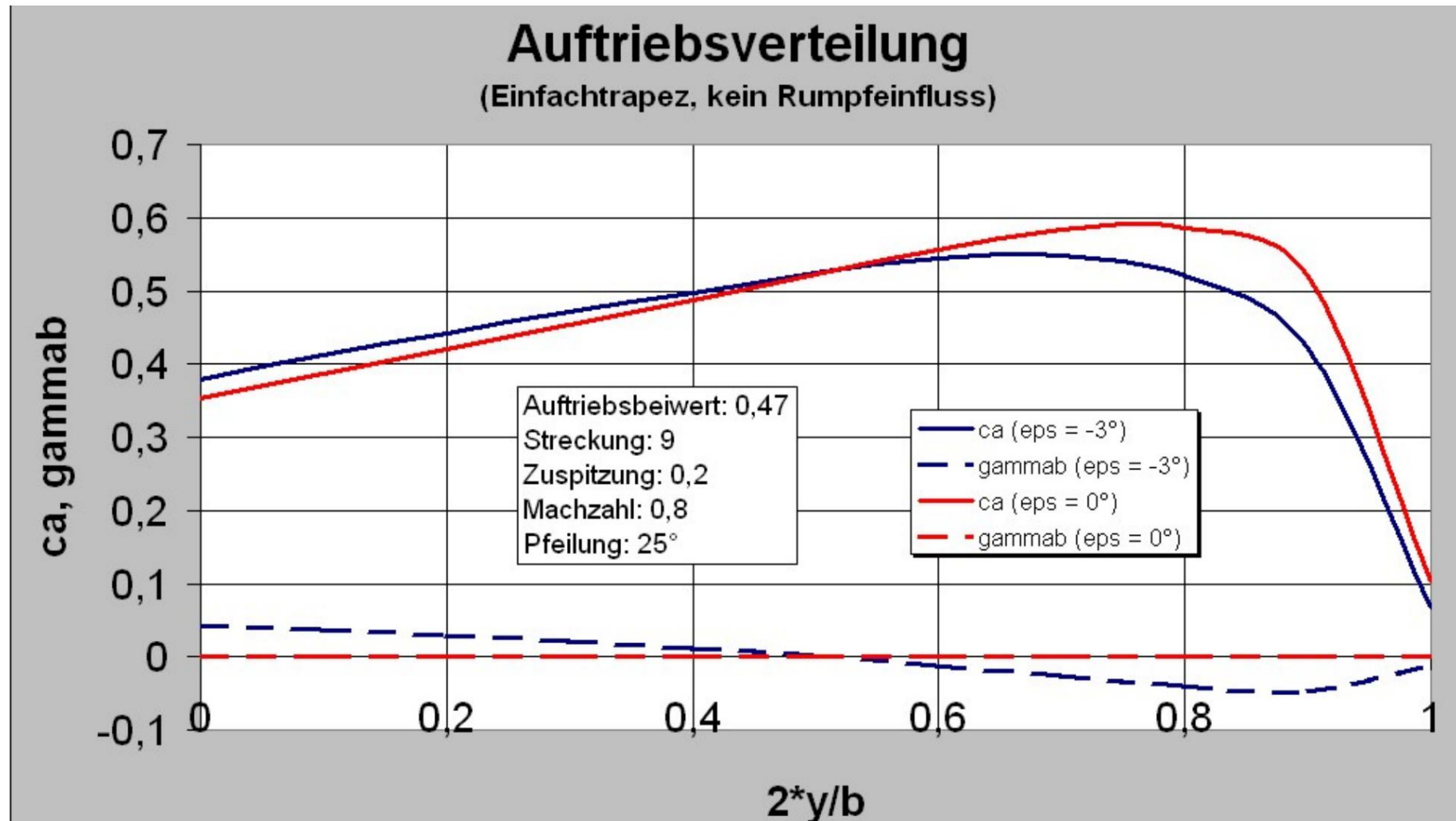
## D Basics of aerodynamic design

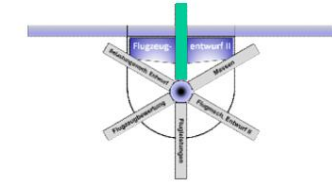
### 1.4.8 Influence of torsion

- In connection with the calculation of the lift distribution, the influence of the twist on the basic circulation distribution has already been mentioned. • By using a negative twist, one can achieve that this base distribution becomes negative in the outer area of the wing and thus both the ca -superelevation is reduced and the position of the ca -maximum is shifted inwards.



## D Basics of aerodynamic design 1.4.8 Influence of torsion

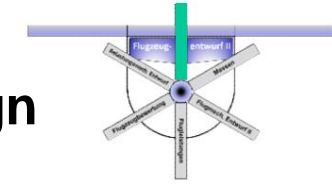




# D Basics of aerodynamic design

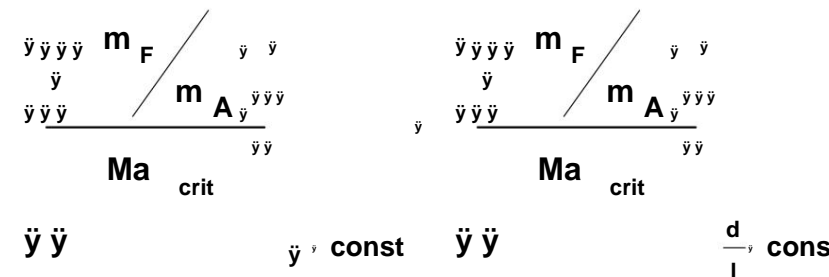
## 1.5 Optimal wing design

- The wing parameters act in an extremely complex way  
A final statement about an optimal design is not possible for all influencing factors.
- It is possible to optimize some parameters that have a very strong counteracting effect while retaining all the others with regard to a target function (example: interaction of the profile thickness with the sweep)
- There are many combinations of profile thickness and sweep which meet the condition of a limiting Mach number (eg critical Mach number), because this goal can be achieved simultaneously by
  - reducing the profile thickness or
  - Increase in arrow size.

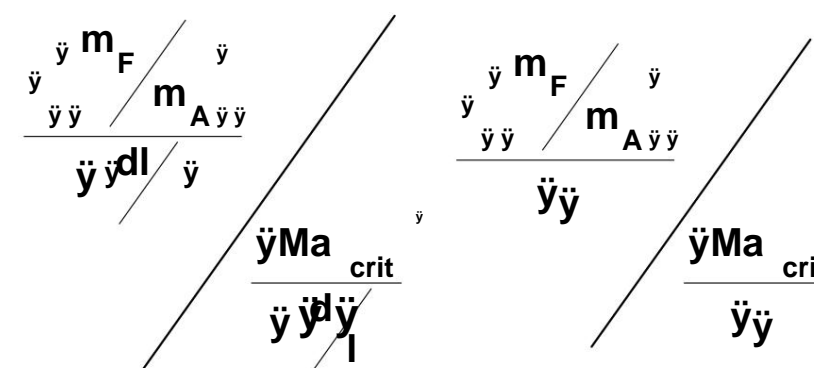


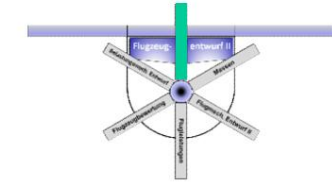
## D Basics of aerodynamic design 1.5 Optimal wing design

- With reduced relative profile thickness and increased wing sweep, critical Mach number and wing mass increase
- The resulting optimization problem for the lowest Wing mass (here related to take-off mass) is:



• or.

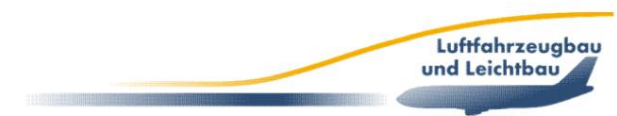


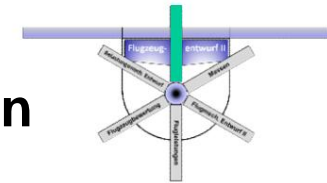


# D Basics of aerodynamic design

## 1.5 Optimal wing design

- This means that the optimal allocation of sweep and profile thickness is achieved when the ratio of the weight change to the change in the limiting Mach number of both measures is the same.





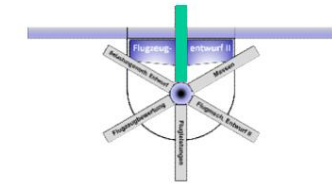
## D Basics of aerodynamic design 1.5 Optimal wing design

- Under the condition that the maximum lift remains constant (ie fulfillment of the given take-off and landing requirements), the change in wing mass also results from the change in wing area:

$$\frac{\ddot{m}_F}{\ddot{m}_A} = \frac{c_{A_{Max}}}{c_A} = \frac{\ddot{c}_{A_{Max}}}{c_{A_{Max}}} = \frac{\ddot{F}}{F}$$

and

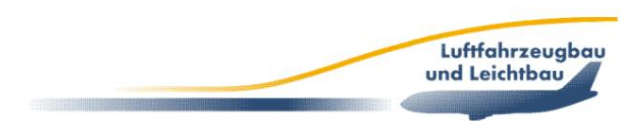
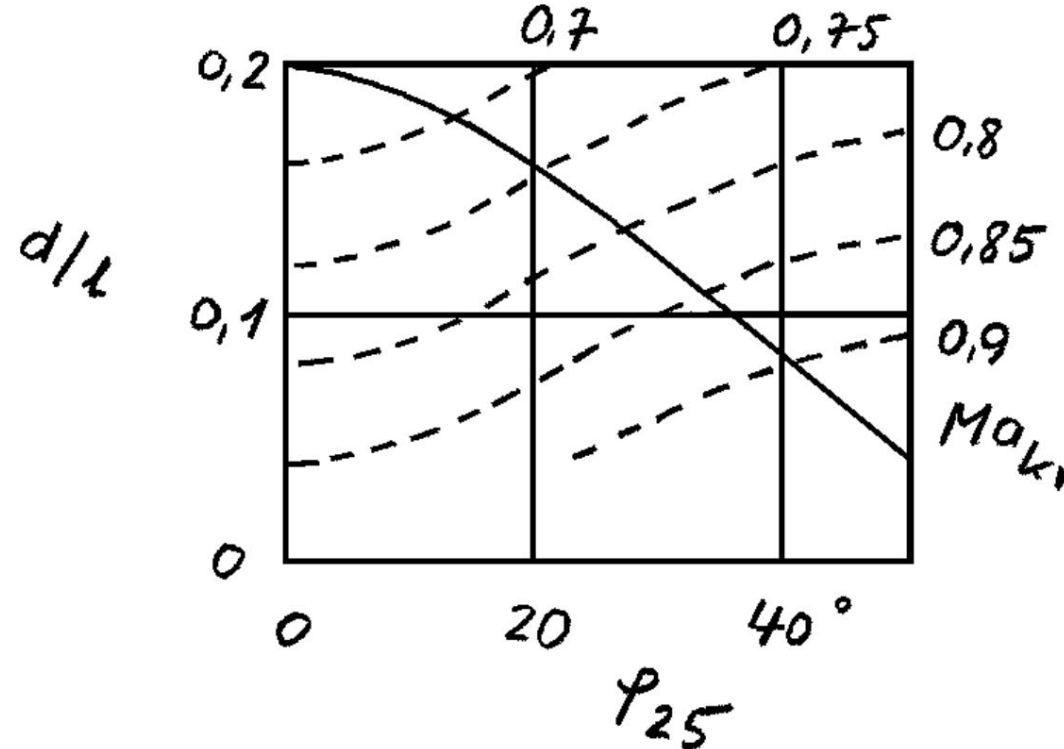
$$\frac{\ddot{m}_F}{\ddot{m}_A} = \frac{c_{A_{Max}}}{c_A} = \frac{\ddot{c}_{A_{Max}}}{c_{A_{Max}}} = \frac{\ddot{y}}{y}$$

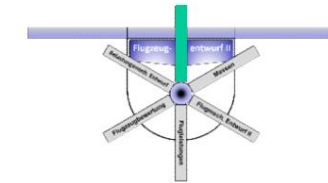


# D Basics of aerodynamic design

## 1.5 Optimal wing design

- Such an optimization of profile thickness and sweep  
Visible from the wing mass, the preliminary design shows good results.
- Aspects such as the influence of the flaps on  
the lift ( $c_{A\max}$ ) and drag influence of the wing area, ...





# D Basics of aerodynamic design

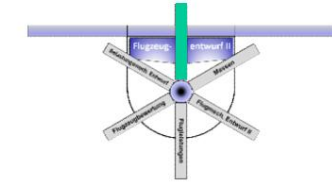
## 1.5 Optimal wing design

- The wing mass is not a comprehensive criterion for wing optimization.
- Optimizing direct operating costs provides a better goal.
- The optimization task for the wing design is to maximize the transport work TKO at minimal operating costs DOC.
- These DOC (see Chapter G) are approximately the sum from capital and fuel costs:

$$\text{DOC/TKO} = \frac{C_1 \cdot m_{\text{RU}}}{N} + C_2 \cdot K$$

- The first constant  $C_1$  contains an annuity (annual fixed costs) for depreciation, interest and insurance and the second factor  $C_2$  the fuel price.



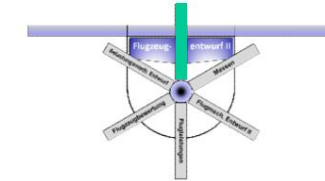


# D Basics of aerodynamic design

## 1.5 Optimal wing design

- The equipment mass  $m_R$  consists of the airframe, engine, equipment and crew mass.
- The wing mass is part of the cell mass and itself a function of several quantities (take-off mass, aspect ratio, max. wing loading, sweep, profile thickness, taper, maximum design speed).

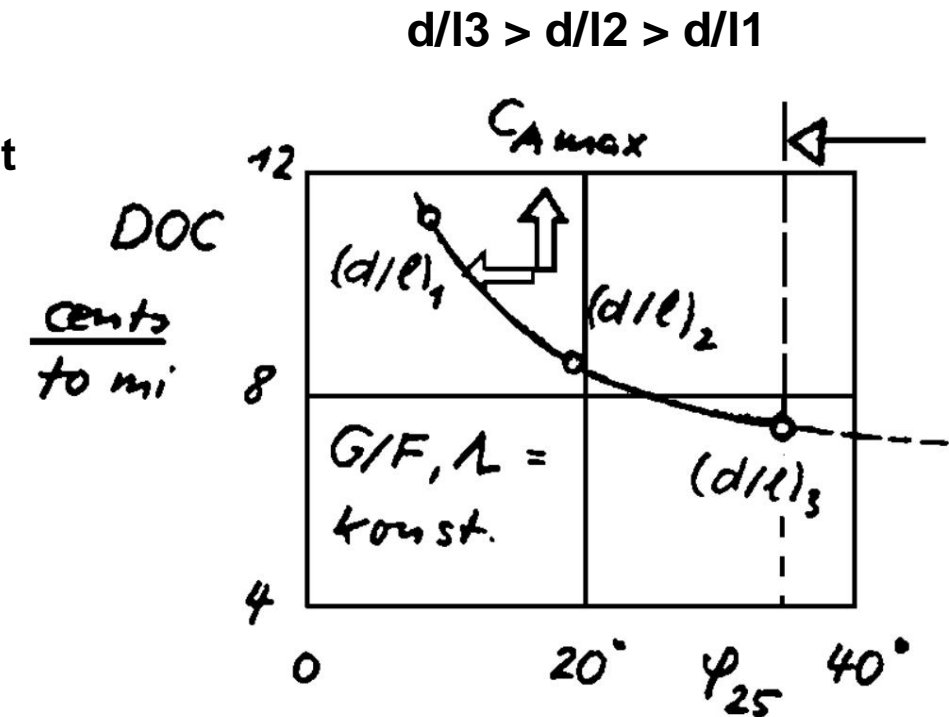




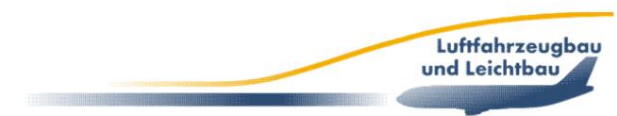
# D Basics of aerodynamic design

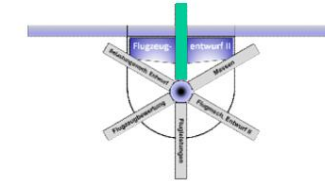
## 1.5 Optimal wing design

- A parameter variation for sweep and profile thickness in a cost calculation for a wing with an aspect ratio of 10 leads to a combination of the two parameters, which can already lead to aeroelastic problems, because it results in a relatively large sweep or a very low overall height for a cost-optimized design.



- The two arrows indicate that for more stringent starting requirements (eg STOL) there will be deviations for the optimal parameter combination in the manner shown.





# D Basics of aerodynamic design

## 1.5 Optimal wing design

- A very frequently employed Cost optimization is carried out in addition to the sweep and profile thickness for the wing aspect ratio and wing loading  $\frac{G/F}{L}$

- The result depends heavily on the  $\frac{G/F}{L}$   
Fuel prices are increasing and make wing design for an aircraft project that is to be successful in the future an extremely sensitive task.

$$d/l_3 > d/l_2 > d/l_1$$

